## *An investigation into the role of lamin A in the progression of colorectal cancer*

Willis, Naomi Daphne

University of Durham

School of Biological and Biomedical Sciences

# An Investigation into the Role of Lamin A in the Progression of Colorectal Cancer

**Naomi Daphne Willis**

Thesis submitted for the degree of Doctor of Philosophy



October 2005

# TABLE OF CONTENTS

# TABLE OF FIGURES

## CHAPTER 1



## CHAPTER 2



## CHAPTER 3

## CHAPTER 4



## CHAPTER 5

## DECLARATION

I declare that all experiments described herein are my own work and were carried out at the School of Biological and Biomedical Sciences, University of Durham under the supervision of Prof. C.J. Hutchison and Dr S.A. Przyborski. This thesis has been composed by myself. No material has been submitted previously for a degree at this or any other university. The copyright of this thesis rests with the author. No quotation from it should be published in any format, including electronic and the internet, without the author's prior written consent. All information derived from this thesis must be acknowledged appropriately.

Naomi D. Willis

## ACKNOWLEDGEMENTS

This project was funded by 'Against Bowel Cancer', registered charity number 1068476.

I would like to acknowledge the excellent support and guidance given to me throughout my Ph.D. and particularly during the writing up process by my supervisors Professor Christopher J. Hutchison and Dr Stefan A. Przyborski. Additionally I am grateful to Professor Robert G. Wilson, Consultant Colorectal Surgeon / Director of Research & Development, The James Cook University Hospital, Middlesbrough for providing an important clinical perspective during the development of this thesis and who, in his capacity as Chairman of the charity 'Against Bowel Cancer', enabled the commencement of this project.

I am also indebted to many researchers and technical staff working at the School of Biological and Biomedical Sciences, University of Durham during my period of study: Dr Rekha Rao, without whom none of the microarray analysis would have been possible; Mrs A. Christine Richardson and Dr Martin W. Goldberg for their invaluable expertise in electron microscopy; Mrs Pamela Ritchie for her superb technical support and always going beyond the call of duty to help; Dr Rebecca Stewart for her technical proficiency, particularly regarding flow cytometry; Dr Ewa Markiewicz, Miss Georgia Salpingidou and especially Dr Mauricio Alvarez-Reyes whose support and advice from the beginning has always been greatly valued.

I would like also to acknowledge the important contribution made to this thesis by our collaborators at the University of Maastricht, Maastricht, The Netherlands. Dr Adriaan P. de Bruïne and Dr Manon van Engeland enabled access to part of the Dutch archive of colorectal cancer tissue and facilitated the completion of an immunohistochemical analysis of these specimens; Dr Jos L.V. Broers and his family showed tremendous kindness towards me during my visit to the University.

# ABBREVIATIONS

| | |
|---|---|
| *A* | Absorbance |
| A | Adenine nucleotide |
| aa | Amino acid |
| ABD | Actin binding domain |
| AC | Astler-Coller |
| ACF | Aberrant crypt foci |
| AD | Autosomal dominant |
| AD-EDMD | Autosomal dominant - Emery-Dreifuss muscular dystrophy |
| AJCC | American Joint Committee on Cancer |
| AKAP149 | A kinase (PRKA) anchor protein 149 kDa |
| AMV-RT | Avian Myeblastosis Virus - Reverse Transcriptase |
| APC | Adenomatous polyposis coli |
| APS | Ammonium persulphate |
| AR | Antigen retrieval |
| ARMS-PCR | Allelic Refractory Mutation Specific – Polymerase Chain Reaction |
| BAF | Barrier-to-autointegration factor |
| BCC | Basal cell carcinoma (of the skin) |
| BDMA | N-benzyl-N,N-dimethylamine |
| BHK | Baby hamster kidney |
| BMP4 | Bone morphogenetic protein 4 |
| bp | base pair |
| BRB | Blot rinse buffer |
| BRR | Bannayan-Riley-Ruvulcaba syndrome |
| BSA | Bovine serum albumin |
| C | Cytosine nucleotide |
| $CaCl_2$ | Calcium chloride |
| CA2 | Carbonic anhydrase II |
| CCD | Charge-coupled device |
| cdc2 | Cell division cycle 2 |
| cDNA | complementary DNA |
| cds | coding sequence / coding region |
| CEA | Carcinoembryonic antigen |

| | |
|---|---|
| *C. elegans* | *Caenorhabditis elegans* |
| CIN | Chromosomal instability |
| cis | carcinoma *in situ* |
| CD44 | CD44 antigen |
| CKI | Casein kinase I |
| CLDN1 | Claudin 1 |
| CMD-1A | Dilated cardiomyopathy-1A |
| CMT1 | Charcot-Marie-Tooth disease, type 1 |
| CMT2 | Charcot-Marie-Tooth disease, type 2 |
| c-MYB | v-myb avian myeloblastosis viral oncogene homolog |
| c-MYC | v-myc avian myelocytomatosis viral oncogene homolog |
| CRC | Colorectal cancer |
| CS | Cowden syndrome |
| C-terminal | Carboxy-terminal |
| Cy3 | Cyanine 3-dUTP |
| Cy5 | Cyanine 5-dUTP |
| DAB | 3,3'-diaminobenzidine tetrahydrochloride |
| DABCO | 1,4-diazabicyclo[2.2.2]octane |
| DAPI | 4',6-diamidine-2-phenyl indole |
| DCC | Deleted in colorectal cancer |
| $ddH_2O$ | Double distilled water |
| DDSA | Dodecenylsuccinic anhydride |
| DEPC | Diethyl pyrocarbonate |
| *df* | degrees of freedom - Student's *t*-test |
| $dH_2O$ | Distilled water |
| D-MEM | Dulbecco's modified eagle medium |
| DMSO | Dimethyl sulphoxide |
| DNA | Deoxyribonucleic acid |
| dnTCF-4 | dominant negative TCF-4 |
| dNTP | deoxynucleotide triphosphate |
| Dsh | Dishevelled |
| DTT | Dithiothreitol |
| dUTP | 2'-deoxyuridine 5'-triphosphate |
| EC | Embryonal carcinoma |
| ECACC | European Collection of Cell Cultures |

| | |
|---|---|
| ECL | Enhanced chemiluminescence |
| EDMD | Emery-Dreifuss muscular dystrophy |
| EDTA | Ethylenediaminetetraacetic acid |
| EGFP | Enhanced green fluorescent protein |
| EGTA | Ethylene glycol-bis[β-aminoethyl ether]-N,N,N'N'-tetraacetic acid |
| *EMD* | Emerin gene (see also *STA*) |
| ENC1 | Ectodermal-neural cortex 1 |
| EPHB2 | Ephrin receptor B2 |
| ER | Endoplasmic reticulum |
| EST | Expressed sequence tag |
| EtBr | Ethidium bromide |
| FABP1 | Fatty acid binding protein 1, liver |
| FAP | Familial adenomatous polyposis |
| FBS | Foetal bovine serum |
| FITC | Fluorescein isothiocyanate |
| FL3 | Fluorescent channel 3 |
| FOB | Faecal Occult Blood |
| FPLD | Familial partial lipodystrophy |
| FS | Forward scatter |
| Fz | Frizzled |
| G | Guanine nucleotide |
| GCL | Germ-cell-less |
| gDNA | genomic DNA |
| GFP | Green fluorescent protein |
| GI tract | Gastrointestinal tract |
| GSK3β | Glycogen synthase kinase 3β |
| $H_2O_2$ | Hydrogen peroxide |
| HCl | Hydrochloric acid |
| HGPS | Hutchinson-Gilford progeria syndrome |
| HNPCC | Hereditary non-polyposis colorectal cancer |
| HPSF | High purity salt free |
| HRP | Horse-radish peroxidase |
| Hyb. station | Hybridization station |
| IF | Intermediate filament |
| IFAP | IF-associated protein |

| | |
|---|---|
| IgG | Immunoglobulin |
| IHC | Immunohistochemistry |
| INM | Inner nuclear membrane |
| JPS | Juvenile polyposis syndrome |
| kb | kilobase |
| KCl | Potassium chloride |
| kDa | kilodalton |
| KLS | Klarsicht-like domain |
| LAP | Lamina-associated protein |
| LBR | Lamin B receptor |
| LDL | Low density lipoprotein |
| LEF | Lymphoid enhancing factor |
| LEM | LAP2, Emerin & MAN1 |
| LGMD | Limb girdle muscular dystrophy 1B |
| *LMNA* | Lamin A/C gene |
| *LMNB1* | Lamin B1 gene |
| *LMNB2* | Lamin B2 gene |
| LRP | LDL receptor-related protein |
| m | monoclonal antibody |
| M | Molar / marker |
| mAb | monoclonal antibody |
| MAD | Mandibuloacral dysplasia |
| $MgCl_2$ | Magnesium chloride |
| $MgSO_4$ | Magnesium sulphate |
| mg | milligram |
| ml | millilitre |
| mM | millimolar |
| MMR | Mismatch repair |
| MPF | Maturation promoting factor |
| mRNA | messenger RNA |
| MSI | Microsatellite instability |
| MW | Molecular weight |
| NaCl | Sodium chloride |
| NaOAc | Sodium acetate |
| NaOH | Sodium hydroxide |

| | |
|---|---|
| NCS | Newborn calf serum |
| NCSC | Neural crest stem cell |
| NE | Nuclear envelope |
| NEP-A | Nuclear envelope precursor – fraction A |
| NEP-B | Nuclear envelope precursor – fraction B |
| ng | nanogram |
| NL | Nuclear lamina |
| NLS | Nuclear localization signal |
| nm | nanometre |
| NORCCAG | Northern Region Colorectal Cancer Audit Group |
| NPC | Nuclear pore complex |
| N-terminal | Amino-terminal |
| NUANCE | Nucleus & ActiN Connecting Element |
| NUP | Nucleoporin |
| ONM | Outer nuclear membrane |
| p | polyclonal antiserum |
| *P* | Probability – Student's *t*-test |
| $p21^{CIP1/WAF1}$ | Cyclin-dependent kinase inhibitor 1A |
| PBS | Phosphate-buffered saline |
| PCNA | Proliferating cell nuclear antigen |
| PCR | Polymerase chain reaction |
| PI | Propidium iodide |
| PJS | Peutz-Jeghers syndrome |
| pmol | picomolar |
| PP1 | Protein phosphatase 1 |
| PPARγ | Peroxisome proliferator activator receptor gamma |
| pRb | Retinoblastoma protein |
| PTC | Peltier Thermal Cycler |
| RECQL2 | DNA helicase-like / Werner syndrome ATP-dependent helicase |
| REST | RE1-silencing transcription factor |
| RNA | Ribonucleic acid |
| RPL31 | Ribosomal protein L31 |
| RT | Room temperature |
| RT-PCR | Reverse transcriptase – polymerase chain reaction |
| SCC | Squamous cell carcinoma |

| | |
|---|---|
| SCLC | Small cell lung cancer |
| S.D. / s.d. | Standard deviation |
| SDS | Sodium dioecyl sulphate |
| SDS-PAGE | Sodium dioecyl sulphate – polyacrylamide gel electrophoresis |
| SREBP1 | Sterol-response-element-binding protein 1 |
| SS | Side scatter |
| *STA* | Emerin gene (see also *EMD*) |
| SUN | sad1 / UNC-84 homology |
| *t* | *t* value – Student's *t*-test |
| T | Thymine nucleotide |
| $T_m$ | Melt temperature |
| TAE | Tris-acetate EDTA |
| *Taq* | *Thermus aquaticus* |
| TBE | Tris-borate EDTA |
| TBS | Tris buffered saline |
| TCF | T-cell factor |
| TE | Tris / EDTA |
| TEM | Transmission Electron Microscope |
| TEMED | N,N,N',N'-tetramethylethylenediamine |
| TMD | Transmembrane domain |
| TP53 | Tumour protein 53 |
| β-TrCP | β-transducin repeat-containing protein |
| TRITC | Tetramethyl rhodamine isothiocyanate |
| TSG | Tumour suppressor gene |
| V | Volts |
| vs | versus |
| v/v | volume / volume |
| w/v | weight / volume |
| XL | X-linked |
| XL-EDMD | X-linked Emery-Dreifuss muscular dystrophy |
| Ub | Ubiquitin |
| µg | microgram |
| µl | microlitre |
| µm | micrometre |
| µmol | micromolar |

## ABSTRACT

Nuclear lamins are type V intermediate filaments which form a proteinaceous meshwork, termed the nuclear lamina, which underlines the inner nuclear membrane and provides mechanical strength to the nucleus and maintains nuclear shape. A-type lamins in particular have been implicated in DNA replication, the regulation of gene transcription, apoptosis and nuclear migration. Expression of lamin A/C is closely associated with the differentiated phenotype and loss of lamin A/C expression has been correlated with increased proliferation, especially in tumours. I sought to investigate the expression and regulation of A- and B-type lamins during colorectal cancer (CRC) progression.

Preferential down-regulation of lamin A expression over lamin C was observed in the most dedifferentiated CRC cell lines. Semi-quantitative RT-PCR suggested that this was achieved by both transcriptional and post-transcriptional mechanisms. A connection between loss of lamin A/C and proliferation was ruled out. Instead immunohistochemical analysis of CRC tissue sections indicated loss of lamin A may correlate with the differentiation status of cells. In normal colonic crypts lamin A/C expression was greatest in the differentiated compartment, whereas lamin A was absent and lamin A/C was present at barely detectable levels in Dukes' A malignant polyps with high grade dysplasia.

Stable re-expression of lamin A constructs in SW480 colon cancer cells which expressed almost no endogenous lamin A rescued two-dimensional growth. Subsequent RNA profiling of 325 genes with reported relevance to colorectal carcinogenesis and general tumourigenesis confirmed that proliferation indices were unaffected by changes in the level of lamin A. Synemin, a cytoskeletal linker protein, was found to be significantly down-regulated in SW480 GFP-lamin A transfected cells versus SW480 GFP transfected cells. This suggests that lamin A functions to maintain nuclear and cellular integrity by indirect modulation of components of cytoskeletal architecture.

# CHAPTER 1 - INTRODUCTION

## *1.1 Colorectal cancer*

### 1.1.1 National perspective

Cancer is a major cause of morbidity and mortality in the UK. Annually more than a quarter of a million people are newly diagnosed with cancer and more than 150,000 people die from the disease (Toms, 2004). Nationally colorectal cancer (CRC) is the third most commonly diagnosed cancer with 35,000 new cases detected every year (**Figure 1.1**). Incidence is similar in men (14% of all new cancer cases) and women (12% of all new cancer cases), although more men present with rectal cancer and show a higher rate of incidence above 40 years of age. CRC accounts for about 10% of all cancer deaths which translates into more than 16,000 people a year (**Figure 1.2**) (Toms, 2004). Only lung and prostate cancer account for more male cancer deaths. In females CRC is also third in importance as a cause of cancer death, behind lung and breast cancer. Compared to the rest of the European Union, the UK has the 14$^{th}$ highest incidence of CRC and the 12$^{th}$ highest mortality rate, based on year 2000 estimates (Toms, 2004). Consequently CRC constitutes a major burden on public health.

In an attempt to improve the prospects for patients diagnosed with cancer, the UK Department of Health has invested in Centres of Excellence for cancer treatment and care throughout the country. The James Cook University Hospital which serves the South Tees area of Northern England has been designated a Centre of Excellence for research and treatment of CRC. The predominant reason for this is the high incidence of



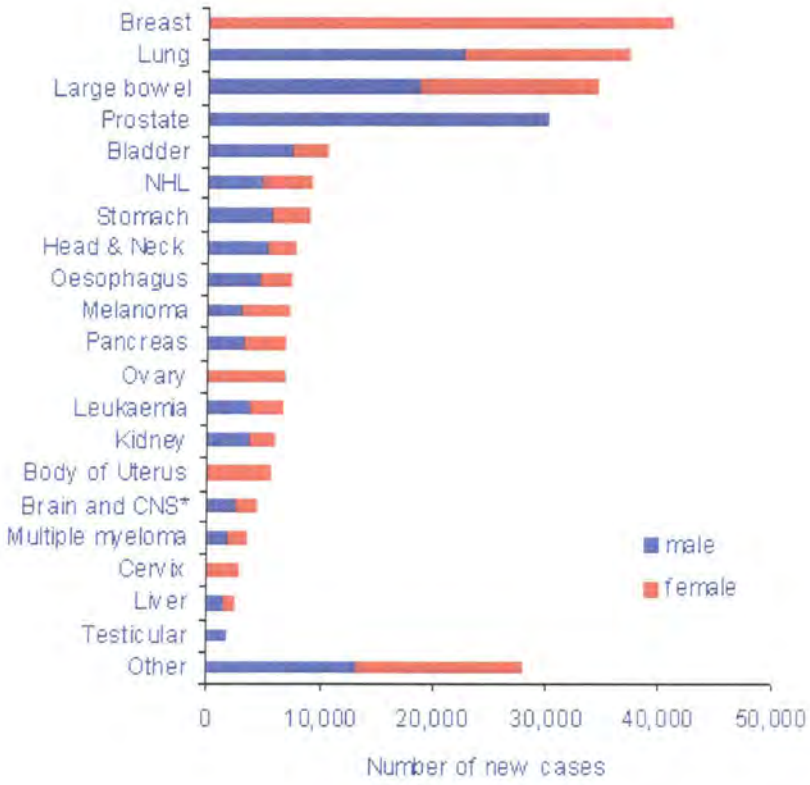


Figure 1.1 The most commonly diagnosed cancers, UK 2001.

*Source: Cancer Research UK (October 2005),*

*http://info.cancerresearchuk.org/cancerstats/incidence/commoncancers/.*

CRC in this area. Approximately 200 patients are seen each year with CRC (Prof. R.G. Wilson, personal communication). Ten percent of patients present with the earliest stages of the disease and usually survive, however, 25% have advanced tumours when first admitted and can often only be offered palliative treatment. In addition, approximately 20% of patients have a family history of the disease. A similar distribution of cases is seen across the whole Northern Region of England. In 2004, the Northern Region Colorectal Cancer Audit Group (NORCCAG) published an audit of all patients with a primary diagnosis of CRC who were treated in the 17 participating hospitals in the Northern Region of England during 2002. Out of 1413 patients who underwent abdominal surgery, 15.92% had Dukes' stage A (early stage) tumours,

30.29% had Dukes' stage B tumours, 29.30% had Dukes' stage C tumours and 21.44% had Dukes' stage D (late stage) tumours which had already spread to a secondary site. (N.B. Dukes' staging was not recorded for 3.04% of cases.) A positive family history was found in the records of between 10 – 15% of patients (NORCCAG, 2004).

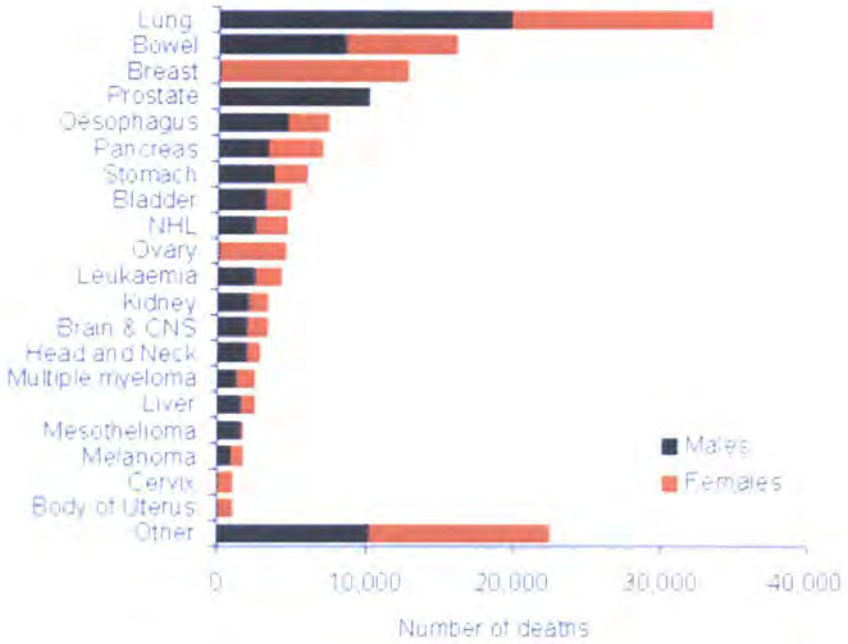


Figure 1.2 The 20 most common causes of cancer death, UK 2003.

*Source: Cancer Research UK (October 2005),*

*http://info.cancerresearchuk.org/cancerstats/mortality/cancerdeaths/.*

The benchmark indicator of successful diagnosis and management of cancer patients is survival rate. In 2001 the national five year relative survival rate (standardized against age) for colon cancer in men was estimated to be 52% and for women, 53% (Toms, 2004). Based on data from the Northern Region, NORCCAG have demonstrated that survival rate after surgery is progressively reduced the later the stage of the resected tumour. They observed that more than 80% of patients with Dukes' A tumours were alive after three years, whereas less than 20% of patients with Dukes' D tumours were alive after three years (NORCCAG, 2004). By reflecting on the situation being faced in

the South Tees area and by the Northern Region of England as a whole it becomes apparent that patient prognosis could be improved in two ways: First, by earlier diagnosis of tumours and second, by improved understanding of advanced tumours. If scientific investigators were to learn more about the nature of changes in late stage tumours it could lead to among other benefits: 1) Identification of new drug therapy targets and 2) An insight into the differences between an individual who responds well to therapy and an individual who responds badly so that treatment regimes may be tailored to suit the individual.

### 1.1.2 Population-based screening for colorectal cancer

The main reason that so many CRC patients present with advanced tumours is due to the asymptomatic nature of the disease in the initial stages when it can be most effectively treated. Accordingly different methods of screening have been trialled which aim to identify those members of the population most at risk from developing CRC. Two screening methods have so far been piloted in the UK: faecal occult blood (FOB) testing and flexible sygmoidoscopy (Alexander and Weller, 2003; Atkin, 2002; Hardcastle *et al.*, 1996). The first randomised trial of screening using FOB testing took place in Nottingham and looked at individuals between 45 - 75 years of age (Hardcastle *et al.*, 1996). The screened group were subjected to biennial FOB tests and those patients giving a positive result underwent further colonoscopic investigation. The control group was not invited to participate in any screening tests. FOB screening detects non-visible or 'occult' blood in stools which can be indicative of colorectal neoplasia. FOB screening was found to be a good predictor of neoplasia in 46% of cases. In addition a larger proportion of tumours detected by screening were Dukes' A (early stage tumours) suggesting that FOB testing facilitated earlier diagnosis.

Importantly Hardcastle *et al.* (1996) also reported a positive effect on survival. The mortality rate in patients who took the FOB test when first invited to do so was reduced by 39% compared to the control group.

These findings were generally supported by those of a similar study carried out in Minnesota, US (Mandel *et al.*, 1993; Mandel *et al.*, 1999). The Minnesota study made additional comparisons between the effectiveness of biennial FOB testing and annual FOB testing and reported a more favourable reduction in mortality rate in the group which were offered annual screening than in the group who were screened biennially, compared to the control group. These studies indicated that FOB screening may have potential benefits for improving survival if applied to the whole population.

To determine the feasibility of screening for CRC in the UK population using FOB testing, the UK Colorectal Cancer Screening Pilot was established in 2000 and an independent report commissioned by the UK Department of Health. A population-based trial was set up in two pilot sites: Coventry and Warwickshire in England and Fife, Tayside and Grampian in Scotland. Men and women between 50 and 69 years of age were invited to participate and close to 60% took up the offer of a FOB test. Overall the outcome was positive and the UK Colorectal Cancer Evaluation Team concluded in their final report that the benefits of FOB testing for the whole population in enabling earlier CRC diagnosis and improved survival far outweighed the financial costs, logistical considerations and risks from complications associated with follow-up colonoscopy in the event of a positive FOB test (Alexander and Weller, 2003). To this effect the National Bowel Cancer Screening Programme is due to be implemented across the UK from April 2006 and aims to monitor all individuals in their sixth decade.

The benefit of single flexible sygmoidoscopy screening has also been investigated in a multicentre randomised controlled trial in the UK (Atkin, 2002). Flexible sygmoidoscopy is the visual examination of the rectum and sigmoid colon with a flexible endoscope. It has the additional advantage of being able to detect pre-malignant lesions or polyps which the FOB test is less likely to pick up. However it is associated with a greater risk to the individual due to accidental perforations of the bowel which can occur during the procedure. Atkin (2002) reported that almost three quarters of cancers detected in the screened group were localized, i.e. Dukes stage A or B, of which 62% were Dukes stage A. (Polyps were generally removed by diathermy snare the same day.) This is a much higher percentage than was detected in the Nottingham study suggesting flexible sygmoidoscopy may be more sensitive than FOB. Additionally there was only one case of a perforated bowel out of 40,000 patients receiving sygmoidoscopy, indicating that it is both safe and effective. There is however one caveat with this screening method. The estimated cost of a diagnostic colonoscopy is £127, whereas the cost of a FOB test including processing is estimated at £5 (Alexander and Weller, 2003). Screening by flexible sygmoidoscopy would have to deliver vast improvements in early diagnosis and CRC survival rate for the benefits of rolling out such a programme nationwide to outweigh the associated financial burden on the UK Nation Health Service.

## *1.2 Colorectal carcinogenesis*

### 1.2.1 Epithelial versus mesenchymal tumours of the colon

The adult gastrointestinal tract is radially organized into four histologically distinct layers: the mucosa, submucosa, muscularis propria and serosa (Burkitt *et al.*, 1993). Colonic crypts are folds of simple columnar epithelium adjacent to the lumenal surface which are embedded in the mucosa and underlined by layers of mesenchymal tissue. **Figure 1.3** shows the histological organization of the colorectum. Colorectal cancer in the context of this thesis constitutes epithelial tumours which have arisen in the colonic crypt. Epithelial tumours are by far the most common cancerous lesion of the colorectum and the best studied. Smooth muscle and stromal tumours of the colon and appendix do occur in the form of leiomyomas and leiomyosarcomas, although they are rare by comparison to the prevalence of their epithelial counterparts (Hatch *et al.*, 2000). However, similar to epithelial tumours, one of the most common sites for smooth muscle tumours is the sigmoid colon (Hatch *et al.*, 2000; Toms, 2004).

Metastasis from a colon carcinoma occurs by either lymphatic or haematogenous spread. The most common sites for metastases of epithelial tumours are the liver and the lungs. Lower rectal carcinomas metastasize first to the lungs, while upper rectal tumours tend to colonize the liver and are further disseminated by the arterial route to the lungs (Weiss and Ward, 1988). Other less common sites of secondary colon tumours include brain and bone (Hammoud *et al.*, 1996; Sundermeyer *et al.*, 2005), skeletal muscle (Torosian *et al.*, 1987), adrenal glands (Murakami *et al.*, 2003), bladder and chin (Hobdy *et al.*, 2003) and oral soft tissues (Bhutani and Pacheco, 1992). It has been determined that if metastases to the brain are involved, other organs are most likely also

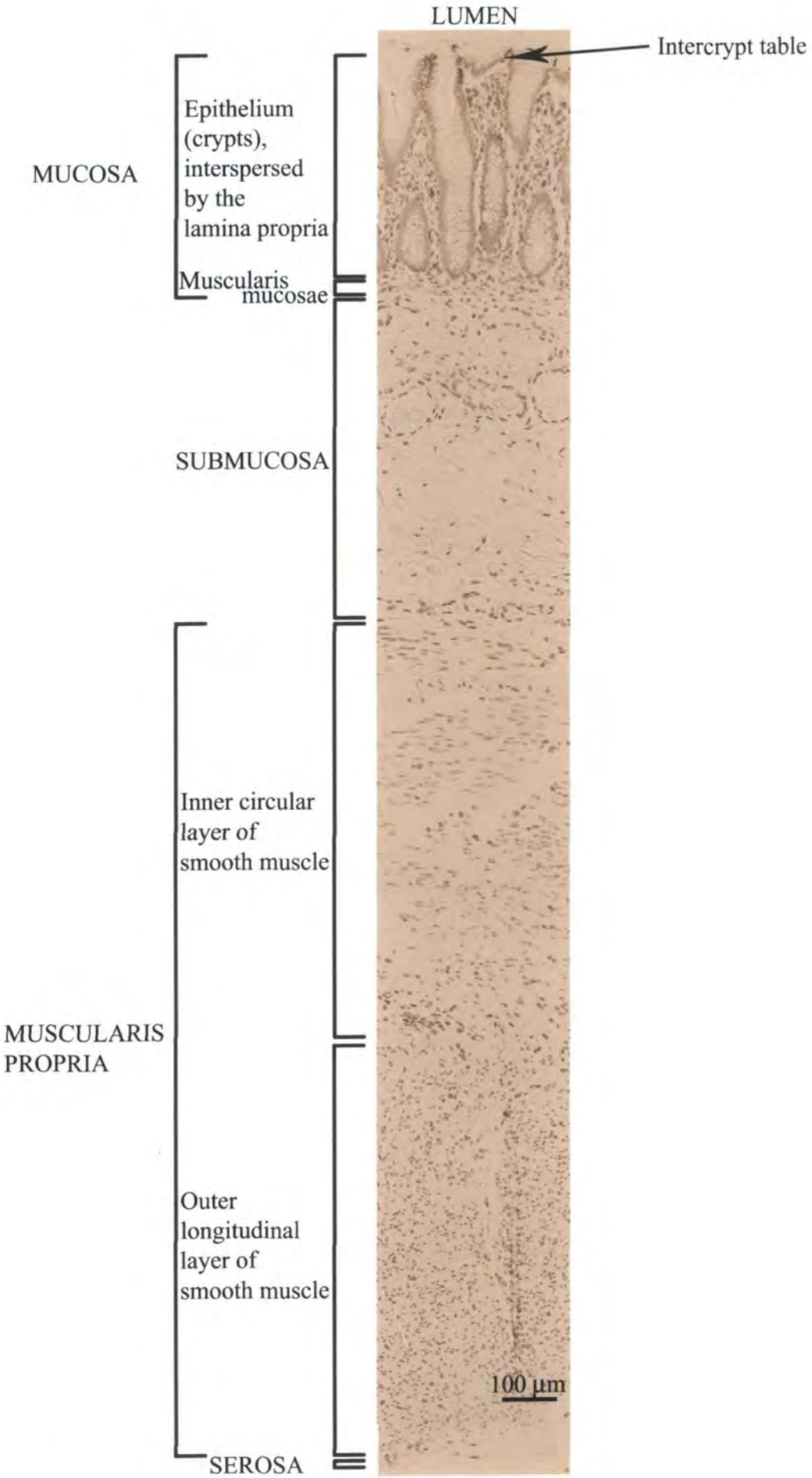


Figure 1.3 Four-layer histology of the colorectum, defined by immunoperoxidase staining with lamin A/C antibodies and counterstaining with haematoxylin.

to harbour metastatic deposits (Alden *et al.*, 1996). The most common malignancy to metastasize to the colon is malignant melanoma, although it is more likely to colonize the small intestine (Reintgen *et al.*, 1984).

### 1.2.2 Genetic control of colonic crypt topology and its implications for colorectal cancer development

Healthy colonic crypts contain three specialized cell types which are mainly concentrated in the upper third of the crypt: mucus-secreting goblet cells, absorptive enterocytes and the less abundant enteroendocrine cells which function to lubricate the passage of waste material, absorb water and salts and secrete hormones respectively (Marshman *et al.*, 2002; Potten *et al.*, 1997). Cell turnover at the intercrypt table is very high, therefore the differentiated population must be perpetually replenished by unidirectional transit amplification and lineage-specific differentiation of multipotent stem cells located in the base of the crypt (Booth and Potten, 2000; Gordon and Hermiston, 1994; Marshman *et al.*, 2002). The transition from proliferation to differentiation in healthy crypts constitutes the crypt-villus axis which is maintained by the canonical Wnt signalling pathway (**Figure 1.4**). This is considered to be the most significant regulator of normal crypt homeostasis and CRC development (Bienz and Clevers, 2000; Giles *et al.*, 2003; Pinto and Clevers, 2005; van de Wetering *et al.*, 2002).

Wnt factors are secreted glycoproteins thought to emanate in the base of intestinal crypts and / or underlying mesenchymal tissue, although their exact location has not been determined (Batlle *et al.*, 2002; Pinto and Clevers, 2005). They pervade the

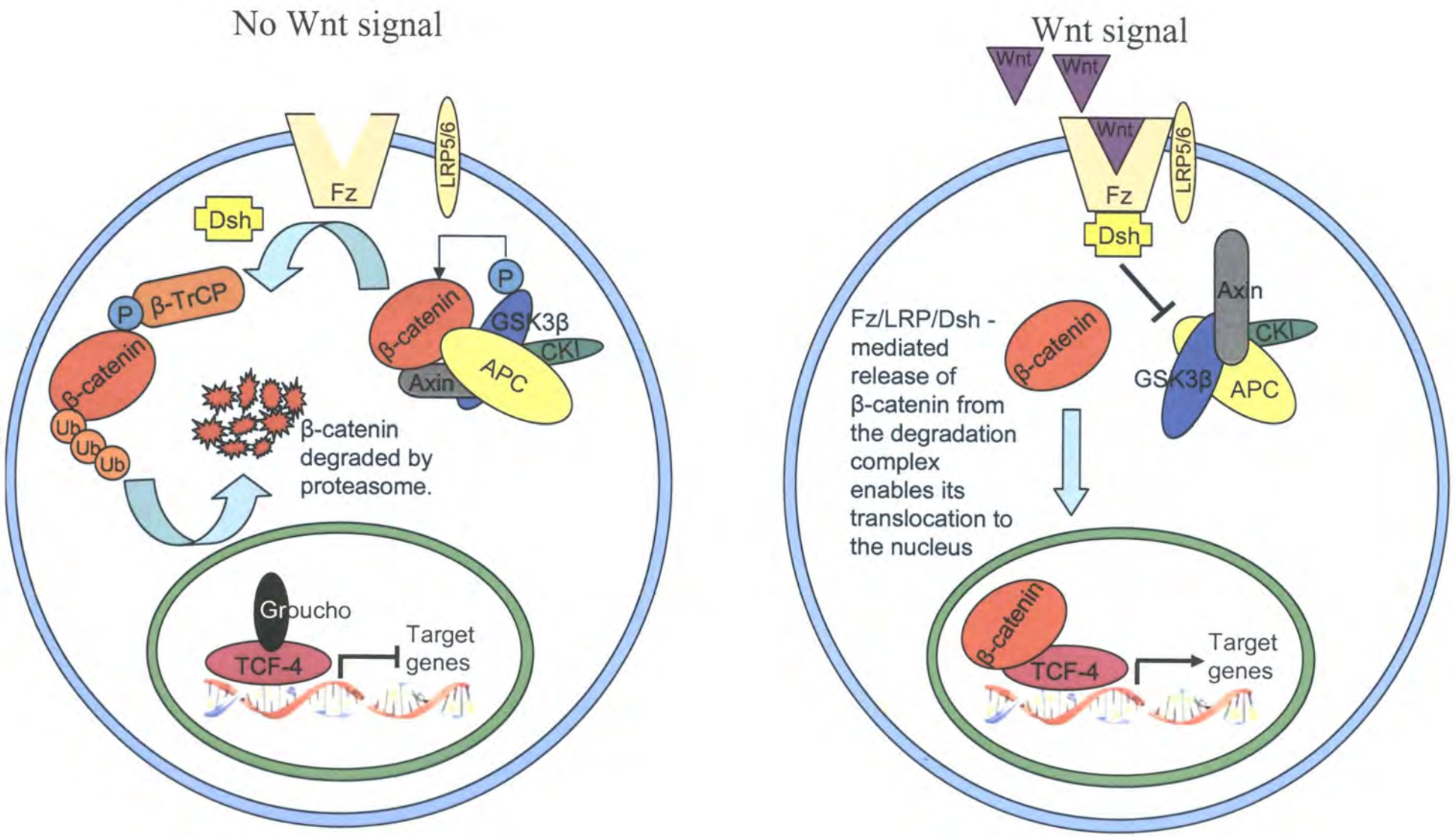


Figure 1.4 The canonical Wnt signalling pathway functional in colonic crypts.

intestinal epithelium, imposing a proliferative phenotype through Frizzled/LRP - mediated stabilization of the cytoplasmic protein, β-catenin, leading to transcription of Wnt target genes (Logan and Nusse, 2004; Pinto *et al.*, 2003; Pinto and Clevers, 2005). The process is negatively regulated by adenomatous polyposis coli (APC) (Korinek *et al.*, 1997), a key component of the multiprotein degradation complex which presents β-catenin for phosphorylation, consequently targeting it for ubiquitination by β-transducin repeat-containing protein (β-TrCP) and subsequent degradation by the proteasome in the absence of a Wnt signal (Bienz and Clevers, 2000). In addition to APC, the multiprotein degradation complex comprises a scaffold protein, Axin and two serine/threonine kinases, glycogen synthase 3β (GSK3β) and casein kinase I (CKI). Upon activation of the canonical Wnt signalling pathway [reviewed in depth by Logan and Nusse (2004)], interaction of Wnt ligands with their membrane spanning co-receptors, Frizzled (Fz) and LRP5/6, at the cell surface results in the recruitment of Axin and another protein, Dishevelled (Dsh), to the plasma membrane. Consequently, the multiprotein complex is dissociated, liberating β-catenin and leaving it free to translocate to the nucleus. When there is no Wnt signal, members of the T-cell factor / lymphoid enhancing factor (TCF/LEF) family of transcription factors are bound to the transcriptional repressor Groucho (Cavallo *et al.*, 1998). In the presence of Wnt, β-catenin overcomes this repression by direct association with TCF/LEF factors, namely TCF-4 in the colon, transactivating the transcription of genes such as c-*MYC* which represses the cell cycle inhibitor $p21^{CIP1/WAF1}$ and pushes cells from G1 to S phase of the cell cycle. Thus active β-catenin/TCF-4 complexes appear to preserve a stem cell and proliferating progenitor population in the lower crypt region which is essential for sustaining the turnover of differentiated cells at the surface (van de Wetering *et al.*, 1997; van de Wetering *et al.*, 2002).

Wnt signalling is switched off in the differentiated compartment of intestinal crypts, but appears to be re-initiated at the earliest stage of colorectal tumour development. Immunohistochemical studies have shown accumulation of β-catenin in the nucleus of aberrant crypt foci (ACF) which are the benign precursors of colorectal cancer (van de Wetering *et al.*, 2002). In addition, mutations in *APC* which constitutively activate β-catenin/TCF signalling (Korinek *et al.*, 1997; Morin *et al.*, 1997) are estimated to account for 85% of all colorectal tumours (Kinzler and Vogelstein, 1996). It has therefore been reasoned that activation of β-catenin/TCF-4 may constitute the dominant switch in the malignant transformation of colon epithelial cells by imposing a proliferative phenotype at an early stage (van de Wetering *et al.*, 2002).

### 1.2.3 Molecular basis of colorectal carcinogenesis

Colorectal carcinogenesis is a multistep process characterized by well-defined histopathological and morphological changes which have an underlying molecular basis (Fearon and Vogelstein, 1990). CRC development encompasses four distinct stages: aberrant crypt foci – adenoma – carcinoma – metastasis. In turn adenomas are subdivided into early (small), intermediate and late (large) stages. Early adenomas are also known as polyps. Malignant adenomas are termed carcinoma *in situ* (cis) or non-invasive cancer because they have yet to breach the colonic wall.

Hyperproliferation of the intestinal epithelium is the foremost preneoplastic event in CRC characterized by morphological changes in the colorectal mucosa, termed aberrant crypt foci. First identified by Bird (1987) in an animal model, ACF represent the clonal expansion of cells associated with the earliest stages of CRC in both rodent and human (Bird and Good, 2000; Roncucci *et al.*, 2000). ACF display expanded lumenal openings

and vary in histology from hyperplasia to dysplasia, although dysplastic morphology appears to be associated with increased size of ACF (Siu *et al.*, 1997). Up-regulation of β-catenin, which is essential for transducing the proliferation-driving Wnt signal, has been associated with ACF (van de Wetering *et al.*, 2002). (See Section 1.2.2 for a description of Wnt signalling.) This is most likely the result of loss or inactivation of *APC*, a tumour suppresor gene (TSG) which negatively regulates β-catenin (Korinek *et al.*, 1997). Mutations in *APC* are present only in dysplastic ACF (Jen *et al.*, 1994) and have come to be considered as the leading mutations predisposing individuals to CRC (Fodde *et al.*, 2001).

'Polyp' is a descriptive term for any elevation in the intestinal surface. They are categorized as neoplastic, hamartomatous, inflammatory (pseudopolyp) or metaplastic. Neoplastic or dysplastic polyps are considered pre-malignant lesions. Other types of polyp have the potential to become malignant, although this is not the case for metaplastic polyps in which transdifferentiation from columnar to stratified epithelium occurs (Misiewicz *et al.*, 1988). Dysplastic polyps are the first visible sign of the onset of CRC which can be diagnosed by colonoscopy or barium enema. Dysplastic polyps protrude like a mushroom stalk from the lumenal wall of the colon and develop from dysplastic ACF, therefore they are associated primarily with loss of *APC*. They can take on three forms representing increasing malignant potential: tubular (single projection only), tubulo-villous (projection with finger-like fronds) and villous (projection with multiple fronds).

Activation of the oncogene K-*ras* by somatic mutation has been associated with the development of intermediate adenomas based on the observation that the majority of adenomas greater than 1 cm in diameter exhibit mutations in *ras* (Vogelstein et al.,

1988). Progression to a large adenoma appears to require loss of the *DCC* gene, which stands for Deleted in colorectal cancer (Fearon *et al.*, 1990).

Finally the development of a full-blown carcinoma is caused by a change in one of the most ubiquitous cancer-associated TSGs, *TP53* (Nigro *et al.*, 1989). Chromosome 17p allelic losses were found to correlate with advancement of the disease and were at a maximum level in carcinomas (Vogelstein *et al.*, 1988). The tumour suppressor gene *TP53* was mapped to the common region of loss on chromosome 17p (Baker *et al.*, 1989) and is consequently considered the key genetic alteration driving the progression of a large colorectal adenoma into a carcinoma (Fearon and Vogelstein, 1990). To encapsulate this evidence a genetic model for colorectal tumourigenesis was proposed by Fearon and Vogelstein (1990). Importantly they emphasized that the pre-requisite accumulation of multiple genetic and possibly epigenetic alterations was more critical for colorectal carcinogenesis than the order of specific alterations. Furthermore, hitherto unidentified genetic alterations are required after loss of *TP53* for a carcinoma to spread to a secondary site. **Figure 1.5** highlights the key molecular alterations during the progression of CRC.

Mutations in *APC* are associated with chromosomal instability (CIN) which is a feature of both sporadic and inherited form of CRC and leads to genetic instability. A second pathway leading to genetic instability has also been identified, termed microsatellite instability (MSI) and results from defects in genes involved in the DNA mismatch repair (MMR) system. MSI is a particular feature of the hereditary form of CRC, Hereditary non-polyposis colorectal cancer (HNPCC). The effect of defective *APC* and DNA MMR genes on genetic stability in CRC is reviewed by Narayan and Roy (2003).

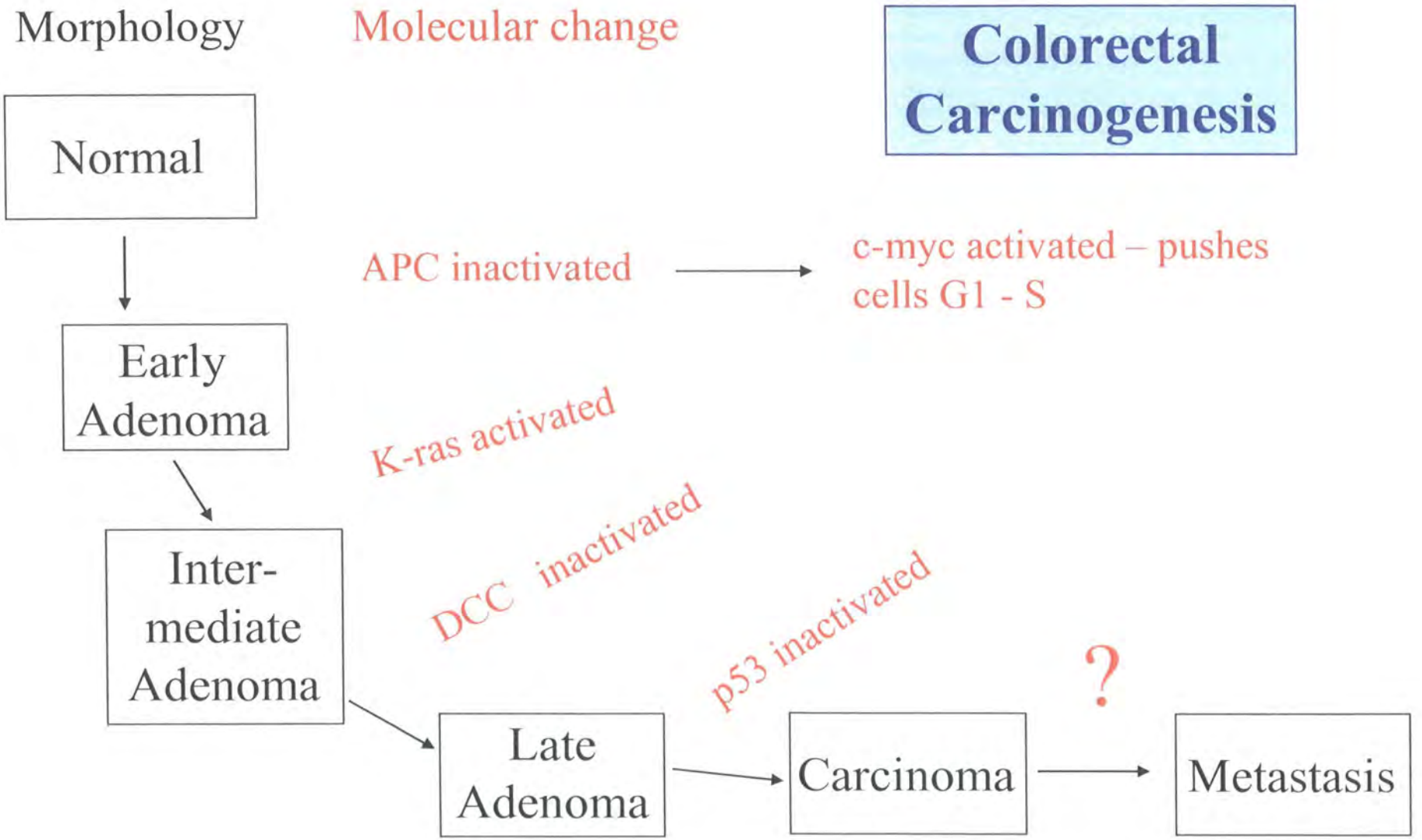


Figure 1.5 Key molecular changes during the development of colorectal cancer.

### 1.2.4 Sporadic versus familial colorectal cancer

Sporadic cases of colorectal cancer are estimated to account for 75% of all CRC cases and are strongly associated with the aged population (Toms, 2004). **Figure 1.6** illustrates the age distribution of CRC incidence. The majority (85%) of cancers are diagnosed in patients over 60 years of age. CRC causing genetic alterations are understood to start accumulating approximately 10 years prior to the development of cancer. Cases of CRC in younger individuals are likely to be the result of an inherited predisposition to the disease.

Sporadic cases of CRC are generally later onset and thought to be related to certain risk factors including diet (high fat / low consumption of fruit and vegetables) and exposure to chemicals (Potter, 1999; Terry *et al.*, 2001). Patients have two normal germ-line *APC* alleles. Somatic mutations in both *APC* alleles are required for polyps to form. Inherited cases of CRC, on the other hand, are the consequence of a genetic predisposition. Patients generally inherit a mutation in one allele of the gene and only require a somatic mutation in the other for a tumour to develop [discussed by Muller *et al.* (2000)]. Genetic predisposition greatly increases the chances of polyps forming and leads to earlier onset of the disease. Hereditary forms of the disease are autosomal dominant and categorized according to symptoms, tumour pathology and age of onset. 'Cancer families' have been identified which carry a hereditary CRC-causing mutation. The first such family to be diagnosed with hereditary bowel cancer in Britain originates from West Cornforth, County Durham (Dunstone and Knaggs, 1972). Three types of hereditary CRC syndrome are recognized and described below. In most cases the predisposing germ-line aberration has been identified.

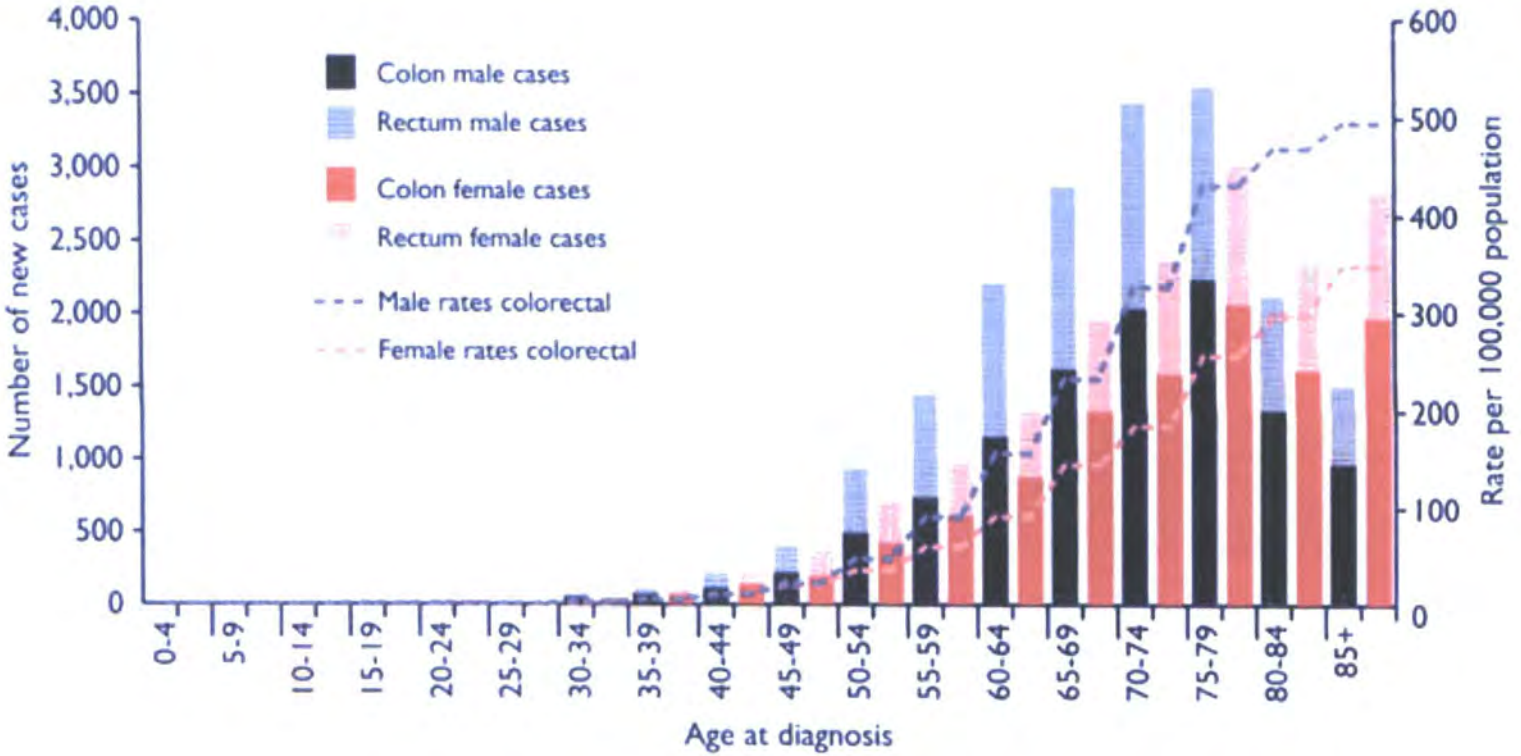


Figure 1.6 Number of new cases and rates by age and sex, colorectal cancer, UK, 2000. *Source: Toms (2004).*

### *1.2.4.1 Familial adenomatous polyposis*

Familial adenomatous polyposis (FAP) represents 0.2 – 1% of all colorectal cancers. It is easy to identify clinically because it is characterized by a colorectal mucosa which is studded with hundreds of polyps [reviewed by Muller *et al.* (2000) and de la Chapelle (2004)]. Patients with this disease have statistically a much higher chance of contracting CRC by virtue of the multiple polyps that arise. FAP is known to be caused by an inherited germ-line mutation in one *APC* allele. The most acute cases are observed when the germ-line mutation resides between codons 1250 - 1330 (Nagase and Nakamura, 1993). The unaffected *APC* allele is lost prior to adenoma appearance.

### *1.2.4.2 Hereditary non-polyposis colorectal cancer*

HNPCC accounts for 2 - 10% of all CRC cases making it the most common inherited CRC predisposition and increases a sufferers life-time risk of cancer to 80 - 85% (Aarnio *et al.*, 1995; de la Chapelle, 2004; Lynch and de la Chapelle, 1999). Also known as Lynch syndrome, affected individuals have a higher chance of contracting cancer in at least seven other organs, including endometrium, stomach, ovaries, small bowel and brain. It is caused by inactivating mutations in DNA MMR genes which enable deleterious mutations in familiar cancer genes (*APC*, K-*ras*, *TP53*) to persist (Parsons *et al.*, 1993; Thibodeau *et al.*, 1993). It differs from FAP because fewer polyps form and crypts with *APC* mutations are found side by side normal crypts without *APC* mutations.

### *1.2.4.3 Hamartomatous polyposis syndromes*

Hamartomatous polyposis can be subdivided into four separate syndromes: Cowden syndrome (CS), Bannayan-Riley-Ruvalcaba syndrome (BRR), Juvenile polyposis syndrome (JPS) and Peutz-Jeghers syndrome (PJS) (Muller *et al.*, 2000). All are characterized by the presence of gastrointestinal hamartomatous polyps and an increased risk of gastrointestinal malignancy. A germ-line mutation in the tumour suppressor gene *PTEN* has been implicated in CS, BRR and JPS (Li *et al.*, 1997; Marsh *et al.*, 1998), while germ-line mutations in serine/threonine kinases *LBK1* & *STK11* have been implicated in PJS (Hemminki *et al.*, 1998; Jenne *et al.*, 1998). *PTEN* & *STK11* mutations are rarely seen in sporadic CRC.

## 1.2.5 Clinicopathological classification of colorectal cancer

The pathologist Cuthbert Dukes studied the progression of rectal cancer in detail and classified it into distinct stages based on the extent of tumour spread (Dukes, 1932). The resulting Dukes' staging system was subsequently used to categorize colorectal tumours. Dukes' stage A tumours are localized to the bowel; stage B tumours extend through the colonic wall, i.e. they breach the serosa; stage C tumours show evidence of regional lymph node invasion as well as mural invasion; stage D was added later by Turnbull *et al.* (1967) and indicates that secondary deposits have been found. Dukes' C tumours can be further subdivided according to the extent of lymph node invasion. C1 tumours are positive only in perirectal nodes; C2 tumours show positive invasion of nodes at the point of mesenteric blood vessel ligature (Gabriel *et al.*, 1935).

Dukes' staging of colorectal tumours is still used routinely, although the TNM method of tumour identification, last modified in 1997 (AJCC, 1997), is often used in conjunction with the Dukes' system because it is more precise. The TNM staging system categorizes tumours according to depth of migration through the histological layers of the colon (T), the number of lymph nodes involved (N) and the presence of distant metastses (M).

One other staging system exists for the classification of CRC, the Astler-Coller (AC) staging system (Astler and Coller, 1954). It has elements which liken it to both the Dukes' and TNM systems and describes both extent of mural invasion and lymph node involvement. AC stage A tumours are limited to the mucosa, stage B1 tumours remain within the boundaries of the serosa, while B2 tumours have begun to invade extra-colonic tissues. Stage C1 and C2 are stage B1 and B2 tumours respectively, but with nodal metastases.

Although the Dukes' staging system has undeniably been of great benefit in diagnosing patients, it has been in use for the best part of a century and does not accurately predict prognosis or response to therapy. Ideally a staging system based on the molecular characteristics of the disease is required which may enable earlier diagnosis, tailored therapy and more accurate predictions of patient survival.

### 1.3.1 The nuclear envelope

The eukaryotic cell is characterized by compartmentalization into two distinct regions: the nucleus and the cytoplasm. The nucleus is demarcated by a double membrane structure, termed the nuclear envelope, punctuated by nuclear pore complexes (NPCs) [reviewed by Franke *et al.* (1981), including an historical perspective]. This results in the physical separation of genetic material and the transcriptional apparatus, which reside in the nucleus, from other organelles and the process of translation which occurs in the cytoplasm. The major architectural components of the nucleus are shown in **Figure 1.7** (not to scale).

The outer nuclear membrane (ONM) represents the cytoplasmic face of the nuclear envelope and is physically and functionally continuous with the endoplasmic reticulum (ER). The inner nuclear membrane (INM) faces the nucleoplasm. Together they enclose a lumenal or perinuclear space, thereby creating a dynamic structure estimated to be 30 nm in width (Franke *et al.*, 1981; Gerace and Burke, 1988). The perinuclear space may provide an optimal environment for signal transduction between the nucleus and the cytoplasm (Sullivan *et al.*, 1993). In higher eukaryotes or metazoans a proteinaceous network, termed the nuclear lamina (NL), underlines the INM on the nucleoplasmic surface (Gerace, 1986; Gerace and Burke, 1988) and is composed of filamentous units known as lamins (Aebi *et al.*, 1986; Gerace and Blobel, 1980). Since they were first observed in rat liver lamina (Gerace *et al.*, 1978) several functions have been ascribed to lamin polypeptides including: Provision of mechanical support, organization of interphase chromatin and regulation of DNA replication, cell cycle progression, nuclear

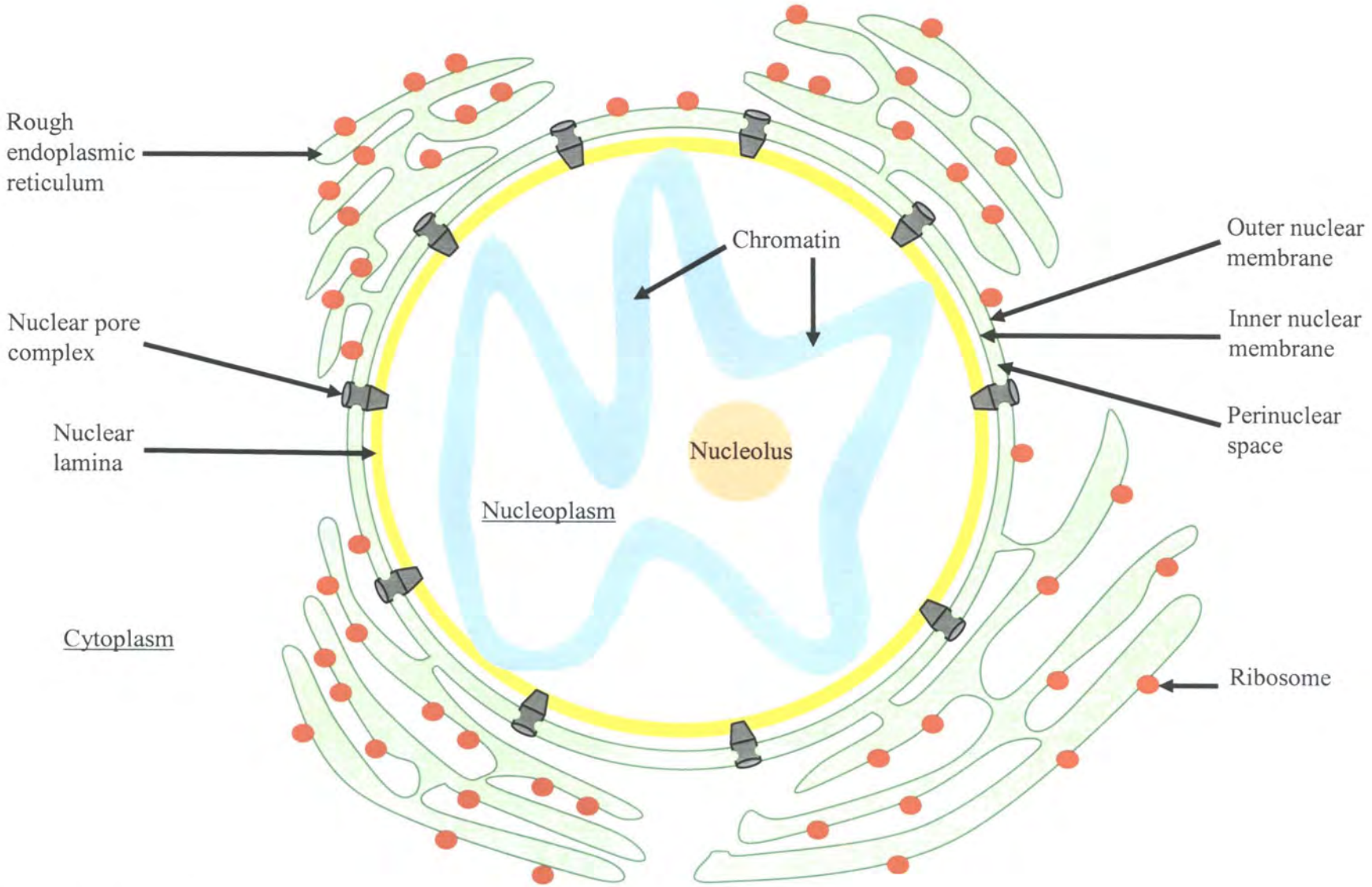


Figure 1.7 The major structural components of the metazoan nucleus.

shape and size, differentiation, transcription and apoptosis [reviewed by Gruenbaum *et al.* (2003) and Hutchison (2002)].

### 1.3.2 The nuclear lamina

The NL was first isolated from rat liver nuclei (Dwyer and Blobel, 1976) and has been reported to vary in thickness between 10 - 100 nm (Aaronson and Blobel, 1975; Dwyer and Blobel, 1976; Fawcett, 1966; Hoger *et al.*, 1991; Scheer *et al.*, 1976). Stabilization of the nuclear lamina is mediated though interactions with various integral membrane proteins of the INM. The best characterized binding partners of lamins are lamina-associated proteins (LAPs), emerin, MAN1 and lamin B receptor (LBR) (Hutchison, 2002).

Nuclear lamins are classified as type V intermediate filaments based on similarities in secondary structural organization and striking sequence homology to the characteristic α-helical rod domain of intermediate filaments (Fisher *et al.*, 1986; McKeon *et al.*, 1986). Intermediate filaments (IFs) in conjunction with microfilaments and microtubules, which are two other distinct filament systems, provide an architectural scaffold within eukaryotic cells (Herrmann and Aebi, 2000). IFs in particular are considered to be mechanical integrators of cellular space (Lazarides, 1980).

The common secondary structure of intermediate filaments comprises a non-helical amino-terminal (N-terminal) head domain and a carboxy-terminal (C-terminal) tail domain positioned either side of a central coiled-coil α-helical domain (rod). The rod domain is further subdivided into four helical regions, termed 1A, 1B, 2A and 2B, characterized by heptad repeats and separated by three non-helical linker segments

(Fuchs and Weber, 1994). Compared to vertebrate cytoplasmic IFs, lamins possess an extended rod domain by virtue of a 42 amino acid (six heptad repeat) insertion within coil 1B (Erber *et al.*, 1998) and a shorter head domain (Fisher *et al.*, 1986). To facilitate targeting of lamins to the nucleus they harbour a nuclear localization signal (NLS) in their tail domain (Loewinger and McKeon, 1988) and most lamins (except lamin C) have a C-terminal CAAX motif (C, cysteine; A, any aliphatic residue; X, any amino acid) which is important for localization at the INM (Nigg, 1992).

Upon reviewing the literature it would appear that the more complex the organism, the more lamin genes and splicing isoforms it possesses. A single lamin (LMN-1) has been identified in nematodes (*Caenorhabditis elegans*) (Liu *et al.*, 2000), two lamin sub-types (Dm0 and lamin C) have been reported in arthropods (*Drosophila melanogaster)* (Bossie and Sanders, 1993; Gruenbaum et al., 1988; Riemer et al., 1995), three in birds (Lehner *et al.*, 1987) and five in amphibians (Benavente *et al.*, 1985; Hofemeister *et al.*, 2002; Stick, 1988). Seven lamins have been identified in mammalian cells. They are categorized into two groups, A-type and B-type, based on their biochemical properties (i.e. isoelectric point), ultrastructural characteristics and mitotic fate (Gerace and Blobel, 1980; Gerace *et al.*, 1984; Gerace and Burke, 1988).

Lamins A, AΔ10, C and C2 are A-type and are alternatively spliced products of the *LMNA* gene (Fisher *et al.*, 1986; Furukawa *et al.*, 1994; Machiels *et al.*, 1996; McKeon *et al.*, 1986) located at chromosome 1q21.1 – 21.3 (Lin and Worman, 1993; Wydner *et al.*, 1996). Lamins B1, B2 and B3 are B-type. Lamin B1 is the only product of *LMNB1*, located at chromosome 5q23.3 – 31.1 (Lin and Worman, 1995; Wydner *et al.*, 1996); while both lamins B2 and B3 are alternatively spliced products of *LMNB2* (Furukawa and Hotta, 1993), chromosome locus 19p13.3 (Biamonti *et al.*, 1992). Both lamin C2

and B3 have only been detected in male germ cells (Furukawa and Hotta, 1993; Furukawa *et al.*, 1994). Consequently lamins A, C, AΔ10, B1 and B2 are important in somatic cells.

The *LMNA* gene is composed of twelve exons. Codon 566, situated in exon 10, constitutes the alternative splice site for prelamin A and lamin C and gives rise to the 3'-most amino acid common to both lamin A and lamin C (Lin and Worman, 1993). Codons 567 to 572 follow on from codon 566 and are lamin C-specific. Lamin C terminates at the amino acid encoded by codon 572. For prelamin A the remaining 743 nucleotides of exons 11 and 12 adjoin the 3'-end of codon 566, making exons 11 and 12 lamin A-specific. Lamin AΔ10 retains the lamin A-specific tail domain, but is missing all 30 amino acids (90 nucleotides) encoded by exon 10 (Machiels *et al.*, 1996). Thus lamin A, lamin C and lamin AΔ10 only differ in the sequence of their tail domains. Alternative splicing of the *LMNA* gene is diagrammatically represented in **Figure 1.8** (not to scale).

The main difference between A-type and B-type lamins is that A-type are developmentally regulated and synthesis appears to accompany cellular differentiation, whereas B-type are believed to be essential for cell survival because at least one B-type lamin is expressed at every point of development (Broers *et al.*, 1997; Coates *et al.*, 1996; Lebel *et al.*, 1987; Lehner *et al.*, 1987; Paulin-Levasseur *et al.*, 1989; Rober *et al.*, 1989; Stewart and Burke, 1987; Stick and Hausen, 1985).

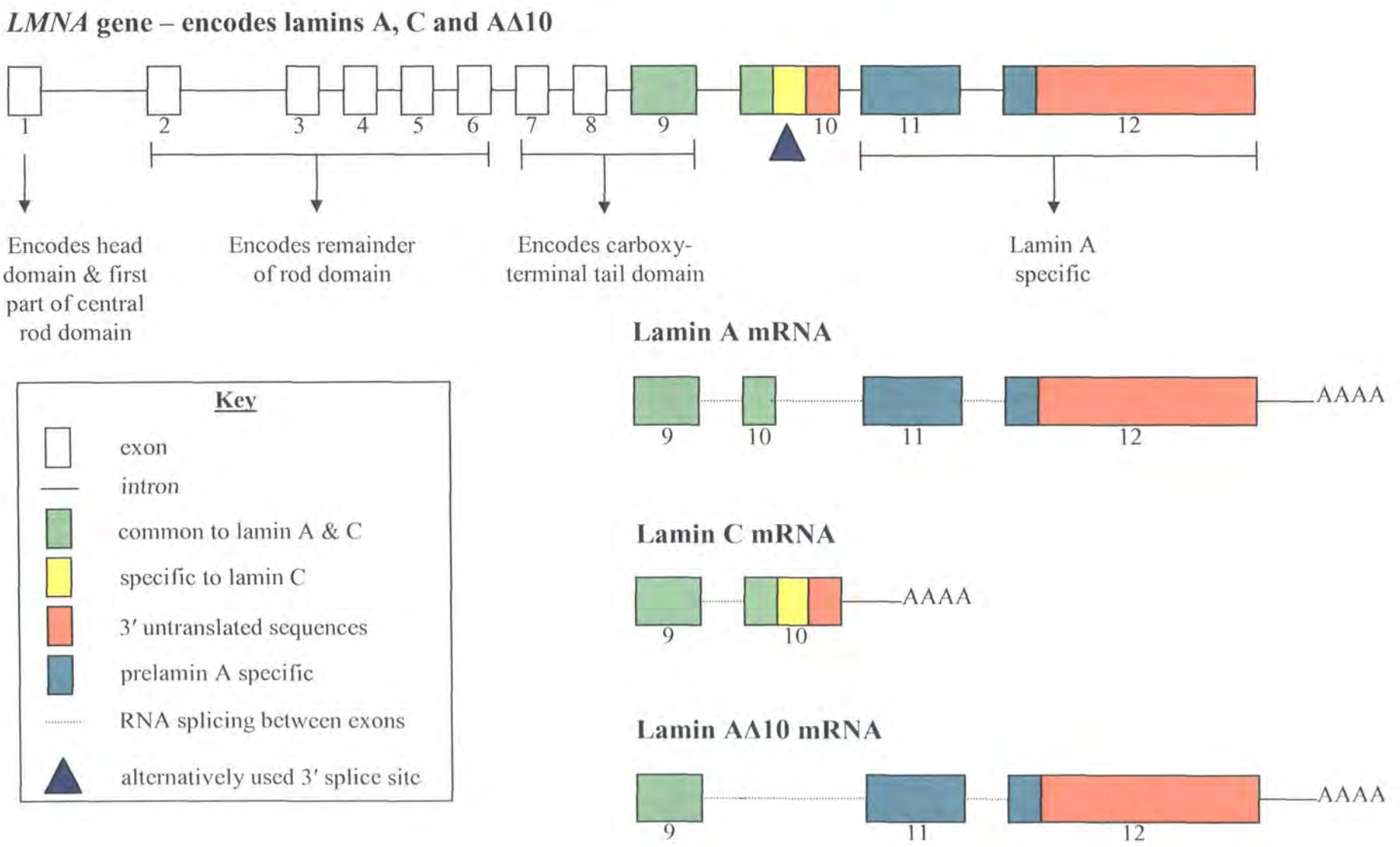


Figure 1.8 Splice variants of the *LMNA* gene.

### 1.3.3 Dynamic behaviour of the nuclear envelope

Vertebrate cells undergo open mitosis which is accompanied by complete, but reversible dissassembly of the nuclear membranes, the nuclear lamina and NPCs. Signs of disassembly are first observed at prometaphase (Georgatos *et al.*, 1997). Components are reassembled in a co-ordinated, step-wise process in late anaphase / telophase (Chaudhary and Courvalin, 1993).

Nuclear envelope dynamics have been investigated in the *Xenopus* cell-free system. Studies by Vigers and Lohka (1991) suggested that nuclear envelope components become vesicularized upon NE disintegration as NE protein-enriched vesicles were assembly competent. Groups such as Drummond *et al.* (1999) have further extended this idea by charting the progress of NE assembly by immunolabelling specific markers of two distinct vesicle populations, known as NEP-A and NEP-B, which appear to be NE precursors. Temporal and functional differences between NEP-A and NEP-B vesicles were determined. NEP-B were recruited first to chromatin and bound to it. The arrival of NEP-A vesicles followed. While NEP-A were unable to bind chromatin, they possessed fusogenic properties and appeared to support the expansion of the NE by fusing to NEP-B vesicles. Recruitment of NE precursor vesicles seems to be triggered by the association of NPC proteins with chromatid surfaces (Belgareh *et al.*, 2001; Bodoor *et al.*, 1999).

Whether vesicularization of NE components occurs *in vivo* has been called into question as a result of studies in somatic systems (mammalian culture cells) which have reported dispersal of NE proteins in the ER in metaphase (Ellenberg *et al.*, 1997; Yang *et al.*, 1997). However, what does seem clear is that NE disassembly is regulated by

phosphorylation of both nuclear membrane and lamin proteins and accompanied by mechanical disruption. During prophase the minus-end-directed microtubule associated motor protein dynein translocates the mitotic spindle which is cross-linked to invaginated regions of the nuclear membrane via centrosomes. This physically tears apart the lamina and nuclear membranes, a process completed by metaphase (Beaudouin *et al.*, 2002; Salina *et al.*, 2002).

The NL itself plays an important role in the breakdown and reassembly of the NE. The integrity of the NL is heavily dependent on the phosphorylation status of individual lamin polypeptides (Ottaviano and Gerace, 1985). Dephosphorylation of the NL concomitant with NE disassembly appears to be regulated primarily by the maturation promoting factor (MPF), a $p34^{cdc2}$ kinase / cyclin B complex activated early in mitosis, but also by other protein kinases such as protein kinase C (Collas *et al.*, 1997; Dessev *et al.*, 1991). Phosphorylation of serine residues close to the lamin rod domain drives lamin polymer assembly (Dessev *et al.*, 1991; Peter *et al.*, 1990; Ward and Kirschner, 1990).

The mitotic fate of A-type and B-type lamins was originally thought to be quite distinct. Gerace and Blobel (1980) were the first to report that lamins A and C were solubilized and not associated with membrane fractions in mitotic cells, whereas lamin B was insoluble. Lamin B was predicted to remain associated with membrane fragments upon nuclear disassembly as disruption of membranes with detergent resulted in almost complete solubilization of lamin B. Similar observations were made in chicken (Stick *et al.*, 1988). More recent investigations have proposed that both A- and B-type lamins become soluble upon depolymerization of lamin polymers (Beaudouin *et al.*, 2002; Daigle *et al.*, 2001).

By contrast reformation of the NL follows dephosphorylation of individual components. Clear temporal variation in the recruitment of lamin sub-types to decondensing chromosomes at the end of mitosis has been demonstrated, although the exact timing of these events is still a matter of debate. Independent of their fate upon onset of mitosis, B-type lamins are the first to be incorporated into an organized polymeric meshwork at the nuclear periphery (Moir *et al.*, 2000a; Moir *et al.*, 2000b). They are rendered functional by post-translational modifications. Permanent farnesylation of the cysteine residue in their very C-terminal isoprenylation signal, the CAAX motif; subsequent endoproteolytic cleavage of the AAX tripeptide and carboxymethylation of the terminal cysteine appears to facilitate anchorage to the INM and interaction with integral proteins of the INM, such as LBR (Farnsworth *et al.*, 1989; Firmbach-Kraft and Stick, 1993; Sobotka-Briner and Chelsky, 1992). Studies completed so far have not led to conclusive agreement regarding the exact timepoint at which B-type lamins start accumulating at the nuclear periphery, but they are believed to localize at some point between late anaphase and late telophase / cytokinesis (Daigle *et al.*, 2001; Moir *et al.*, 2000b). Incorporation of B-type lamins into the NL is regulated by the activity of protein phosphatase 1 (PP1) which is dependent on binding to the membrane associated protein AKAP149 (Steen and Collas, 2001).

By following the progress of GFP-tagged nuclear lamins, it has been determined that A-type lamins do not migrate to the nuclear periphery until the end of cytokinesis when the entire NE has been fully reconstituted (Broers *et al.*, 1999) and appear to persist in the nucleoplasm in a soluble form for a few hours into G1 phase of the cell cycle (Moir *et al.*, 2000b). A-type lamins are considered non-essential for NE assembly because they are absent at the earliest stages of development, but their importance in maintaining a proper functioning nucleus is underlined by a growing number of diseases which are

the result of specific mutations in *LMNA* or lamin A/C interacting proteins. Lamin A specifically is synthesized initially as a precursor molecule, termed prelamin A. It undergoes similar processing to B-type lamins inside the nucleus, except a further 15 amino acids are removed from the carboxy terminus (Sasseville and Raymond, 1995; Sinensky *et al.*, 1994; Weber *et al.*, 1989). Isoprenylation of the CAAX box is a pre-requisite for all other processing steps (Sinensky *et al.*, 1994). It appears that prelamin A is assembly competent when isoprenylation activity is artificially suppressed, but under normal circumstances lamin A is converted into a mature form within four hours and the lamin A precursor molecules are restricted to intranuclear foci (Sasseville and Raymond, 1995).

Thus the skeleton of the NL is first outlined by a lattice arrangement of lamins B1 and B2 which is fleshed out by subsequent incorporation of A-type lamins which is entirely dependent on the prior organization of B-type lamin filaments (Dyer *et al.*, 1999; Moir *et al.*, 2000b).

#### *1.3.3.1 Lamin filament assembly*

Models of NL assembly have been proposed and modified over the past two decades based on both *in vitro* and *in vivo* observations. The formation of lamin filaments is thought to result from the following series of sequential steps. First, parallel unstaggered coiled-coil dimers are formed involving the α-helical central rod domain, similar to cytoplasmic IF assembly (Aebi *et al.*, 1986; Heitlinger *et al.*, 1991; Heitlinger *et al.*, 1992). Subsequently, lamin dimers associate head-to-tail, but unlike vertebrate cytoplasmic IFs, they extend longitudinally to form long protofilaments before making lateral associations. *In vitro*, lateral growth of protofilaments results in the formation of

paracrystals with a 24 – 25 nm transverse banding repeat. This has been interpreted to represent anti-parallel, half-staggered associations of lamin head-to-tail polymers (protofilaments) which give rise to ~10 nm wide mature filaments. The organization of these filaments was first observed in *Xenopus* oocytes where they were arranged into a two-dimensional orthogonal lattice with an average crossover spacing of 52 nm (Aebi *et al.*, 1986; Goldberg *et al.*, 1999; Heitlinger *et al.*, 1991; Heitlinger *et al.*, 1992; Moir *et al.*, 1991; Stuurman *et al.*, 1998).

In 2001, Hutchison and co-workers (Hutchison *et al.*, 2001) proposed a model by which lamins A and C are incorporated into the NL once B-type lamins have associated with the INM. Lamin C does not possess an isoprenylation signal, therefore it was suggested that it becomes incorporated into the lamina on the back of lamin A. The group proposed that lamin A and lamin C form anti-parallel, half-staggered tetramers which then make head-to-tail associations with lamin B tetramers which are already arranged subjacent to the INM. Subsequently, Vaughan *et al.* (2001) reported that lamin C and emerin are dependent on lamin A for localization at the NE. The presence of lamin C and emerin may be essential to stabilize the NL as emerin's interaction with the NL is destabilized in the absence of lamin C (Vaughan *et al.*, 2001).

### 1.3.4 Functions of the nuclear lamina

#### *1.3.4.1 Structural organization of the nuclear envelope and DNA replication*

Increased awareness of the process of NL formation during NE assembly has greatly enhanced our understanding of the functions of the NL. First of all, the NL is essential

for the organization of the nuclear envelope. Using a cell-free system based around the mitotic components of Chinese hamster ovary cells, Burke and Gerace (1986) reported inhibition of NE formation after immunological depletion of the lamin complement. Dabauvalle *et al.* (1991) made a similar connection between lamin activity and NE assembly. Benevente and Krohne (1986) reported that lamin-depleted nuclei were also unable to decondense chromatin and reform nucleoli, rendering the nucleus structurally and functionally incompetent.

However, some researchers have found that the NE can reform in the absence of a lamin pool, but observed that cells depleted of functional B-type lamins could not support DNA replication (Meier *et al.*, 1991; Newport *et al.*, 1990). Goldberg *et al.* (1995) provided the first direct evidence that lamins influence DNA replication. Upon addition of purified lamin B3 (Liii) to depleted extracts in the *Xenopus* nuclear assembly system, they observed that DNA replication was reinitiated. Nevertheless, it is clear that the absence of a functional lamina leads to extreme mechanical fragility of the NE (Liu *et al.*, 2000; Newport *et al.*, 1990) resulting in nuclear deformities, such as invaginations and herniations and a much reduced resistance to physical pressure (Broers *et al.*, 2004).

Localization of lamins to the nuclear periphery is also believed to be important for the assembly and spatial organization of NPCs (Lenz-Bohme *et al.*, 1997; Liu *et al.*, 2000; Stuurman *et al.*, 1998) and more specifically the recruitment of nucleoporin NUP153 (Smythe *et al.*, 2000), one of the proteins making up the terminal ring of the nuclear pore basket [reviewed by Bagley et al. (2000)].

### *1.3.4.2 Role for lamins in apoptosis and nuclear migration*

In the context of this study it is very interesting that a role for nuclear lamins has been proposed in the regulation of apoptosis, the programming of nuclear migration and the regulation of gene transcriptional activity – all functional targets in cancer. I will briefly explain the current position regarding lamin involvement in apoptosis and nuclear migration before concentrating on the functional consequences of lamin influence on interphase chromatin in Section 1.3.4.3.

Classic morphological features of apoptosis including chromatin condensation, clustering of NPCs and membrane blebbing are also seen in lamin-deficient nuclei (Sullivan *et al.*, 1999; Tzur *et al.*, 2002). In vertebrates, caspase induced cleavage of lamins appears to be one of the earliest events in apoptosis and thus constitutes a critical and possibly rate-limiting step which precedes DNA fragmentation (Rao *et al.*, 1996; Takahashi *et al.*, 1996) and degradation of other INM-associated proteins (Buendia *et al.*, 2001; Duband-Goulet *et al.*, 1998).

Morphological changes in nuclear shape and size, plus translocation of nuclei from a basal to apical position are classic features of colorectal epithelial dysplasia. The degree of nuclear migration correlates with malignant potential. During the normal development of *C. elegans* nuclear migration has been associated with microtubule-lamina connections mediated by SUN (sad1 / UNC-84 homology) domain proteins that traverse the double membrane structure of the NE (Lee *et al.*, 2002; Starr *et al.*, 2001). The microtubule network and corresponding motor proteins responsible for nuclear positioning exist in the cytoplasm, therefore SUN domain proteins are emerging as one of two candidate groups of nuclear membrane-associated proteins (the other group

being the spectrin-repeat proteins, nesprins) predicted to mediate influence of the NL on cytoarchitechture. In *C. elegans*, two SUN domain proteins - UNC-84 (which associates with the INM and colocalizes with Ce-lamin) and UNC-83 (which is located at the ONM) - are predicted to interact within the perinuclear space of the NE (Gruenbaum *et al.*, 2005; Starr *et al.*, 2001). UNC-84 is expected to interact with or initiate a signalling cascade which modifies the cytoplasmic microtubule network resulting in nuclear migration (Lee *et al.*, 2002). Certainly, further work is required to elucidate all the components regulating nuclear migration in *C. elegans* and to confirm a similar relationship in mammalian cells. In mammals only one SUN domain protein has been described so far, UNC-84/Sun. It is anticipated that UNC-84 may form a bridge linking nesprin-2 molecules which localize to both the nucleoplasmic and cytoplasmic faces of the NE, thereby co-ordinating a functional link between lamin A/C, nesprin and actin (Libotte *et al.*, 2005).

#### *1.3.4.3 Role for lamins in the regulation of transcription*

Lamins appear to affect gene transcription through interaction with transcriptional machinery, chromatin or transcriptional repressors. Lamins do not always bind directly to transcriptional regulatory complexes or transcription factors, but may influence transcription indirectly through interactions with their binding partners which either associate with chromatin or with class II nuclear components.

The main lamin-interacting proteins integral to the INM are the so-called LEM domain proteins [LAP2, Emerin and MAN1], although interaction between lamins and MAN1 has not been determined. [See Foisner (2001) for a diagrammatic representation of lamin interactions at the INM and with peripheral heterochromatin.] The LEM domain

is a characteristic 43 amino acid sequence in the N-terminal domain of these proteins (Cohen *et al.*, 2001). Seemingly independent of lamins, LAP2β interacts with chromatin via BAF (barrier-to-autointegration factor) and its LEM domain (Furukawa, 1999). It also binds the transcription factor GCL (germ-cell-less), a peripheral INM protein, and represses activity of the E2F-DP transcriptional complex, known to be under tight control by the retinoblastoma protein (pRb) in G1 phase of the cell cycle (Nili *et al.*, 2001). The LAP2α isoform is one of only two LAP2 sub-types out of a total of six currently recognized which do not integrate into the INM (Berger *et al.*, 1996; Dechat *et al.*, 1998). It binds chromatin and targets lamin A/C to intranuclear sites during interphase where the two proteins form tight complexes and have consequently been implicated in the structural organization of the nucleus (Dechat *et al.*, 1998; Dechat *et al.*, 2000). Hence it is conceivable that changes in lamin A/C activity could be reflected in chromatin modification by LAP2α.

Emerin probably represents one of the most interesting integral membrane protein targets of lamin A/C. It binds to both lamin A/C and BAF (Lee *et al.*, 2001), constituting a functional link with chromatin. Its localization to the INM is highly sensitive to the availability of lamin A polymers (Vaughan *et al.*, 2001) and it is redistributed to the cytoplasm, presumably the ER when the lamina is not properly formed (Gruenbaum *et al.*, 2002). Additionally, mutations in the *STA* gene which encodes emerin cause the muscle wasting disease X-linked Emery-Dreifuss muscular dystrophy (Bione *et al.*, 1994) which exhibits very similar clinical features to autosomal dominant Emery-Dreifuss muscular dystrophy which is caused by mutations in *LMNA* (Bonne *et al.*, 1999). Other class II nuclear proteins also interact with lamins, including LBR which binds lamin B (Ye *et al.*, 1997) and LAP1 proteins which bind all lamin sub-types (Foisner and Gerace, 1993).

In the context of cancer biology, the reported interaction between pRb and lamin A is particularly noteworthy and suggests a mechanism by which A-type lamins may promote tumour development. Hypophosphorylated pRb represses transcription of genes necessary for G1 - S phase transition and activates genes which promote differentiation by negatively regulating the activity of E2F transcriptional complexes (Chellappan *et al.*, 1991; Korenjak and Brehm, 2005). Lamin A/C in complex with LAP2α was found to interact with hypophosphorylated pRb via pocket C of pRb, thus tethering pRb at the nuclear periphery during G1 phase of the cell cycle (Markiewicz *et al.*, 2002). Evidence suggests that nuclear anchorage of pRb is essential for its appropriate function because deletion mutants in pocket C of pRb are no longer tethered to the nucleus and have been shown to have oncogenic properties (Mittnacht and Weinberg, 1991).

Finally, lamins also appear to regulate gene transcription by modulating RNA synthesis. Addition of headless lamin A to BHK cells or transcriptionally active *Xenopus* nuclei caused disintegration of the NL and specifically abrogated the activity of RNA polymerase II (Spann *et al.*, 2002). The dissolved units of the NL formed nuclear foci which sequestered some transcription factors. Splicing factors were redistributed into unrelated nuclear speckles.

### 1.3.5 Lamins in disease

In recent years lamin A/C has been found to be responsible for a plethora of human genetic disorders which generally display tissue-specific phenotypes and are collectively known as the laminopathies. These diseases can be subdivided into the following groups: Those that primarily affect striated muscle - muscular dystrophies and

cardiomyopathies; those that primarily affect fat distribution - the lypodystrophies; those that affect bone formation; those that predominately affect nerve conduction and lastly, the premature ageing syndromes. No disease has so far been reported to be caused by mutations in *LMNB1* or *LMNB2*, possibly reflecting an essential role in cell survival (Gruenbaum *et al.*, 2005).

### *1.3.5.1 Diseases affecting striated muscle*

#### 1.3.5.1.1 Emery-Dreifuss muscular dystrophy (EDMD)

Three inherited forms of EDMD are recognized, an autosomal dominant (AD) form, an autosomal recessive form and an X-linked (XL) form. Both the autosomal forms are the result of mutations in the *LMNA* gene (Bonne *et al.*, 1999; Raffaele Di Barletta *et al.*, 2000), whereas the X-linked form arises through loss-of-function mutations in emerin (Wulff *et al.*, 1997), an integral protein of the INM. Both autosomal dominant and X-linked forms of the disease display a similar triad of clinical features, including early contractures of the elbows, Achilles tendons and posterior cervical muscles; progressive weakness and wasting of skeletal muscles, particularly humeral and peroneal muscles; and cardiac conduction defects (cardiomyopathy) which can result in sudden heart failure and therefore represent the most life-threatening clinical feature of the disease (Dreifuss and Hogan, 1961; Emery and Dreifuss, 1966; Miller *et al.*, 1985).

The locus for AD-EDMD was mapped to chromosome 1q11-q23, a region which contains the *LMNA* gene, in a large French pedigree. Mutations in the *LMNA* gene co-segregated with the disease in five families. Consequently, this became the first

inherited disorder to be explained by mutations in a component of the nuclear lamina, namely lamin A/C (Bonne *et al.*, 1999). Mutations in the head, rod and tail domain of *LMNA* have been identified in AD-EDMD patients (Raffaele Di Barletta *et al.*, 2000). Only one case of EDMD has been reported to involve both *LMNA* alleles (Raffaele Di Barletta *et al.*, 2000). The patient experienced severe muscle wasting and contractures, although there were no cardiac abnormalities.

The X-linked form of Emery-Dreifuss muscular dystrophy, a recessive disease with 100% penetrance in the second / third decade of life was first reported by Dreifuss and Hogan (1961) and later by Emery and Dreifuss (1966). The locus responsible for inheritance of XL-EDMD was mapped to chromosome region Xq28 (Bione *et al.*, 1993). This region contained the *STA* gene (now also known as the *EMD* gene) which encodes emerin, a protein comprised of 254 amino acids and recognized as a 34 kDa product on a western blot (Manilal *et al.*, 1996). Unique mutations in the emerin gene were found in five XL-EDMD patients resulting in loss or truncation of the protein (Bione *et al.*, 1994). Further mutations in emerin were identified by Wulff *et al.* (1997) at novel locations along the gene, therefore it appears that mutations in emerin are widely distributed and there is no particular hot spot. However, the majority of mutations in emerin are associated with the lamin A binding domain and are known to disrupt emerin – lamin A interaction (Lee *et al.*, 2001). Perhaps this explains the weakened interaction of mutant emerin with the nuclear lamina (Ellis *et al.*, 1999). A role for emerin as a nuclear membrane anchorage element was proposed by Cartegni *et al.* (1997). Immunofluoresence studies have shown positive emerin staining is localized to the nuclear membrane in normal tissues, similar to that of lamin A (Manilal *et al.*, 1996; Manilal *et al.*, 1999; Nagano *et al.*, 1996). However, emerin is noticeably absent from skeletal and cardiac muscle in XL-EDMD patients (Nagano *et al.*, 1996).

#### 1.3.5.1.2 Limb girdle muscular dystrophy 1B (LGMD-1B)

LGMD-1B is another autosomal dominant syndrome associated with progressive muscle weakness and cardiac conduction defects (van der Kooi *et al.*, 1996). Symmetrical weakness in proximal lower-limb muscles begins before the age of 20 years, progressing to the upper-limb muscles at about 30 – 40 years of age. Overall the phenotype is milder than EDMD with a much reduced occurrence of contractures. Similar to EDMD, cardiological abnormalities are the most life-threatening clinical manifestation of the disease. The disorder was linked to chromosome 1q11-q21 (van der Kooi *et al.*, 1997) and mutations in *LMNA* were subsequently identified as the causative lesion upon genetic analysis of three LGMD-1B families (Muchir *et al.*, 2000).

#### 1.3.5.1.3 Dilated cardiomyopathy-1A (CMD-1A)

Dilated cardiomyopathies per se affect cardiac function and show minimal skeletal muscle involvement (Olson and Keating, 1996). Sudden heart failure is the primary cause of death. The familial form of the disease (i.e. CMD-1A) is inherited in an autosomal dominant pattern and is characterized by the onset of cardiac conduction defects in the third or fourth decade of life. Mutations in the *LMNA* gene account for the autosomal dominant form and occur predominantly within the coiled-coil regions 1A and 1B of the rod domain (Brodsky *et al.*, 2000; Fatkin *et al.*, 1999), but result in varied skeletal muscular dystrophic phenotypes. Interestingly, lamins A and C can be affected independently, with the R571S mutation substituting an arginine residue in the lamin C-specific carboxy terminus (Bonne *et al.*, 2000) and the R644C mutation, also substituting an arginine residue, but in the unique lamin A tail domain (Genschel *et al.*, 2001).

### *1.3.5.2 Diseases of adipose tissue, bone and nerve*

#### 1.3.5.2.1 Dunnigan type - familial partial lipodystrophy (FPLD) - affects adipose tissue

Similar to dilated cardiomyopathy, FPLD is a family of diseases with only one form (Dunnigan type) being associated with mutations in lamin A/C. Clinical features of FPLD are evident with the onset of puberty and are characterized by abnormal distribution of subcutaneous fat. In Dunnigan type - FPLD, adipose tissue progressively disappears (lipoatrophy) from upper and lower extremities, gluteal and truncal areas, yet accumulates on the face, neck, back and groin (Dunnigan *et al.*, 1974). Patients generally develop insulin resistance. The disease was linked to chromosome 1q21 and missense mutations in *LMNA* were identified in five Canadian families (Cao and Hegele, 2000). Unlike muscular dystrophy-associated mutations, which are mostly found within the core of the C-terminal globular Ig domain of lamin A and expected to disturb lamin structure (Krimm *et al.*, 2002), Dunnigan type - FPLD-associated mutations are mostly distributed on the surface of the Ig domain and therefore not expected to disturb lamin structure (Hegele *et al.*, 2000; Speckman *et al.*, 2000), but contribute to NE fragility and disorganization, resulting in herniations such as those reported in lipodystrophic patients by Vigouroux et al. (2001).

#### 1.3.5.2.2 Mandibuloacral dysplasia (MAD) - affects bone

MAD patients exhibit progeria-like abnormalities in bone and skin growth with lipodystrophic elements. The disease has an autosomal recessive character and only

homozygous patients show the classic clinical features of postnatal growth retardation; craniofacial malformations including an hypoplastic mandible producing severe dental crowding; skeletal abnormalities including hypoplastic clavicles; atrophy of the skin over hands and feet with mottled cutaneous pigmentation; alopecia and partial lipodystrophy of either pattern A or B, often accompanied by extreme insulin resistance (Cutler *et al.*, 1991; Simha and Garg, 2002; Young *et al.*, 1971). Only MAD sufferers with type A lipodystrophy have been found to harbour a homozygous mutation, R527H, in the lamin A/C tail domain (Novelli *et al.*, 2002; Simha *et al.*, 2003) which appears to affect the normal distribution of lamin A/C at the NE resulting in lobulations and a 'honey-comb' staining pattern (Novelli *et al.*, 2002).

#### 1.3.5.2.3 Charcot-Marie-Tooth type 2B1 (CMT2B1) - affects neural lineages

Charcot-Marie-Tooth disease is another group of disorders which appear clinically and genetically heterogeneous, affecting motor and sensory nerves, particularly nerve conduction velocity, in the second decade of life. They are inherited in an autosomal recessive pattern. CMT type 1 (CMT1) describes the demyelinating form of the disease, whereas CMT type 2 (CMT2) describes the axonal form which can be further subdivided into CMT2B1 and CMT2B2 according to genetic linkage. CMT2 patients experience reduced nerve conduction velocity concomitant with weakness and wasting of distal lower limb muscles and proximal muscle involvement in a subset of cases. In separate studies on consanguinous families with CMT2B1 the disorder was linked to chromosome region 1q21 which harbours the *LMNA* gene (Bouhouche *et al.*, 1999). A unique homozygous mutation was later identified in the rod domain of lamin A/C in three consanguinous Algerian families (De Sandre-Giovannoli *et al.*, 2002). The locus for the CMT2B2 was otherwise mapped to chromosome 19q13.3 (Leal *et al.*, 2001).

### *1.3.5.3 Progeroid / premature ageing syndromes*

#### 1.3.5.3.1 Hutchinson-Gilford progeria syndrome

Hutchsinson-Gilford progeria syndrome (HGPS) is a premature ageing syndrome which can result from both consanguinous and non-consanginous unions suggesting both autosomal recessive and autosomal dominant modes of inheritance. The HGPS gene was initially mapped to chromosome 1q by observing two cases of uniparental isodisomy of 1q and one case with a 6 megabase paternal interstitial deletion. Identical *de novo* single-base substitutions affecting codon 608 (GGC > GGT) which do not result in an amino acid change in exon 11 (lamin A-specific), but partially activate a cryptic splice site were identified in 18 out of 20 patients with classic HGPS (Eriksson *et al.*, 2003). In one case a G-A transition was reported in the same codon, G608S (GGC > AGC), resulting in a substitution of serine for glycine. Activation of the cryptic splice site results in a 50 amino acid deletion at the C-terminal end of lamin A removing the site for endoproteolytic cleavage as well as the site for cell-cycle-dependent phosphorylation (Ser 625), both of which are necessary for the post-translational modification of prelamin A into mature lamin A. It is thought that incompletely processed lamin A may act as a dominant negative mutant at the NE (Eriksson *et al.*, 2003).

Mouse models carrying an autosomal recessive mutation in *LMNA* ($LMNA^{L530P/L530P}$) show demonstrable defects in A-type lamins and many of the clinical features associated with HGPS in humans including growth retardation, abnormal dentition, loss of subcutaneous tissue, alopecia, reduced bone density, incomplete sexual maturation and poor muscle development (Mounkes *et al.*, 2003). HGPS patients usually suffer

disproportionate craniofacial development and atherosclerosis and die of congestive heart failure in the first or second decade of life. The mouse model for HGPS was shown to have a much smaller heart and smaller myocytes compared to wild-type. Mutant mice also presented with defects in nuclear morphology (Mounkes *et al.*, 2003). Immunofluorescence and electron microscopic investigations using fibroblasts derived from HGPS patients with the G608G mutation demonstrated age-dependent defects in nuclear structure, including nuclear lobulations, thickening of the NL, clustering of nuclear pores and loss of peripheral heterochromatin (Goldman *et al.*, 2004).

#### 1.3.5.3.2 Werner syndrome

Werner syndrome comprises clinical features such as premature arteriosclerosis, scleroderma-like skin changes, subcutaneous calcification and a wizened / aged facial appearance (McKusick, 1963). Atypical Werner Syndrome has a more severe phenotype than the 'typical' form which is caused by homozygous mutations in the DNA helicase-like gene, *RECQL2*. Four atypical Werner Syndrome patients were found to express normal RECQL2, but were heterozygous for novel missense mutations in *LMNA* (Chen *et al.*, 2003). Changes in nuclear morphology and mislocalization of lamins in fibroblasts of a patient with mutation L140R were described (Chen *et al.*, 2003). Therefore atypical Werner Syndrome is characterized by autosomal dominant inheritance of *LMNA* mutations believed to induce nuclear malformations.

### *1.3.5.4 Differential lamin expression in cancer*

Differential expression of lamins, particularly lamin A/C has been associated with epithelial, lymphoid and mesenchymal tumours, including basal skin cell carcinoma (Tilli *et al.*, 2003; Venables *et al.*, 2001), human non-small cell lung cancer, small cell lung cancer (Broers *et al.*, 1993; Kaufmann *et al.*, 1991), acute lymphoblastic leukaemia, non-Hodgkin's lymphoma (Stadelmann *et al.*, 1990), metastatic leiomyosarcoma, rhabdomyosarcoma and chondrosarcoma (Cance *et al.*, 1992). Two groups have investigated the changes in lamin A/C and lamin B1 expression in colorectal neoplasms, but their findings appear somewhat contradictory. Cance *et al.*, (1992) reported constitutive expression of lamin B and heterogeneous expression of lamin A/C in two colon adenocarcinomas, as determined by immunohistochemistry; whereas Moss *et al.* (1999) reported reduced nuclear immunostaining for both lamins A/C and B1 in colon adenomas and adenocarcinomas, compared to normal tissue.

Venables *et al.* (2001) correlated down-regulation of lamin A in basal cell carcinoma (BCC) of the skin with a high proliferation index and a loss of lamin C with slower growing tumours. However, a relationship between loss of lamin A and increased proliferation was not borne out in work completed by Oguchi *et al.* (2002) which associated loss of lamin A/C with poor differentiation status in keratinocytic tumours of the skin and not increased proliferation. Therefore the relationship between A-type lamins and proliferation / differentiation appears not to be straightforward. This was highlighted by analyses of keratinocytic tumours carried out by Tilli et al. (2003). Lamin A/C expression correlated with well-differentiated tumours and more cells expressed Ki67 in poorly differentiated tumours. However, simultaneous expression of lamin A/C and Ki67 occurred in approximately 50% of the proliferating cells in BCC

and squamous cell carcinoma (SCC), indicating that proliferating cells may also maintain a certain degree of differentiation and that lamin A/C and Ki67 are not mutually exclusive.

### *1.3.5.5 Structural hypothesis versus gene expression hypothesis for laminopathies*

Debate surrounds the function of the nuclear lamina - whether its functions are merely architectural or extend to regulating gene transcription, and how it may achieve this. The study of laminopathies which affect striated muscle has led to the formation of a structural hypothesis for the role of lamins in these diseases. Lamin-associated lipodystrophies, on the other hand, are less readily explained by loss of mechanical integrity. The gene expression hypothesis is a more plausible explanation for these diseases.

The structural hypothesis proposes that the lamina maintains the structural integrity of the nucleus and resists mechanical pressure which could damage cells (Goldman *et al.*, 2002; Hutchison *et al.*, 2001). Degradation of the NL would lead to weakness in the NE making it less resistant to deformation. Morphological abnormalities of the NE including herniations (abnormal shape), invaginations and honeycombs (tears in the NE) are reported features in laminopathy patient fibroblasts. Under normal circumstances skeletal and cardiac muscles are subjected to harsh mechanical stress. Together, this strongly suggests a link between lamin mutations and structural weakness of the nuclear envelope in muscular dystrophies and cardiomyopathies.

However, diseases such as Dunnigan type – FPLD and CMT2B1 affect adipose tissue and neurons which are not placed under great mechanical strain, therefore the loss of

lamin A/C must impact on another important function of the NL, other than or as well as maintenance of nuclear architecture. This led to the proposal of the gene expression model, whereby diseases arise through altered gene expression in specific tissues (Cohen *et al.*, 2001). The strongest evidence comes from studies on Dunnigan type – FPLD. FPLD mutations in *LMNA* cause a decrease in the binding of prelamin A to SREBP1 which is proposed to reduce the pool available for activation of peroxisome proliferator activator receptor gamma (PPARγ) (Capanni *et al.*, 2005), a transcription factor which activates adipogenic genes (Akerblad *et al.*, 2005).

### *1.4 Aims of this thesis*

The implications of non-functional lamin A/C are borne out in tissue-specific familial disorders such as autosomal inherited EDMD, MAD, Dunnigan type – FPLD and CMT2B1. In addition mutations in the lamin A binding region of emerin also give rise to an X-linked form of EDMD with identical clinical features to AD-EDMD. Biochemical and immunofluorescence analyses of lamin distribution in a broad range of malignancies affecting epithelial, mesenchymal and lymphoid tissue have demonstrated altered expression of A-type lamins and to a lesser extent B-type lamins in relation to normal cells. Changes in expression of lamin A/C in colorectal cancer has been reported, but the exact nature of these alterations and the driving force behind them has not been investigated. Previous work on keratinocytic tumours of the skin suggests that both the proliferation and differentiation status of a tumour may influence lamin activity.

Chapter 3 describes the simple cancer model set up to observe changes in expression of nuclear lamin sub-types A, C, B1 and B2 during CRC progression. It comprised

cultured colorectal carcinoma cells derived from tumours representing different degrees of differentiation. A down-regulation of lamin A was detected but it did not appear to correlate with proliferation indices, but rather the progression of the disease to a pre-metastatic stage. It coincided therefore with increasing dedifferentiation.

Chapter 4 further explores the relationship between lamin A and cellular proliferation / differentiation in SW480 colon cancer cells which express almost no endogenous lamin A and show highly abnormal growth characteristics. Ectopic expression of lamin A was able to rescue two-dimensional growth and normal cell morphology. cDNA microarray analysis identified down-regulation of a cytoplasmic intermediate filament protein, synemin, upon re-expression of lamin A. This suggested that lamin A may influence cell morphology through functional interactions with components of cytoarchitecture.

Finally, Chapter 5 demonstrates successful re-exposure of lamin A and lamin C epitopes in paraffin-embedded sections of colorectal tumour and normal colon tissue. A-type lamin expression in Dukes' stage A, B, C, D and metastasized tumours was examined by immunoperoxidase staining in a pilot study. In healthy colonic crypts lamin A/C expression correlated with the differentiated phenotype, whereas analysis of Dukes' A malignant polyps determined a relationship between aberrant nuclear morphology and loss of lamin A/C expression.

# CHAPTER 2 – MATERIALS AND METHODS

## *2.1 General chemicals / materials*

All general chemicals were purchased from BDH Laboratory Supplies (VWR International Ltd, Leicestershire, England), Sigma-Aldrich Company Ltd, Dorset, England or Melford Laboratories Ltd, Suffolk, England, unless otherwise stated. Chemicals from BDH were AnalaR® analytical grade and all other reagents were Molecular Biology grade. All plasticware for tissue culture was supplied by Greiner Bio-One Ltd, Gloucestershire, GB.

## *2.2 Mammalian cell culture and transfection*

### 2.2.1 Cell lines

Colon carcinoma cell lines HT29, SW948, SW480 and T84 were obtained from the European Collection of Cell Cultures (ECACC), Wiltshire, UK as growing cultures. These cell lines were chosen because they represented different stages of colorectal cancer from grade II to metastasis. They were routinely cultured in 75 $cm^2$ plastic tissue culture flasks (25 $cm^2$ flasks for SW948) under the following conditions: HT29 – McCoy's 5A medium (Sigma) supplemented with 10% foetal bovine serum (FBS), 2 mM L-Glutamine and 100 units/ml penicillin / 100 µg/ml streptomycin (Invitrogen Ltd, Paisley, UK); SW948 and SW480 – L-15 (Leibovitz) medium with 2 mM L-Glutamine (Invitrogen) supplemented with 10% FBS, 100 units/ml penicillin and 100

μg/ml streptomycin and T84 – DMEM / Ham's F-12 (1:1) medium with 2 mM Glutamax® (Invitrogen) supplemented with 10% FBS, 100 units/ml penicillin and 100 μg/ml streptomycin. All cultures were maintained in a humidified environment at 37°C with 5% $CO_2$, except SW948 and SW480 which were grown without $CO_2$. For all experiments cells were cultured in FBS from lot 111K3366, obtained from Sigma. Cells were routinely subcultured between 70 – 80% confluency, detached from the substrate in the presence of 0.25% trypsin in 0.5 mM EDTA / phosphate-buffered saline (PBS) at 37°C, 5% $CO_2$ in a humidified atmosphere for 2 minutes (cell lines HT29 and SW480), 4 minutes (SW948), 5 - 10 minutes (T84) or 30 seconds – 1 minute (transfected SW480 cells) and neutralized in the corresponding serum-containing medium. HT29 were routinely split 1:10 – 1:12, SW948 were split 1:2, SW480 were split 1:4 and T84 were split 1:3. In the case of SW948, cells were additionally centrifuged at 200 x g for 5 minutes before re-seeding in tissue culture flasks. This was to help create a single cell suspension as these cells tended to aggregate upon trypsinization.

### 2.2.2 Transfection of GFP-reporters into cell line SW480

#### *2.2.2.1 DNA constructs*

SW480 cells were transfected with DNA constructs encoding fusion proteins of EGFP-lamin A, EGFP-emerin or EGFP. EGFP-lamin A full length was a gift from Dr M. Ozumi, Institute of Physical and Chemical Research, Saitama, Japan and EGFP-emerin was a gift from Dr W.G.F. Whitfield, University of Dundee, UK.

### *2.2.2.2 Transfection using GeneJammer® transfection reagent*

In preparation for transfection cells were grown in 6-well plates (35mm diameter) until 60% confluent, under standard culture conditions outlined in Section 2.2.1. The culture medium was aspirated and cells were washed once with fresh culture medium. A transfection mixture of 100 µl L-15 (Leibovitz) media (non-supplemented), 6 µl GeneJammer® transfection reagent (Stratagene, La Jolla, CA) and chosen DNA construct [3 µl EGFP-lamin A (1 µg/µl), 1 µl EGFP-emerin (1 µg/µl) or 1 µl EGFP (1 µg/µl)] was prepared according to the manufacturer's instructions and added dropwise to 900 µl fresh serum-containing media [L-15 (Leibovitz) + 10% FBS] in a tissue culture well. The transfection mixture was swirled gently to evenly distribute it over the cells. Initially cells were incubated for 3 hours in a humidified environment at 37°C, without $CO_2$, after which 1 ml media [L-15 (Leibovitz) + 10% FBS + 2% P/S] was added. For stable tranfection cells were grown for 5 days, with one media change after 48 hours, under standard growth conditions and then split 1:3 into standard growth media. Geneticin® (G-418 sulphate, Invitrogen) selective antibiotic was added to a final concentration of 200 µg/ml 24 hours later. Thereafter media was changed every 72 hours with fresh Geneticin added. The presence of transfected colonies was determined when all cells from the negative control (DNA construct replaced by 1 µl $ddH_20$ in transfection mixture) died off.

### *2.2.2.3 Single cell cloning of stably-tranfected colonies*

Once transfected colonies had been established transfectants were cloned out by limited dilution in 96-well plates. Single cell clones were scaled up using standard growth conditions and kept under constant antibiotic selection.

### *2.2.2.4 Determining GFP-reporter stability within clones*

Loss of GFP-reporter expression over time when cells were not under constant antibiotic selection proved a problem in the first few weeks after transfection, hence cells were kept under constant antibiotic selection during single cell cloning and scaling up of cultures. To confirm the GFP-reporter stability, all cloned cell lines were split 1:2. One flask of cells was cultured in media containing Geneticin® (200 μg/ml), while the other flask was grown in Geneticin®-free media. After four weeks culture, cells were seeded at high density on glass coverslips for 24 hours and then fixed in methanol / acetone (v/v, 1:1), 4°C, for 10 minutes and mounted in Mowiol mountant containing 2.5% DABCO (1,4-diazabicyclo[2.2.2]octane) and 1 μg/ml DAPI (4',6-diamidine-2-phenyl indole) (see Appendix I, A). GFP expression in clones grown with or without antibiotic selection was examined using a Zeiss Axioskop microscope (Carl Zeiss MicroImaging, Inc., Thornwood, NY) equipped for epifluorescence. Any single cell cloned line showing loss of expression when grown without Geneticin® was pronounced unstably transfected and discarded. All other cell lines which showed no difference in GFP expression were grown in Geneticin®-free media for all subsequent work.

### *2.2.2.5 Basis for selection of clones for oligonucleotide microarray analysis*

Out of 47 EGFP-lamin A, 12 EGFP-emerin and 6 EGFP stably transfected single cell clones successfully grown out, 6, 3 and 2 clones respectively were eventually selected on the basis of their GFP expression (assessed by fluorescence microscopy). To maximize future experimental possibilities, clones with low, medium and high levels of GFP expression were chosen, where possible. Assignation of different GFP expression

levels was based on the overall range of GFP expression levels observed across all the single cell cloned lines.

To enable selection of the final clones to be used in microarray analysis, GFP-reporter and endogenous protein expression was quantified by western analysis (see Section 2.4) using antibodies against lamin A/C (JoL2), emerin and GFP (see **Tables 2.1, a & b**). The following clones were chosen: GFP-lamin A 2bb3, GFP-emerin 2 and GFP 2.

The SW480 colon adenocarcinoma cell line is populated by two cell types: One, bipolar and the other, epithelial-like (polygonal shaped) and over time epithelial-like cells have predominated (Leibovitz *et al.*, 1976). In the absence of evidence to the contrary, distinction was made between single cell cloned colonies that appeared to be composed entirely of bipolar-shaped or polygonal-shaped cells. The final clones selected for microarray analysis were, to the best of our ability, identified as being of polygonal shape and therefore epithelial-like.

### *2.3 Indirect immunofluorescence*

CRC cell lines HT29, SW948, SW480 and T84 were seeded at an initial density of 4.1 x $10^5$, 1.0 x $10^6$, 1.0 x $10^6$ and 5.0 x $10^5$ cells/well respectively in 35 mm diameter tissue culture wells containing 13 mm diameter glass coverslips pre-coated with Poly-D-lysine (0.01 mg/ml) for 16 hours prior to use. Cells were grown for 24 hours, washed once in PBS, then fixed in methanol / acetone (1:1, v/v, chilled to -20°C) for 10 minutes at 4°C, washed 3 times in PBS, 5 minutes/wash at room temperature (RT) and air dried for 5 - 10 minutes before immunostaining. GFP-lamin A, GFP-emerin and GFP transfected SW480 cells were grown to 70% confluency, washed once in PBS,

incubated in pre-warmed (37°C) 4% Paraformaldehyde in PBS, pH 7.4 for 12 minutes at RT, permeabilized using 0.5% Triton X-100 in PBS for 5 minutes at RT and washed twice in PBS, 4 minutes/wash at RT. This was followed by a blocking step involving incubation in 1% newborn calf serum (NCS) in PBS for 30 minutes at RT. Coverslips were then washed twice in PBS, 5 minutes/wash at RT and air dried for 5 - 10 minutes.

Cells were single- or double-stained with primary antibodies (25 µl/coverslip) for 1 hour at RT in a wet chamber, using dilutions detailed in **Table 2.1 (a)** and **2.1 (b)** and then washed 5 times in PBS. Incubation with Rhodamine (TRITC)- or Fluorescein (FITC)-conjugated IgG secondary antibodies (Jackson ImmunoResearch Laboratories, Inc., West Grove, PA) was for 1 hour at RT in a wet chamber, followed by 5 washes in PBS. Coverslips were mounted in Mowiol mounting media containing 2.5% DABCO and 1 µg/ml DAPI (see Appendix I, A). Single indirect immunofluorescence images were captured using a Zeiss Axiovert 10 microscope equipped with a Plan-Neofluar 40x N/A 1.3 oil immersion lens and a 12 bit CCD camera, directed by IPLab software. Images of double immunostained cells were captured using a Zeiss Axioskop microscope equipped with a Plan-Neofluar 40x / 1.3 oil immersion lens and fitted with a Bio-Rad Radiance 2000 confocal scanning system, operated by LaserSharp 2000™ software (Zeiss). Z-series were collected in Sequential mode using Kalman averaging (4 times) at a resolution of 1024 x 1024 pixels with an additional 2x digital zoom. Images were projected into z-stacks. Immunocytochemical analyses on GFP-lamin A, GFP-emerin and GFP transfected SW480 cells were completed using a Zeiss LSM 510-META microscope equipped with a Plan-Neofluar 40x / 1.3 oil immersion lens. Images were collected with a Zeiss Axiocam CCD camera directed by Zeiss Axiovision software, version 3.0. Parameters were set individually for each antibody and DAPI, depending on the microscope being utilized, and were kept constant thereafter. Images were

**Table 2.1 (a) Lamin antibodies and corresponding secondary antibodies used for immunofluorescence, SDS-PAGE and immunohistochemistry.**

| Primary antibody | Target | Type | Reference | Assay | Dilution | Secondary antibody | Dilution |
|---|---|---|---|---|---|---|---|
| JoL4 | Lamin A tail | Mouse/m | Dyer *et al.* (1997) | Immunofluorescence<br>Western blot | Undiluted<br>1:200 | TRITC / FITC-DαM<br>DαM HRP | 1:50<br>1:2000 |
| 133A2 | Lamin A tail | Mouse/m | Gift from J.L.V Broers[#] / Hozak *et al.* (1995) | Immunohistochemistry | 1:50 | Biotinylated DαM HRP | 1:400 |
| JoL2 | Lamin A/C tail | Mouse/m | Dyer *et al.* (1997) | Immunofluorescence<br>Western blot<br>Immunohistochemistry | 1:10 or 1:25<br>1:200 / 1:400<br>1:100 | TRITC / FITC-DαM<br>DαM HRP<br>Biotinylated DαM HRP | 1:50<br>1:2000 / 1:4000<br>1:400 |
| RaLC | Lamin C tail | Rabbit/p | Venables *et al.* (2001) | Immunofluorescence<br>Western blot<br>Immunohistochemistry | 1:20<br>1:150<br>1:20 | FITC-DαR<br>DαR HRP<br>Biotinylated GαR HRP | 1:50<br>1:2000<br>1:400 |
| Lamin B (M-20) | Lamin B1 | Goat/p | Santa Cruz[§] | Immunofluorescence<br>Western blot | 1:25<br>1:250 | TRITC / FITC-DαG<br>DαG HRP | 1:50<br>1:2000 |
| LN43 | Lamin B2 | Mouse/m | Gift from E.B Lane[¥] / Kill and Hutchison (1995) | Immunofluorescence<br>Western blot | 1:10 or 1:25<br>1:250 | TRITC / FITC-DαM<br>DαM HRP | 1:50<br>1:2000 |

m = monoclonal antibody; p = polyclonal antiserum, affinity purified; HRP = horse-radish peroxidase

[#]Dr J.L.V. Broers, University of Maastricht, The Netherlands.

[§]Santa Cruz Biotechnology, Inc., Santa Cruz, CA. [¥]Professor E.B. Lane, University of Dundee, UK.

**Table 2.1 (b) Other primary antibodies and corresponding secondary antibodies used for immunofluorescence and SDS-PAGE.**

| Primary antibody | Target | Type | Reference | Assay | Dilution | Secondary antibody | Dilution |
|---|---|---|---|---|---|---|---|
| Emerin, clone 4G5 | Emerin | Mouse/m | Novocastra[¶] / Vector[Φ] | Immunofluoresence | 1:50 | TRITC DαM | 1:50 |
| | | | | Western blot | 1:250 | DαM HRP | 1:4000 |
| αGFP | GFP | Mouse/m | Clontech[†] | Western blot | 1:500 | DαM HRP | 1:4000 |
| Ki67 | Ki67 | Rabbit/p | Dako* | Immunofluorescence | 1:100 | TRITC DαR | 1:50 |
| Ki67, clone Ki67 | Ki67 | Mouse/m | Dako* | Immunofluorescence | 1:10 | TRITC DαM | 1:50 |
| PCNA | PCNA | Human/p | Immuno Concepts[ε] | Immunofluorescence | 1:10 | TRITC GαH | 1:50 |
| Actin, clone AC-40 | β-actin | Mouse/m | Sigma[ξ] | Western blot | 1:1500 / 1:1750 | DαM HRP | 1:2000 / 1:4000 |

m = monoclonal antibody; p = polyclonal antiserum, affinity purified; HRP = horse-radish peroxidase.

[¶]Novocastra Laboratories Ltd, Newcastle-upon-Tyne, UK.

[Φ]Vector Laboratories Inc., Burlingame, CA.

[†]BD Biosciences Clontech, Palo Alto, CA.

*DakoCytomation Denmark A/S, Glostrup, Denmark.

[ε]Immuno Concepts N.A. Ltd, Sacramento, CA.

[ξ]Sigma-Aldrich Company Ltd, Dorset, England.

organized using Adobe® Photoshop® 7.0 (Adobe Systems, Inc., San Jose, CA).

### *2.4 One-dimensional SDS-PAGE and immunoblotting*

Cultured cells were harvested at 80% confluency and protein was extracted from 7 x $10^6$ cells per cell line. Cell pellets were re-suspended in 500 µl Lysis buffer [10 mM Tris-HCl (pH 7.4), 10 mM KCl, 3 mM $MgCl_2$, 0.1% Triton X-100 and 1X Protease inhibitor cocktail (Sigma)] and then incubated with 0.1 units/µl DNase I on ice for 10 minutes. Cell extracts were dissolved in 500 µl 2X Sample buffer [125 mM Tris-HCl (pH 6.8), 2% Sodium dioecyl sulphate (SDS), 2 mM Dithiothreitol (DTT), 20% Glycerol, 5% β-mercaptoethanol and 0.25% Bromophenol blue (w/v)], boiled at 95°C for 3 minutes and finally centrifuged at 14,000 x g for 3 minutes. Protein samples were resolved using one-dimensional SDS-PAGE on a 10 or 12% poly-acrylamide resolving gel with a 5% poly-acrylamide stacking gel (see Appendix I, B), both made using ProSieve® 50 acrylamide gel solution (Cambrex Bio Science Wokingham Ltd, Berkshire, UK) and containing 0.1% SDS. Samples were run at 100 volts (V) for 2 hours in Tank buffer (25 mM Tris, 192 mM Glycine and 0.1% SDS) and transferred to nitrocellulose membrane (Protran®, grade BA85, Schleider and Schuell BioScience Inc., Keene, NH) at 30 V for 16 hours at 4°C in Transfer buffer (25 mM Tris and 192 mM Glycine, pH 9.2, plus 20% methanol and 0.1% SDS). Nitrocellulose membranes were subsequently washed once in Blot rinse buffer (BRB) [10 mM Tris-HCl, 150 mM NaCl and 1 mM EDTA, pH 7.4, plus 0.1% Tween® 20 (v/v)] and incubated initially in 4% blocking buffer [4% skimmed milk powder (w/v) in BRB] for 10 minutes at RT on a shaker, after which the blocking buffer was replaced with fresh blocking solution for a further 16 hours at 4°C with constant agitation. After blocking, nitrocellulose membranes were washed twice in BRB for 5 minutes. Detection of individual lamins and other proteins was accomplished

using a series of specific antibodies listed in **Table 2.1 (a)** and **Table 2.1 (b)**. β-actin was used as a control for loading. Nitrocellulose membranes were incubated with primary antibodies diluted to their optimum concentration in BRB + 1% NCS for 1 hour at RT on a shaker and then rinsed 3 times with BRB, 5 minutes/rinse at RT on a shaker. Secondary antibodies were horse-radish peroxidase (HRP)-conjugated IgG and used at a concentration of 1:2000 – 1:4000 in BRB + 1% NCS. Membranes were incubated with secondary antibodies for 1 hour at RT with continuous agitation and then washed with BRB, 3 times for 5 minutes and Tris buffered saline (TBS) (20 mM Tris and 0.5 M NaCl, pH 7.5), once for 3 minutes to remove Tween® 20. Nitrocellulose membranes were exposed to ECL™ western blotting reagents 1 and 2 (1:1, v/v) (Amersham Biosciences, Buckinghamshire, UK) for 1 minute and immunoreactivity was measured by recovering the signal of chemiluminescence on Hyperfilm™ ECL films (Amersham Biosciences) using a Compact X4 Automatic X-ray Film Processor (Xograph Imaging Systems Ltd, Gloucestershire, UK). Differences between lamin expression were quantified using densitometry (see Section 2.10.1).

### *2.5 Flow cytometry*

Cells were grown to 70% confluency and trypsinized according to standard procedures (see Section 2.2.1). Media was added up to 10 ml and cells were pelleted at 200 x g for 5 minutes. The supernatant was aspirated and cells re-suspended in 0.5 ml PBS. Cells were fixed in 4.5 ml methanol (pre-chilled to -20°C) added drop-wise with constant, mild vortexing of cells. After incubation at -20°C overnight, cells were centrifuged at 1500 x g for 5 minutes, re-suspended in 5 ml PBS and pelleted again by centrifugation at 1500 x g for 5 minutes. The supernatant was removed and cells re-suspended in 400 µl PBS. 100 µg/ml RNase and 25 µg/ml Propidium iodide (PI) (Sigma) was added

and samples incubated for 5 minutes on ice before further centrifugation at 1500 x g for 5 minutes to remove enzyme and PI stain. Finally cells were re-suspended in 1 ml PBS and placed on ice. Flow cytometric analyses were carried out using a Coulter® EPICS® XL-MCL™ Flow Cytometer (Beckman Coulter, Inc., Fullerton, CA) using System II™, version 3.0 software. A monodisperse suspension of cells were excited at 488 nm by an argon ion laser and fluorescence from PI was collected through a 620 nm band-pass filter, transmitting light between 605 – 635 nm to the fluorescent channel 3 (FL3) sensor.

The parameters set for forward scatter (FS) and side scatter (SS) of light as cells pass through laser and for the PI fluorescence collector, FL3, are given in **Table 2.2** for each cell line. For non-transfected cell lines HT29 and SW480 – see **Table 2.2 (a)**, SW948 – see **Table 2.2 (b)** and T84 – see **Table 2.2 (c)**. For transfected cell lines SW480 GFP-lamin A 2bb3 – see **Table 2.2 (d)**, SW480 GFP-emerin 2 – see **Table 2.2 (e)** and SW480 GFP 2 – see **Table 2.2 (f)**. Data for a minimum 10,000 single cell events was collected for each sample.

| | Voltage | Gain |
|---|---|---|
| **FS** | 593 | 1.0 |
| **SS** | 689 | 2.0 |
| **FL3** | 650 | 1.0 |

**Table 2.2 (a)** Parameters for HT29 and SW480-untransfected.

| | Voltage | Gain |
|---|---|---|
| **FS** | 593 | 1.0 |
| **SS** | 689 | 2.0 |
| **FL3** | 810 | 1.0 |

**Table 2.2 (b)** Parameters for SW948.

| | Voltage | Gain |
|---|---|---|
| **FS** | 593 | 1.0 |
| **SS** | 689 | 2.0 |
| **FL3** | 568 | 1.0 |

**Table 2.2 (c)** Parameters for T84.

| | Voltage | Gain |
|---|---|---|
| **FS** | 593 | 1.0 |
| **SS** | 689 | 2.0 |
| **FL3** | 750 | 1.0 |

**Table 2.2 (d)** Parameters for SW480 GFP-lamin A 2bb3.

| | Voltage | Gain |
|---|---|---|
| **FS** | 443 | 1.0 |
| **SS** | 509 | 2.0 |
| **FL3** | 620 | 1.0 |

**Table 2.2 (e)** Parameters for SW480 GFP-emerin 2.

| | Voltage | Gain |
|---|---|---|
| **FS** | 393 | 1.0 |
| **SS** | 499 | 2.0 |
| **FL3** | 710 | 1.0 |

**Table 2.2 (f)** Parameters for SW480 GFP 2.

**Table 2.2 (a - f)**
**Flow cytometry parameters.**

## *2.6 Preparation of cells for electron microscopy*

In untransfected and transfected SW480 cultures, cells floating in the media were separated from those adhering to the culture dish. Media was removed from 70 – 80% confluent cultures and floating cells were collected by centrifugation at 200 x g for 5 minutes. Adherent cells were harvested using standard procedures and pelleted at 200 x g for 5 minutes. All pelleted samples were re-suspended in Karnovsky's fixative (Karnovsky, 1965) - 2% Paraformaldehyde, 2.5% Glutaraldehyde in 0.1 M Sodium cacodylate buffer, pH 7.3 - for 1 - 1.5 hours at 4°C. Fixative was replaced with 2% Osmium tetroxide buffered with an equal volume of 0.2 M Sodium cacodylate, pH 7.3 for 30 minutes to 1 hour at 4°C. Fixative was poured off and cells were dehydrated through an ethanol series: 70%, 3 times 5 minutes; 95%, 3 times 5 minutes and 100%, 3 times 10 minutes. Subsequently cells were infiltrated with intermediate solution - 100% ethanol and Propylene oxide, combined 1:1 (v/v) - 3 times 10 minutes and Propylene oxide alone, 3 times 10 minutes. Cells were then infiltrated with Propylene oxide / araldite resin [49% Araldite CY212, 49% Dodecenylsuccinic anhydride (DDSA) and 2% Benzyl dimethylamine (BDMA)] combined 1:1 (v/v) for 30 minutes at 45°C or overnight at RT in tubes with the lids off and with pure araldite for 30 minutes at 45°C in tubes with the lids off. Samples were orientated and embedded in a suitable mould, covered with fresh araldite and left to polymerize for 12 hours at 45°C and for a further 24 hours at 60°C.

Samples were sectioned at a thickness of 60 - 90 nm using a Reichert Ultracut S (Leica Microsystems (UK) Ltd, Milton Keynes, Buckinghamshire, UK), collected onto Formvar® coated copper grids (Agar Scientific Ltd. Stansted, Essex, England) and stained with uranyl acetate and Reynolds' lead citrate (Reynolds, 1963) for 10 minutes

each at RT. Sections were examined for evidence of apoptosis on a Phillips 400 Transmission Electron Microscope (TEM) (FEI UK Ltd, Cambridge, UK) or a Hitachi H7600 TEM (Hitachi High-Technologies Corporation, Tokyo, Japan).

## *2.7 Immunohistochemistry*

### 2.7.1 Colorectal tissue specimens

Normal and tumour human tissues were procured from the Department of Pathology, University Hospital, Maastricht, The Netherlands without patient identifying codes. Thirty-six tumour specimens were selected from the archive based on their clinical stage, along with 11 examples of normal mucosa. The number of Dukes' stage A and D specimens available was limited, therefore the following tumour types were included for immunohistochemical analysis of A-type lamin expression: Dukes' stage A (n = 2), Dukes' stage B (n = 10), Dukes' stage C (n = 11), Dukes' stage D (n = 2), metastasis to liver (n = 8), lung (n = 1), pancreas / duodenum (n = 1) and small intestine (n = 1). All specimens had been grossly dissected and immersed in 4% formalin fixative for 30 minutes at 35°C. Dehydration and embedding of tissues was fully automated and the procedure was as follows: 70% ethanol, 60 minutes at 35°C; 70% ethanol, 60 minutes at 37°C; 96% ethanol, 60 minutes at 37°C; 96% ethanol, 1 hour 30 minutes at 40°C; 100% ethanol, 1 hour 30 minutes at 40°C and 100% ethanol, 2 hours at 45°C. Samples were cleared in xylene for 15 minutes at 45°C, 15 minutes at 50°C, followed by another 30 minutes at 50°C before embedding in paraffin at 60°C for two 60 minute periods and finally for 1 hour 30 minutes. The clinical stage was confirmed histologically.

### 2.7.2 Antigen retrieval

Formalin-fixed, paraffin-embedded tissue specimens were sectioned into 4 μm thick slices and left overnight at 37°C to bond to Starfrost® adhesive microscope slides (Knittel Glaser, Braunschweig, Germany). Tissue sections were de-paraffinized in xylene, 2 times for 5 minutes and rehydrated through an ethanol series: 100% ethanol, 5 minutes; 100% ethanol, 5 minutes; 96% ethanol, 2 minutes and 70% ethanol, 2 minutes.

The process of antigen retrieval used was adapted from the method described by Barker *et al.* (1999). Endogenous peroxidase activity was quenched in 1.5% $H_2O_2$ in methanol (fresh) for 20 minutes at RT. Thereafter tissue sections were immersed in 0.01 M citrate buffer, pH 6.0 (pre-heated to 90°C) for 15 minutes in a water bath at 90°C. Afterwards slides were placed directly into PBS for at least 10 minutes to cool and to limit evaporation.

### 2.7.3 Peroxidase staining

Non-specific binding was blocked using 2% goat serum / 2% bovine serum albumin (BSA) in PBS or 2% rabbit serum / 2% BSA in PBS, depending on the animal the secondary antibody was raised in, 100 μl/section, for 25 minutes at RT. Sections were washed 3 times with PBS and incubated with primary antibody diluted in 0.1% BSA in PBS, 100 μl/section, for 45 minutes at RT. Primary antibodies were used at the following concentrations: JoL2, 1:100; 133A2, 1:50 and RaLC, 1:20 (see **Table 2.1, a**). Antibody was removed by washing 3 times in PBS. Biotinylated IgG secondary antibodies were used at a concentration of 1:400 in 0.1% BSA in PBS, 100 μl/section, for 45 minutes at RT. Sections were washed 3 times with PBS followed by a 30 minute

incubation at RT with StreptABComplex / HRP (DakoCytomation, Glostrup, Denmark) [50 µl Streptavidin and 50 µl biotinylated peroxidase in 5 ml wash buffer (0.1% BSA in PBS)], 100 µl/section, prepared 30 minutes prior to use. The complex was removed by washing 3 times with PBS. Immunological detection was achieved by adding 100 µl activated DAB chromogen (DakoCytomation) at working concentration (0.0225% $H_2O_2$ in 1 mg/ml filtered DAB in PBS). DAB was added directly to tissue sections for the following lengths of time: JoL2-stained sections for 3 minutes, 133A2-stained sections for 6 minutes and RaLC-stained sections for 5 minutes. Reactions were stopped by immersing sections in $dH_2O$. All incubations were carried out in a humidified staining box. Negative controls were sections stained as above, except the primary antibody was replaced with 0.1% BSA in PBS.

### 2.7.4 Counterstaining

To visualize all nuclei, sections were counterstained with undiluted Ehrlich's haematoxylin (Raymond A Lamb Ltd, Eastbourne, East Sussex, UK) for 3 minutes and rinsed in tap water for 1 minute. The stain was differentiated using 1% acid-alcohol (1% HCl in 70% ethanol) for 1 minute 15 seconds and ripened in 0.04% aqueous ammonia for 30 seconds which was washed away by dipping in and out of $dH_2O$ for 1 minute. Sections were dehydrated through a graded ethanol series and cleared as follows: 70% ethanol for 2 minutes, 96% ethanol for 2 minutes, 96% ethanol for 2 minutes, 100% ethanol for 2 minutes, 100% ethanol for 2 minutes, xylene for 3 minutes and xylene for 3 minutes. Specimens were coverslipped with Entellan® (Merck kGaA, Darmstadt, Germany) and left to dry overnight.

### 2.7.5 Analysis

Colorectal tissue sections were analysed using a Nikon Diaphot 300 inverted microscope (Nikon Corporation, Tokyo, Japan) equipped for bright-field microscopy with Plan 4x / 0.13, 10x / 0.25, 20x / 0.4 and 40x / 1.3 lenses. Images were collected with a Nikon DXM1200 digital camera controlled by Nikon Act-1, version 2.20 software. Image processing was carried out in Adobe® Photoshop® 7.0. Intensity of staining was scored using the + / - system.

## *2.8 Semi-quantitative RT-PCR*

### 2.8.1 Primer design

Primers specific for the coding sequence (cds) of human lamin A (NM_170707), lamin C (NM_005572), lamin B2 (NM_032737) and β-actin (NM_001101) were designed using the Primer3 web interface (http://frodo.wi.mit.edu/primer3/primer3_code.html), developed by the Whitehead Institute, Cambridge, MA and the Howard Hughes Medical Institute, Chevy Chase, MD. It selects suitable primers from a given DNA sequence based on a number of parameters including product size, primer length, melt temperature ($T_m$) and GC%. The software was programmed to design primers between 18 and 27 bases long and select primers with a minimum $T_m$ of 57°C, a maximum $T_m$ of 63°, with a maximum $T_m$ difference between the sense and antisense primers of 4°C. The GC/AT ratio was important and a GC content between 45 - 70 % was ensured. NetPrimer online software (PREMIER Biosoft International, CA / http://www.premierbiosoft.com/netprimer/index.html) also predicted primer melt

temperature, using the nearest neighbour thermodynamic theory, and enabled examination of secondary structures in primer pairs, incorporating hairpin loops, self-dimers, cross-dimers, palindromes, runs and repeats, which could impinge their function or lead to non-specific products. **Table 2.3** shows primer sequences.

| Gene | Accession number | Primer direction | Start (5' – 3') | Deoxyoligonucleotide sequence, 5' – 3' | Product size (bp) |
|---|---|---|---|---|---|
| lamin A | NM_170707 | sense | 727 | GATGCGCTGCAGGAACTACG | 1137 |
| | | antisense | 1863 | CGTGACACTGGAGGCAGAAGAG | |
| lamin C | NM_005572 | sense | 727 | GATGCGCTGCAGGAACTACG | 993 |
| | | antisense | 1719 | TCAGCGGCGGCTACCACTCA | |
| lamin B2 | NM_032737 | sense | 980 | ACAAGTTCCGGAAGATGCTG | 481 |
| | | antisense | 1460 | ACCTGCCTCTTGATTCTCCA | |
| c-myc | V00568 | sense | 514 | TCCACCTCCAGCTTGTACCTG | 557 |
| | | antisense | 1070 | CGCCTCTTGACATTCTCCTCG | |
| c-raf | X03484 | sense | 277 | CCAGAGTGCTGTGCAGTGTTC | 589 |
| | | antisense | 865 | AGGCTGATTCGCTGTGACTTC | |
| RPL31 | NM_000993 | sense | 53 | ACGAAGTGGTAACCCGAGAAT | 322 |
| | | antisense | 374 | TTCTCATCCACATTGACTGTCTG | |
| synemin | AJ310522 | sense | 1920 | CGTTACCAGTATCCTGAAGCAG | 518 |
| | | antisense | 2437 | CGTGAGTCGTGTTCTCCTGA | |
| β-actin | NM_001101 | sense | 257 | GGCACCACACCTTCTACAATGAGC | 834 |
| | | antisense | 1090 | CGTCATACTCCTGCTTGCTGATCCAC | |

**Table 2.3 Primers for semi-quantitative RT-PCR.**

### 2.8.2 RNA isolation

Total RNA was isolated from three different passages of CRC cell lines HT29, SW948, SW480 and T84 using TRI Reagent™ (Sigma). The procedure was executed principally as described in Sigma's Technical Bulletin MB-205 (Sigma, 1999). Transfected SW480 cells expanded to approximately 70% confluency in 75 $cm^2$ tissue culture flasks were lysed directly on the culture surface with 2 ml TRI Reagent™ per flask and allowed to stand for 10 minutes at RT. Lysates were transferred to 1.5 ml RNase-free microfuge tubes and centrifuged at 12,000 x g for 10 minutes at 4°C. The supernatant which contains RNA was removed and placed into a fresh tube to which 200 µl RNase-free chloroform was added for every ml of TRI Reagent™ used. Samples were vortexed for 10 seconds and left to stand for 15 minutes at RT or until mixture separated into two layers. Samples were further centrifuged at 12,000 x g for 15 minutes at 4°C. The aqueous phase alone was immediately transferred to a fresh tube and 0.5 ml RNase-free isopropanol per ml of TRI Reagent™ used was added. Samples were inverted 3 times and incubated for 10 minutes at RT before centrifugation at 12,000 x g for 10 minutes at 4°C. The supernatant was aspirated to leave a maximum of 50 µl liquid. The RNA precipitate was washed with 1 ml 75% ethanol in DEPC-treated $dH_2O$ per ml TRI Reagent™ used and pelleted again at 10,000 x g for 10 minutes at 4°C. All supernatant was removed and samples air-dried for 5 - 10 minutes in a laminar flow hood and re-suspended in 15 - 20 µl Nuclease-free water, depending on expected RNA yield. RNA samples were solubilized at 50°C for 2 minutes and stored at -20°C.

### 2.8.3 Confirmation of RNA integrity

Validation of RNA quality, purity and concentration was carried out as explained in Section 2.9.4. Additionally, the human gene β-actin was used to exclude the possibility that genomic DNA (gDNA) may have been co-isolated with total RNA. Before RT-PCR was undertaken, primers to an 834 bp fragment of β-actin were used to amplify any contaminating gDNA in 0.5 µg RNA which had not been reverse transcribed. PCR was carried out in a 25 µl reaction volume comprising 1X ReddyMix™ PCR Master Mix (ABgene, Epsom, Surrey, UK) [25 units/ml Thermoprime Plus DNA polymerase (*Taq*), 75 mM Tris-HCl (pH 8.8 at 25°C), 20 mM $(NH_4)_2SO_4$, 2.5 mM $MgCl_2$, 0.01% Tween® 20 (v/v) and 200 µM each dNTPs], 0.4 pmol/µl β-actin sense primer and 0.4 pmol/µl β-actin antisense primer. Cycling conditions were dependent on the thermal cycler used, see Section 3.8.4 for specific details. The total volume of PCR product (25 µl) was electrophoresed on a 1% agarose / 0.8X Tris-borate EDTA (TBE) gel with 0.3 µg/ml Ethidium bromide (EtBr). RNA samples showing evidence of gDNA contamination were treated with 0.075 units/µg/µl RQ1 RNase-free DNase (Promega) in 1X reaction buffer [40 mM Tris-HCl (pH 8.0), 10 mM $MgSO_4$, 1 mM $CaCl_2$] for 15 minutes at RT. The reaction was terminated by incubating samples with 1 µl DNase stop solution (20 mM EGTA, pH 8.0) for 10 minutes at 65°C.

RNA was precipitated with 1/10 of the total reaction volume of DEPC-treated 3 M Sodium acetate (NaOAc), pH 5.2 and 3 volumes 100% extra-clean ethanol (-20°C), vortexed for 5 seconds and incubated overnight at -20°C. To recover RNA, samples were centrifuged at 12,000 x g for 10 minutes at 4°C, the supernatant removed and pellets washed with 1 ml 70% extra-clean ethanol (in DEPC-treated $dH_2O$). Centrifugation was repeated at 12,000 x g for 5 minutes at 4°C, the supernatant

aspirated and residual ethanol allowed to evaporate for 5 - 10 minutes in a laminar flow hood. The resulting pellet was re-suspended in 20 µl DEPC-treated $dH_2O$ and the quality, purity ($A_{260}/A_{280}$) and concentration ($A_{260}$) of RNA was measured as described in Section 2.9.4.

### 2.8.4 Reverse transcriptase – polymerase chain reaction

Reverse transcription and amplification of human β-actin, lamin A and lamin C mRNA was completed in one step using Promega's AccessQuick™ RT-PCR System; for lamin B2 it was carried out in 2 stages using Promega's Reverse Transcription System (A3500) and PCR Master Mix (M7502). For all samples, RT-PCR was completed in triplicate, except in the case of lamin B2 where samples were analysed in duplicate. In preparation for RT-PCR, all components and samples were kept on ice until loaded into a thermal cycler.

Reactions utilizing Promega's AccessQuick™ RT-PCR System were down-scaled to 50% of the original volume recommended, to a final volume of 25 µl. A master mix comprising 1X AccessQuick™ Master Mix (*Tfl* DNA Polymerase, dNTPs, $MgCl_2$ and reaction buffer), 0.15 pmol/µl sense primer, 0.15 pmol/µl antisense primer and water was mixed thoroughly and aliquoted, 24 µl per PCR tube. One microlitre RNA template (0.1 µg/µl) was added to each tube, except the negative control in which RNA was replaced by RNase-free water. RNA was denatured at 72°C for 5 minutes and then cooled on ice for a further 5 minutes. Avian Myeblastosis Virus - Reverse Transcriptase (AMV-RT) (5 units/µl) (Promega) was added as the final component to a final concentration of 0.1 units/µl. To repudiate contamination of any RT-PCR reaction components with DNA, controls in which AMV-RT was replaced with water were

analysed for each RNA sample. Finally, all components were gently vortexed and briefly spun down before loading into a PTC-0200 DNA Engine Gradient Cycler (Bio-Rad Laboratories, Hercules, CA). Optimized cycling conditions were as follows: RNA was reverse transcribed at 45°C for 60 minutes and the resulting cDNA denatured initially at 94°C for 2 minutes, followed by 26 cycles of 94°C for 30 seconds, 59°C (lamin A primers) or 60°C (β-actin and lamin C primers) for 1 minute (annealing) and 72°C for 1 minute, concluding with a final elongation at 72°C for 5 minutes.

For lamin B2, RT-PCR was separated into two stand-alone reactions. First, a cDNA template was synthesized in a 20 µl reaction using Promega's Reverse Transcription System. Two microlitres total RNA (0.5 µg/µl) and 1 µl Random primers (0.5 µg/µl) were incubated together in a thin-walled microfuge tube at 70°C for 10 minutes, tap spun and snap chilled on ice. A reverse transcription master mix comprising 1X AMV-RT buffer [50 mM Tris-HCl (pH 8.3 at 25°C), 50 mM KCl, 10 mM $MgCl_2$, 0.5 mM spermidine and 10 mM DTT), 1 mM each dNTP mixture, 1 unit/µl Recombinant RNasin® Ribonuclease inhibitor and Nuclease-free water was prepared and aliquoted equally between tubes of denatured RNA and Random primers. AMV-RT (10 units/µl) (Promega) was added to a final concentration of 0.75 units/µl (15 units/µg RNA), except for –AMV-RT controls where AMV-RT was replaced by an equivalent volume of Nuclease-free water for each sample. Reactions were flick mixed, spun briefly and incubated at RT for 10 minutes, followed by 42°C for 30 minutes. Heating samples at 95°C for 5 minutes inactivated AMV-RT and samples were subsequently chilled on ice. cDNA was stored at -20°C.

β-actin was amplified from all cDNAs and their accompanying –AMV-RT controls, plus the negative control where no RNA was added, to show that equals amounts of

cDNA had been reverse transcribed, that there was no contamination in any of the reaction components and that the reverse transcription and PCR reactions were working successfully. A 481bp fragment of lamin B2 was amplified from all reverse transcription reaction products which had AMV-RT added, plus a negative control. A 25 µl reaction volume contained 1X Promega PCR Master Mix [25 units/ml *Taq* DNA polymerase in buffer (pH 8.5), 200 µM each dNTPs and 1.5 mM $MgCl_2$], 0.4 pmol/µl sense primer, 0.4 pmol/µl antisense primer, 2 µl cDNA template and Nuclease-free water. Samples were mixed well and spun down. The succeeding optimized PCR profiles for lamin B2 and β-actin were carried out on an Eppendorf Mastercycler® Gradient Thermal Cycler (Eppendorf UK Ltd, Cambridge, UK): 94°C for 3 minutes, 26 cycles at 94°C for 1 minute, 54°C (lamin B2) or 60°C (β-actin) for 1 minute 30 seconds and 72°C for 3 minutes, and finally 72°C for 5 minutes.

### 2.8.5 Analysis

Amplified products were run on 1% agarose / 0.8X TBE gels, containing 0.3 µg/ml EtBr, at 70V for 60 minutes. Product size was compared to a 100 bp DNA ladder (Promega) and bands were visualized using a Gel Doc™ 2000 UV transilluminator and Quantity One™ software, version 4.0.3 (Bio-Rad). Differences between lamin A, C and B2 mRNA levels were quantified using densitometry (see Section 2.10.1) and expressed as a ratio against β-actin expression.

### 2.8.6 DNA sequencing

Lamin A, lamin C and lamin B2 RT-PCR products were purified using Promega's Wizard® SV Gel and PCR Clean-Up System. An equal volume of Membrane Binding Solution was added to 50 µl PCR product, after which DNA was purified by micro-centrifugation as described in section V.A. of Promega's Technical Bulletin No. 308 (2002). DNA was eluted in 20 – 40 µl Nuclease-free water, depending on the expected yield.

Concentration of DNA was determined by running purified samples against DNA of known concentrations on a 1% agarose / 0.8X TBE gel containing 0.3 µg/ml EtBr, at 80 V for 45 minutes. By measuring intensity of DNA bands of known concentration, using densitometry, to produce a standard curve, the concentration of individual purified DNA samples was determined.

Lamin A, lamin C and lamin B2 were sequenced with primers lamin A antisense, lamin C antisense and lamin B2 sense respectively (primer sequences given in **Table 2.3**) using an ABI Prism® 377 XL automated DNA sequencer (Applied Biosystems, Foster City, CA) which can sequence approximately 800 bp when cDNA concentration is between 20 – 250 ng/µl and the sequencing primer is at the optimum concentration of 3.2 pmol/µl. The sequences were analysed using the Nucleotide-nucleotide BLAST database (BLASTN 2.2.11) [http://www.ncbi.nlm.nih.gov/BLAST / Altschul *et al.* (1997)].

## *2.9 Glass slide oligonucleotide microarray analysis*

### 2.9.1 Design of Colorectal Cancer Oligonucleotide Chip

A unique DNA array comprising 332 oligonucleotide sequences, representing 325 different human genes was designed to investigate the affect of a loss of lamin A expression on the activity of colorectal cancer-associated genes. Genes were chosen according to their association with colorectal cancer and their known role in the development and progression of malignancy in general. Genes were sorted into functional groups (see Appendix II, A) and spotted onto the chip generally in these groups.

### 2.9.2 Spotting of oligonucleotide array

HPSF® purified oligonucleotides were synthesized by MWG Biotech Ltd, London, UK to a scale of 0.01 μmole based on the GenBank® accession numbers for each mRNA sequence (see Appendix II, B). Each oligonucleotide was reconstituted in 50% Nuclease-free water / 50% Dimethyl sulphoxide (DMSO) to a concentration of 50 μmol and placed in a pre-determined location in a 384-well plate (see Appendix II, C).

The oligonucleotide chip was produced by a GeneTAC™ G3 Arrayer (Genomic Solutions, Inc. Ann Arbor, MI) containing a 12 x 4 pin spotting tool. Oligonucleotides were spotted in quadruplicate in 8 x 4 patches, arranged in a 12 x 4 grid, on MWG Epoxy glass slides. The pins were cleaned according to the following procedure between the spotting of each set of oligonucleotides: sonic bath ($ddH_2O$) for 10 seconds,

a second bath of $ddH_2O$ for 5 seconds, 80% ethanol in $ddH_2O$ for 5 seconds, air dry for 5 seconds and heat for 5 seconds. After spotting, slides were arranged spotted side up on a platform in a lidded wet chamber containing 150 ml of a saturated NaCl solution and incubated at 42°C overnight. The next day slides were placed back-to-back in a 50 ml conical tube containing 0.2% SDS in $ddH_2O$ and inverted 5 times. Slides were then transferred to another tube and washed 3 times in $ddH_2O$, inverting tube 5 times per wash. Lastly, slides were removed to fresh $ddH_2O$, pre-warmed to 50°C and incubated for 20 minutes at 50°C away from the light, before drying at 42°C for 10 - 15 minutes and storing in the dark at RT for a maximum of six months.

### 2.9.3 Total RNA isolation

Total RNA was extracted from three different passages of SW480 GFP-lamin A 2bb3, SW480 GFP-emerin 2 and SW480 GFP 2 using TRI Reagent™, exactly as described in Section 2.8.2, except RNA was stored at -80°C.

### 2.9.4 Confirmation of quality, purity and concentration of RNA

Total RNA quality was assessed by gel electrophoresis. RNA was diluted in 6X RNA loading buffer [6X Tris-acetate EDTA (TAE) buffer, 8 M urea, 15% ficoll, 0.25% Xylene cyanol FF (w/v) and 0.25% Bromophenol blue (w/v)] and heated at 70°C for 5 minutes before adding Ethidium bromide to a final concentration of 7 ng/µl. Samples were separated alongside RNA Millennium™ size markers (Ambion, Inc., Austin, TX) on 1% agarose gels in 0.8X TBE buffer at 80 V for 1 hour 10 minutes. Bands were

visualized using a Gel Doc™ 2000 UV transilluminator and Quantity One™, version 4.0.3 software (Bio-Rad).

Purity was determined by measuring the ratio of absorbance in 10 mM Tris-HCl, pH 7.5 at 260 nm and 280 nm ($A_{260}/A_{280}$) in a GeneQuest CE2301 Analyser (Cecil Instruments Ltd, Cambridge, UK) and the concentration was calculated by measuring the absorbance in DEPC-treated $dH_2O$ at 260 nm ($A_{260}$).

### 2.9.5 Hybridization

#### *2.9.5.1 Preparation of RNA for hybridization*

Total RNA was prepared for hybridization to our unique oligonucleotide chip using the Micromax™ Direct labelling kit (PerkinElmer Life Sciences, Boston, MA). Control RNA samples were always assigned Cyanine 3-dUTP (Cy3) fluorescent dye and test RNA samples, Cyanine 5-dUTP (Cy5) fluorescent dye. RNA was reverse transcribed in the following way: To 70 µg test and control RNA, 1 µl Random primers was added and the total volume made up to 20 µl with DEPC-treated water. Samples were given a pulse spin and incubated for 10 minutes at 65°C in a water bath and then for 5 minutes at RT. To each tube 2.5 µl Buffer (A), 1.0 µl Cy3 or Cy5 dye and 2.0 µl Enzyme mix (E) were added in order and incubated for 60 minutes at 42°C in a water bath. Once the fluorescent dyes had been incorporated into the cDNA, samples were kept away from the light as much as possible. When the reverse transcription reaction finished 2.5 µl 0.5 M EDTA, pH 8.0 (RNase-free) and 2.5 µl 1 M Sodium hydroxide (NaOH) (fresh) was added to stop the reaction and degrade residual RNA. The tube contents were

ghtly mixed (not vortexed) and incubated at RT for 15 minutes. At this point the two robes were combined. Any residual probe left in the empty tube was collected by dding 350 µl Tris / EDTA (TE) buffer (10 mM Tris / 1 mM EDTA in DEPC-treated vater) and transferring the contents to the tube containing the combined samples and nixing. The combined samples were pipetted into a Microcon® purification column Millipore Corporation, Bedford, MA) and centrifuged at 11,000 x g for 7 minutes. It was essential that a small volume of probe remained in the column, so it was checked 2 minutes before the centrifugation step was due to end. The flow-through was removed and 400 µl more TE buffer was added to the column, plus 10 µl Human Cot-1 DNA® (1 mg/ml) (Invitrogen) to block cross-hybridization of human repetitive DNA sequences within target. The column was spun at 11,000 x g for 5 minutes or until approximately 80 µl liquid remained in the column. The column was inverted into a fresh RNase-free microfuge tube and the whole set-up was spun at 600 x g for 1 minute to collect probe. If less than 80 µl was collected the volume was made up to 80 µl with TE buffer and the labelled sample was denatured at 94°C for 5 minutes. To the denatured sample, an equivalent volume (80 µl) of EasyHyb® Hybridization Solution (U-Vision Biotech Inc., Taiwan), pre-incubated for 2 minutes at 42°C, was added, pipette mixed very gently to avoid bubbles forming and spun down briefly.

### *2.9.5.2 Hybridization and wash cycles*

Samples were kept at 50°C before loading into the GeneTAC™ Hybridization station (Hyb. station) (Genomic Solutions). The Hyb. station was pre-warmed to 42°C and the prepared probe was introduced to the module, position 1, containing one oligonucleotide chip, counterbalanced by an unspotted glass slide in position 2. The Hyb. station was programmed to complete hybridization of RNA to chip in 1 hour 50

minutes at 42°C. Subsequently the chip was washed in buffers of increasing stringency to remove any unbound probe. The optimized wash cycle programme was completed as follows at 25°C:

1. Purge manifold
2. Wash slide 1, Reservoir 2 (Wash I), 1 minute
3. Wash slide 2, Reservoir 2 (Wash I), 1 minute
4. Hold at temperature Wash I, 2 minutes
5. Purge manifold
6. Wash slide 1, Reservoir 3 (Wash II), Pass 1, 1 minute
7. Wash slide 2, Reservoir 3 (Wash II), Pass 1, 1 minute
8. Hold at temperature Wash II, 2 minutes
9. Wash slide 1, Reservoir 3 (Wash II), Pass 2, 1minute
10. Wash slide 2, Reservoir 3 (Wash II), Pass 2, 1minute
11. Hold at temperature Wash II, 2 minutes
12. Purge manifold
13. Wash slide 1, Reservoir 4 (Wash III), 1 minute
14. Wash slide 2, Reservoir 4 (Wash III), 1 minute
15. Hold at temperature Wash III, 2 minutes
16. Slide 1 and 2, drain and dry, 1 minute

The components of the wash buffers, Wash I, Wash II and Wash III, also known as Reservoirs 2, 3 and 4 respectively are detailed in **Table 2.4**. It was essential to dilute Solution B (part of EasyHyb® Hybridization Solution Kit) in $ddH_2O$ before adding Solution A (part of EasyHyb® Hybridization Solution Kit).

| Reservoir / Wash | Solution | Volume |
|---|---|---|
| Reservoir 2 / Wash I | B | 20 ml |
| | $ddH_20$ | 178 ml |
| | A | 2 ml |
| | Total | 200ml |
| | | |
| Reservoir 3 / Wash II | B | 2 ml |
| | $ddH_20$ | 196 ml |
| | A | 2 ml |
| | Total | 200 ml |
| | | |
| Reservoir 4 / Wash III | B | 1 ml |
| | $ddH_20$ | 199 ml |
| | Total | 200 ml |

**Table 2.4 Components of GeneTAC™ Hybridization station wash buffers**

### 2.9.6 Image acquisition and analysis

Arrays were scanned immediately after hybridization in a GeneTAC™ LS IV Biochip Analyzer operated by GeneTAC GT LS, version 3.11 software (Genomic Solutions). Scanning was stopped at a particular Gain when the landmarks in positions A1.a1, A12.a1, D1.a1 and D12.a1 lit up, to enable alignment of array. Gain for Cy3 did not exceed 55, Gain for Cy5 was never greater than 65. The Black (Offset) was adjusted to give minimum background. Scan dimensions were X = 1000, Y = 3000 with 5 point averaging.

Image analysis was enabled by the GeneTAC™ Integrator, version 3.3.0 microarray analysis software (Genomic Solutions). A 12 x 4 patch grid was overlaid and landmarks

assigned to spots positioned in A1.a1, A12.a1, D1.a1 and D12.a1 (see Appendix II, B & C). Spacing of grid circles was standardized at 500 μm and circle diameter set to 350 μm. The grid was moved to align with the majority of spots. Each patch was examined individually and any bad spots (i.e. ones which were not uniform in size, did not fit into their grid circle or did not follow the same pattern as other replicates) were flagged as such and excluded from analysis.

Only arrays with a Mean Normalisation Factor greater than 0.8 were included in the analysis. In addition a linear relationship between Cy3 and Cy5 intensities was desired. Fold changes were given relative to the control channel, Cy3. The reports of composite ratios between Cy5 / Cy3 were filtered to show genes which were 1.5 fold or more up- or down-regulated in test versus control samples.

Microarray analysis of cell lines SW480 GFP-lamin A 2bb3, GFP-emerin 2 and GFP 2 was done in a three-way pair-wise manner, where each pair of cell lines were analysed in triplicate and significant gene changes common to all repeats were chosen to be confirmed by RT-PCR.

### 2.9.7 RT-PCR confirmation of changes in expression of selected genes

Primers to c-myc (V00568), c-raf (X03484), ribosomal protein L31 (RPL31) (NM_000993) and synemin, isoform H (AJ310522), were designed (**Table 2.3**) as described in Section 2.8.1, Primer design. Semi-quantitative RT-PCR was set up exactly as for lamin B2, including the appropriate negative controls (see Section 2.8.4), using the same total RNA isolated for microarray analysis. Thus RT-PCR using each pair of primers was replicated on three separate RNA samples for each cell line.

Optimized PCR cycling conditions for c-myc and synemin: 1 cycle at 94°C for 2 minutes, 25 cycles (26 cycles for synemin) at 94°C for 45 seconds, 59°C for 1 minute and 72°C for 1 minute and 1 cycle at 72°C for 5 minutes; c-raf: 1 cycle at 94°C for 2 minutes, 25 cycles at 94°C for 45 seconds, 60°C for 1 minute and 72°C for 1 minute and 1 cycle at 72°C for 5 minutes and RPL31: 1 cycle at 94°C for 2 minutes, 25 cycles at 94°C for 45 seconds, 56°C for 1 minute and 72°C for 40 seconds and 1 cycle at 72°C for 5 minutes. β-actin RT-PCR was performed as a positive and loading control utilizing the same PCR profile standardized in Section 2.8.4.

PCR products were analysed by gel electrophoresis and subsequent densitometry as outlined in Section 2.8.5 and Section 2.10.1. Products were confirmed by DNA sequencing with c-myc antisense, c-raf antisense, synemin antisense and RPL31 antisense primers (**Table 2.3**) using an ABI Prism® 377 XL automated DNA sequencer (Applied Biosystems), exactly as described in Section 2.8.6.

## *2.10 Miscellaneous: applications relevant to more than one experimental procedure*

### 2.10.1 Densitometry

Western blot and RT-PCR bands were digitally scanned in a Fujifilm Intelligent Dark Box II (Fujifilm Medical Systems, Edison, NJ) directed by Fujifilm Image Reader LAS-1000 Pro Ver. 2.11 software and intensities quantified in Image Gauge version 4.0 (Fujifilm).

# CHAPTER 3 – CHARACTERIZATION OF COLORECTAL CANCER CELL LINES

## *3.1 Introduction*

### 3.1.1 Nuclear lamin expression in cancer

Differential expression of lamins, particularly lamin A/C has been associated with epithelial, lymphoid and mesenchymal tumours, including basal skin cell carcinoma (Tilli *et al.*, 2003; Venables *et al.*, 2001), human non-small cell lung cancer, small cell lung cancer (Broers *et al.*, 1993; Kaufmann *et al.*, 1991), acute lymphoblastic leukaemia, non-Hodgkin's lymphoma (Stadelmann *et al.*, 1990), metastatic leiomyosarcoma, rhabdomyosarcoma and chondrosarcoma (Cance *et al.*, 1992). Two groups have investigated the changes in lamin A/C and lamin B1 expression in colorectal neoplasms, but their findings appear somewhat contradictory. Cance *et al.*, (1992) reported constitutive expression of lamin B (antibody did not differentiate between lamin B1 and B2) and heterogeneous expression of lamin A/C in two colon adenocarcinomas, determined by immunohistochemistry; Moss *et al.* (1999) reported reduced nuclear immunostaining for both lamins A/C and B1 in colon adenomas and adenocarcinomas, compared to normal tissue. Neither group was able to corroborate their observations by western blot analysis.

After considering the findings by Venables *et al.* (2001) which correlated a down-regulation of lamin A in basal skin cell carcinomas with a high proliferative index and a loss of lamin C with slower growth, the following seemed clear: First, that examining

the changes in expression of lamin A/C together may not in fact disclose the true nature of the relationship between A-type lamins and the development and progression of colon cancer. Second, that a panel of highly sensitive antibodies specific for individual lamin sub-types was required to quantify any change in lamin expression by western analysis. Fortunately, in our laboratory we have access to such a panel of lamin antibodies.

Monoclonal antibody JoL4 (anti-lamin A) reacts only with the lamin A tail domain, amino acids (aa) 573 to end and detects a 70 kDa band on a western blot of whole cell extracts. Monoclonal antibody JoL2 (anti-lamin A/C) reacts with the common domain of the lamin A/C tail, aa 464 - 572 and identifies both lamins A and C, seen on an immunoblot as 70 and 65 kDa bands respectively (Dyer *et al.*, 1997). An additional antibody, RalC (anti-lamin C), was raised in rabbit against the last eight amino acids of the lamin C tail domain making it specific for lamin C only (Venables *et al.*, 2001). This antibody detects a band of 65 kDa on western blot. LN43 (anti-lamin B2) is a monoclonal antibody specific for lamin B2 (Bridger *et al.*, 1993; Kill and Hutchison, 1995), seen as a 68 kDa band on immunoblot (Venables *et al.*, 2001). GaLB1 (anti-lamin B1), a polyclonal lamin B1 antibody raised in goat, was commercially obtained (Santa Cruz) and is visualized as a 67 kDa band on western blot (Venables *et al.*, 2001).

Original investigations into the presence of A- and B-type lamins in mammalian somatic cells led to the conclusion that they were constitutively expressed [reviewed by Gerace (1986)]. However, subsequent biochemical studies on developing mouse embryos, young animals and embryonal carcinoma (EC) cells and their differentiated derivatives revealed that expression of lamins A and C is not only developmentally regulated (Stewart and Burke, 1987) in a cell-type specific manner (Rober *et al.*, 1989),

but is closely associated with differentiation (Lebel *et al.*, 1987; Stewart and Burke, 1987). In general, an increased expression of lamin A/C appears to accompany tissue and cellular differentiation (Broers *et al.*, 1997; Coates *et al.*, 1996; Lebel *et al.*, 1987; Paulin-Levasseur *et al.*, 1989; Rober *et al.*, 1989; Stewart and Burke, 1987). Some of these studies show the synthesis of B-type lamins to be unaffected during differentiation (Lebel *et al.*, 1987; Paulin-Levasseur *et al.*, 1989), but analyses on adult human tissues using antibodies which distinguish between lamin B1 and B2 suggest individual B-type lamins may have different patterns of expression. Broers *et al.* (1997) found lamin B2 was universally distributed in all normal human tissues, except hepatocytes, whereas lamin B1 was expressed in a more cell-specific manner which appeared to be inversely correlated with differentiation in epithelial cells.

Originally described as units of architecture, lamins are type V intermediate filaments which form an orthogonal meshwork underlining the inner nuclear membrane, termed the nuclear lamina, which conveys mechanical strength to the nucleus (Aebi *et al.*, 1986), resisting deformation (Broers *et al.*, 2004; Lui and et al., 2000; Moir *et al.*, 2000b) and regulating nuclear shape (Schirmer *et al.*, 2001; Sullivan *et al.*, 1999) and size (Spann *et al.*, 1997). Lamins shape the nucleoskeleton by anchoring integral proteins of the inner nuclear membrane, positioning nuclear pore complexes and recruiting lamins to the nuclear lamina itself [reviewed by Hutchison (2002)]. Current evidence implicates lamins in the control of DNA replication and most interestingly, suggests they may organize interphase chromatin and play a role in regulating transcription.

In the quest to elucidate the function of lamins, nuclear binding partners of lamin A/C have been identified, revealing a possible mechanism by which A-type lamins may

promote tumour development. Markiewicz *et al.* (2002) demonstrated that lamin A/C in complex with LAP2α interacts with hypophosphorylated retinoblastoma protein, via pRb's nuclear localization signal sequence, located in pocket C, thus tethering it in the nucleus in G1 phase of the cell cycle. Previously, *in vitro* interaction between pRb and lamin A has been described by Ozaki *et al.* (1994). Hypophosphorylated pRb functions to silence genes necessary for cell proliferation by negatively regulating the transcription factor E2F (Chellappan *et al.*, 1991). Evidence suggests that nuclear anchorage of pRb is essential for its appropriate function: deletion mutants in pocket C of pRb, which are no longer tethered in the nucleus, have been shown to have oncogenic properties (Mittnacht and Weinberg, 1991). In addition, down-regulation of lamin A has been shown to accompany rapid tumour advancement (Venables *et al.*, 2001).

Based on these findings our group proposes that there is a causal link between lamin A expression and loss of pRb silencing function in tumour cells. We believe that down-regulation of lamin A will promote hyper-proliferation and dedifferentiation during carcinogenesis through an epigenetic mechanism. Here colorectal cancer is used as a model system for testing our hypothesis.

### 3.1.2 Selection of colorectal cancer cell lines

Colorectal carcinoma is known to develop over many years through a series of pathologically and histologically distinct stages. By explanting tissue from individual stages, cell lines can be created representing each order of malignancy, thus enabling *in vitro* studies of the molecular characteristics concomitant with disease progression. The initial aim of this project was to assemble a model system of cell lines with which the

nature of lamin expression with respect to colorectal cancer development could be investigated.

ECACC is an international provider of cell lines, particularly those derived from tumours. From this source the following four cell lines were selected which best represented the different Broders' grades (Broders, 1925) recognized in CRC: HT29 - a grade II colon adenocarcinoma cell line originating from a malignant primary tumour in a 44 year old Caucasion female (Fogh and Trempe, 1975); SW948 - a colon adenocarcinoma cell line isolated from a grade III (Dukes' class C) tumour in an 81 year old Caucasian female (Leibovitz *et al.*, 1976); SW480 - established from a grade IV (Dukes' class B) adenocarcinoma of the colon in a 50 year old Caucasian male (Leibovitz *et al.*, 1976) and T84 – a cell line derived from lung metastases of a colon carcinoma in a 72 year old male (Murakami and Masui, 1980). Metastatic tumour tissue was inoculated subcutaneously into BALB/c athymic mice, serially transplanted and established in *in vitro* culture without any change to the original histological characteristics of the tumour (Murakami and Masui, 1980; Reid *et al.*, 1978). Both SW948 and SW480 produce carcinoembryonic antigen (CEA), SW948 significantly more than SW480. Although HT29 was derived from a grade II colon adenocarcinoma it actually forms well-differentiated cultures consistent with grade I primary colonies, therefore an additional cell line, SW1116, was selected originally to be incorporated into this study. SW1116 represented a grade II adenocarcinoma of the colon which extended into the muscularis mucosae and was isolated from a 73 year old Caucasian male (Leibovitz *et al.*, 1976). However, this was later withdrawn from use in any experiments as it proved impossible to culture successfully. All cell lines used had an epithelial-like morphology.

### 3.1.3 Broders' grading compared to Dukes' staging of CRC tumours

At this point it is pertinent to explain how the classification of our CRC cell lines into grades compares to the accepted clinicopathological classification of colon carcinomas according to the Dukes' staging system (Dukes, 1932). As detailed in the Chapter 1, Section 1.2.5, the Dukes' staging system comprises Dukes' stages A, B and C and is based on the extent of spread. Stage D was added later by Turnbull *et al.* (1967) and indicates that a tumour has metastasized. On the other hand, Broders (1925) pioneered a system of categorizing tumours histologically according to their degree of differentiation. Tumours with 75 - 100% of cells differentiated are classified as grade I, tumours with 50 - 75% of cells differentiated as grade II, those with 25 - 50% of cells differentiated as grade III and those with 0 - 25% of cells differentiated as grade IV. Thus the CRC cell lines HT29, SW948 and SW480 can be thought of as representing increasing levels of dedifferentiation. The metastasized cell line T84 falls outside both Dukes' (1932) and Broders' (1925) original classification schemes because the cells were derived from a secondary site (lung).

However, the two systems of classification appear to compare favourably. Dukes (1932) showed that most grade I cases could also be categorized as Dukes' stage A; most grade II tumours were stage B and the majority of grade III and IV tumours were stage C. However, there was a degree of overlap and Dukes' stages A, B and C could not be correlated absolutely with Broders' grades I, II, III and IV. This system of grading also appears to correlate with prognosis, in that patients with grade I adenocarcinomas have the best prospects for survival after one year and the outlook becomes progressively poorer the higher the grade of tumour (Dukes, 1932; Rankin and Broders, 1928).

### 3.1.4 Summary

Previous analyses investigating the expression of nuclear lamins in colorectal cancer have proved inconclusive (Cance *et al.*, 1992; Moss *et al.*, 1999). Here a comprehensive expression study of lamins A, C, B1 and B2 in CRC cell lines HT29, SW948, SW480 and T84 using a panel of antibodies specific for individual lamin sub-types is presented. Correlation between proliferation / differentiation status of tumours and alteration in lamin behaviour is examined.

## *3.2 Results*

### 3.2.1 Optimization of cell culture conditions

The cell lines described previously were grown following the culture conditions stipulated by ECACC, recorded *verbatim* in Chapter 2, Section 2.2.1. Importantly, HT29 and T84 were grown in a 5% $CO_2$ equilibrated environment, whereas SW948 and SW480 were cultured under atmospheric conditions, necessitated by the use of Leibovitz's L-15 medium which was developed without a sodium bicarbonate buffering system and therefore formulated to support cells in a non-$CO_2$ environment (Leibovitz, 1963). The benefits of weaning all the cultures onto the same media and growing all in 5% $CO_2$ were considered. However, it was deemed judicious to maintain the cell lines in the growth conditions recommended by the supplier as, for the most part, they were those under which the cell lines had been isolated originally and therefore had been shown previously to give rise to healthy cultures (Fogh and Trempe, 1975; Leibovitz *et al.*, 1976; Murakami and Masui, 1980). Additionally, it was felt that altering the culture

conditions may, in fact, also alter some molecular characteristics which may inadvertently affect the accuracy of future data.

During the process of establishing the cell lines in our laboratory, it was necessary to make some modifications to the sub-culture routine of all the cell lines, despite consistent adherence to the culture conditions prescribed by ECACC, to ensure the healthiest cultures for experimental analysis. The improvements were mainly related to split ratio / re-seeding density and the trypsinization procedure. In brief: HT29 was the most robust cell line and grew more vigorously than any other, hence it was necessary to increase the split ratio recommended by ECACC to 1:10 – 1:12. SW948 had to be maintained at a high density and therefore was not split more than 1:2 in order to counteract the cells' predisposition to growing on top of each other. If allowed, this resulted in a sparse culture that never became fully confluent, but formed colonies that were extremely difficult to disaggregate. SW480 grew most actively if split no more than 1:4, while T84 were always slow growing and best if split 1:3. Interestingly, T84 proved more challenging to dissociate from the culture surface than the other cell lines. The optimized procedure involved 10 minutes incubation in 0.25% trypsin / EDTA at 37°C, yet still up to 20% of cells ordinarily remained adhered to the substrate.

### 3.2.2 Morphological and growth characteristics

From the outset it was clear that each cell line had distinctive morphological and developmental features, despite all cultures being epithelial in origin. **Figure 3.1** shows our model CRC cell system in a series of phase contrast micrographs which illustrate all the significant features of morphology and growth associated with each cell line.

Cell line HT29 grew as a homogeneous culture comprising cells shaped as moderately elongated spheres with a high nucleoplasmic to cytoplasmic ratio. It formed closely associated, adherent colonies which converged to form a monolayer. Contact inhibition was not obvious at sub-confluent levels, but when grown beyond 100% confluency cells continued to proliferate and became progressively more tightly packed. HT29 appeared least predisposed to cellular stratification, rather overgrowth ultimately led to monolayer sloughing.

In T84, examples of stratified (multi-layered) growth were only seen if cells were seeded too thinly, or if they were allowed to become over-confluent. Growth of T84 cells was noticeably constrained when cells were seeded at less than 25% density. In this situation, rather than expanding across the surface of the dish, cells accumulated in multi-layered clusters and took longer to fill the culture plate. As a rule healthy T84 cells were polyhedral in shape and formed a tightly packed and adherent monolayer. Neither cell size nor nucleoplasmic to cytoplasmic ratio appeared uniform. Cells varied from small size, with a high nuclear compared to cytoplasmic volume to large size with a low nucleoplasmic to cytoplasmic ratio. Nucleoli were sharply demarcated at 32X objective magnification, roundish to irregular in shape, sometimes presenting as bi-lobed structures, and varied greatly in diameter. Nuclei often contained more than the maximum number of four nucleoli expected in normal cells.

In contrast, SW948 and SW480 cells were highly anchorage independent. Cellular stratification was a feature of the cultures from the beginning and there was no clearer exponent of this phenomenon than SW480, a grade IV cell line. These cells were significantly larger than SW948, predominately epithelial-like (polygonal shaped cells), although a sub-population were bipolar, and frequently multinucleate. It was not

uncommon to see up to eight nuclei within a single cell. They grew in an uninhibited and non-uniform fashion. Some cells would grow as a single layer, while a proportion of neighbouring cells would grow in multiple layers (**Figure 3.1, C**). In contrast to the observation by Leibovitz *et al.* (1976) that only the bipolar cell population grew individually, I observed the epithelial-like cells forming islands and growing as individuals. A large proportion of cells were routinely observed floating in the media. At 32X magnification these 'floaters' were seen to be round, shrunken and displaying small, pericellular, bulbous protrusions (**Figure 3.1, G**). Although this culture appeared highly proliferative, these observations were thought to indicate that a high level of apoptosis was occurring within the culture.

SW948 cells were small and formed highly aggregated, stratified colonies making it impossible to identify individuals at 32X magnification. Although essentially adherent, their propensity to form multiple layers left them susceptible to mass detachment unless the culture was maintained above 50% density, seeded as monodisperse as possible and provided with fresh media every 48 hours. These cells have been reported to contain both microvesicular bodies and an evident glycocalyx (Leibovitz *et al.*, 1976). Similar to SW480, healthy cultures displayed increasing numbers of floating cells as the number of days growth increased. Again this was thought to be the consequence of apoptosis which is addressed in Section 3.2.3.

### 3.2.3 Cell cycle analysis

To determine the proportion of cells in each phase of the cell cycle and the presence of cells undergoing apoptosis, cell lines HT29, SW948, SW480 and T84 were expanded to 70% confluency, fixed in methanol, stained with the DNA intercalating dye Propidium

iodide (25 μg/ml) containing 100 μg/ml RNase to remove RNA and subjected to flow cytometric analysis.

Overall SW480 and T84 cells spent proportionally more time in S and G2/M phases of the cell cycle than in G0/G1, compared to HT29 and SW948 cells (**Figure 3.2**). Approximately two thirds of HT29 and SW948 cells were in G0/G1 and therefore proportionally less were in S and G2/M phases. The difference between the proportion of HT29 and SW948 cells compared to SW480 and T84 cells in G0/G1 was significant and indicates that while all cultures were proliferating, SW480 and T84 exhibited a higher rate of cell growth compared to HT29 and SW948.

Nuclear fragmentation, incorporating DNA fragmentation and DNA loss, is a key feature associated with apoptosis, thus apoptotic cells can be identified through their reduced stainability with PI resulting in a sub-G0/G1 peak (Sgonc and Gruber, 1998). A distinct region below the G0/G1 peak was expected but not detected for SW480. However, this may be explained by the method used to prepare the cells (see Chapter 2, Section 2.5). All floating cells were removed and discarded prior to trypsinization and consequently adherent cells only were prepared for flow cytometry. Hence this protocol may have resulted in the inadvertent removal of any apoptotic population. Nevertheless a sub-G0/G1 peak was identified in SW948 cells, supporting the idea that a degree of apoptosis was occurring in this culture. In all replicate analyses of T84 it appeared that a very small proportion of cells exhibited reduced PI staining which may therefore be indicative of low-level apoptosis within this culture. No evidence of apoptosis in HT29 cells was apparent, however the potential inadequacies of the protocol used should be taken into consideration before making any firm conclusions regarding the four cell lines examined.

### 3.2.4 The relationship between lamin expression and colorectal cancer progression

#### *3.2.4.1 Lamin A is down-regulated in pre-metastatic cells*

To investigate the expression pattern of individual lamins in relation to the degree of tumour differentiation, both western blotting and immunofluorescence techniques were applied to the colorectal carcinoma cell lines HT29, SW948, SW480 and T84 which represented tumour grades II, III, IV and a lung metastasis of a colon carcinoma respectively.

Protein expression profiles (**Figure 3.3**) revealed differential expression of lamin A (**A**) and B2 (**D**) with respect to the degree of cellular differentiation. Lamin C and B1 expression appeared unchanged. Lamin A expression was significantly decreased in tumour grades III and IV. Expression was reduced by an average 52% in grade III and 57.7% in grade IV tumour cells compared to grade II cells (**Figure 3.4, A**). Higher levels of lamin A expression were maintained in grade II and metastasis samples, although lamin A expression in lung metastasis cells was, on average, 15.5% greater than in grade II cells. Standardizing the level of lamin C expression against β-actin showed that it was overall similar at every stage of the disease (**Figure 3.4, B**). Expression in grade II, IV and metastasis cultures was nearly 100%, although a 20.5% reduction in lamin C expression between grade II and grade III cells was observed.

Expression of lamin B1 was similar, if not identical across all grades of colorectal carcinoma - no cell line exhibited less than 90% expression compared to the grade IV sample which was designated 100% (**Figure 3.4, C**). Densitometric analysis of lamin B2 immunoblots (**Figure 3.4, D**) demonstrated that the average expression of lamin B2

increased by 29.5% between grade II and grade III, reduced by 68% between grades III and IV before recovering in the metastasized cells to a level of expression which was 22% higher than in grade IV, but 46% lower than in grade II.

To analyse the nuclear distribution of lamins in our model system of colorectal cancer cell lines, single indirect immunofluorescence with the aforementioned panel of anti-lamin antibodies was performed (**Figures 3.5, 3.6 & 3.7**). Double immunostaining analyses followed to investigate the relationship between lamin A and A/C expression and cellular proliferation, using proliferation indices Ki67 and PCNA (**Figure 3.8**). Initial attempts to perform single indirect immunofluorescence with the lamin A-specific antibody JoL4 resulted in poor quality staining, therefore JoL2 (anti-lamin A/C) was used preferentially to determine the distribution of lamin A (**Figure 3.5.1**) compared to the distribution of lamin C, ascertained by single staining with the lamin C-specific antibody, RaLC (**Figure 3.5.2**).

Lamin A/C staining (**Figure 3.5.1**) was nuclear specific in all colorectal cancer cell lines and was generally localized to the nuclear rim. Only in T84 did a minority of cells show nucleoplasmic distribution of lamin A/C. The majority of cells were positive for lamin A/C. Limited cells in HT29, SW948, SW480 and T84 were not stained, although the intensity of staining was brightest in HT29 and T84 cells. HT29 nuclei exhibited multiple lamin A/C positive invaginations (arrows). Using RaLC, lamin C appeared evenly distributed around the nuclear rim in all cancer cell lines and the intensity of staining was equivalent across all grades (**Figure 3.5.2**). All cells, barring a negligible number of T84 cells, were positive for lamin C.

Indirect immunofluorescence of B-type lamins showed that, as expected, staining was associated very strongly with the nuclear envelope. Lamin B1 staining was similar in all cancer grades (**Figure 3.5.3**), whereas lamin B2 exhibited dynamic changes in expression levels as the cell lines became progressively more neoplastic (**Figure 3.5.4**). All SW948 cells strongly expressed lamin B2, compared to HT29 and T84 cells which showed positive, but weaker staining. SW480 cells displayed a unique mosaic pattern of lamin B2 expression. While 41.7% of cells were brightly positive (for example, see arrows in panels G and I), 58.3% of cells were lamin B2 negative (for example, see arrow heads in panels G and I). Two hundred cells were analysed.

To confirm that this mosaic-like pattern of lamin B2 expression was a consistent feature of SW480 cells alone, all cell lines were immunostained with the lamin B2 antibody, LN43, serially diluted from 1:10 to 1:100 (**Figure 3.6**). Concomitant with increasing antibody dilution, the intensity of lamin B2 staining decreased in cell lines HT29 (**Figure 3.6.1**), SW948 (**Figure 3.6.2**) and T84 (**Figure 3.6.4**), but the protein remained uniformly expressed in all cells. In SW480 (**Figure 3.6.3**), cells expressing lamin B2 showed a reduction in staining intensity as antibody concentration decreased, but positive staining was still detected at 1:100 antibody dilution. However, a large population of lamin B2 negative cells was always present. This offers an explanation as to why there was a 68.1% reduction in lamin B2 protein levels between grade III and grade IV cells when assessed by western blot (**Figure 3.3, D / 3.4, D**): It is not the overall level of lamin B2 expression which is diminished across the SW480 culture, but rather a selective loss of lamin B2 in the majority of cells.

To confirm immunoblotting and immunofluorescence data indicating that lamin A is down-regulated to a pre-metastatic stage, the colorectal cancer cells lines were stained

with JoL2 at a dilution of 1:50 which just detected lamin A/C expression in the cell line HT29 (**Figure 3.7**). The aim of this experiment was to accurately observe differences in lamin A/C expression between the cell lines by ensuring the signal was not saturated. Interesting differences became apparent. While lamin A/C staining was readily detectable in HT29 and SW948 cells, it was almost completely absent from SW480 cells. Staining was comparatively high in T84 cells. Western analysis indicated that SW480 cells express the least amount of lamin A (**Figure 3.3, A / 3.4, A**) and this immunocytochemical experiment supports a uniform down-regulation of lamin A in grade IV CRC cells.

### *3.2.4.2 Down-regulation of lamin A in SW948 and SW480 cells does not correlate with proliferation indices*

Given that reduced expression of lamin A has been associated with more proliferative cell types (Broers *et al.*, 1997; Venables *et al.*, 2001) and our CRC cell lines represent progressive dedifferentiation, it was reasoned that loss of lamin A expression in the least differentiated cell lines SW948 and SW480 may be concomitant with increased expression of proliferation markers Ki67 and PCNA. To investigate this hypothesis the CRC cells lines were subjected to further immunocytochemical analyses involving double-staining with lamin antibodies, JoL4 (anti-lamin A) or JoL2 (anti-lamin A/C) and proliferation marker antibodies, Ki67 or PCNA (**Figure 3.8**).

Importantly, **Figures 3.8.1** and **3.8.3** confirm that there is a down-regulation of lamin A in SW948 and SW480 cells compared to HT29 and T84, demonstrated by reduced nuclear staining with JoL4. However, there appeared to be no correlation between loss of lamin A or A/C expression and expression of proliferation marker Ki67 (**Figures**

**3.8.1** & **3.8.2**) or PCNA (**Figures 3.8.3** & **3.8.4**). For each cell line co-stained with anti-lamin A/C and Ki67, two hundred cells were analysed. In each cell line the percentage of Ki67 expressing cells was comparable at approximately 95% (HT29 - 95%, SW948 - 98%, SW480 - 99% and T84 - 94.5%), although clear variations in lamin A/C expression were observed.

### *3.2.4.3 Loss of lamin A in SW948 and SW480 cells appears to be the result of both transcriptional and post-transcriptional mechanisms*

The loss of expression of lamin A from SW948 and SW480 cells leads to the question: At what level is expression of lamin A regulated in these cells? Lamin A and lamin C mRNA instability or preferential use of the alternative splice site, favouring the generation of one mRNA over the other, have been suggested previously as mechanisms for transcriptional control of cell-type specific expression of A-type lamins (Lin and Worman, 1997). Hence the amount of lamin A and lamin C transcript present in each colorectal cancer cell line was assessed.

Semi-quantitative RT-PCR was carried out on equal concentrations of total RNA (verified by β-actin RT-PCR – **Figure 3.9, C**) using primers specific for lamin A (**Figure 3.9, A**) and lamin C (**Figure 3.9, B**). The *LMNA* gene yields three transcript variants in somatic cells - lamin A, lamin C and the less abundant lamin AΔ10 - by alternative splicing of exon 10 (Machiels *et al.*, 1996). Although the lamin C messenger sequence lacks the whole of exon 11 and 12 it is in complete consensus with lamin A but for 21 nucleotides at the 3′ terminus which constitutes six lamin C-specific codons and a TGA termination codon which are spliced during the synthesis of prelamin A (Lin and Worman, 1993). Therefore to amplify lamins A and C independently a system was

used whereby a universal sense primer complementary to lamin A/C was combined either with an antisense primer specific for exons 11 / 12 in order to amplify lamin A, or with an antisense primer specific for the unique 21 bases at the 3′ end of lamin C in order to amplify lamin C specifically. Consequently the lamin A and lamin C RT-PCR products could be separated by size on an agarose gel. Primers for this experiment were already available in the laboratory, but were originally designed for Allelic Refractory Mutation Specific - Polymerase Chain Reaction (ARMS-PCR) to detect single nucleotide polymorphisms in AD-EDMD cell lines with known mutations in the *LMNA* gene (Alvarez-Reyes, 2003). The ARMS-PCR strategy necessitates a mismatch in the second or third last base of one primer, in this case the sense primer, whether it is to be used to distinguish the mutant or the wild-type allele.

Thus the lamin A/C wild-type sense primer used in this thesis had the sequence:

5′-GATGCGCTGCAGGAACTACG- 3′.

But the actual wild-type lamin A/C sequence is:

5′-GATGCGCTGCAGGAACTGCG-3′.

However, this mismatch was designed to stabilize the primer and facilitate a more efficient RT-PCR, rather than restrict it.

RT-PCR experiments revealed that in grade III (SW948) cells levels of lamin A mRNA were largely reduced compared to the other CRC cell lines examined (**Figure 3.10, A**). The difference in lamin A mRNA expression between grade II (HT29) and grade III cells was statistically significant. Grade IV (SW480) cells expressed similar levels of lamin A messenger as grade II and metastasis (T84) cells, suggesting that lamin A is down-regulated at the protein level by different mechanisms in grade III and grade IV CRC cells. Quantitative variation in the amount of lamin C transcript in each cell line

was calculated using densitometry (**Figure 3.10, B**), but deviation between replicates meant that relative differences in lamin C mRNA expression were not significant. Sequence analysis of lamin A and lamin C RT-PCR products demonstrated that the primers used were sub-type specific (**Figure 3.11**).

#### *3.2.4.4 Changes in lamin B2 expression are transcriptionally regulated*

Grade II, III, IV and metastasis CRC cell lines were subjected to semi-quantitative RT-PCR using primers specific for lamin B2 (**Figure 3.12**). Changes in lamin B2 at the mRNA level followed a similar pattern to those observed at the protein level (**Figure 3.3, D** & **Figure 3.4, D**). Grade III cells exhibited the highest level of mRNA expression which correlates with their protein profile. Lamin B2 mRNA expression in grade IV and metastasis cells also followed the same pattern as that seen at the protein level, i.e. the metastasis cells displayed more lamin B2 transcript than grade IV cells. However, in grade II cells messenger RNA expression appeared proportionally lower than protein expression, relative to grade III cells. In general it appears that the dynamic changes in lamin B2 protein expression observed in CRC cell lines HT29, SW948, SW480 and T84 (**Figure 3.3, D** & **Figure 3.4, D**) are predominantly the result of transcriptional regulation. Sequence analysis of lamin B2 RT-PCR products confirmed the specificity of the lamin B2 primers (**Figure 3.13**).

### *3.3 Discussion*

Expression and distribution of nuclear lamins A, C, B1 and B2 was investigated in a model system of cell lines representing the progression of colorectal cancer from a

relatively differentiated phenotype (Broders' grade II) to a highly dedifferentiated phenotype (Broders' grade IV), to metastasis. Protein profiling and indirect immunofluorescence analyses identified changes in the expression of lamins A and B2 during the advancement of CRC. In contrast lamin C and B1 expression appeared constant in all grades of the disease. Specifically, lamin A was down-regulated in the more dedifferentiated cell lines SW948 and SW480 (grade III and IV respectively) which displayed morphological abnormalities including loss of contact inhibition, stratified growth and an apparently weaker adherence to the tissue culture substrate. Lamin A expression was not similarly reduced in the lung metastasis cell line T84 which displayed a higher level of lamin A expression than in HT29 (grade II) cells. Interestingly, although T84 is derived from metastases, in the presence of serum it has been shown to grow in a monolayer, establish tight junctions between cells and form microvilli on the plasma membrane facing the media (Dharmsathaphorn *et al.*, 1984). In short it retains the structural polarity and morphology associated with differentiated epithelial cells. The corollary of this is that loss of lamin A appears to accompany dedifferentiation of colorectal cancer cells and therefore their progression towards neoplasia.

Lamin B2 expression appeared to be dynamically regulated in CRC cells, primarily at the level of transcription, given that SW948 cells were found to exhibit the highest relative level of protein expression and the highest relative transcript copy number. However, unlike lamin A, changes in lamin B2 expression cannot be described as a dedifferentiation-associated event. Despite a very large reduction in relative protein expression between SW948 and SW480 cells, HT29 cells expressed only very low levels of lamin B2 compared to the less well differentiated SW948 cell line. However, it was established that lower levels of lamin B2 expression in a cell line were not

necessarily the result of uniform diminution of the protein across all cells, but could be attributed to large variations within a cell line. This was demonstrated in SW480 cells in which the majority of cells displayed complete loss of expression, while the remaining cells expressed lamin B2 at levels similar to those observed in cell lines expressing uniformly high levels of lamin B2.

The first evidence of a differential relationship between lamins A and C and tumour growth was presented by Venables *et al.* (2001). Studies on lamin expression in basal cell carcinomas of the skin found a correlation between loss of lamin A and fast tumour growth, whereas a down-regulation of lamin C appeared to coincide with slower tumour growth. Hence I decided to investigate the relationship between lamin A, C, B1 and B2 expression and the proliferative capacity of CRC cells.

Flow cytometric analyses showed HT29 and SW948 cells to be slow growing and SW480 and T84 cells to be faster growing. Comparative immunofluorescence analyses revealed that Ki67 expression was fairly constant in all cell lines despite a clear reduction in lamin A expression in SW948 and SW480 cells. In addition, no appreciable relationship between PCNA expression and lamin A levels was observed. Thus no correlation between lamin A expression and overall cell growth rate or proliferation status could be engendered in our chosen colorectal cancer cell lines. There does appear, however, to be an inverse correlation between lamin B2 expression and growth rate - the slower growing cells (HT29 and SW948) expressed the highest level of lamin B2.

The loss of lamin A in SW948 and SW480 cells posed the intriguing question: Was this regulated at the level of transcription or post-transcriptionally? Semi-quantitative RT-PCR was performed on RNA extracted from all four CRC cell lines using primers

which differentiated between lamin A and lamin C transcript variants. As expected no significant change in lamin C mRNA levels was observed. In SW948 cells, the lamin A message was barely detectable, whereas in HT29, SW480 and T84 cells it was more strongly expressed. This suggests that loss of lamin A in SW948 cells is regulated at the level of transcription, but in SW480 cells it is most likely regulated post-transcriptionally. Essentially, down-regulation of lamin A appears to result from two different mechanisms in the cell lines investigated.

Previously, transcriptional regulation of *lamin A/C* gene expression has been reported. Research by Kaufmann *et al.* (1991) demonstrated that an up-regulation of lamins A and C in v-*ras*$^{H}$-expressing small cell lung carcinoma (SCLC) cells was the result of an augmentation in mRNA synthesis. Later, Broers *et al.* (1993) ascribed down-regulation of lamin A/C in the SCLC sub-type to the absence of A-type lamin transcripts. Furthermore, the same group observed preferential repression of lamin A expression relative to lamin C in a human lung adenocarcinoma cell line. Similar to our findings with SW948 CRC cells this imbalance was later shown to be controlled at the mRNA level (Machiels *et al.*, 1995). Recently, studies on the premature ageing disease Hutchinson-Gilford progeria syndrome have also illustrated a post-transcriptional mechanism by which lamin A expression may be abrogated but lamin C unaffected. In HGPS loss of functional lamin A has been attributed to incomplete processing of prelamin A to mature lamin A as the result of single-base substitutions in the lamin A tail domain which do not affect lamin C (Eriksson *et al.*, 2003).

In summary these results indicate that lamin A alone is down-regulated by both transcriptional and post-transcriptional mechanisms in morphologically abnormal cultured colorectal carcinoma cells. Furthermore the regulation of lamin A expression

appears not to be correlated with cell proliferation, but rather the differentiation status of cells. This suggests that expression of lamin A may be functionally significant in maintaining the typical epithelial morphology associated with differentiated tissue. Performing a functional rescue of lamin A negative cells would enable the effect of lamin A on morphology to be studied. Comparing overall gene expression profiles in lamin A positive and lamin A negative cells would facilitate more detailed investigations into the role of lamin A as a possible epigenetic regulator of colorectal cancer-associated genes.

### *3.4 Figures*

**Figure 3.1**

**Morphology of colorectal cancer cell lines.** Phase contrast micrographs of human colon cancer cell lines HT29, SW948, SW480 and T84 were taken at 10X (panel I) and 32X (panel II) objective magnification. These cell lines formed the basis of a model cell system used to investigate changes in lamin expression with respect to CRC progression. HT29, SW948 and SW480 originated from grade II, III and IV colon adenocarcinomas respectively and T84 represents a lung metastasis of colon carcinoma. HT29 and T84 cells formed compact, adherent colonies (**A**) which converged, in general, to form a single sheet of cells (**B**). SW948 and SW480 cells were conspicuously anchorage independent. The tightly packed colonies formed by SW948 were universally stratified and in SW480 islands of epithelial cells (**C**) were consistently observed. SW480 contained a mixture of epithelial-like (**E**) and bipolar (**F**) cells, epithelial cells predominating, and exhibited a high proportion of multinucleate cells (**M**).

Few floating cells (**D**) were observed in HT29 and T84 cultures, but significantly more were routinely found in SW948 and SW480 cultures. In SW480 these 'floaters' (**G**) appeared shrunken and displayed small, pericellular protuberances.

Scale bar: Panel I – 40 μm; panel II – 20 μm.

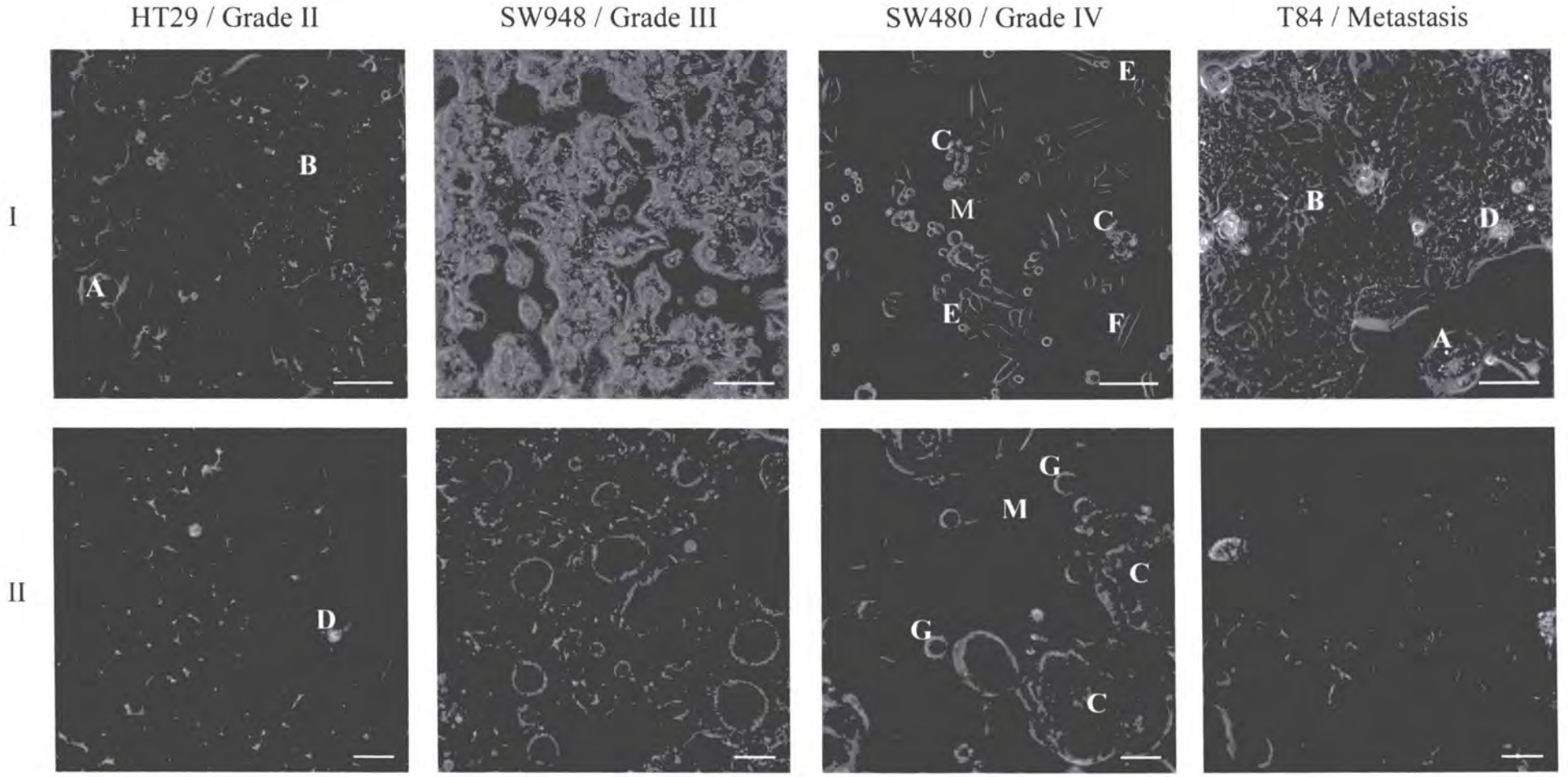
HT29 / Grade II
SW948 / Grade III
SW480 / Grade IV
T84 / Metastasis
I
II
A
B
C
D
E
F
G
M

Figure 3.1

**Figure 3.2**

**Cell cycle characteristics of human colorectal cancer cell lines.** HT29 (grade II), SW948 (grade III), SW480 (grade IV) and T84 (metastasis) cells, upon reaching 70% confluency, were fixed in ice-cold methanol, stained with a 25 μg/ml Propidium iodide solution and analysed by flow cytometry. Relative cell size and granularity is characterized by forward scatter (FS) and side scatter (SS) intensity, left panels (a, c, e & g). Data for more than 10,000 monodisperse events were collected and PI fluorescence is shown in the right panels (b, d, f & h). Cells in G0/G1 are indicated by gate E, cells in S-phase, by gate F and cells in G2/M, by gate G. The proportion of cells in G0/G1 phase of the cell cycle [given as mean ± standard deviation (s.d) of three replicates] was significantly higher in HT29 and SW948 cells compared to SW480 cells (HT29: $t = 4.46$, $df = 4$, $P < 0.05$; SW948: $t = 3.77$, $df = 4$, $P < 0.05$) and in HT29 and SW948 cells compared to T84 cells (HT29: $t = 7.73$, $df = 4$, $P < 0.005$; SW948: $t = 3.71$, $df = 4$, $P < 0.05$) showing that HT29 and SW948 cells were less proliferative than SW480 and T84 cells. Student's *t*-test was 'two-tailed'.

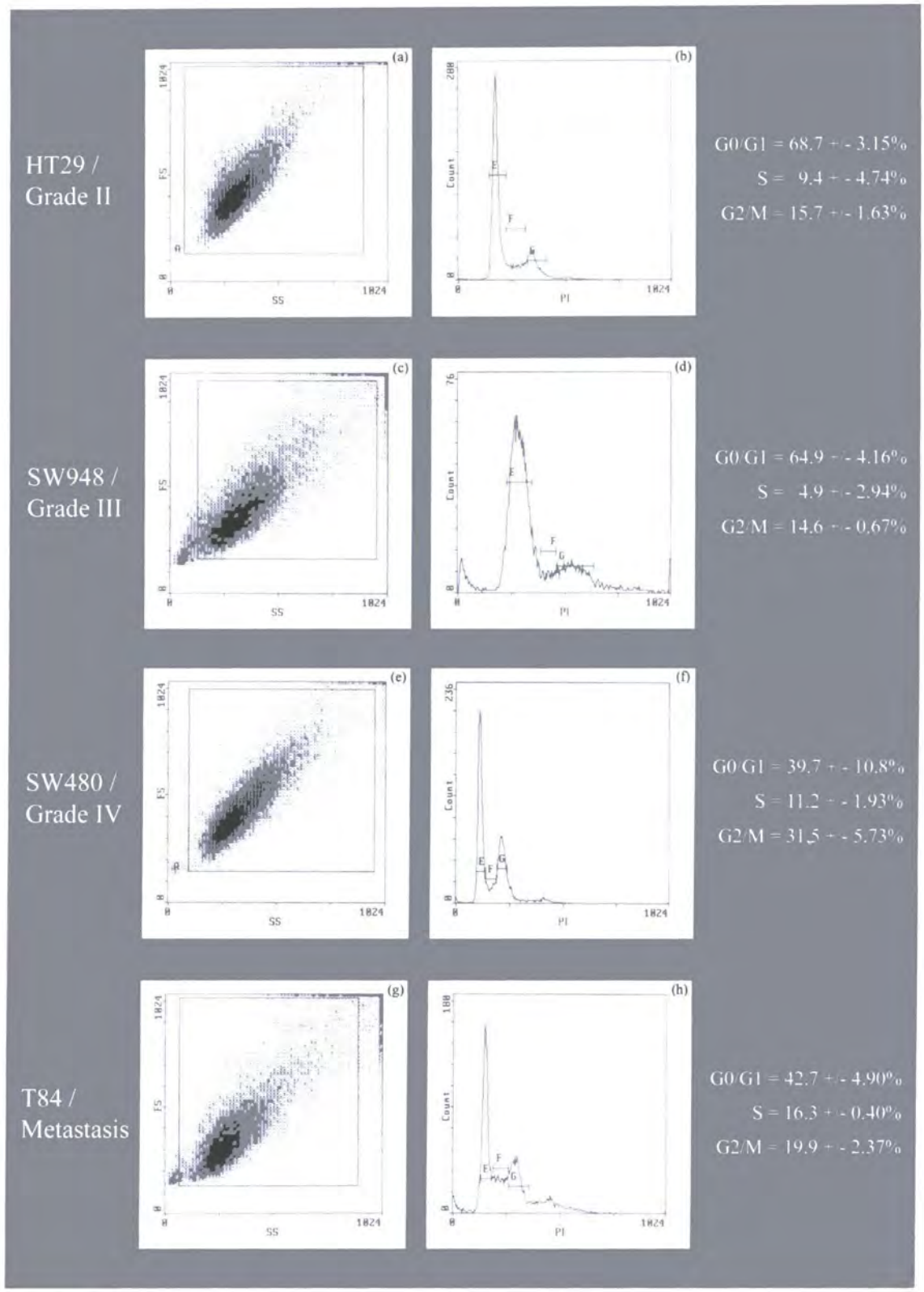
HT29 /
Grade II
(a)
(b)
G0/G1 = 68.7 +/- 3.15%
S = 9.4 +/- 4.74%
G2/M = 15.7 +/- 1.63%
SW948 /
Grade III
(c)
(d)
G0/G1 = 64.9 +/- 4.16%
S = 4.9 +/- 2.94%
G2/M = 14.6 +/- 0.67%
SW480 /
Grade IV
(e)
(f)
G0/G1 = 39.7 +/- 10.8%
S = 11.2 +/- 1.93%
G2/M = 31.5 +/- 5.73%
T84 /
Metastasis
(g)
(h)
G0/G1 = 42.7 +/- 4.90%
S = 16.3 +/- 0.40%
G2/M = 19.9 +/- 2.37%
FS
SS
Count
PI
1024

Figure 3.2

**Figure 3.3**

**Characterization of A- and B-type lamin expression in colorectal cancer cell lines by western analysis.** Whole cell extracts from cells lines representing different grades of colon carcinoma - grade II (HT29) – lane 1, grade III (SW948) – lane 2, grade IV (SW480) – lane 3 and metastasis (T84) – lane 4 - were resolved on 10% SDS-PAGE, transferred to nitrocellulose and immunoblotted with one of monoclonal antibody JoL4 – anti-lamin A (**A**), rabbit polyclonal antibody RaLC – anti-lamin C (**B**), goat polyclonal anti-lamin B1 (**C**) and monoclonal antibody LN43 – anti-lamin B2 (**D**). β-actin was used as a loading control (**A** - **D**). Molecular weight markers (MW) are in kDa.

Immunoblots using specific anti-lamin A antibody, JoL4, revealed a down-regulation of lamin A to a pre-metastatic stage. Lamin C protein profiles appeared to change little as colon cancer developed.

It was expected that the B-type lamins would be equivalent in all grades of colorectal carcinoma as at least one B-type lamin is required for cell survival. While SDS-PAGE for lamin B1 supported this theory - lamin B1 expression was similar across all cell lines, lamin B2 exhibited dynamic changes as the disease progressed. A strong up-regulation was observed in grade III colorectal cancer cells compared to grade II cells, followed by a dramatic decline in expression in grade IV samples. In metastasized cells lamin B2 protein expression was partly recovered, but to a level lower than that detected in grade II cells.

A-type lamins

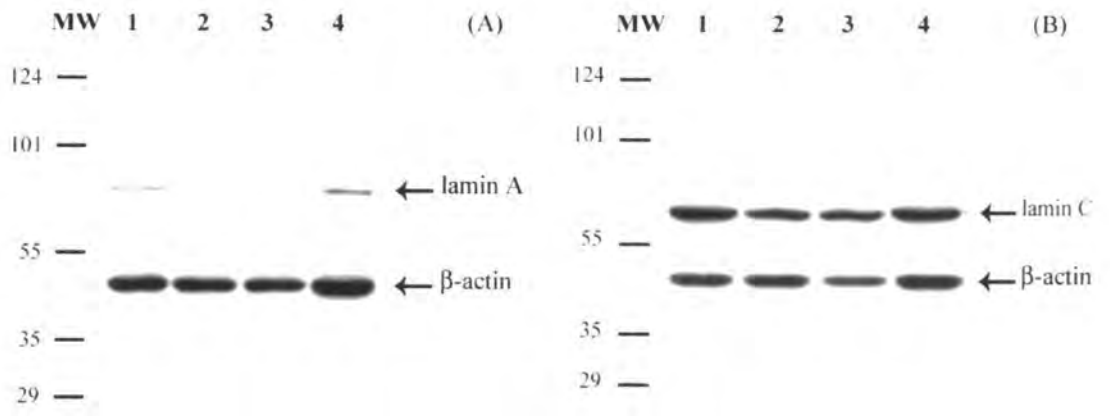


B-type lamins

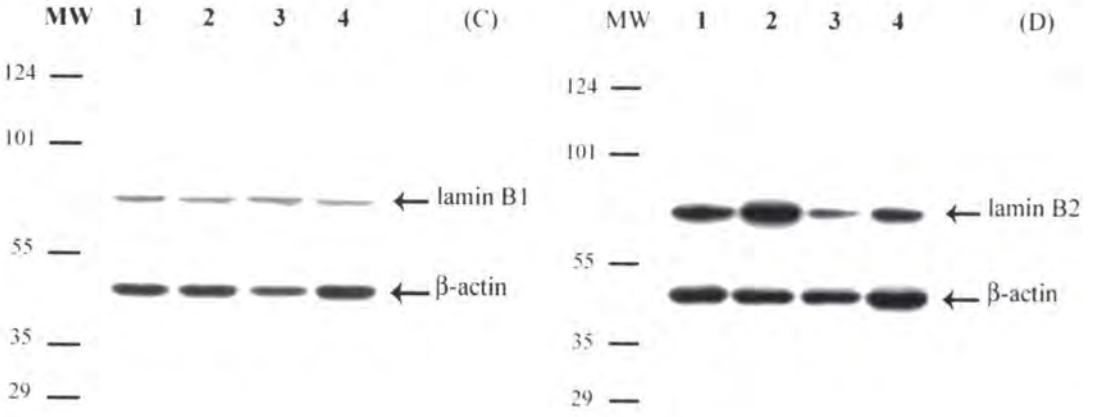


Figure 3.3

**Figure 3.4**

**Expression of lamins during colorectal cancer progression, normalized against β-actin.** Protein expression profiles of lamins A, C, B1 and B2 in grade II (HT29), grade III (SW948), grade IV (SW480) and metastasis (T84) colon carcinoma cells, see **Figure 3.3**, were digitally scanned in a Fujifilm LAS-1000 Intelligent Dark Box II Image Reader and quantified by densitometry using Fujifilm Image Gauge software, version 4.0. Measurements (in arbitrary units) of individual protein levels in each cell line were standardized against β-actin expression for both replicate experiments and an average taken. Relative expression levels for individual lamins were calculated, considering the cell line with the highest average expression level for each protein to be 100%.

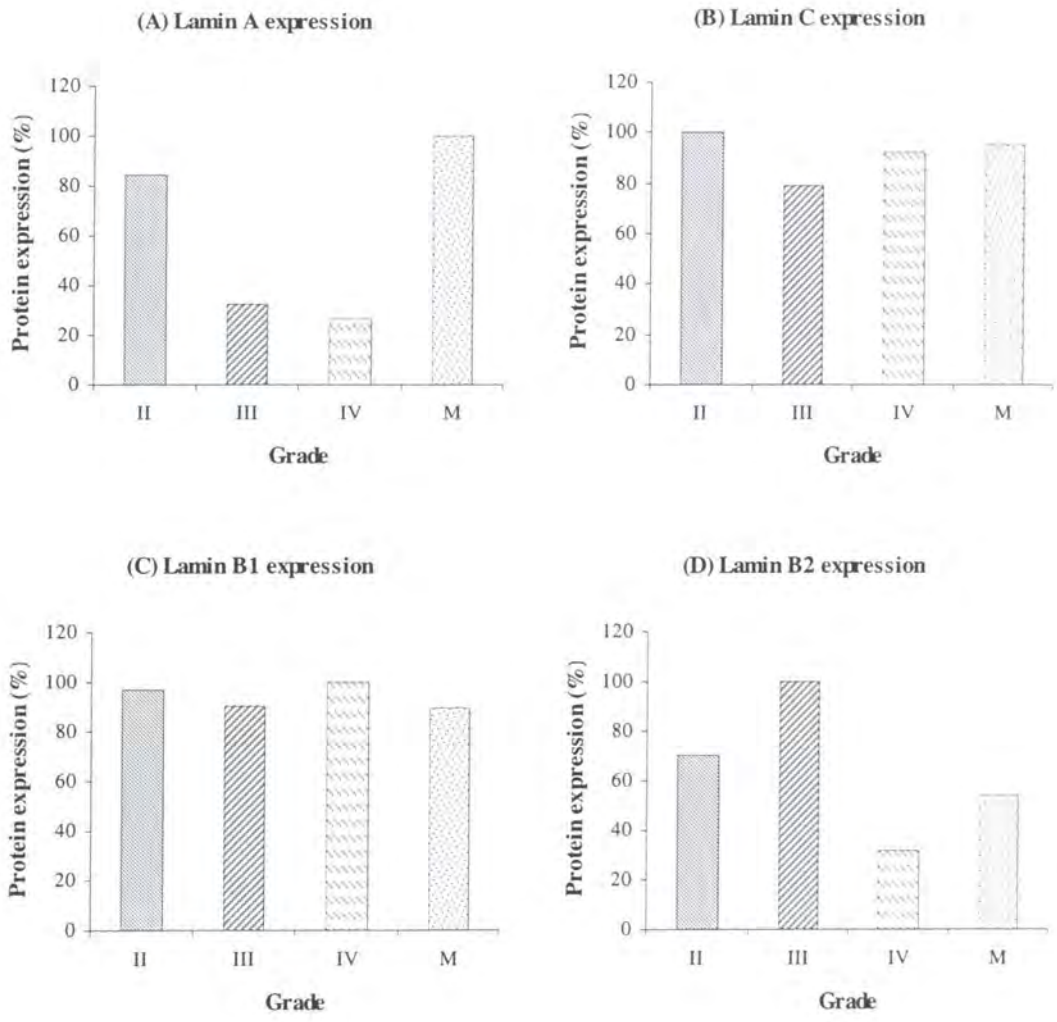
(A) Lamin A expression
Protein expression (%)
120
100
80
60
40
20
0
II
III
IV
M
Grade
(B) Lamin C expression
Protein expression (%)
120
100
80
60
40
20
0
II
III
IV
M
Grade
(C) Lamin B1 expression
Protein expression (%)
120
100
80
60
40
20
0
II
III
IV
M
Grade
(D) Lamin B2 expression
Protein expression (%)
120
100
80
60
40
20
0
II
III
IV
M
Grade

Figure 3.4

**Figure 3.5**

**An immunocytochemical study of lamin distribution in colon tumour cells.** Grade II (HT29), III (SW948), IV (SW480) and metastasis (T84) colorectal carcinoma cells were fixed in methanol:acetone (1:1) and co-stained with either mAb anti-lamin A/C – JoL2, diluted 1:10 (**Figure 3.5.1**), rabbit anti-lamin C – RaLC, diluted 1:20 (**Figure 3.5.2**), goat anti-lamin B1, diluted 1:25 (**Figure 3.5.3**) or mAb anti-lamin B2 – LN43, diluted 1:10 (**Figure 3.5.4**) and DAPI to reveal the distribution of DNA. Lamin and DAPI staining are displayed separately in black and white micrographs (left panels - A, D, G & J and central panels - B, E, H & K) and as a composite image (right panels - C, F, I & L) in which lamin staining is shown in red or green, superimposed over DNA staining, shown in blue. Scale bar = 10 μm.

***Figure 3.5.1*** - arrows indicate nuclear invaginations.

***Figure 3.5.4*** - arrows demarcate lamin B2 positive cells, arrow heads indicate lamin B2 negative cells.

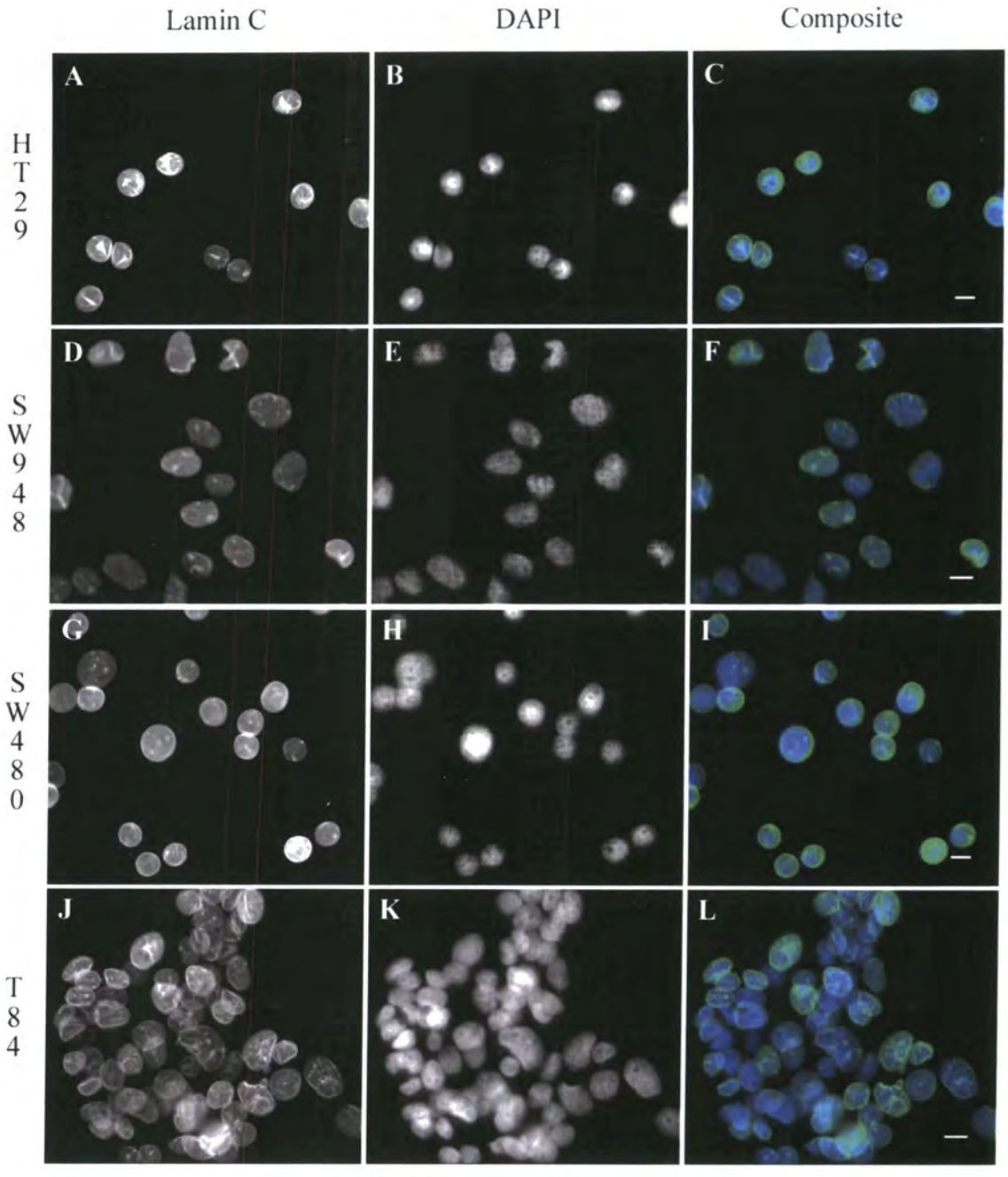


Figure 3.5.2

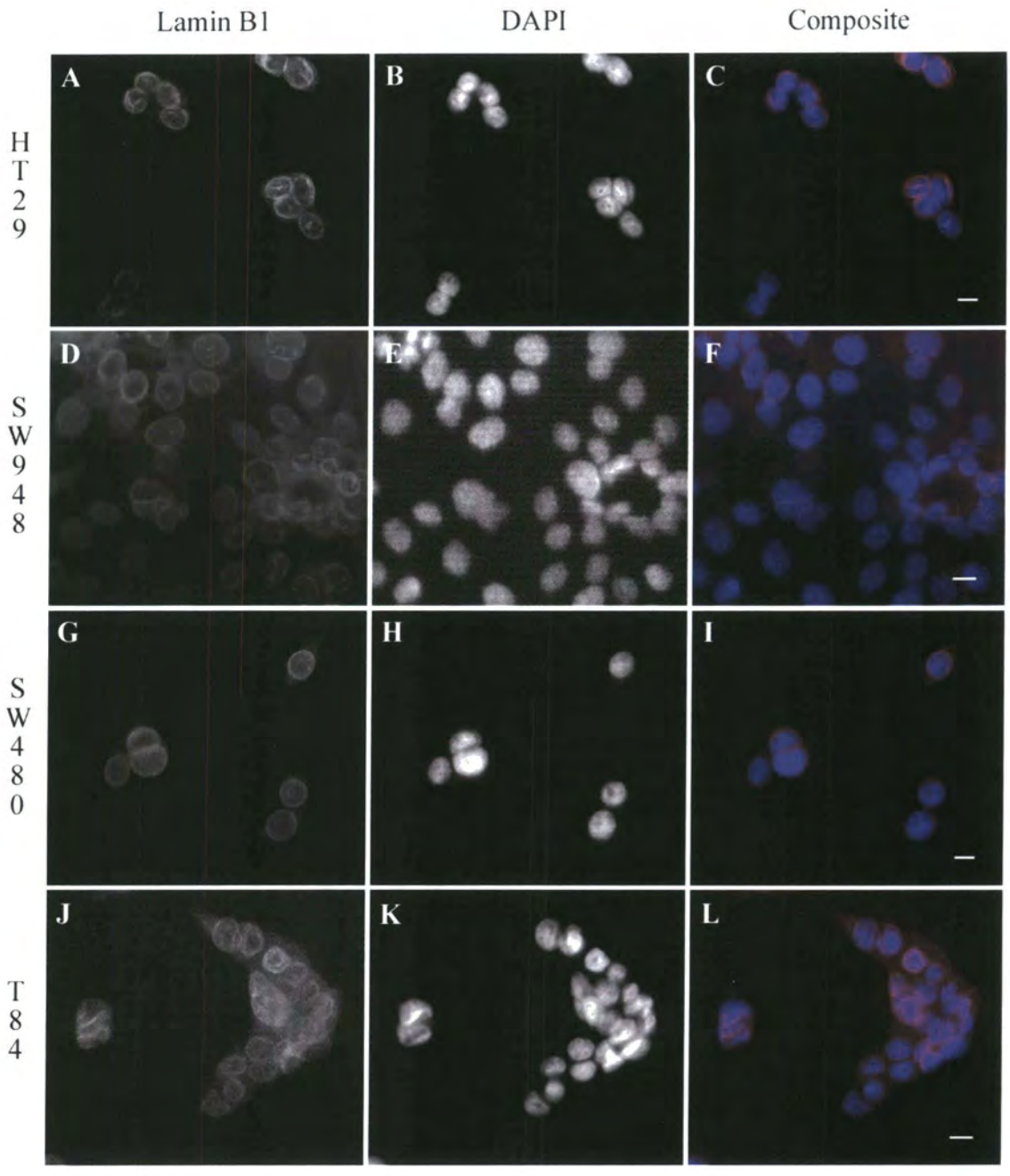


Figure 3.5.3

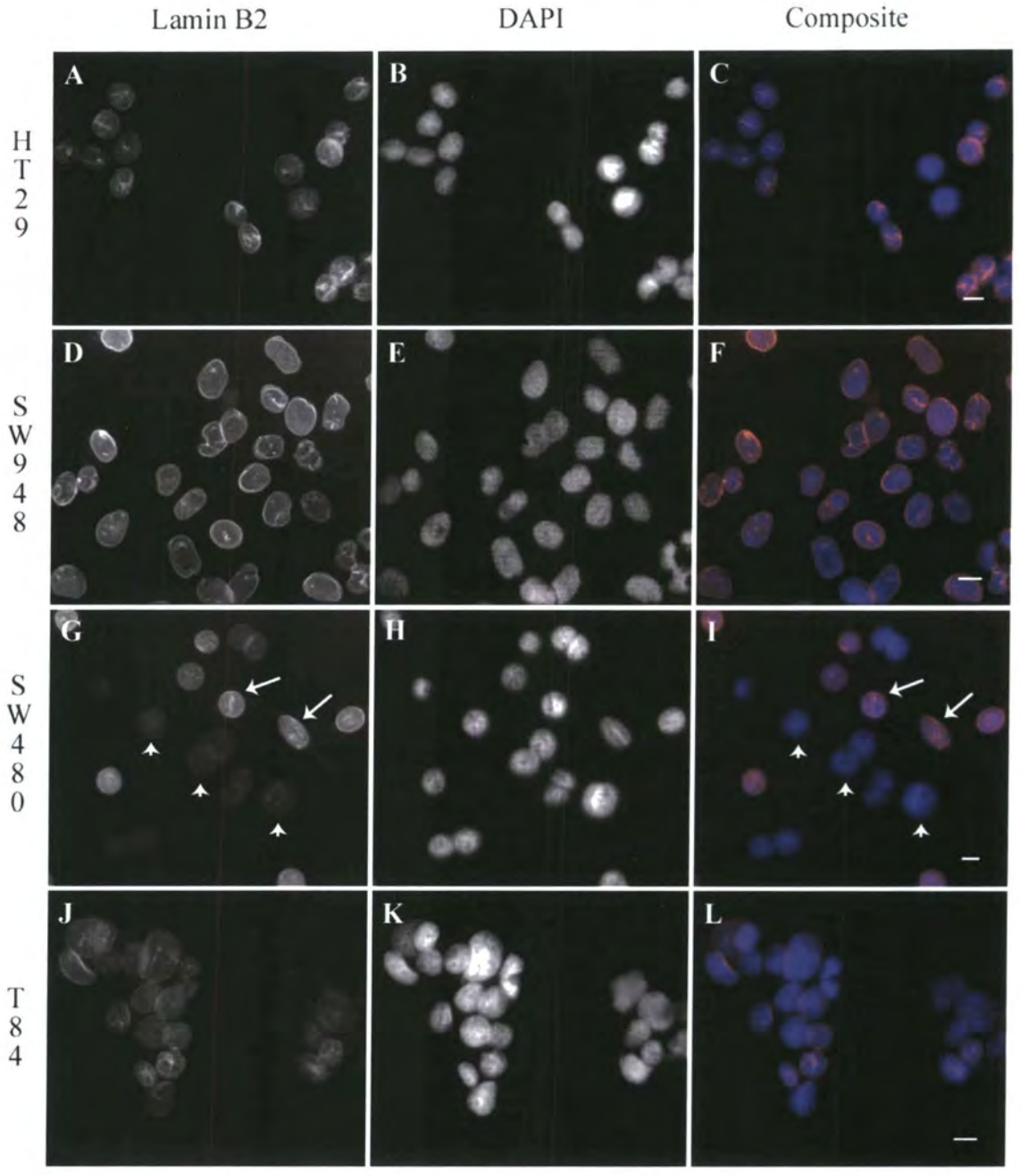


Figure 3.5.4

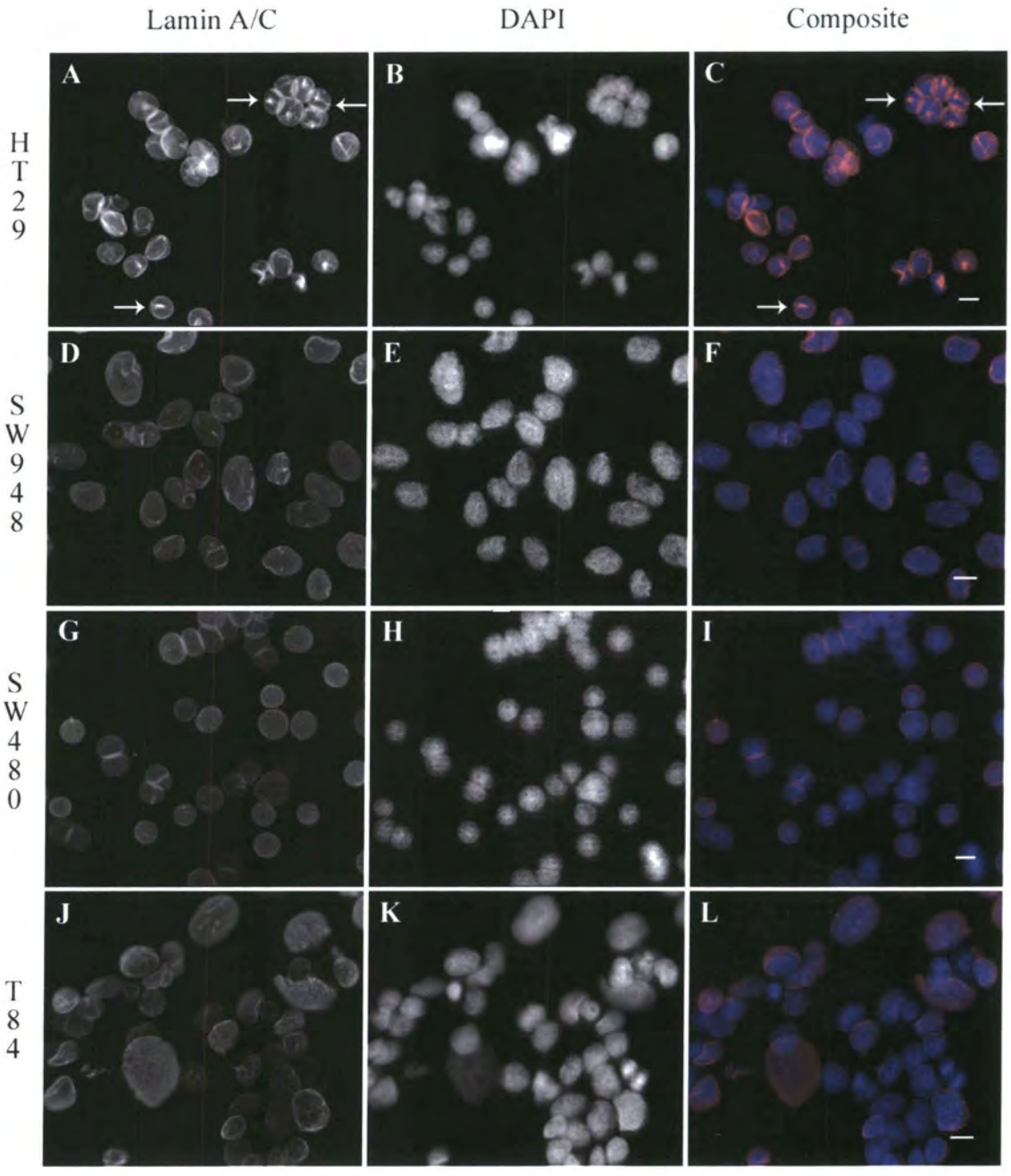


Figure 3.5.1

**Figure 3.6**

**Lamin B2 displays a unique pattern of distribution in SW480 cells which is not affected by antibody dilution.** HT29 (**Figure 3.6.1**), SW948 (**Figure 3.6.2**), SW480 (**Figure 3.6.3**) and T84 (**Figure 3.6.4**) colorectal carcinoma cells were immunostained with anti-lamin B2 – LN43 serially diluted 1:10 (panels A, B and C), 1:25 (panels D, E and F), 1:50 (panels G, H and I) and 1:100 (panels J, K and L) after fixation in methanol:acetone (1:1). The distribution of DNA was detected by co-staining with DAPI. Composite two-colour images (panels C, F, I and L) show lamin expression in red, superimposed over DNA staining, identified in blue. Individual black and white micrographs show lamin (panels A, D, G and J) and DAPI (panels B, E, H and K) staining separately. Scale bar = 10 μm.

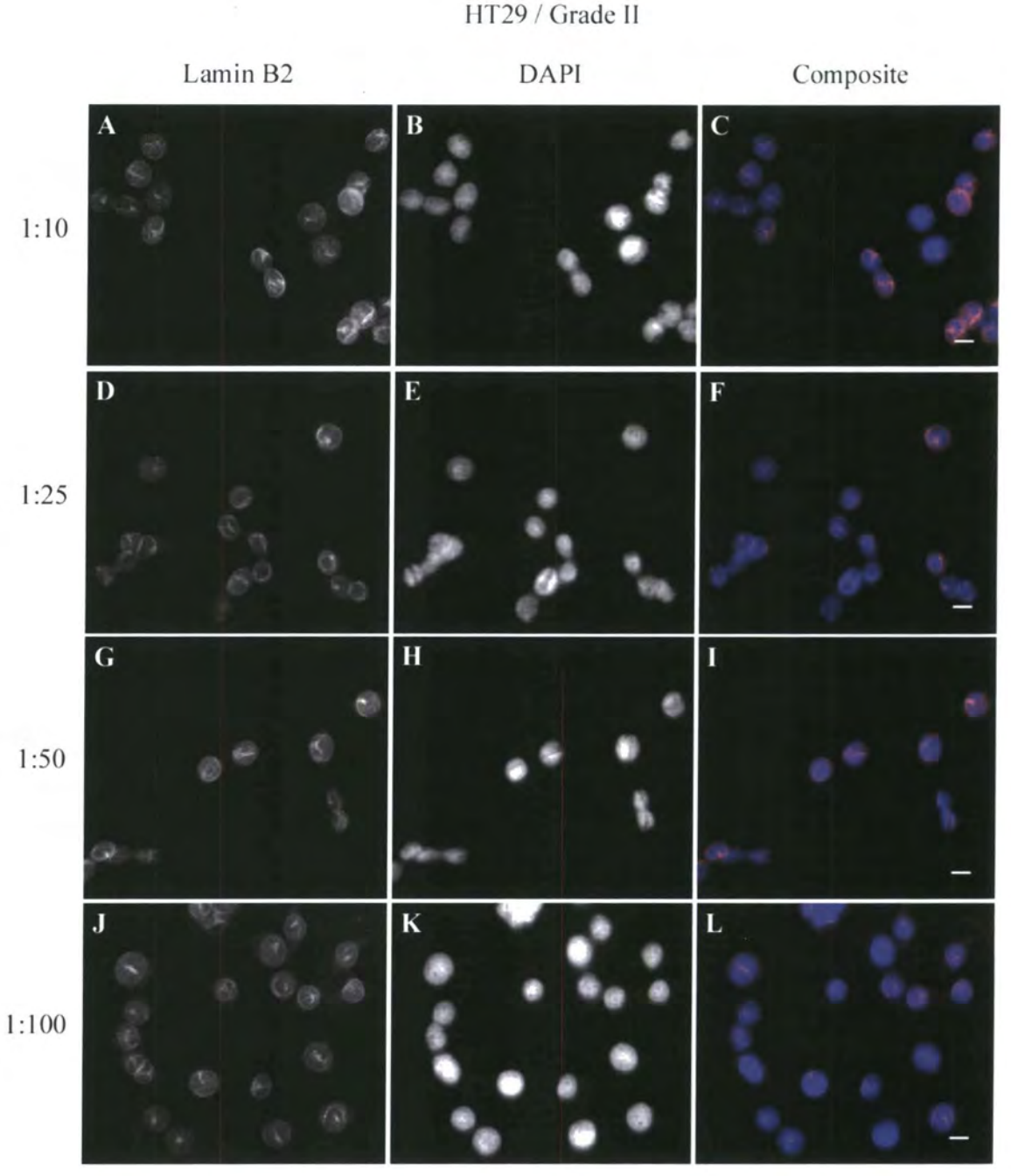
HT29 / Grade II
Lamin B2
DAPI
Composite
1:10
1:25
1:50
1:100
A
B
C
D
E
F
G
H
I
J
K
L

Figure 3.6.1

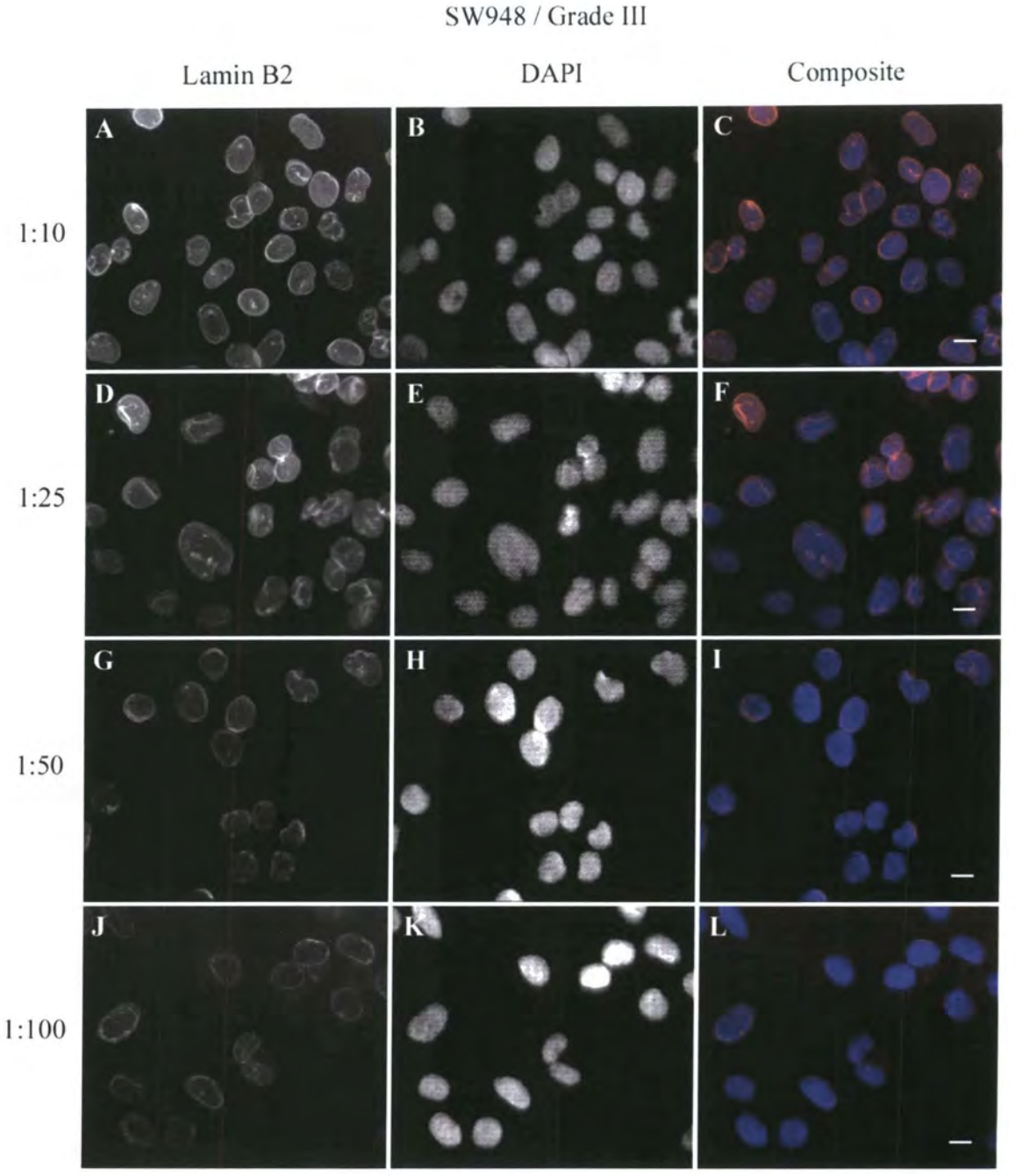
SW948 / Grade III
Lamin B2
DAPI
Composite
1:10
1:25
1:50
1:100
A
B
C
D
E
F
G
H
I
J
K
L

Figure 3.6.2

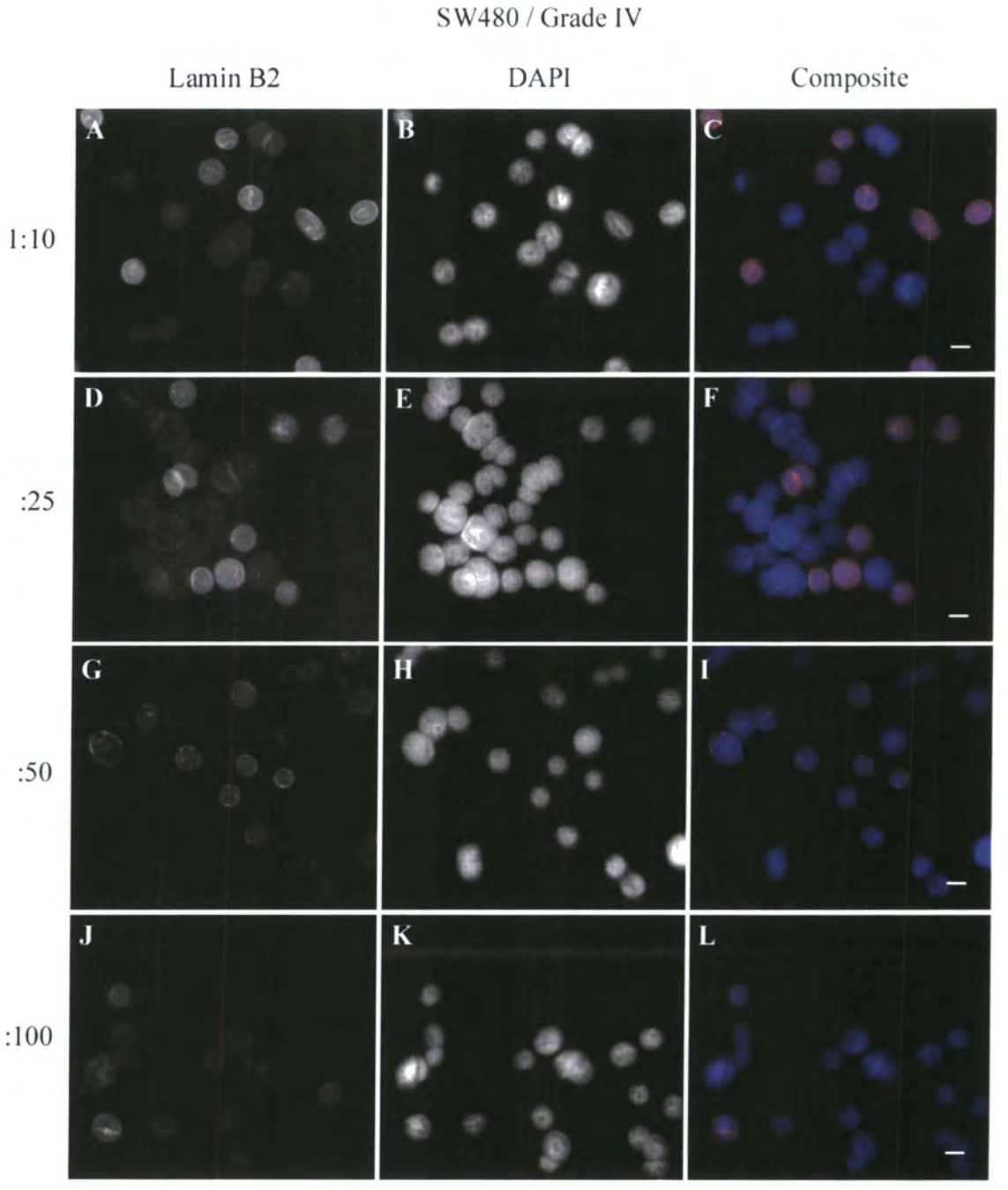
SW480 / Grade IV
Lamin B2
DAPI
Composite
1:10
:25
:50
:100
A
B
C
D
E
F
G
H
I
J
K
L

Figure 3.6.3

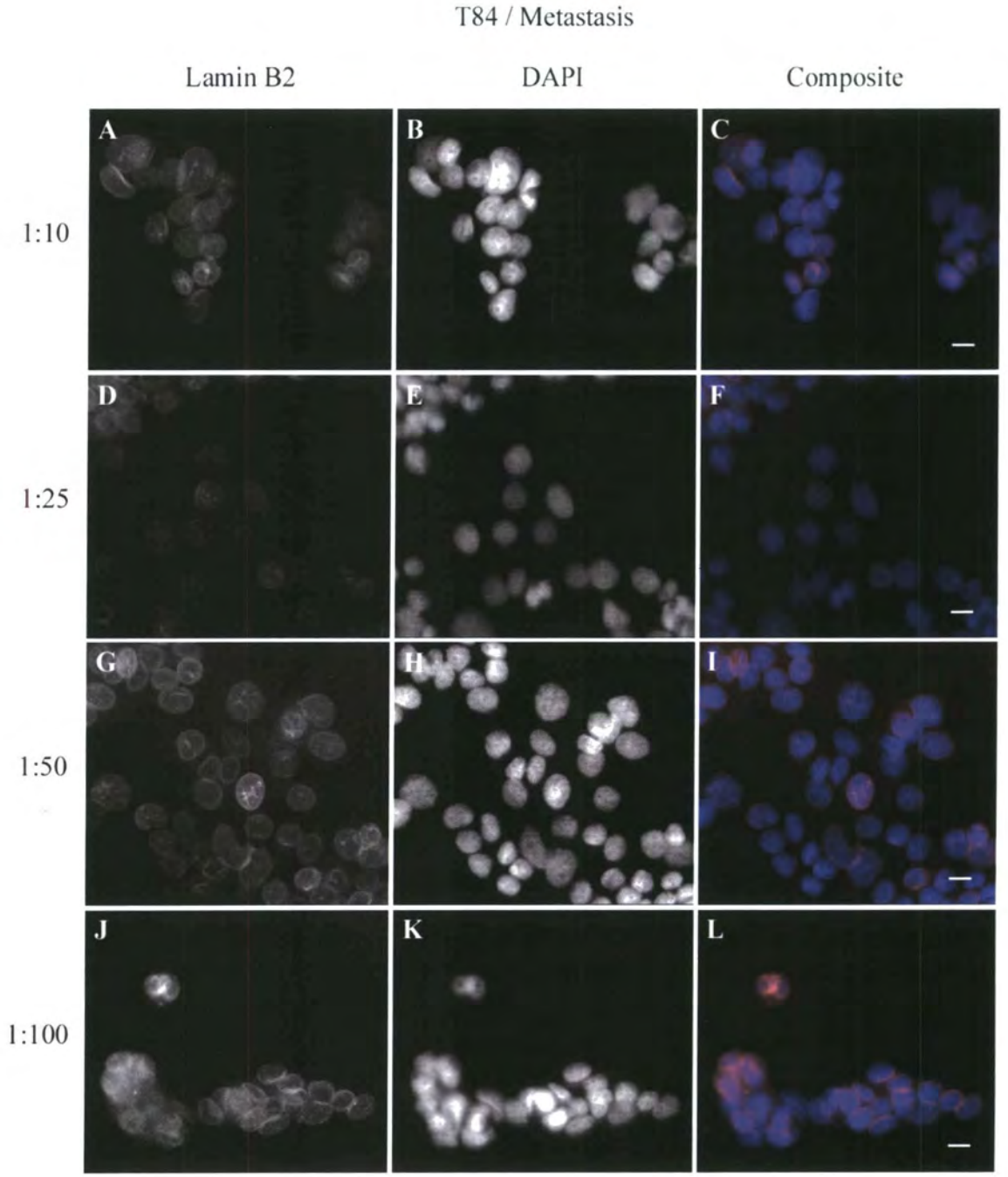
T84 / Metastasis
Lamin B2
DAPI
Composite
1:10
1:25
1:50
1:100
A
B
C
D
E
F
G
H
I
J
K
L

Figure 3.6.4

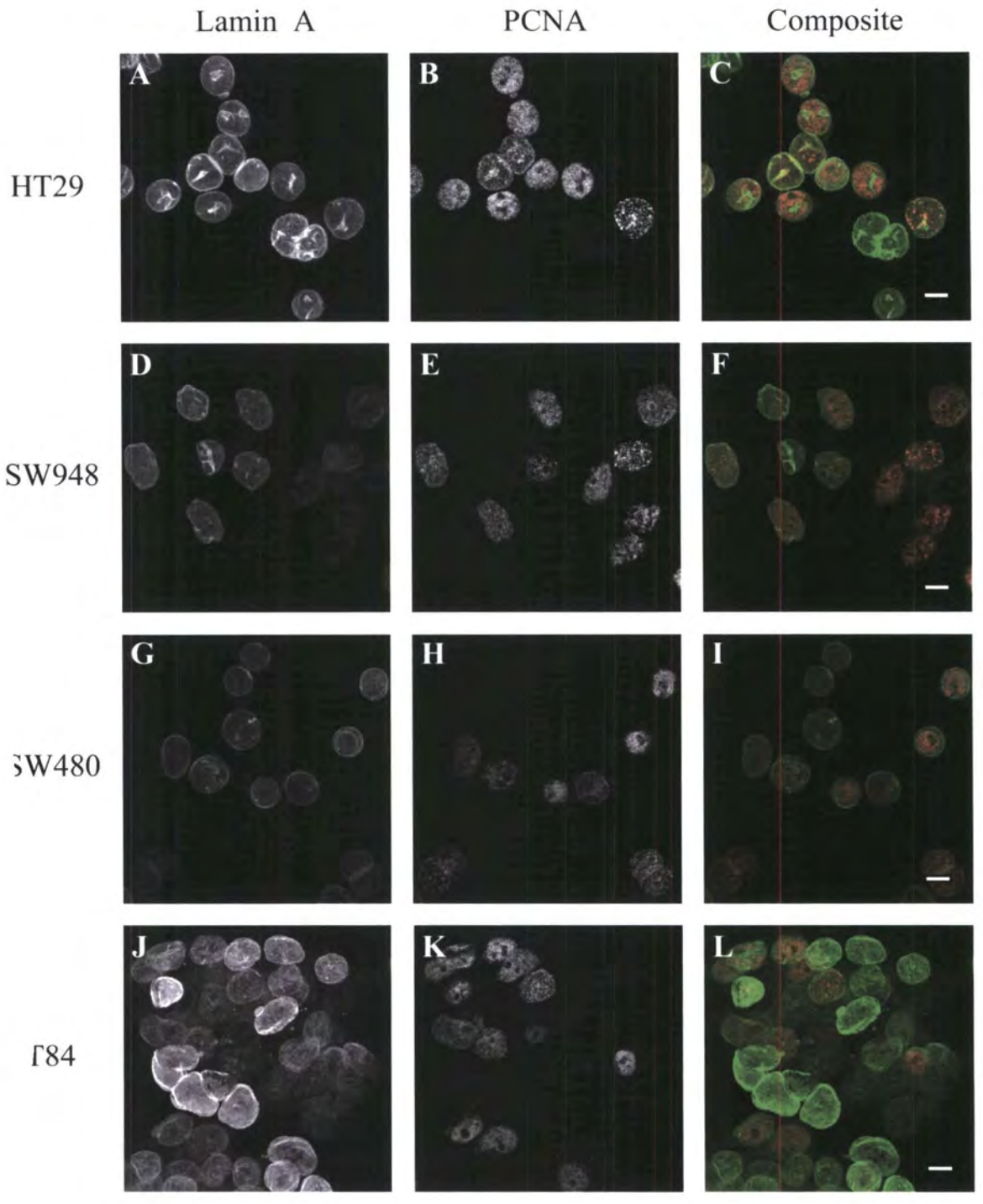


Figure 3.8.3

**Figure 3.7**

**Colorectal carcinoma cell lines stained with lamin A/C antibody JoL2 at the lowest dilution required for signal.** HT29, SW948, SW480 and T84 cells representing tumour grades II, III, IV and metastasis respectively were immunostained with mAb JoL2, diluted 1:50 after fixation in methanol:acetone (1:1). The distribution of chromatin was revealed using DAPI. Panels A, D, G and J show lamin A/C staining. Panels B, E, H and K show DNA staining. Panels C, F, I and L show two-colour merged images in which antibody staining is shown in red and DAPI staining in blue. Scale bar = 10 μm.

**Figure 3.8**

**The expression of lamin A in colorectal carcinoma cells is independent of their proliferation status.** The relationship between the distribution of A-type lamins and the expression of proliferation markers Ki67 and PCNA was investigated in four grades of colorectal carcinoma by double indirect immunofluorescence.

***Figures 3.8.1 and 3.8.2***

Grade II (HT29, panels A - C), grade III (SW948, panels D - F), grade IV (SW480, panels G - I) and metastasis (T84, panels J - L) colorectal carcinoma cells were fixed in methanol:acetone (1:1) and co-stained with either mAb anti-lamin A – JoL4 (**Figure 3.8.1**) or mAb anti-lamin A/C – JoL2 (**Figure 3.8.2**) and rabbit anti-Ki67 after 72 hours in culture. Panels A, D, G and J show lamin stained images; panels B, E, H and K show Ki67 stained images and panels C, F, I and L show merged images in which lamin is presented in green and Ki67 in red. Scale bar = 10 μm.

*Figure 3.8.3 and 3.8.4*

Grade II (HT29, panels A - C), grade III (SW948, panels D - F), grade IV (SW480, panels G - I) and metastasis (T84, panels J - L) colorectal carcinoma cells were fixed in methanol:acetone (1:1) and co-stained with antibodies JoL4 – anti-lamin A and PCNA – human anti-PCNA (**Figure 3.8.3**) or antibodies JoL2 – anti-lamin A/C and PCNA (**Figure 3.8.4**) after 16 hours in culture. Panels A, D, G and J show lamin stained images; panels B, E, H and K show PCNA stained images and panels C, F, I and L show merged images in which lamin is presented in green and PCNA in red. Scale bar = 10 μm.

**Figure 3.9**

**Analysis of lamin A and C mRNA expression in different grades of colorectal cancer by semi-quantitative RT-PCR.** One-step RT-PCR was performed on 0.1 μg total RNA isolated from three different passages of grade II (HT29) – lane 1, grade III (SW948) – lane 2, grade IV (SW480) – lane 3 and metastasis (T84) – lane 4 CRC cell lines under non-saturating conditions. Expression of the *LMNA* gene was investigated using primers specific for the lamin A transcript, yielding a 1137 bp product (**A**) and the lamin C transcript, yielding a 993 bp product (**B**). Equal loading of RNA in each sample was verified by monitoring the transcriptional level of β-actin (**C**). Primers produced an 834 bp product.

**Figure 3.10**

**Densitometric assessment of lamin A and C transcript levels.** Messenger RNA expression levels for lamins A (**A**) & C (**B**) in grade II, III, IV and metastasis colorectal carcinoma cells was determined by semi-quantitative RT-PCR, followed by densitometry. Bands were digitally scanned in a Fujifilm Intelligent Dark Box II operated by Image Reader LAS-1000 Pro Ver. 2.11 software and intensities measured using Fujifilm Image Gauge, version 4.0. For each of three replicates, mRNA expression was standardized against β-actin and relative expression of lamin A and C transcripts calculated, considering the cell line with the highest band intensity to be 100%. Values are mean ± standard deviation.

The level of lamin A mRNA expression in grade III (SW948) cells (mean = 33.0 ± 21.3%) was significantly lower than in grade II (HT29) cells (mean = 96.5 ± 6.0%), $t$ = 4.97, $df$ = 4, $P < 0.01$ in 'two-tailed' Student's $t$-test. The difference in mRNA expression between grade III and grade IV (SW480) cells (mean = 79.4 ± 31.2%) and grade III and metastasis (T84) cells (mean = 75.8 ± 28.2%) was not statistically significant.

Lamin C mRNA expression did not change significantly between grades. Grade mean = 45.8 ± 35.3%; grade III, mean = 26.4 ± 16.9%; grade IV, mean = 61.7 ± 37. and grade metastasis, mean = 89.3 ± 18.6%.

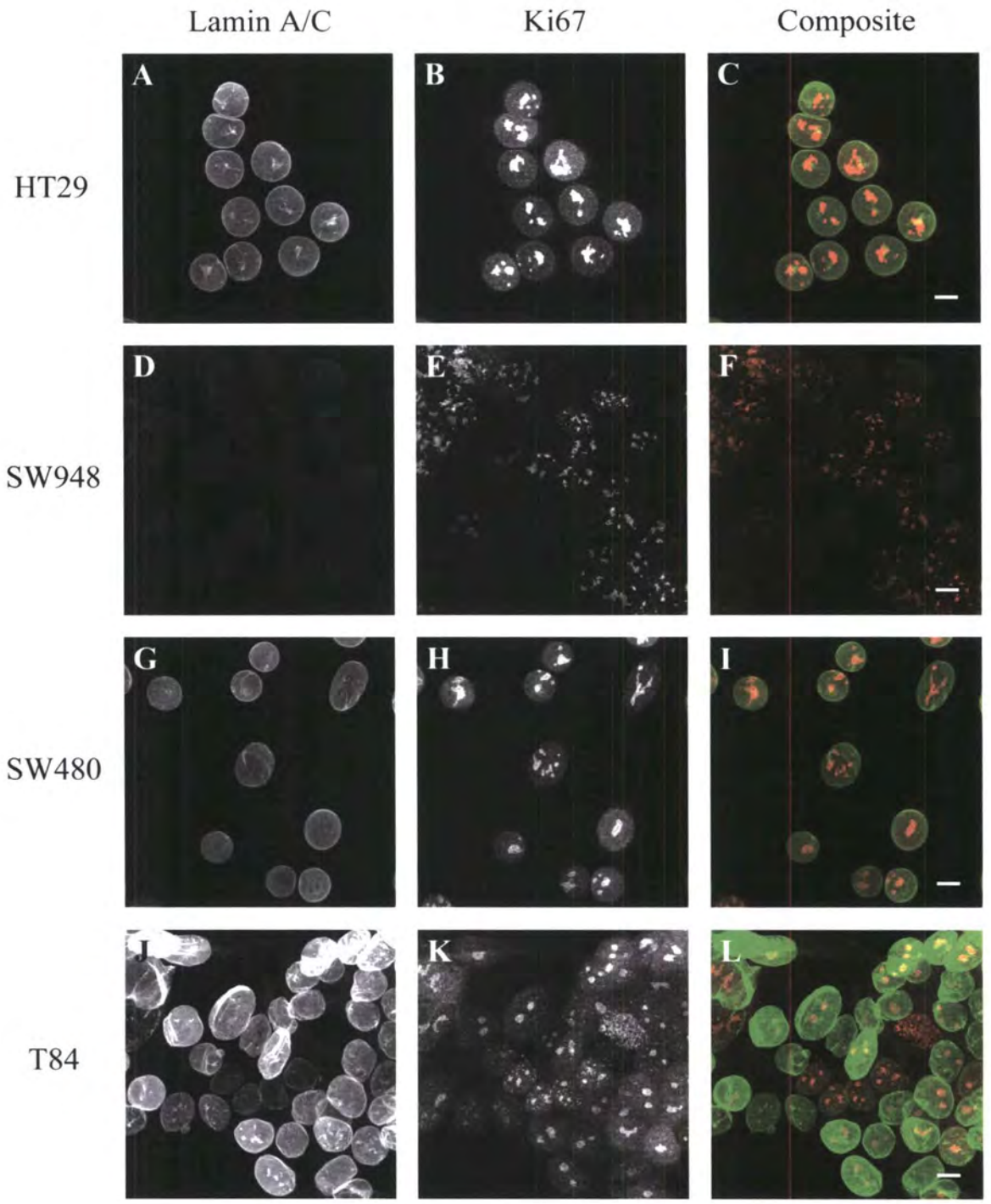


Figure 3.8.2

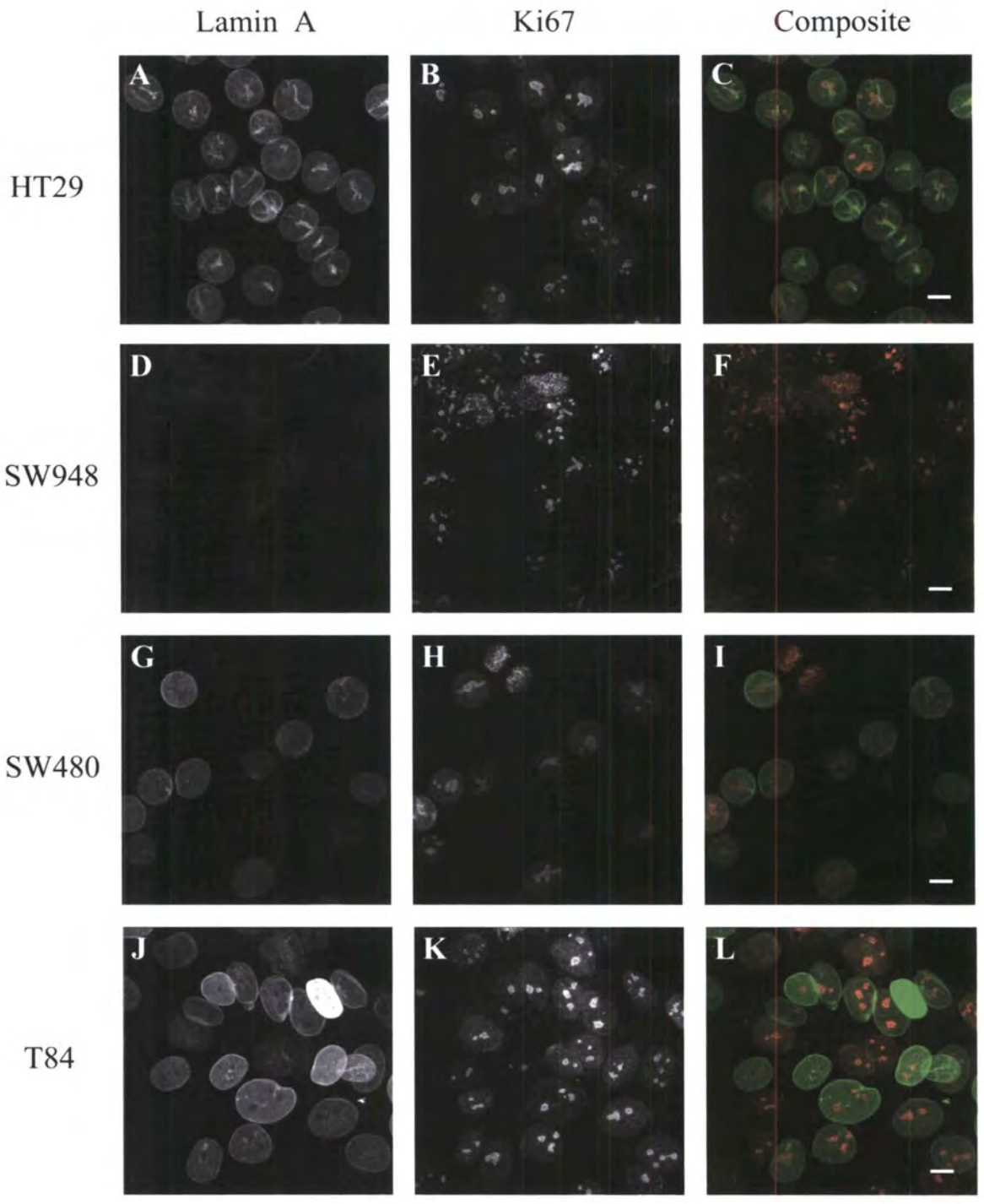


Figure 3.8.1

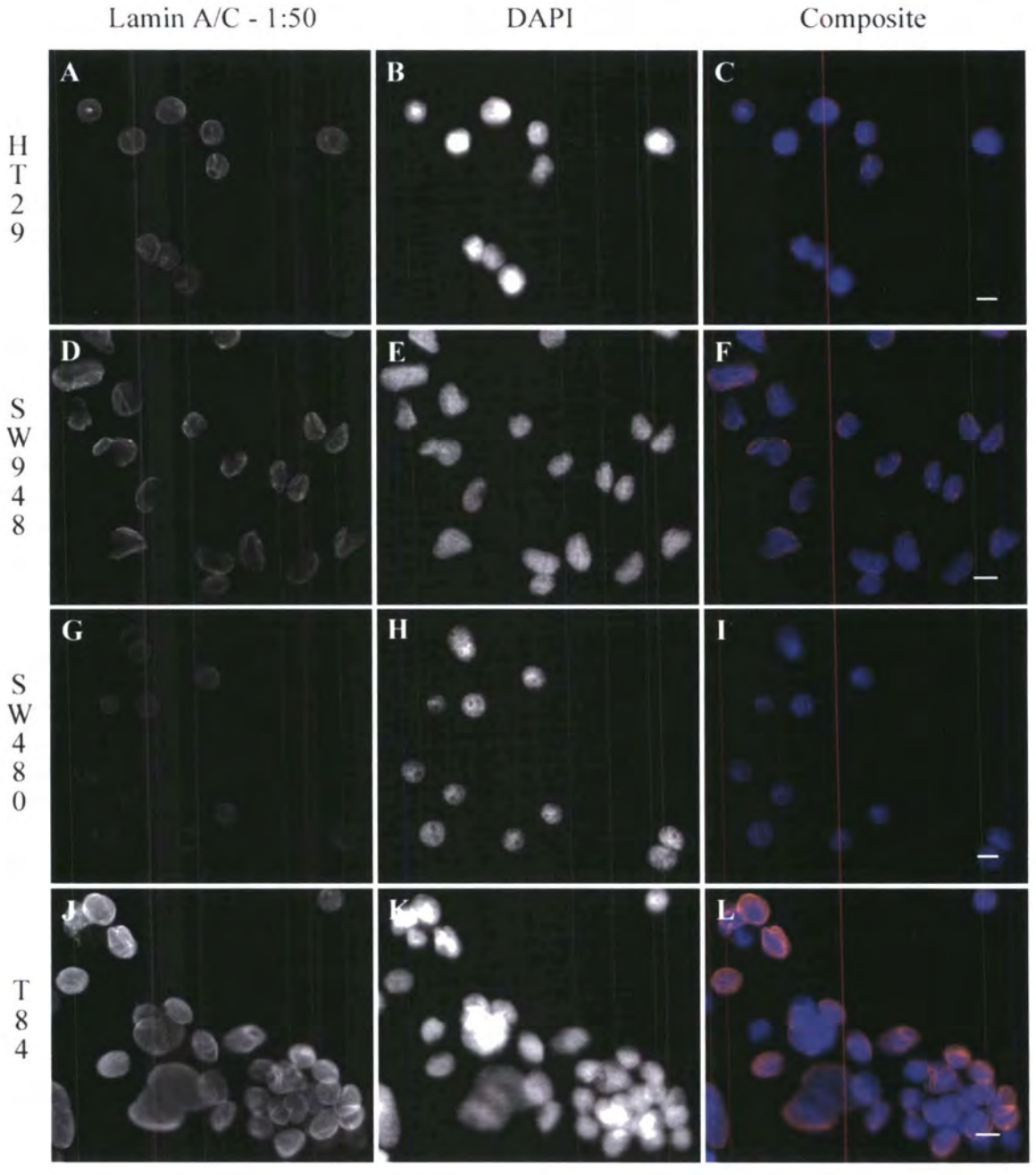
Lamin A/C - 1:50
DAPI
Composite
HT29
SW948
SW480
T84
A
B
C
D
E
F
G
H
I
J
K
L

Figure 3.7

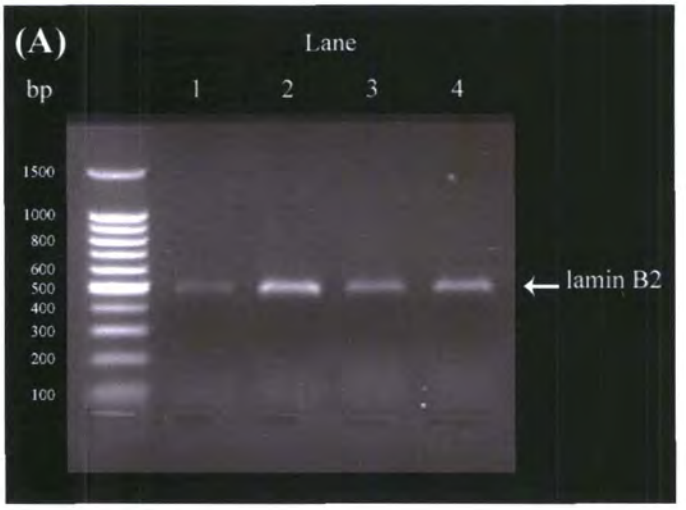
(A)
Lane
bp
1
2
3
4
1500
1000
800
600
500
400
300
200
100
lamin B2

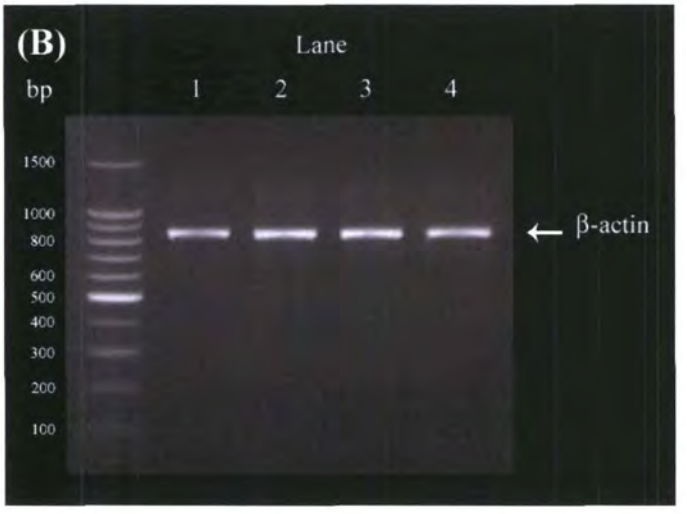
(B)
Lane
bp
1
2
3
4
1500
1000
800
600
500
400
300
200
100
β-actin

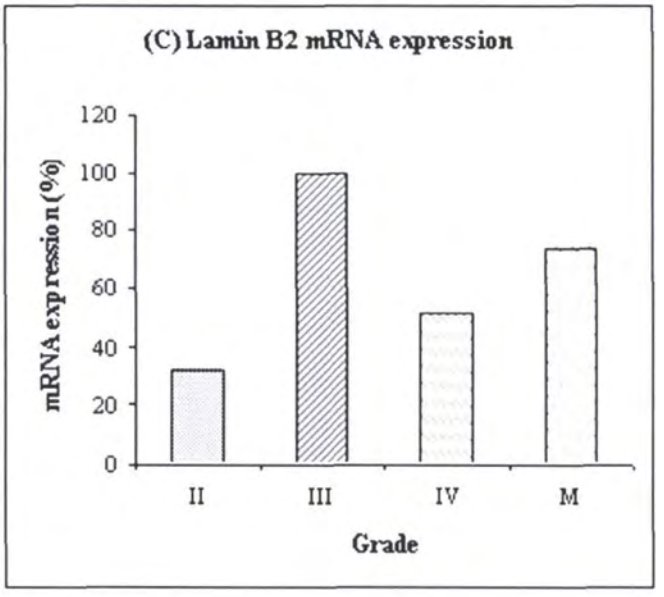
(C) Lamin B2 mRNA expression
mRNA expression (%)
120
100
80
60
40
20
0
II
III
IV
M
Grade

Figure 3.12

**Figure 3.11**

**Confirmation of lamin A and lamin C primer specificity**. Lamin A and C RT-PCR products were sequenced in the reverse direction using an ABI Prism® 377 XL automated DNA sequencer. The 3'-most end of the sequences were compared using the Nucleotide-nucleotide BLAST database (BLASTN 2.2.11). The figure shows three of the highest scoring BLAST hits for the lamin A (**A**) and lamin C (**B**) RT-PCR products, plus an example sequence alignment for each. The BLAST results show that the lamin A RT-PCR products align preferentially with lamin A specific mRNA sequences, while the lamin C RT-PCR products align more significantly with lamin C specific mRNA sequences.

**Figure 3.12**

**Study of lamin B2 mRNA expression in CRC cell lines by semi-quantitative RT-PCR.** Total RNA extracted from cell lines delineating grade II (HT29), III (SW948), IV (SW480) and metastasized (T84) colorectal tumours was reverse transcribed and subjected to 26 rounds of amplification using primers to a 481 bp fragment of lamin B2 (**A**). Equal loading of cDNA in each sample was monitored using primers to an 834 bp fragment of β-actin (**B**).

**C.** Densitometric evaluation of lamin B2 transcript level. Measurements (in arbitrary units) for each replicate were normalized against β-actin. Values are average relative mRNA expression, considering tumour grade III with the highest copy number to be 100%. Relative expression of lamin B2 mRNA was 32.2% in grade II cells, 100% in grade III cells, 51.8% in grade IV cells, rising to 74.2% in metastasized cultures.

NCBI results of BLAST

## A. Lamin A

| Sequences producing significant alignments: | Score (Bits) | E Value |
|---|---|---|
| gi\|34782765\|gb\|BC018863.2\| Homo sapiens lamin A/C, mRNA (cDNA cl | 170 | 1e-40 |
| gi\|57014046\|gb\|AY847597.1\| Homo sapiens lamin A/C transcript ... | 170 | 1e-40 |
| gi\|27436945\|ref\|NM_170707.1\| Homo sapiens lamin A/C (LMNA), tran | 170 | 1e-40 |

> gi|27436945|ref|NM_170707.1| Homo sapiens lamin A/C (LMNA), transcript variant 1, mRNA
Length=3181

Score = 170 bits (86), Expect = 1e-40
Identities = 90/92 (97%), Gaps = 0/92 (0%)
Strand=Plus/Plus

```
Query  1     TCGGGGGACCCCGCTGAGTACAACCTGCGCTCGCGCACCGTGCTGTGCGGGACCTGCGGG  60
             ||||||||||||||||||||||||||||||||||||||||||||||||||||||||||||
Sbjct  1929  TCGGGGGACCCCGCTGAGTACAACCTGCGCTCGCGCACCGTGCTGTGCGGGACCTGCGGG  1988

Query  61    CAGCCTGCCGACAANGCATNTGCCAGCGGCTC  92
             |||||||||||||| |||| ||||||||||||
Sbjct  1989  CAGCCTGCCGACAAGGCATCTGCCAGCGGCTC  2020
```

## B. Lamin C

| Sequences producing significant alignments: | Score (Bits) | E Value |
|---|---|---|
| gi\|27436944\|ref\|NM_005572.2\| Homo sapiens lamin A/C (LMNA), tran | 180 | 1e-43 |
| gi\|33991068\|gb\|BC000511.2\| Homo sapiens lamin A/C, transcript... | 180 | 1e-43 |
| gi\|186925\|gb\|M13451.1\|HUMLAMC Human lamin C mRNA, complete cds | 180 | 1e-43 |

> gi|27436944|ref|NM_005572.2| Homo sapiens lamin A/C (LMNA), transcript variant 2, mRNA
Length=2032

Score = 180 bits (91), Expect = 1e-43
Identities = 94/95 (98%), Gaps = 0/95 (0%)
Strand=Plus/Plus

```
Query  1     CACTGGGGAAGAAGTGGCCATGCGCAAGCTGGTGCGCTCAGTGACTGTGGTTGAGGACGA  60
             ||||||||||||||||||||||||||||||||||||||||||||||||||||||||||||
Sbjct  1811  CACTGGGGAAGAAGTGGCCATGCGCAAGCTGGTGCGCTCAGTGACTGTGGTTGAGGACGA  1870

Query  61    CGAGGATGAGGATGGAGATGACCTGCTCCCTCACC  95
             ||||||||||||||||||||||||||| |||||
Sbjct  1871  CGAGGATGAGGATGGAGATGACCTGCTCCATCACC  1905
```

Figure 3.11

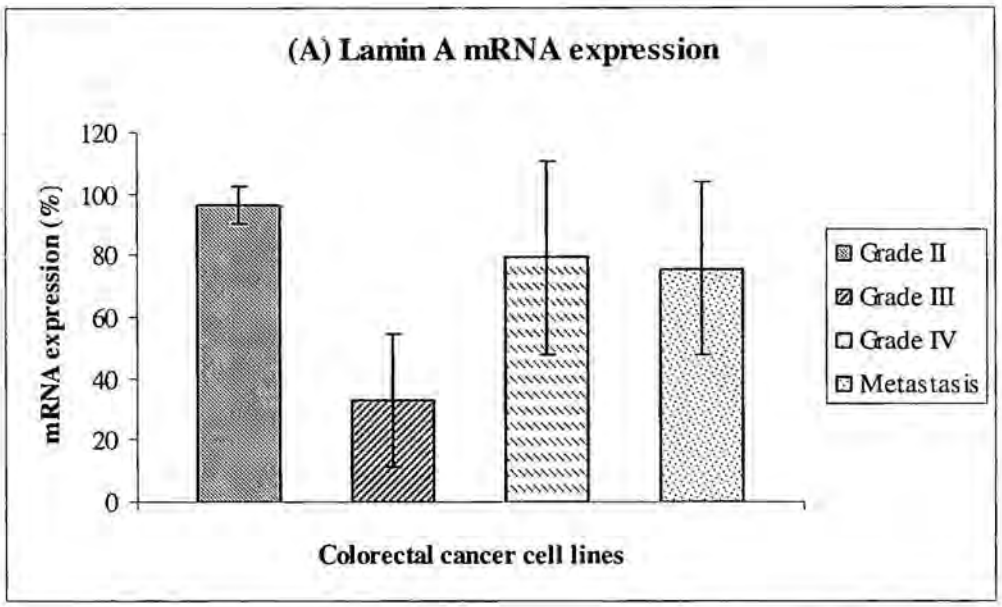
(A) Lamin A mRNA expression
mRNA expression (%)
120
100
80
60
40
20
0
Grade II
Grade III
Grade IV
Metastasis
Colorectal cancer cell lines

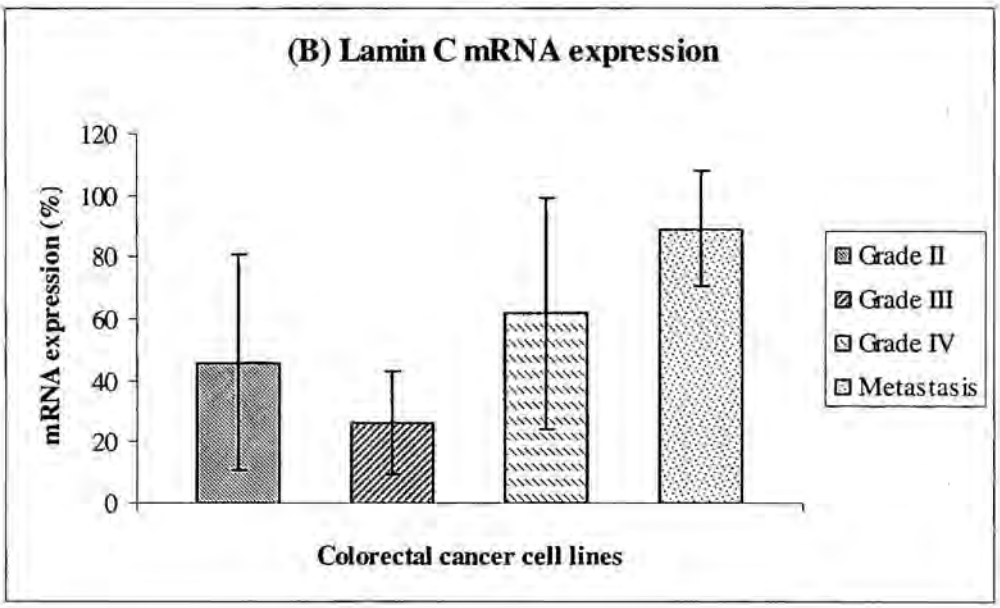
(B) Lamin C mRNA expression
mRNA expression (%)
120
100
80
60
40
20
0
Grade II
Grade III
Grade IV
Metastasis
Colorectal cancer cell lines

Figure 3.10

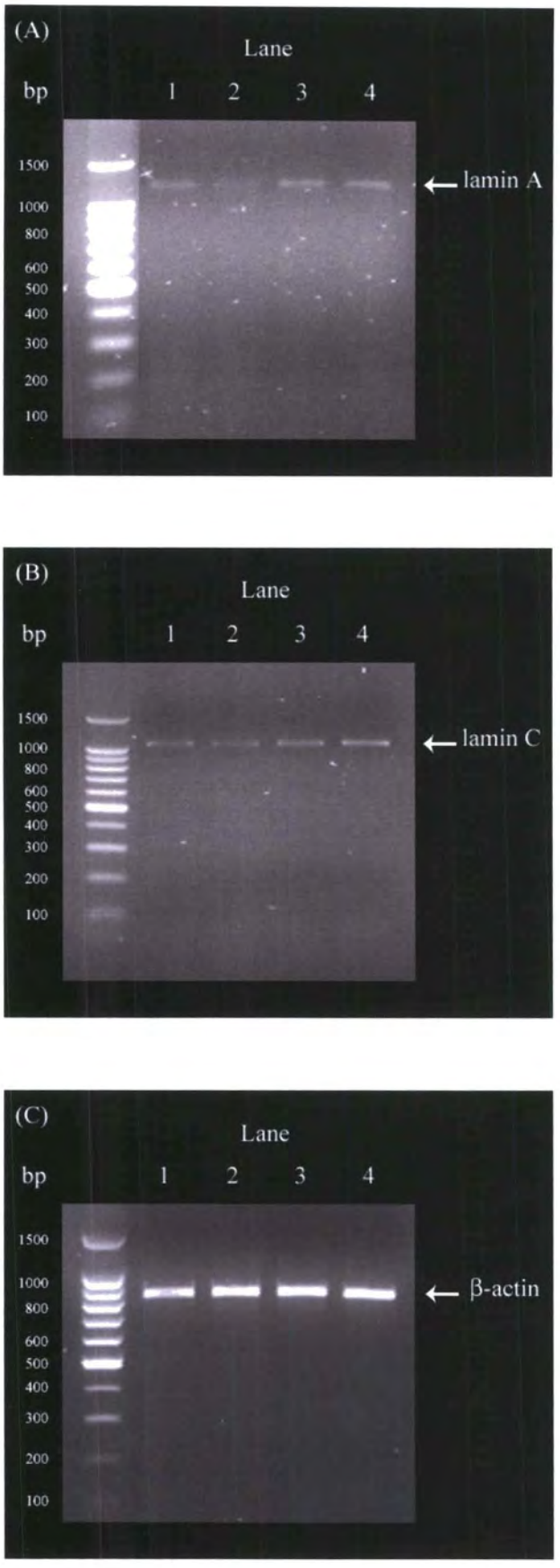
(A)
Lane
bp
1
2
3
4
1500
1000
800
600
500
400
300
200
100
lamin A
(B)
Lane
bp
1
2
3
4
1500
1000
800
600
500
400
300
200
100
lamin C
(C)
Lane
bp
1
2
3
4
1500
1000
800
600
500
400
300
200
100
β-actin

Figure 3.9

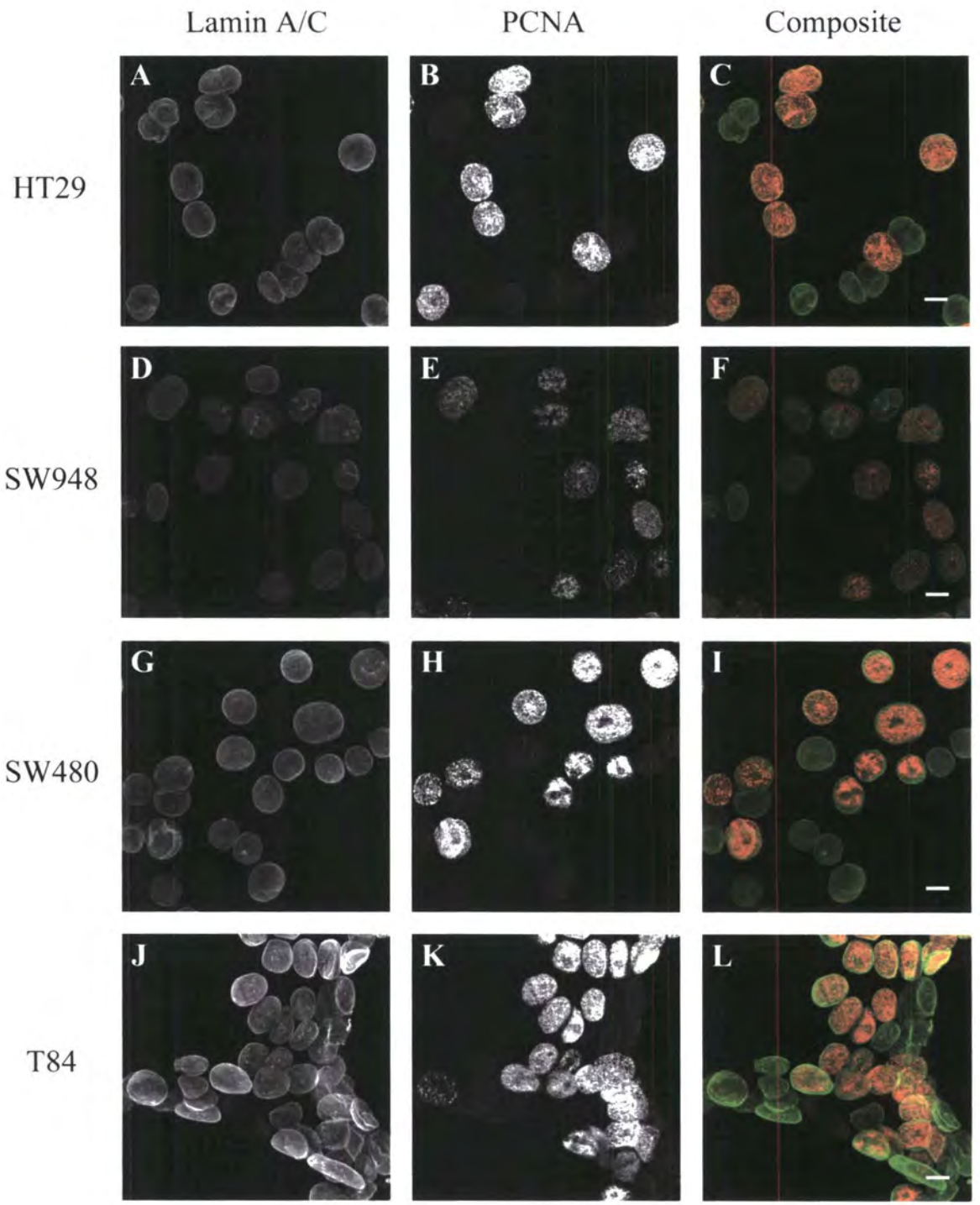


Figure 3.8.4

**Figure 3.13**

**Confirmation of lamin B2 primer specificity**. Lamin B2 RT-PCR products were sequenced in the forward direction using an ABI Prism® 377 XL automated DNA sequencer. The sequences in GenBank® with greatest homology were identified using the Nucleotide-nucleotide BLAST database (BLASTN 2.2.11). The figure shows three of the highest scoring BLAST hits for the lamin B2 RT-PCR products, plus an example sequence alignment.


results of BLAST

## Lamin B2

| Sequences producing significant alignments: | Score (Bits) | E Value |
|---|---|---|
| gi\|33873549\|gb\|BC006551.2\| Homo sapiens lamin B2, mRNA (cDNA ... | 198 | 5e-49 |
| gi\|186918\|gb\|M94362.1\|HUMLAMBBA Human lamin B2 (LAMB2) mRNA, par | 198 | 5e-49 |
| gi\|27436950\|ref\|NM_032737.2\| Homo sapiens lamin B2 (LMNB2), mRNA | 198 | 5e-49 |

> gi|27436950|ref|NM_032737.2| Homo sapiens lamin B2 (LMNB2), mRNA
Length=4653

Score = 198 bits (100), Expect = 5e-49
Identities = 100/100 (100%), Gaps = 0/100 (0%)
Strand=Plus/Plus

```
Query  1     ATGCGGGACGTGATGCAGCAGCAGCTGGCCGAGTACCAGGAGCTGCTGGACGTGAAGCTG  60
             ||||||||||||||||||||||||||||||||||||||||||||||||||||||||||||
Sbjct  1114  ATGCGGGACGTGATGCAGCAGCAGCTGGCCGAGTACCAGGAGCTGCTGGACGTGAAGCTG  1173

Query  61    GCCCTGGACATGGAGATCAACGCCTACCGGAAGCTCCTGG  100
             ||||||||||||||||||||||||||||||||||||||||
Sbjct  1174  GCCCTGGACATGGAGATCAACGCCTACCGGAAGCTCCTGG  1213
```

Figure 3.13

# CHAPTER 4 – STABLE RE-EXPRESSION OF LAMIN A CONSTRUCTS IN SW480 COLON CANCER CELLS

## *4.1 Introduction*

### 4.1.1 Embryonic development of the gastrointestinal tract

Embryonic development is understood to be a highly regulated series of events which are subject to fine genetic control (Touchette, 1994; Wolpert, 1994). The key elements of vertebrate embryogenesis are cell division, determination, migration, differentiation and apoptosis (Raven and Johnson, 1996; Touchette, 1994; Wolpert, 1994). Organogenesis is characterized by the differentiation of positioned cells into pre-determined functional tissues and organs and is accompanied by large-scale cell expansion (Raven and Johnson, 1996). The purpose of cell determination, tissue patterning and differentiation during development is to make sure a cell identifies with and performs the specific function required of it. The consequences of a failure to co-ordinate developmental signals can be seen in a plethora of human disorders which have a broad phenotypic spectrum. Hirschsprung's disease is one such disorder affecting the colon. It is characterized by impaired enteric innervation of the large intestine resulting in chronic constipation and intestinal obstructions in the infant, often requiring surgery immediately after birth. This disease is thought to be the result of defects in the migratory pattern of neural crest stem cells (NCSCs) which are responsible for the formation of the gastrointestinal nervous system. Ordinarily, NCSCs colonize the entire developing digestive tract, but in embryos with Hirschsprung's disease they do not

reach the primitive hindgut, rendering it incapable of generating a normal, functioning nervous system of it own (Iwashita *et al.*, 2003).

The vertebrate gastrointestinal tract (GI tract) first appears as a hollow tube of undifferentiated stratified endoderm surrounded by undifferentiated splachnic mesoderm. The former gives rise to the epithelial lining of the gut, while the latter differentiates into the mesenchymal components. The entire structure is innervated by the ectoderm-derived enteric nervous system [discussed by Kedinger *et al.* (1998) and de Santa Barbara *et al.* (2003)].

Development of the GI tract is characterized by the patterning of embryonic gut along four axes of symmetry [reviewed by de Santa Barbara *et al.* (2003) and Stanier (2005)]. Differentiation along the anterior-posterior or longitudinal axis compartmentalizes the gut into three regions known as the foregut, midgut and hindgut which develop into the specialized structures of the adult gut along a functional gradient. The pharynx, oesophagus and stomach are derived from the foregut, the small intestine originates from the midgut and the colon develops predominantly from the hindgut. Part of the colon, from caecum to right two-thirds of the transverse colon, is derived from the midgut (Sadler and Langman, 2000). Patterning along the dorsoventral and left-right axes determines the body position of the digestive organs as well as derivatives of the GI tract such as the lungs, liver, pancreas and thyroid which bud from the foregut early in embryonic development. Development along the radial axis gives rise to regional morphological specialization of the gut epithelium. In the large intestine this results in the formation of tubular invaginations, called crypts, interrupted by flat surface epithelium (intercrypt table) which maximize the available surface area, facilitating the absorptive function of the colon (de Santa Barbara *et al.*, 2003; Potten *et al.*, 1997).

### 4.1.2 Genetic control of colonic epithelial morphogenesis and its implications for CRC development

The adult GI tract is radially organized into four histologically distinct layers: the mucosa, submucosa, muscularis propria and serosa (Burkitt *et al.*, 1993). Colonic crypts are folds of simple columnar epithelium, analogous to the crypts of Lieberkuhn of the small intestine, which form part of the mucosa and are adjacent to the lumenal surface. They possess three specialized cell types which are found in the upper part of the crypt: mucus-secreting goblet cells, absorptive enterocytes and the less abundant enteroendocrine cells which function to lubricate the passage of waste material, absorb water and salts and secrete hormones respectively (Marshman *et al.*, 2002; Potten *et al.*, 1997). The differentiated cells are perpetually extruded into the lumen and replenished through a process of transit amplification and lineage-specific differentiation of multipotent stem cells located in the base of the crypt (Gordon and Hermiston, 1994; Marshman *et al.*, 2002). In the colon, maturing cells migrate unidirectionally from the crypt base to the intercrypt table (Marshman *et al.*, 2002).

In many ways the perpetual self-renewal of the colonic epithelium, involving proliferation of stem cells followed by differentiation, migration and finally programmed cell death of mature cells, recapitulates the process of embryonic development described above (de Santa Barbara *et al.*, 2003). Similarly, homeostasis of the intestinal epithelium is necessarily kept under tight genetic control through the modulation of multiple signalling pathways (Radtke and Clevers, 2005; Sancho *et al.*, 2004). Likewise, failure to activate or repress the correct signals can result in a disastrous outcome. If this occurs within the colonic epithelium, one of the consequences is cancer (Radtke and Clevers, 2005; Sancho *et al.*, 2004).

Research into the pathology of colorectal cancer has revealed as much about the molecular mechanisms of disease development as it has about the physiological maintenance of crypt topology in normal colonic epithelium. Currently the canonical Wnt signalling pathway (see Chapter 1, Figure 1.4) is considered to be the most significant regulator of normal crypt homeostasis and CRC development (Bienz and Clevers, 2000; Giles *et al.*, 2003; Pinto and Clevers, 2005; van de Wetering *et al.*, 2002).

Normal colonic crypts can essentially be divided into three compartments (see Chapter 5, Figure 5.2). Lying above the stem cell niche located at the crypt base, is the transit amplifying region which contains the proliferative progenitor cells. Together they occupy the lower two thirds of the crypt. The differentiated region which harbours fully functional differentiated cell types is located in the upper third of the crypt and will hereafter be additionally described as the villus* (Booth and Potten, 2000; Marshman *et al.*, 2002). The transition from proliferation to differentiation constitutes the crypt-villus axis which is maintained by the Wnt signal (Pinto and Clevers, 2005; van de Wetering *et al.*, 2002).

Wnt factors are secreted glycoproteins thought to emanate in the base of intestinal crypts and / or underlying mesenchymal tissue, although their exact location has not been determined (Batlle *et al.*, 2002; Pinto and Clevers, 2005). They pervade the

---

*Strictly speaking the colonic epithelium does not possess villi. In the small intestine the differentiated epithelial compartment involved in digestion and absorption is morphologically distinguishable as a long, finger-like projection (villus) into the gut lumen, but this is replaced by flat surface epithelium in the colon (de Santa Barbara *et al.*, 2003). However, explaining the signalling mechanisms which control homeostasis in normal colonic epithelium and which become dysregulated in CRC is made simpler by referring to the differentiated zone in the epithelium of both the small and large intestines as the villus.

intestinal epithelium, imposing a proliferative phenotype through Frizzled/LRP - mediated stabilization of the cytoplasmic protein, β-catenin, leading to transcription of Wnt target genes (Logan and Nusse, 2004; Pinto *et al.*, 2003; Pinto and Clevers, 2005). The process is negatively regulated by APC (Korinek *et al.*, 1997), a key component of the multiprotein degradation complex which presents β-catenin for phosphorylation, consequently targeting it for ubiquitination by β-TrCP and subsequent degradation by the proteasome in the absence of a Wnt signal (Bienz and Clevers, 2000). In addition to APC, the multiprotein degradation complex comprises a scaffold protein, Axin and two serine/threonine kinases, GSK3β and CKI. Upon activation of the canonical Wnt signalling pathway [reviewed in depth by Logan and Nusse (2004)], interaction of Wnt ligands with their membrane spanning co-receptors, Fz and LRP5/6, at the cell surface results in the recruitment of Axin and another protein, Dsh to the plasma membrane. Consequently, the multiprotein complex is dissociated, liberating β-catenin and leaving it free to translocate to the nucleus. When there is no Wnt signal, members of the TCF/LEF family of transcription factors are bound to the transcriptional repressor Groucho (Cavallo *et al.*, 1998). In the presence of Wnt, β-catenin overcomes this repression by direct association with TCF/LEF factors, transactivating the transcription of downstream targets (van de Wetering *et al.*, 1997).

TCF-4, the most prominently expressed member of the TCF/LEF family in epithelial cells of the colon, forms functionally active complexes with β-catenin (Korinek *et al.*, 1997). Latterly the Wnt-induced β-catenin/TCF-4 complex has been described as the principal governor of cell dynamics at the crypt-villus junction, preserving a stem cell and proliferating progenitor population in the lower crypt region essential for sustaining the turnover of differentiated cells at the surface (van de Wetering *et al.*, 2002). By inhibiting the β-catenin/TCF-4 complex with inducible expression of dominant negative

TCF-4 (dnTCF-4), van de Wetering *et al.* (2002) were able to demonstrate: First, a concomitant G1 arrest. Second, a down-regulation of intestinal markers of proliferation such as *EPHB2*, *c-MYB*, *BMP4*, *ENC1*, *CD44*, *CLDN1* and c-*MYC* which were known to or subsequently shown to be expressed in the proliferative compartment of normal crypts. Third, an up-regulation of intestinal markers of differentiation including carbonic anhydrase II (*CA2*), fatty acid binding protein 1, liver (*FABP1*) and most significantly $p21^{CIP1/WAF1}$. One of the most important downstream targets of the β-catenin/TCF-4 complex appears to be c-myc which is known to push cells from G1 to S-phase of the cell cycle and is a well-known oncogene (He *et al.*, 1998; Oster *et al.*, 2002). Expression of c-myc at endogenous levels in dnTCF-4 cells caused re-entry into the cell cycle and $p21^{CIP1/WAF1}$ expression was reduced. Thus β-catenin/TCF-4 complexes appear to maintain a progenitor / stem cell phenotype in intestinal crypts through c-myc-mediated repression of the cell cycle inhibitor $p21^{CIP1/WAF1}$. In the differentiated compartment the Wnt signal is absent, β-catenin is exported from the nucleus by APC and sequestrated by the aforementioned degradation complex. c-*MYC* is not activated, therefore $p21^{CIP1/WAF1}$ expression is induced, facilitating cell cycle arrest and differentiation (van de Wetering *et al.*, 2002).

Immunohistochemical studies have clearly shown accumulation of β-catenin in the nucleus of crypt progenitor cells and in aberrant crypt foci which are the benign precursors of colorectal cancer (van de Wetering *et al.*, 2002). This indicates that Wnt signalling is re-initiated in colon tumour cells. In addition, mutations in *APC* which constitutively activate β-catenin/TCF signalling (Korinek *et al.*, 1997; Morin *et al.*, 1997) are estimated to account for 85% of all colorectal tumours (Kinzler and Vogelstein, 1996). It has therefore been reasoned that activation of β-catenin/TCF-4 may constitute the dominant switch in the malignant transformation of a colon epithelial

cell by imposing a proliferative phenotype at an early stage (van de Wetering *et al.*, 2002). The corollary of this is that the development and progression of colorectal cancer is a process of dedifferentiation, as well as increased proliferation. Essentially it is the story of a colon epithelial cell losing its identity with the intestine step-by-step and could be viewed as development in reverse.

In the light of my own findings that lamin A is down-regulated in late grade, highly dedifferentiated colorectal cancer cell lines (see Chapter 3), it was postulated that loss of lamin A may be an important event in the progression of CRC. Fundamentally, lamin A provides mechanical support to the nucleus (Aebi *et al.*, 1986; Broers *et al.*, 2004). However, evidence has been accumulating which suggests that it may also function as a regulator of gene transcription (Csoka *et al.*, 2004; Hutchison, 2002; Spann *et al.*, 2002). Consequently a DNA microarray approach seemed the most effective method to investigate the downstream implications of a loss of lamin A and thereby determine if lamin A affects global gene expression of CRC-associated genes in a way that promotes dedifferentiation, hyperproliferation and disease advancement.

### 4.1.3 DNA microarray analysis

#### *4.1.3.1 Relevance to this study*

The development of cancer involves the accumulation of genetic mutations over a long period of time. Colorectal cancer is no exception (Fearon and Vogelstein, 1990). Research carried out over the last decade has also brought scientists attention to the possible role of epigenetic changes as the result of DNA promoter methylation in the

progression of cancer (Herman and Baylin, 2003; Jones and Laird, 1999). For example, CpG island promoter hypermethylation of the *lamin A/C* gene in leukaemias and lymphomas has been correlated with abrogation of lamin A expression at the level of transcription and has been associated with poor survival in diffuse large B-cell lymphomas (Agrelo *et al.*, 2005). It was speculated that loss of lamin A may have an equivalent epigenetic influence on the development of CRC. In summary, where cancer is concerned a complicated picture emerges in which the expression of multiple genes can be affected as the result of direct mutation and/or by epigenetic silencing.

To investigate all possible genetic aberrations in cancer using traditional techniques is inconceivable, hence the development of genetic expression microarray technologies has revolutionized our understanding of the cancer genome because they can evaluate changes in expression of thousands of genes at once (Basik *et al.*, 2003; Clarke *et al.*, 2001; Stremmel *et al.*, 2002). DNA microarrays have enabled high-throughput identification of novel diagnostic and prognostic indicators which would not have been discovered otherwise (Agrawal *et al.*, 2002; Dhanasekaran *et al.*, 2001; Korkola *et al.*, 2003). Additionally they have enabled classification of tumours according to their genetic signature (Fuller *et al.*, 2002; Golub *et al.*, 1999; Korkola *et al.*, 2005; Perou *et al.*, 2000) and allowed genome-wide investigations into chemotherapeutic drug targets (Marton *et al.*, 1998; Scherf *et al.*, 2000) which is necessary if new treatments are to be found.

In 2002 a US research group performed oligonucleotide arrays on different stages of colon cancer and identified osteopontin as a possible marker of tumour progression out of a total of 8900 genes on the chip (Agrawal *et al.*, 2002). Most microarray studies like this one aim to screen for the activity of as many genes as possible. Affymetrix

GeneChip® technology now offers the ESTs of the whole human genome, that is approximately 33,000 genes, on one chip. While this all-encompassing approach leaves no stone unturned, it is highly unlikely that any more than 10% of the genome will be differentially regulated at any one time. Furthermore, microarray analysis on this scale can produce copious amounts of insignificant data which must be processed. Therefore, it was reasoned that a targeted microarray approach would best suit the purpose of this chapter. To this end, a unique chip was created in-house comprising 325 genes.

### *4.1.3.2 Selection of genes for the Colorectal Cancer Oligonucleotide Chip*

The genes included on our Colorectal Cancer Chip were organized into functional groups and are tabulated in Appendix II, A. The list was assembled by myself and Dr Rekha Rao, a former post-doctoral scientist in our laboratory. It was the product of both a review of the literature as it stood at the end of 2002 and to a larger extent contributions made by Prinicipal Investigators at the School of Biological and Biomedical Sciences, University of Durham. The result was an oligonucleotide chip comprising 325 genes. The majority of the genes were associated with either intestinal epithelial morphogenesis, maintenance of the proliferative and differentiated compartments of mature crypts, the promotion of colorectal cancer or had been established as commonly affected in neoplasms. This included important tumour suppressor genes and oncogenes. Given the involvement of other researchers in developing this list, there were inevitably a few genes included on the basis of personal interest alone and consequently expression in normal colon or colorectal tumours was not expected. One such example is *FOXE3* which is expressed exclusively in lens epithelial cells (Blixt *et al.*, 2000). However, due to the strict localization of its expression, *FOXE3* could be considered an unorthodox negative control.

A large proportion of the chip was made up of downstream targets of the Wnt-activated β-catenin/TCF-4 complex which were identified using DNA microarray analysis by van de Wetering *et al.* (2002). Canonical Wnt signalling has been implicated in the control of the intestinal crypt-villus axis and appears to be turned on in the earliest stages of the disease (van de Wetering *et al.*, 2002). [N.B. One downstream target of the β-catenin/TCF-4 complex, c-*MYC* and the upstream regulator of β-catenin levels, *APC* were not placed in the Wnt signalling group because they are recognized oncogenes and were classified according to this function (see Appendix II, A).] All the genes were divided into 22 different groups in all.

The following gene sets are also particularly noteworthy. Fifty-two genes known to be involved in early stem cell differentiation were included on the chip because our laboratory had previously identified differential expression of a subset of these genes in cells expressing different levels of lamin A (unpublished). The cell cycle progression / cell proliferation and growth cluster of genes was compiled because an increase in their expression would generally indicate loss of proliferative control, therefore they were prime candidates for alteration in colorectal cancer. The number of nucleoskeletal and cytoskeletal genes added to this chip reflects the common interest of the main research groups in our department who contributed genes to the final list. The requisite positive (β-actin and GAPDH) and negative controls (Oct4 / POU5F1 and muscarinic receptors, M1 - M5) were naturally incorporated into the array.

### 4.1.4 Summary

This chapter describes a genomic study which was undertaken to understand the implications of lamin A dysregulation in colorectal cancer cells. This included RNA

profiling using microarray analysis with a colorectal cancer-specific oligonucleotide chip. This approach was employed on lamin A-transfected SW480 cells versus control cells to study how changes in lamin A levels would affect global gene expression.

## *4.2 Results*

### 4.2.1 Establishment of GFP-reporter transfected SW480 cell lines

Previously (Chapter 3) I showed by western blotting and immunofluorescence that lamin A expression is diminished in SW948 and SW480 colon carcinoma cells. To explore the downstream implications of this molecular change on the expression of genes associated with intestinal epithelial morphogenesis and colorectal cancer, SW480 cells were transfected with three different enhanced GFP-reporters. (SW480 cells were chosen because they were easier to culture and individual cells could be visualized at relatively low magnification.) These included GFP-lamin A, GFP-emerin and GFP. Both GFP-emerin and GFP were originally intended to be controls. Emerin is one of a group of lamina-associated proteins responsible for the association of the nuclear lamina with the inner nuclear membrane (Vaughan *et al.*, 2001) and is mutated in X-linked Emery-Dreifuss muscular dystrophy (Bione *et al.*, 1994). No role has been reported for emerin in tumourigenicity.

Forty-seven GFP-lamin A, 12 GFP-emerin and six GFP stably transfected clones were successfully scaled up and the percentage of GFP positive cells was examined. Six GFP-lamin A (11, 12, 1a3, 2c3, 1b4 and 2bb3), three GFP-emerin (1, 2 and 3) and two GFP (1 and 2) clones with 100% of cells expressing the GFP-reporter (**Figure 4.1**) were

selected and maintained in culture. The GFP-lamin A clones were grouped on the basis of GFP fluorescence intensity. Clones 11, 12 and 1b4 had low expression, clones 1a3, 2c3 and 2bb3 had medium expression. The intention was to investigate changes in gene expression in lamin A negative cells versus cells expressing lamin A equivalent to the normal endogenous level. Accordingly, cells strongly expressing GFP-lamin A were rejected as this represented a commensurate over-expression of lamin A.

### 4.2.2 Endogenous lamin A and emerin remains localized to the nuclear membrane in GFP-reporter transfected cell lines

Sub-confluent GFP-reporter transfected cells were fixed in Paraformaldehyde and stained with monoclonal anti-emerin (GFP-lamin A clones), anti-lamin A – JoL4 (GFP-emerin clones) or both (GFP clones) (**Figure 4.1**). Endogenous emerin staining was strongly associated with the nuclear rim in both GFP-lamin A and GFP transfected cells. Endogenous lamin A was located at the nuclear rim in GFP transfected cells, but appeared also in the cytoplasm of GFP-emerin transfected cells. All GFP fusion proteins localized predominantly to the nucleus. Only GFP-emerin showed some cytoplasmic localization.

### 4.2.3 Expression levels of lamin A, emerin and GFP-reporters in transfected cell lines

Protein expression profiles were determined for endogenous and exogenous lamin A, emerin and GFP in each of the selected clonal lines: SW480 GFP-lamin A 11, 12, 1a3, 2c3, 1b4 and 2bb3; SW480 GFP-emerin 1, 2 and 3 and SW480 GFP 1 and 2 (**Figure**

**4.2.1**). No endogenous lamin A was present in SW480 GFP 1 cells and it was barely detectable in SW480 GFP 2, GFP-emerin 1 and GFP-lamin A 1a3 cells. Generally, more endogenous lamin A was present in GFP-emerin and GFP-lamin A transfected clones, compared to GFP transfected clones, possibly due to the stabilization of endogenous lamin A by GFP-emerin and GFP-lamin A. SW480 GFP-lamin A clones 2bb3 and 12 showed appreciable levels of GFP-lamin A fusion protein. Expression was highest in 2bb3 cells, effectively doubling the endogenous level of lamin A (**Figure 4.2.1, A**).

Endogenous emerin expression levels were variable, but generally higher in GFP-emerin transfected clones and clonal lines with the highest level of GFP-lamin A reporter (clones 2bb3 and 12), suggesting reciprocal stabilization of endogenous emerin by the GFP forms of both emerin and lamin A (**Figure 4.2.1, B**). Cells transfected with GFP expressed the lowest levels of emerin. Blotting with anti-GFP antibodies confirmed the variation in GFP-reporter expression between clones which had been identified using anti-lamin A and anti-emerin antibodies (**Figure 4.2.1, C**).

Clones over-expressing GFP-lamin A were excluded by visual screen. From the remaining clones SW480 GFP-lamin A 2bb3, GFP-emerin 2 and GFP 2, which expressed the highest level of their respective GFP fusion protein, were selected for comparison using microarray analysis. These cell lines were compared on the same western blot (**Figure 4.2.2**) which confirmed that GFP 2 cells expressed almost no endogenous lamin A (**Figure 4.2.2, A**). In GFP-emerin 2 cells endogenous lamin A levels were eqivalent to the combined amount of endogenous and exogenous lamin A in GFP-lamin A 2bb3 cells. Consequently, rather than functioning as a negative control,

SW480 GFP-emerin 2 represented a second cell line expressing essentially normal levels of lamin A and therefore equivalent to SW480 GFP-lamin A 2bb3 in that respect.

### 4.2.4 Up-regulation of lamin A promotes an epithelial-like phenotype

To begin to determine the consequences of re-expressing lamin A in SW480 cells, cell morphology was investigated using phase contrast microscopy (**Figure 4.3**). There were significant differences between the morphology of SW480 GFP 2, GFP-emerin 2 and GFP-lamin A 2bb3 clones in culture. GFP 2 cells displayed an identical phenotype to untransfected SW480 cells: Cells grew in multiple layers and were not contact inhibited. However, GFP 2 cells did appear to grow more slowly than the parental cell line, probably due to the load placed on the cells by the large GFP construct. A complete rescue of an epithelial-like phenotype was achieved by transfecting SW480 cells with GFP-lamin A. Cells grew in a monolayer and contact inhibition was reintroduced. Transfection of GFP-emerin appeared to constitute a partial rescue of a more normal, epithelial-like phenotype; the vast majority of the culture grew as a monolayer, but the presence of multinucleated cells persisted.

Next, cell growth characteristics were investigated in each cell line by flow cytometry (**Figure 4.4**). Forward and side scatter analysis revealed a reduction in cell size variability and granularity in GFP-emerin 2 and GFP-lamin A 2bb3 cells compared to GFP 2 cells (**Figure 4.4**, panels a, c & e). This correlated with the rescue of a more normal epithelial morphology in these two clonal lines. There were, however, no statistically significant differences in cell cycle distribution between cell lines (**Figure 4.4**, panels b, d & f).

A common feature of all the transfected cell lines and SW480 untransfected cells was the propensity of the cells to dislodge from the culture substrate, resulting in an adherent and a floating population of cells. It was hypothesized that this may be the result of apoptosis. However, flow cytometry revealed no pre-G1 peak (**Figure 4.4**, panels b, d & f) and ultrastructural studies of the cells uncovered no other evidence that apoptosis was occuring in any cell population (**Figure 4.5**). However electron microscopy did reveal an increased incidence of nuclear invaginations in SW480 GFP 2 cells compared to all other cells lines. This could be the result of a malfunctioning nuclear lamina due to the lack of lamin A, consequently reducing the ability of the nucleus to maintain its shape. Additionally there appeared to be a loss of peripheral heterochromatin in SW480 untransfected cells compared to SW480 GFP-lamin A 2bb3 cells.

### 4.2.5 Lamin A facilitates the maintenance of an epithelial-like phenotype through down-regulation of the cytoskeletal protein synemin

A microarray was designed comprising 325 genes associated with intestinal epithelial homeostasis and colorectal / general cancer development and progression. The construction of the array is described in Section 4.1.3.2. Three-way pair-wise analysis of the gene expression profiles of SW480 GFP 2, GFP-emerin 2 and GFP-lamin A 2bb3 cells was performed as detailed in **Figure 4.6**. Equal quantities of control and test RNA of suitable quality (**Figure 4.7**) were labelled with Cy3 and Cy5 fluorescent dyes respectively and hybridized to specific oligonucleotide sequences immobilized on a glass chip. Arrays were laser-scanned producing a dotted image of gene activity (**Figure 4.8**). Hybridization was quantified by measuring the fluorescence from each fluor. Differences in expression of each gene were calculated as a ratio of Cy5 / Cy3 and given as a fold change. (The average fold change for each gene in each replicate array is

tabulated in Appendix II, D.) All genes less than 1.5 fold up- or down-regulated in each array were excluded from further analysis. The remaining genes which were expressed 1.5 fold higher or lower in test versus control samples are shown in **Table 4.1**. The most reproducible results were obtained for the intermediate filament proteins synemin and paranemin, the oncogenes c-myc and c-raf, the stem cell marker REST and ribosomal protein L31. *Synemin*, *paranemin*, c-*MYC* and c-*RAF* appeared to be down-regulated in cells expressing the highest levels of lamin A, whereas *REST* and *RPL31* appeared to be up-regulated. The positions of four of these genes on the microarray are indicated in **Figure 4.8**.

To corroborate the relationship between expression of *synemin*, c-*MYC*, c-*RAF* and *RPL31* and the level of lamin A, semi-quantitative RT-PCR was carried out on the same RNA samples used in the microarray experiments (**Figure 4.9**). Densitometric assessment confirmed that down-regulation of synemin mRNA correlated with increased expression of lamin A (**Figure 4.10, A**). The amount of synemin transcript was significantly reduced in SW480 GFP-lamin A 2bb3 cells compared to GFP 2 cells ($P < 0.05$). However, RT-PCR showed that c-myc, c-raf and RPL31 mRNA levels were similar in all cell lines (**Figure 4.10, B - D**). Primer specificity was demonstrated by sequencing all RT-PCR products (**Figure 4.11**).

### *4.3 Discussion*

The implications of a loss of lamin A in colorectal cancer cells was investigated using the SW480 cell line which had been shown previously (Chapter 3) to express diminished levels of lamin A relative to the more differentiated cell line HT29, but retain lamin C. Transfection of these cells with GFP-emerin or GFP-lamin A elevated

the levels of lamin A and rescued an epithelial-like phenotype in culture which was completely absent from untransfected and GFP transfected SW480 cells. GFP-lamin A transfected cells in particular displayed increased uniformity in size and growth characteristics. Altogether these observations suggested that loss of lamin A may be important in the development of colorectal cancer through a direct or indirect influence on cell morphology.

To understand how lamin A may influence cell morphological changes in the development of colorectal cancer, RNA profiles of three GFP-reporter transfected cell lines expressing increased levels of lamin A (cell lines SW480 GFP-lamin A 2bb3 and SW480 GFP-emerin 2) or no lamin A (cell line SW480 GFP 2) were compared using microarray analysis with a unique colorectal cancer-specific oligonucleotide chip. Fifty-seven percent of the genes (186 out of 325) on the chip showed differential regulation in at least one microarray experiment and of these, changes in expression of six genes were reproducible. Four leads were followed up. Primers to c-*MYC*, c-*RAF*, *synemin* and *RPL31* were used to amplify cDNA transcribed from the original RNA samples used in the microarray analyses. Using the robust technique of RT-PCR, a significant down-regulation in synemin between SW480 GFP 2 and SW480 GFP-lamin A 2bb3 cells was confirmed. However, changes in expression of the other three genes were not confirmed.

Collectively these data suggest that lamin A does not have a role in the Wnt signalling pathway because expression of c-*MYC*, which is directly regulated by the downstream target of Wnt, β-catenin, and promotes proliferation (van de Wetering *et al.*, 2002), remained unchanged in the transfected cell lines. Consistent with this observation, cell proliferation indices also remained unaltered. However, RT-PCR confirmation of

changes in the mRNA levels of synemin indicates that the phenotypic manifestations of lamin A down-regulation observed in cultured cells may reflect alterations in the cytoskeleton.

Communication between the nuclear matrix and cytoskeleton can be achieved through two possible mechanisms: The nuclear pore complex (Allen *et al.*, 2000; Stoffler *et al.*, 1999) or integral proteins of the nuclear envelope which bridge the gap between the nucleoskeleton and the cytoskeleton (Padmakumar *et al.*, 2004; Zhen *et al.*, 2002). Nesprins have emerged as important proteins hypothesized to connect the nuclear lamina to elements of the microfilament system in the cytoplasm (Libotte *et al.*, 2005). Similar to other members of the α-actinin superfamily, nesprin-1 giant, which is also known as Enaptin (Padmakumar *et al.*, 2004), and nesprin-2 giant, which is also termed NUANCE (Zhen *et al.*, 2002), are able to bind to actin fibres and facilitate actin bundling by virtue of their N-terminal α-actinin-related actin binding domain (ABD) (Padmakumar *et al.*, 2004; Zhen *et al.*, 2002). What distinguishes nesprins from other members of the spectrin family is their C-terminal Klarsicht-like domain (KLS) which contains a transmembrane domain (TMD) and targets the proteins to the nuclear membrane (Padmakumar *et al.*, 2004; Zhang *et al.*, 2001; Zhen *et al.*, 2002). Localization of nesprin-2 giant to both sides of the nuclear envelope has been demonstrated, as well as direct interaction of nesprin-2 giant with both lamin A/C and emerin (Libotte *et al.*, 2005; Zhen *et al.*, 2002). Likewise nesprin-1 giant and nesprin-1α [previously named syne-1 (Apel *et al.*, 2000) and myne-1 (Mislow *et al.*, 2002a)] immunostaining has been detected at the nuclear membrane of smooth and skeletal muscle and found to overlap with that of lamin A/C and emerin (Mislow *et al.*, 2002a; Zhang *et al.*, 2001). In addition, direct interaction between nesprin-1α, lamin A and emerin has been shown by Mislow et al. (2002b), as well as cytoplasmic staining of

nesprin-1 giant in COS7 cells (chick cardiac myocytes) (Padmakumar *et al.*, 2004). Based on this evidence Libotte et al. (2005) have proposed a model in which giant nesprin isoforms congregate at the ONM, where they bind actin, and at the INM, where they interact with nuclear lamin A/C and emerin and lie in close proximity to heterochromatin. Via UNC-84/Sun and other hitherto unidentified peripheral and integral membrane proteins nesprins are predicted to form molecular bridges between lamins, emerin and the actin cytoskeleton. If this is the case alterations in nucleoskeletal elements might be expected to have an impact on the form and function of the cytoskeleton.

Synemin was originally identified as an IF-associated protein (IFAP), but was later demonstrated to be a unique member of the IF superfamily and possess the characteristic ~310-amino acid IF rod domain (Becker *et al.*, 1995; Bellin *et al.*, 1999). Based on its domain structure it has been classified as a type VI intermediate filament protein (Mizuno *et al.*, 2001; Steinert *et al.*, 1999). Synemin is believed to require one or both of type III IF proteins desmin and vimentin to assemble and functions as an effective cytoskeletal cross-linker (Bellin *et al.*, 1999; Bilak *et al.*, 1998). As such it could be very important in maintaining cytoskeletal architecture.

Synemin was first identified in avian smooth muscle (Granger and Lazarides, 1980). Two splice variants of the human synemin gene have been identified, α and β (Titeux *et al.*, 2001). In mouse a third, smaller isoform has recently come to light (Xue *et al.*, 2004). The majority of research has focused so far on understanding the nature of synemin's heteropolymeric interactions in muscle (Bellin *et al.*, 1999; Bilak *et al.*, 1998; Mizuno *et al.*, 2004), however work by Jing et al. (2005) now suggests a role for synemin in promoting tumourigenicity. Jing and co-workers showed that α- and β-

synemin were expressed at higher levels in reactive and malignant astrocytes compared to normal brain tissue. They reported that all astrocytoma tissues reacted with synemin antibodies, independent of grade. Additionally they found that α- and β-synemin were differentially increased in some glioblastoma cell lines. Generally α-synemin appeared predominately up-regulated with comparable variation in expression seen at the mRNA level. Interestingly, in these cell lines synemin was found to associate specifically with α-actinin in ruffled membranes which are actin-rich semicircular leading edges important in cell motility. Both nesprin-1 giant and nesprin-2 giant isoforms have also been immunodetected in membrane ruffles / leading edges (Padmakumar *et al.*, 2004; Zhen *et al.*, 2002). Nesprin-1 was shown to largely colocalize with the actin-binding protein α-actinin, while nesprin-2 colocalized with the actin networks. Taken together this evidence suggests a dual role for nesprins and synemin in cell motility.

Cell motility is an important aspect of carcinogenesis and facilitates metastasis. Changes to nuclear shape, including elongation and enlargement, and polarity are strong indicators of dysplasia in colorectal cancer. Experiments by Zhen *et al.* (2002) have, in the first place, implicated nesprin-2 giant in the control of nuclear shape. Drug-induced depolymerization of the actin cytoskeleton in COS7 cells resulted in aberrant nuclear morphology and perinuclear accumulations of nesprin-2 giant and actin, suggesting nesprin-2 functions to mediate control of nuclear shape by the actin cytoskeleton. (Interestingly, irregularly shaped nuclei which also presented several invaginations were a feature of GFP-transfected SW480 cells which expressed almost no endogenous lamin A.) The nesprin-1α isoform was first identified as a novel protein which selectively associated with the nuclear envelope of synaptic nuclei of smooth and striated myotubes, therefore it was considered most likely to be involved in the migration and/or anchorage of myonuclei at the postsynaptic apparatus (Apel *et al.*, 2000). Due to the

strong sequence homology between nesprin-1α and nesprin-2 giant, Zhen *et al.* (2002) have proposed a similar function for nesprin-2 although a direct connection remains to be investigated.

Expression profiles of human nesprin-1 giant and nesprin-2 giant transcripts have been analysed by probing a human multiple tissue expression array (Padmakumar *et al.*, 2004; Zhen *et al.*, 2002). With respect to the colon, the following was discovered. Healthy colon tissue expressed medium levels of nesprin-1 and low levels of nesprin-2. In the colon carcinoma cell line SW480 they reported no change in the level of nesprin-2 compared to normal tissue, but a down-regulation of nesprin-1 to an almost undetectable amount. The same panel of cancer cells lines were tested by both groups and it was noticeable that all expressed little or no nesprin-1 and the majority had only traceable amounts of nesprin-2.

At this point only tentative proposals can be made regarding the possible connection between lamin A, located on the nucleoplasmic face of the nuclear envelope; synemin, which has so far only been reported in the cytosol and the maintenance of cellular integrity. Loss of lamin A affects nuclear and cellular morphology in SW480 cells. A normal epithelial-like phenotype can be rescued by transfection of lamin A and to a lesser extent emerin. RNA profiling of 325 genes predicted to have some importance in the development and progression of colon cancer revealed that synemin was significantly down-regulated in lamin A positive versus lamin A negative cells. It has been noted that synemin is expressed in reactive and neoplastic astrocytes, but not in normal astrocytes (Jing *et al.*, 2005), suggesting that expression of synemin may promote a tumourigenic phenotype. It is therefore plausible that lamin A expression may promote a more normal epithelial-like phenotype in SW480 cells by influencing

the expression of cytoskeletal linker proteins, such as synemin. Nesprins, by virtue of their affinity for lamin polypeptides and α-actinin and their prominence on both sides of the nuclear envelope, have emerged as the most likely mediators of lamin A – cytoplasmic IF interaction.

Of course it should not be forgotten that this chapter has only examined the expression of synemin at the mRNA level. Future work should focus on determining whether equivalent changes in synemin expression are seen at the protein level. The data presented in this chapter suggests further investigations into the expression of other cytoskeletal proteins and their organization with respect to the expression of nuclear lamins will be highly beneficial to our understanding of nucleoskeletal – cytoskeletal communication.

### *4.4 Figures*

**Figure 4.1**

**Comparative assessment of the localization of endogenous lamin A and emerin in SW480 cells transfected with one of GFP-lamin A, GFP-emerin or GFP.** One hundred percent stable transfection of SW480 colorectal cancer cells with GFP-lamin A (**A**), GFP-emerin (**B**) and GFP (**C** & **D**) was achieved (shown in green) as a result of antibiotic selection and subsequent single cell cloning of positive cells. The GFP-reporters localized to the nucleus. Endogenous emerin expression (shown in red) in GFP-lamin A and GFP transfected cells was strongly associated with the nuclear rim. Similarly, endogenous lamin A expression (shown in red) was specific to the nuclear periphery in GFP transfected cells, as determined by staining with the mAb JoL4, but was more heterogeneous in GFP-emerin transfected cells. Here, lamin A expression appeared to be both nucleoplasmic and cytoplasmic. Nuclear shape was uniformly round in GFP-lamin A transfected cells, but varied in GFP-emerin and GFP transfected cells which generally presented elongated, oval shaped nuclei. DNA was stained with DAPI (shown in blue) and a three-colour merge of the green, red and blue channels was created and shown in the final column. Scale bar = 10 μm.

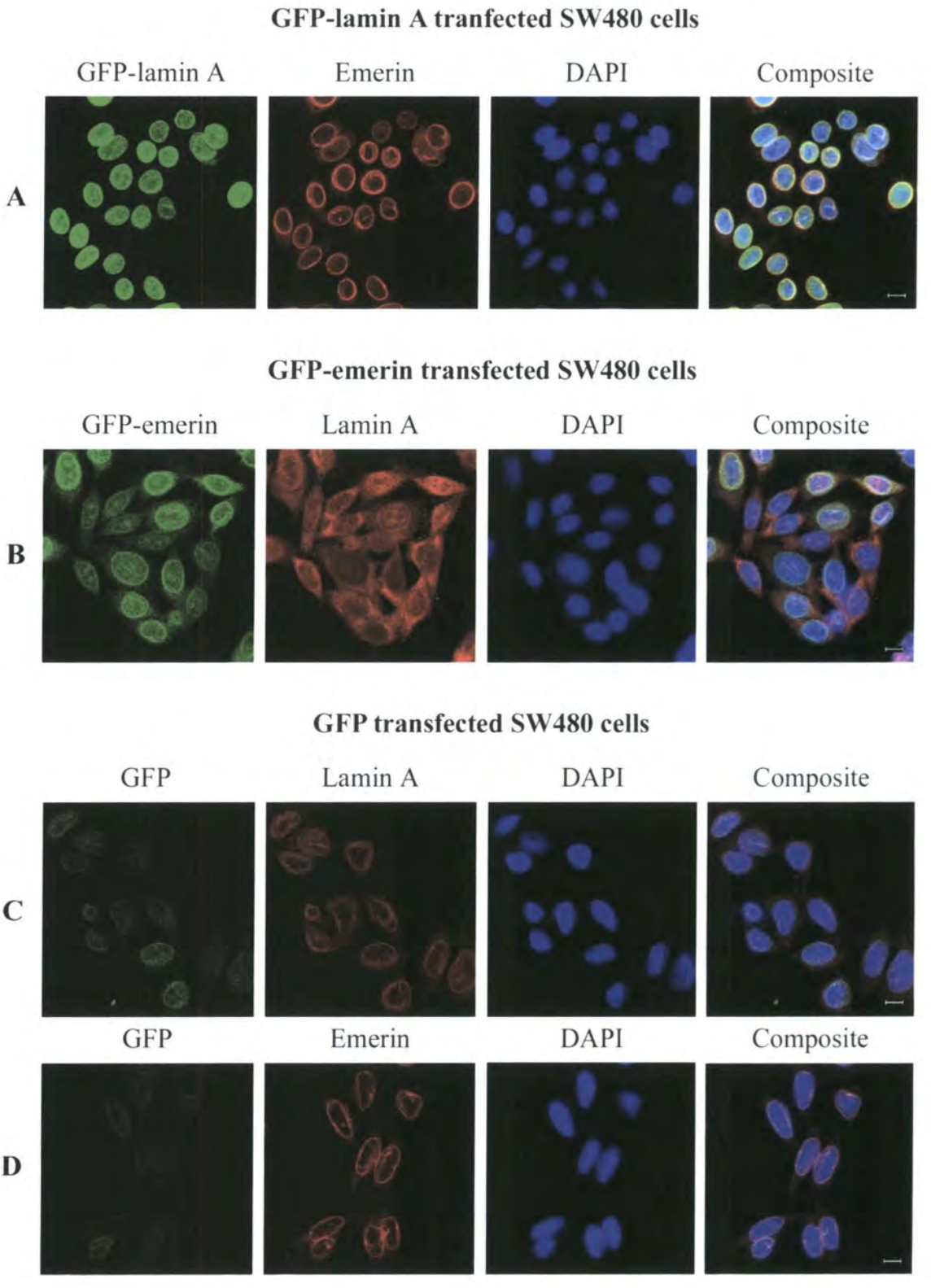
GFP-lamin A tranfected SW480 cells
GFP-lamin A
Emerin
DAPI
Composite
A
GFP-emerin transfected SW480 cells
GFP-emerin
Lamin A
DAPI
Composite
B
GFP transfected SW480 cells
GFP
Lamin A
DAPI
Composite
C
GFP
Emerin
DAPI
Composite
D

Figure 4.1

**Figure 4.2**

**Quantitative characterization of GFP-reporter, endogenous A-type lamin and endogenous emerin expression in transfected SW480 clones.**

***Figure 4.2.1***

Whole cell extracts from two GFP (lanes 1 & 2), three GFP-emerin (lanes 3 - 5) and six GFP-lamin A transfected clones (lanes 6 - 11) were resolved on 10% (**A**) or 12% (**B** & **C**) SDS-PAGE, transferred to nitrocellulose and immunoblotted with mAb JoL2 – anti-lamin A/C (**A**), monoclonal anti-emerin (**B**) and monoclonal anti-GFP (**C**). Equal loading was confirmed by co-blotting for β-actin (**A**). Molecular weight markers (M) are given in kDa.

Transfected SW480 clones run in each lane:

| Lane | Transfected SW480 clone |
|---|---|
| lane 1 | SW480 GFP 1 |
| lane 2 | SW480 GFP 2 |
| lane 3 | SW480 GFP-emerin 1 |
| lane 4 | SW480 GFP-emerin 2 |
| lane 5 | SW480 GFP-emerin 3 |
| lane 6 | SW480 GFP-lamin A 1a3 |
| lane 7 | SW480 GFP-lamin A 2c3 |
| lane 8 | SW480 GFP-lamin A 1b4 |
| lane 9 | SW480 GFP-lamin A 2bb3 |
| lane 10 | SW480 GFP-lamin A 11 |
| lane 11 | SW480 GFP-lamin A 12 |

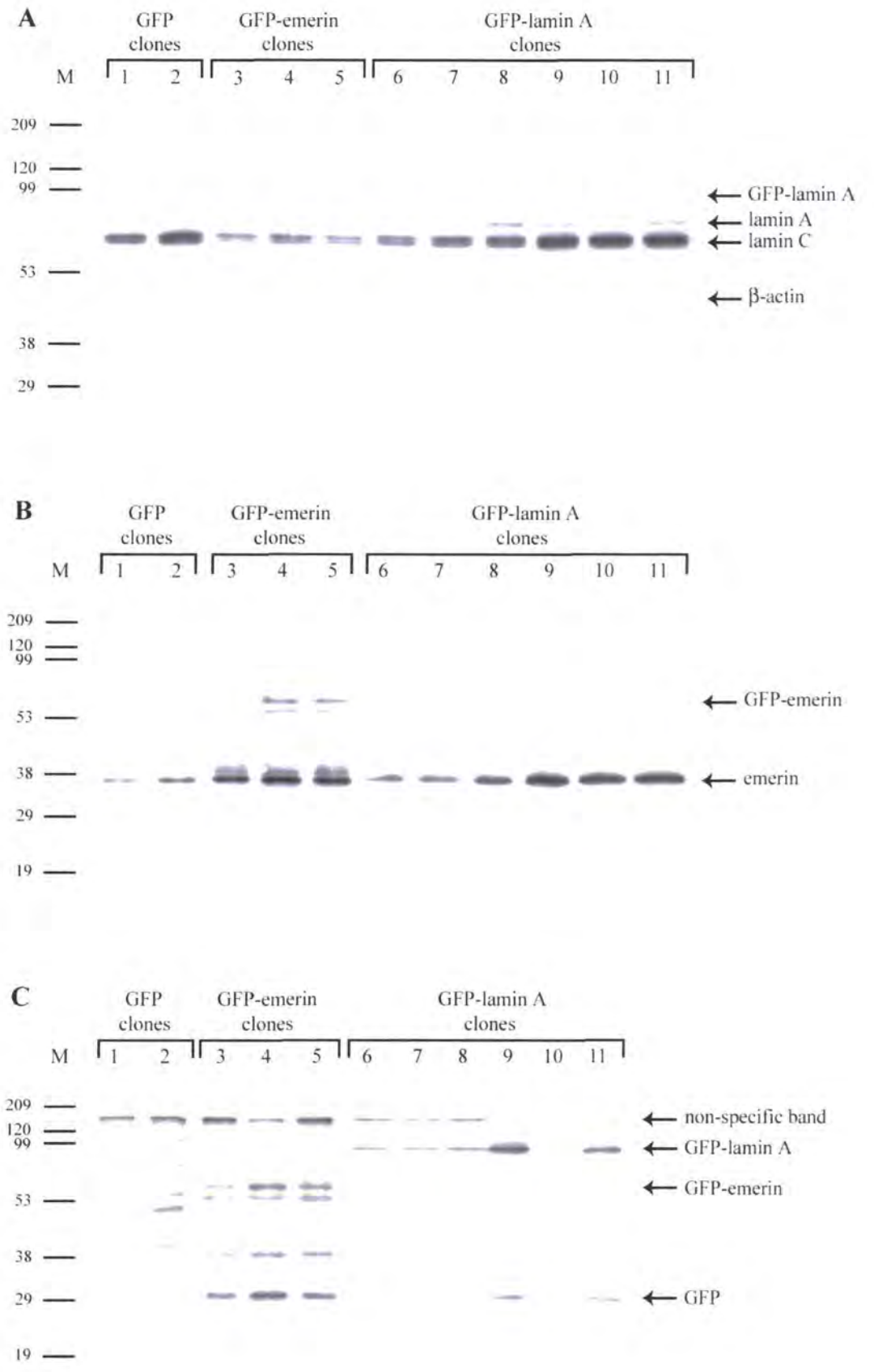
A
GFP clones
GFP-emerin clones
GFP-lamin A clones
M
1 2 3 4 5 6 7 8 9 10 11
209
120
99
53
38
29
GFP-lamin A
lamin A
lamin C
β-actin
B
GFP clones
GFP-emerin clones
GFP-lamin A clones
M
1 2 3 4 5 6 7 8 9 10 11
209
120
99
53
38
29
19
GFP-emerin
emerin
C
GFP clones
GFP-emerin clones
GFP-lamin A clones
M
1 2 3 4 5 6 7 8 9 10 11
209
120
99
53
38
29
19
non-specific band
GFP-lamin A
GFP-emerin
GFP

Figure 4.2.1

*Figure 4.2.2*

SW480 GFP 2 (lane 1), GFP-emerin 2 (lane 2) and GFP-lamin A 2bb3 (lane 3) cells were selected on the basis of their GFP-reporter expression. Whole cell extracts were resolved on 10% (**A**) or 12% (**B** & **C**) SDS-PAGE, transferred to nitrocellulose and immunoblotted with mAb JoL2 – anti-lamin A/C (**A**), monoclonal anti-emerin (**B**) and monoclonal anti-GFP (**C**). Equal loading was confirmed by co-blotting for β-actin (**A**). Molecular weight markers (M) are given in kDa.

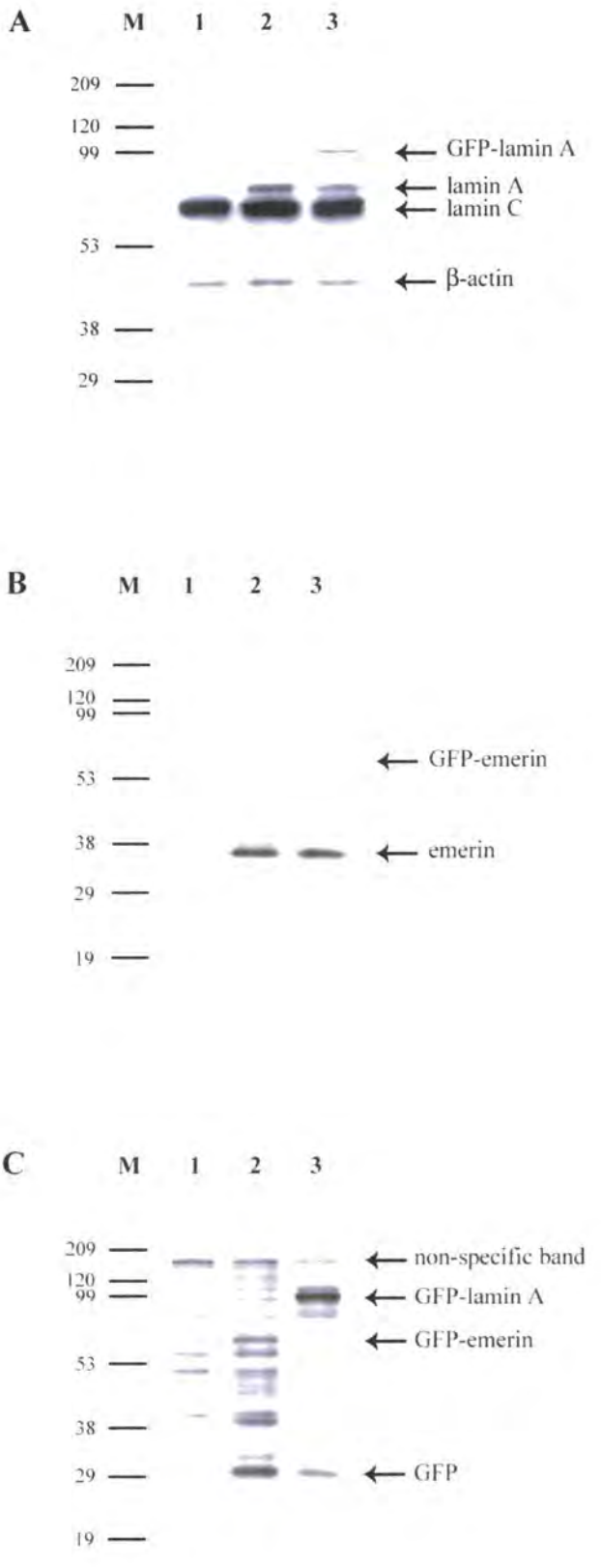
A
M
1
2
3
209
120
99
53
38
29
GFP-lamin A
lamin A
lamin C
β-actin
B
M
1
2
3
209
120
99
53
38
29
19
GFP-emerin
emerin
C
M
1
2
3
209
120
99
53
38
29
19
non-specific band
GFP-lamin A
GFP-emerin
GFP

Figure 4.2.2

**Figure 4.3**

**Morphology of SW480 parental cell line and its transfected derivatives.** Phase contrast images of SW480 colon carcinoma cells (far left panel), found previously to express minimal lamin A, were transfected with GFP, GFP-emerin or GFP-lamin A using Statagene's GeneJammer® tranfection protocol. Stably transfected cells were selected using Geneticin® antibiotic and cloned out by limited dilution. Three specific clones identified as GFP 2, GFP-emerin 2 and GFP-lamin A 2bb3 were chosen on the basis of their GFP-reporter expression, as determined by western analysis (see **Figure 4.2**) and were used in all subsequent experimental work. Clear morphological differences were apparent between the cell lines in culture and are presented in the panels entitled GFP transfected, GFP-emerin transfected and GFP-lamin A transfected respectively.

Transfection of colon carcinoma cells with GFP had no effect on cell morphology - the entire culture continued to display highly disorganized, multi-layered growth (**A**). A partial rescue of SW480 cells was achieved by the transfection of GFP-emerin - the majority of cells grew in a monolayer, although there was a high proportion of multinucleated cells (**B**). A complete rescue of cell morphology was achieved when GFP-lamin A was transfected. Normal epithelial growth was observed - cells grew in a monolayer and there was no evidence of stratified growth. Compared to GFP-emerin 2, the proportion of multinucleate cells (**B**) was very small.

Images were captured at 10X (panel I) and 20X (panel II) objective magnification. Scale bars = 20 μm (panel I) and 10 μm (panel II).

**Figure 4.4**

**Cell cycle characteristics of GFP-reporter transfected SW480 colorectal cancer cells.** Growth rate, cell size and granularity of GFP, GFP-emerin and GFP-lamin A transfected SW480 cell lines GFP 2, GFP-emerin 2 and GFP-lamin A 2bb3 were examined by flow cytometry. Cells were fixed in ice-cold methanol upon reaching 70% confluency and stained with 25 μg/ml Propidium iodide. Data for more than 10,000 single cell events were collected. Left panels (a, c & e) show forward scatter (FS) versus side scatter (SS); right panels (b, d & f) show PI fluorescence relative to cell number (count). Cells in G0/G1 are indicated by gate E, cells in S-phase, by gate F and cells in G2/M, by gate G.

Panels a, c and e showed appreciable differences in overall cell size and granularity between the transfected cell lines. GFP 2 cells varied markedly in cell dimension and granularity, while the GFP-emerin 2 cell population was less heterogeneous. GFP-lamin 2bb3 cells displayed the greatest uniformity in cell size and granularity. Differences between the proportion of transfected cells in G0/G1 phase of the cell cycle (given as mean ± s.d. of three replicates) were not statistically significant ($P > 0.05$ - 'two-tailed' Student's *t*-test), demonstrating that morphological variation had no impact on growth rate.

**Figure 4.5**

**Transmission electron micrographs of untransfected and transfected SW480 cells.** 70 - 80% confluent cultures of SW480 colon cancer cells (first column) and their stably transfected derivatives SW480 GFP 2 (second column), SW480 GFP-emerin 2 (third column) and SW480 GFP-lamin A 2bb3 (fourth column) were separated according to their adherence to the tissue culture substrate and prepared for electron microscopy using Karnovsky's method. There was no evidence of apoptosis in either the adherent (top panels) or floating (bottom panels) population of cells, but pronounced cytoplasmic blebbing, particularly in transfected cells which had been dislodged from the culture surface, was observed. GFP 2 cells exhibited prominent nuclear invaginations (arrows). Scale bar = 2 μm, except GFP-emerin transfected 'floating' cell, bar = 5 μm.

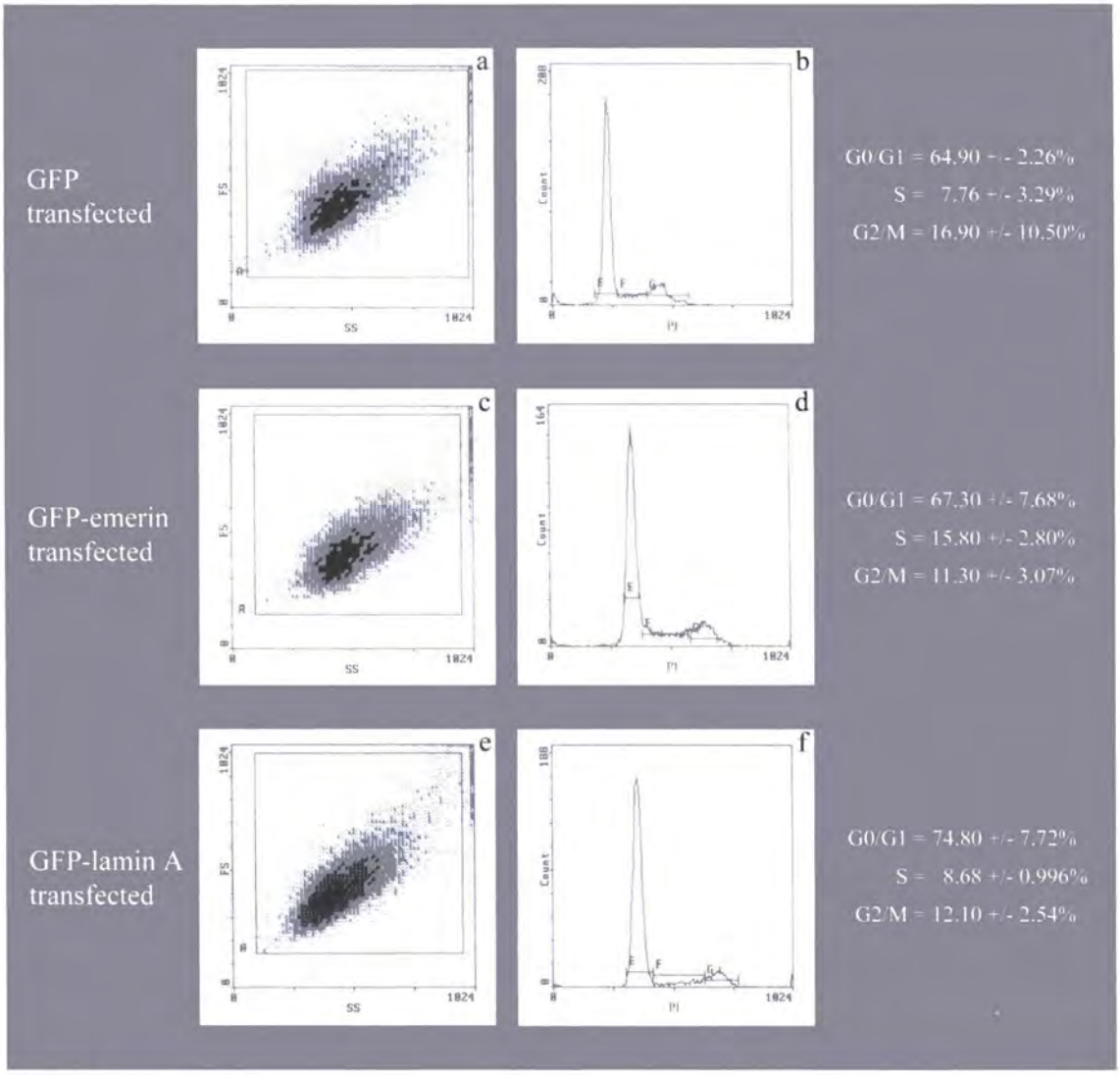
GFP transfected
a
b
G0/G1 = 64.90 +- 2.26%
S = 7.76 +/- 3.29%
G2/M = 16.90 +/- 10.50%
GFP-emerin transfected
c
d
G0/G1 = 67.30 +/- 7.68%
S = 15.80 +/- 2.80%
G2/M = 11.30 +/- 3.07%
GFP-lamin A transfected
e
f
G0/G1 = 74.80 +/- 7.72%
S = 8.68 +/- 0.996%
G2/M = 12.10 +/- 2.54%

Figure 4.4

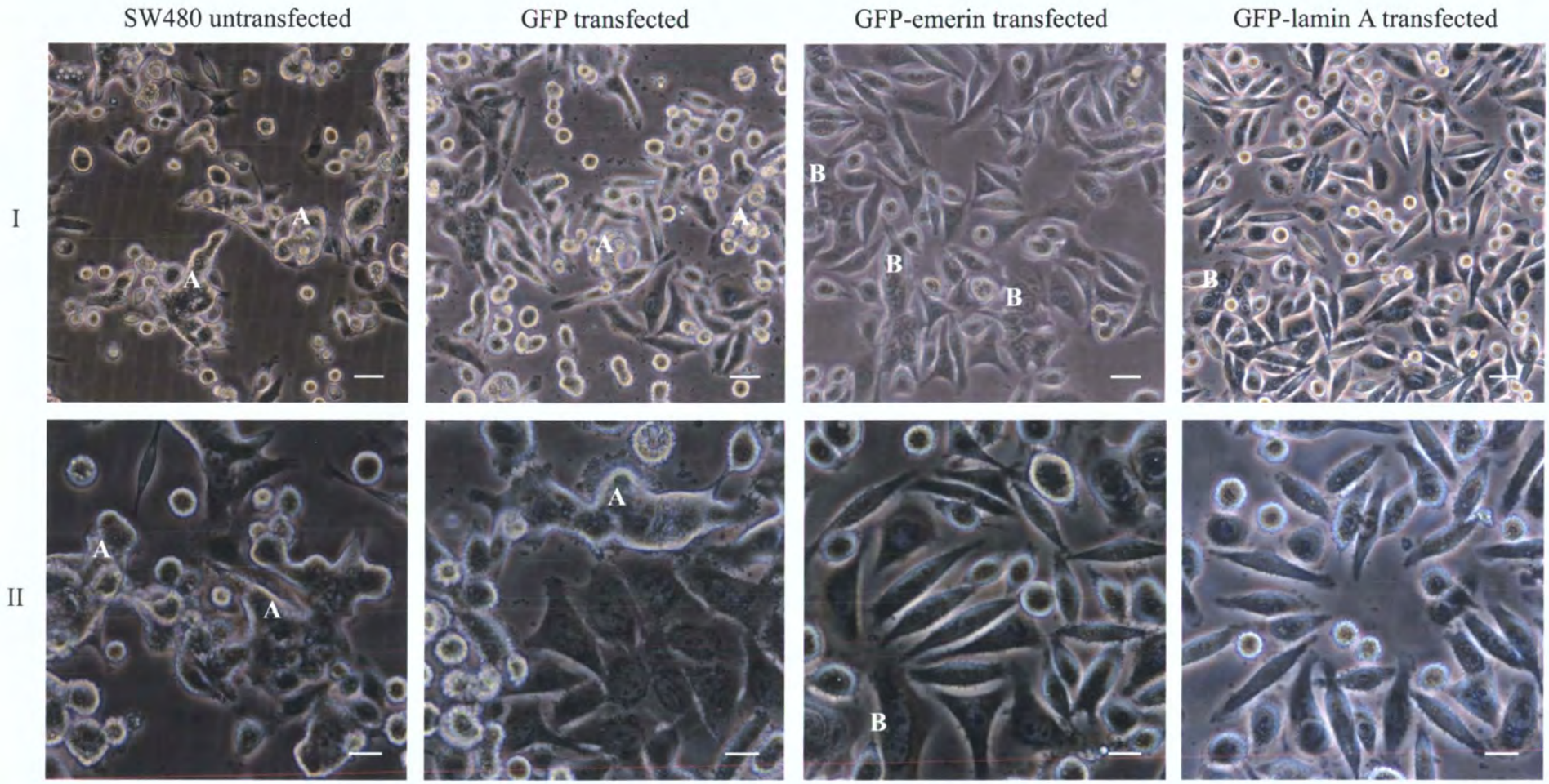
SW480 untransfected
GFP transfected
GFP-emerin transfected
GFP-lamin A transfected
I
II
A
B

Figure 4.3

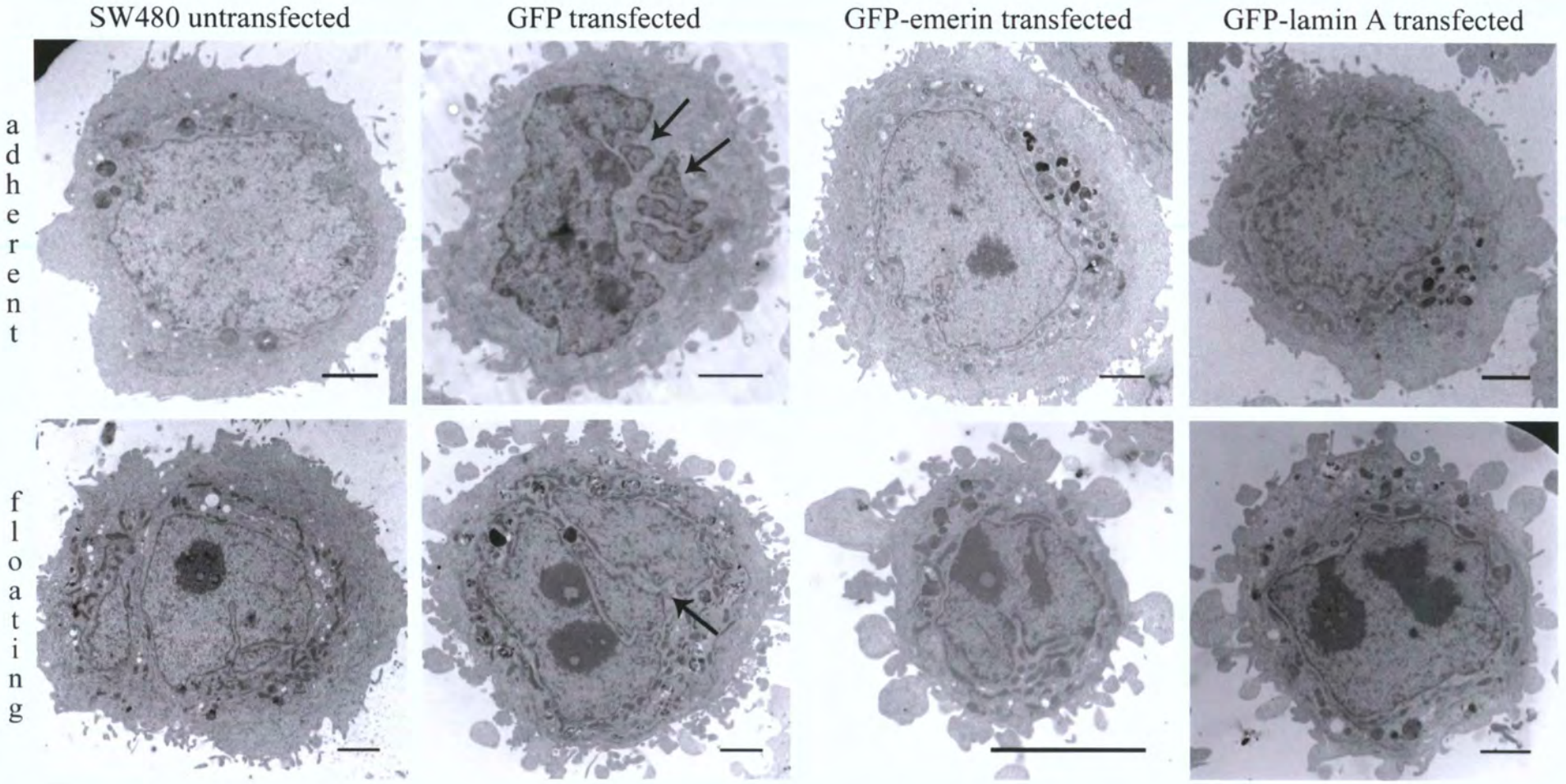
SW480 untransfected
GFP transfected
GFP-emerin transfected
GFP-lamin A transfected
adherent
floating

Figure 4.5

**Figure 4.6**

**Schematic overview of glass slide microarray analysis.** A selection of 332 oligonucleotides, representing 325 different genes, were robotically spotted in quadruplicate in pre-defined locations on a glass slide, creating a DNA chip. Differential levels of corresponding RNA transcripts in transfected SW480 cancer cells were measured by means of simultaneous, two-colour fluorescence hybridization on the chip. The relative intensity of fluorescence signals determined the direction and order of magnitude of any change in gene expression.

## GLASS SLIDE MICROARRAY ANALYSIS

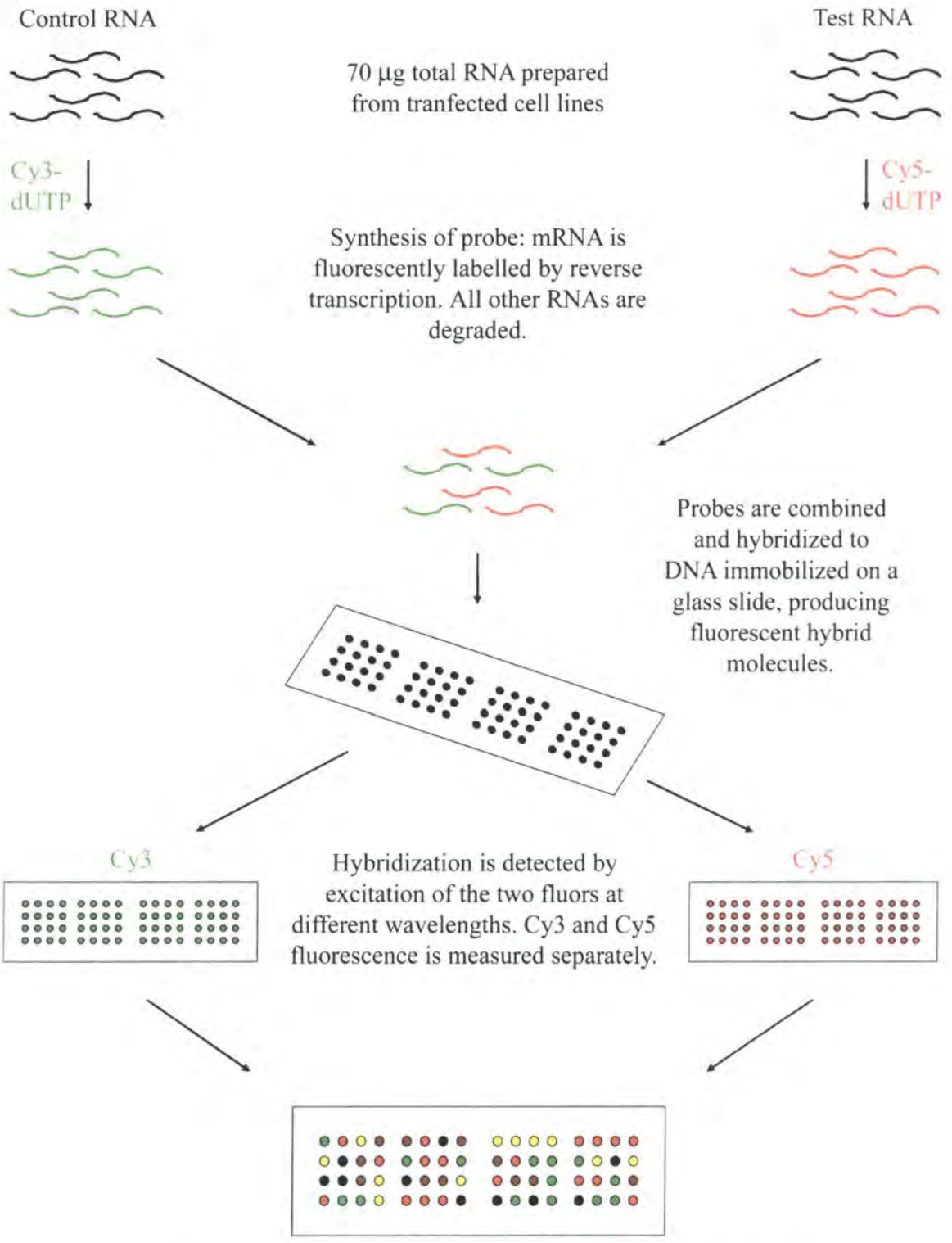


Figure 4.6

**Figure 4.7**

**Quality and purity of total RNA used in microarray experiments.** Total RNA was extracted from three different passages of SW480 GFP 2 (lanes 1, 4 & 7), SW480 GFP-emerin 2 (lanes 2, 5 & 8) and SW480 GFP-lamin A 2bb3 (lanes 3, 6 & 9) cells using TRI Reagent™. Quality was verified by gel electrophoresis. All the hallmarks of good quality RNA were demonstrated. The 28S and 18S ribosomal RNA bands were clearly distinguished, the 28S band being at least twice the intensity of the 18S band. No evidence of DNA contamination or RNA degradation was apparent. RNA purity was determined by measuring the ratio of absorbance in 10 mM Tris-HCl, pH 7.5 at 260 and 280 nm ($A_{260/280}$). An $A_{260/280}$ >1.8 indicates very pure RNA. Only one RNA sample (lane 7) did not meet this specification. M - RNA size markers, shown in kilobases (kb).

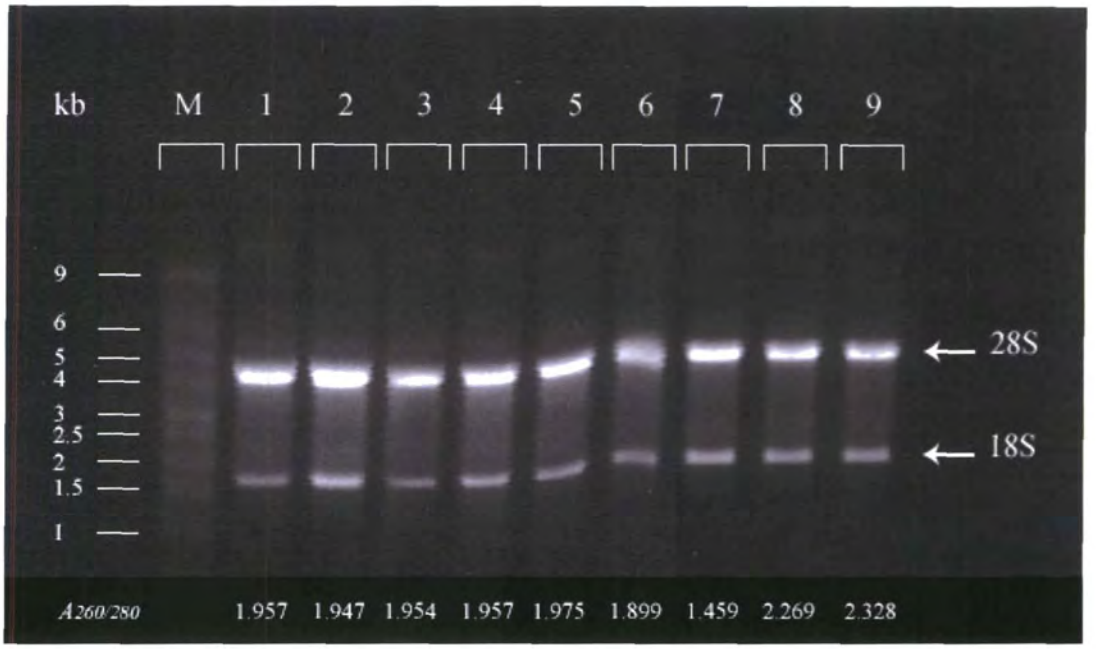
kb
M
1
2
3
4
5
6
7
8
9
9
6
5
4
3
2.5
2
1.5
1
28S
18S
A260/280
1.957
1.947
1.954
1.957
1.975
1.899
1.459
2.269
2.328

Figure 4.7

**Figure 4.8**

**Two-colour dot plots of hybridized microarrays.** For each microarray experiment hybridized chips were scanned in a GeneTAC™ LS IV Biochip Analyzer and Cy5 fluorescence signals superimposed over Cy3 fluorescence signals. Green spots correspond to genes down-regulated in test versus (vs) control cells. Red spots correspond to genes up-regulated in test vs control cells. Genes expressed at approximately equal levels in both cell lines appear yellow. The position of the replicate spots for the four genes encoding RPL31, synemin, c-raf and c-myc, which showed significant fold changes between SW480 GFP 2 (labelled **GFP**), GFP-emerin 2 (labelled **Emerin**) and/or GFP-lamin A 2bb3 (labelled **Lamin A**) cell lines, are highlighted. A red arrow indicates the gene was significantly up-regulated, a green arrow indicates the gene was significantly down-regulated. Example microarray dot plots shown: **A**. Lamin A (test) vs GFP (control); **B**. Emerin (test) vs GFP (control) and **C**. Lamin A (test) vs emerin (control).

**A. Lamin A vs GFP**

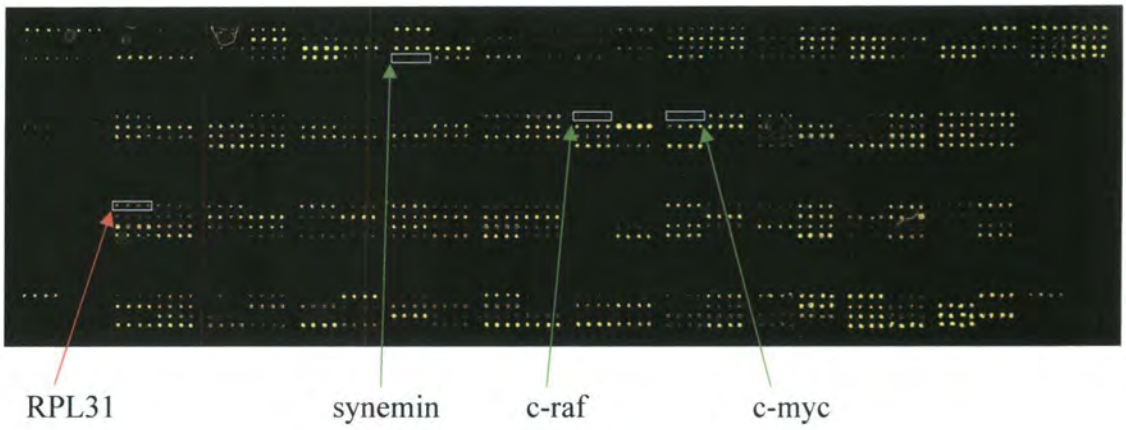


**B. Emerin vs GFP**

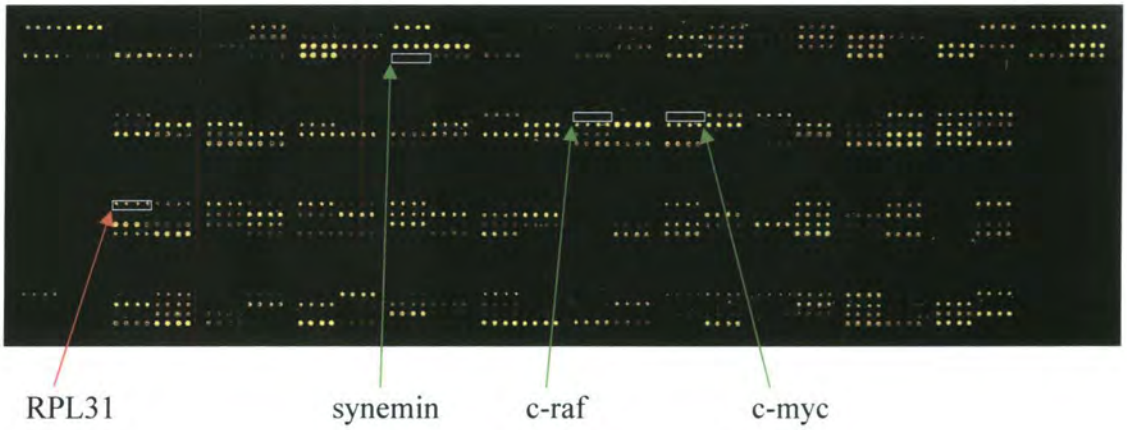


**C. Lamin A vs Emerin**

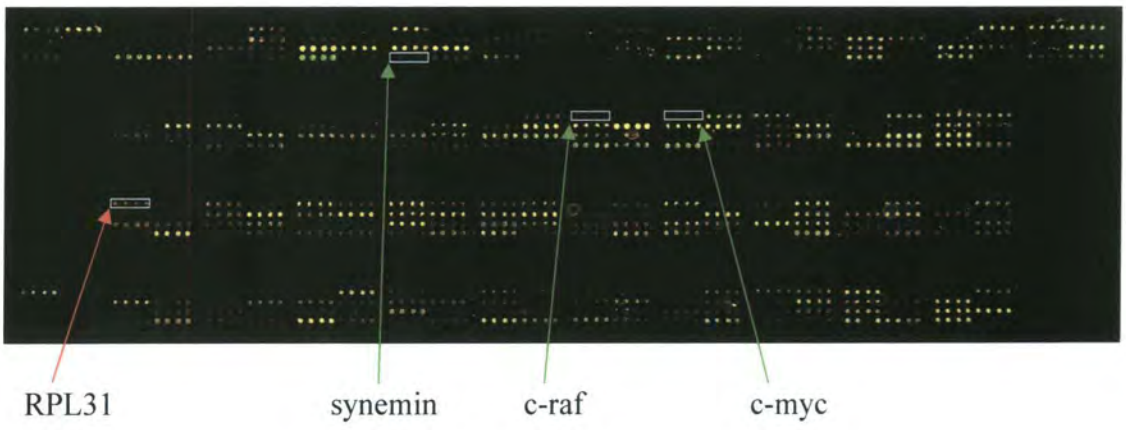


Figure 4.8

**Table 4.1**

**Genes expressed 1.5 fold higher or lower in microarray analyses.** Three-way pair-wise analysis of differential gene expression in SW480 GFP 2, GFP-emerin 2 and GFP-lamin A 2bb3 cells (denoted **GFP**, **Emerin** and **Lamin A** respectively) identified 185 genes which were either 1.5 fold up- or down-regulated in one or more microarray experiments. Pair-wise analysis was repeated three times. For each replicate (denoted **1**, **2** or **3**) the genes expressed at least 1.5 fold higher (**Up**) or lower (**Down**) in test compared to control samples are indicated by a black dot. The most reproducible changes were observed for the genes *REST*, *paranemin*, *synemin*, c-*MYC*, c-*RAF* and *RPL31*, highlighted in grey.

**Table 4.1 All genes differentially expressed by at least 1.5 fold.**

| | Lamin A vs GFP | | | | | | Emerin vs GFP | | | | | | Lamin A vs Emerin | | | | | | |
|---|---|---|---|---|---|---|---|---|---|---|---|---|---|---|---|---|---|---|---|
| | Up | | | Down | | | Up | | | Down | | | Up | | | Down | | | |
| Gene symbol | 1 | 2 | 3 | 1 | 2 | 3 | 1 | 2 | 3 | 1 | 2 | 3 | 1 | 2 | 3 | 1 | 2 | 3 | Gene description |
| Apoptosis and apoptotic inhibitors | | | | | | | | | | | | | | | | | | | |
| *AMID / PRG3* | | | | | | | • | | | | | | | | • | | | | p53-responsive gene 3 |
| *BAK1* | | | | | | | | | | | | | • | | | | | | BCL2-antagonist/killer 1 |
| *CASP3* | | | | | | | | | | • | | | • | | | | | • | caspase 3, apoptosis-related cysteine protease |
| *CAST* | | | | | | | | | | | | | | | | • | | | calpastatin |
| *FASLG* | | | | | | | | | | | | | • | | | | | | Fas ligand (TNF superfamily, member 6) |
| *LITAF* | | | | | | | | | | | | | • | | | | | | lipopolysaccharide-induced TNF factor |
| *NCKAP1 / NAP1* | | | | | | | • | | | | | | | | | | | | NCK-associated protein 1 |
| *TNFRSF10A / TRAILR1* | | | | • | | | | | | | | | | | | | | | tumor necrosis factor receptor superfamily, member 10a |
| | | | | | | | | | | | | | | | | | | | |
| Cell adhesion | | | | | | | | | | | | | | | | | | | |
| *CTNNA1* | • | | | | | | | | | | | | • | | | | | | catenin (cadherin-associated protein), alpha 1, 102kDa |
| | | | | | | | | | | | | | | | | | | | |
| Cell cycle progression / cell proliferation and growth | | | | | | | | | | | | | | | | | | | |
| *CCNA1* | | | | | | | | | | | | | • | | | | | | cyclin A1 |
| *CCNB1* | | | | | | | | | | | | | • | | | | | | cyclin B1 |
| *CCNB2* | | | | | | | | | | • | | | • | | | | | | cyclin B2 |
| *CCND1* | | | | | | | | | | | | | | | • | | | | cyclin D1 |
| *CCND3* | • | | | | | | | | | | | | • | | | | | | cyclin D3 |
| *CDC2* | | | | | | | | | | | | | • | | | | | | cell division cycle 2, G1 to S and G2 to M / cdk1 |
| *CDKN1B* | | | | • | | | | | | | | | | | | | | | cyclin-dependent kinase inhibitor 1B (p27, Kip1) |
| *CHK1* | | | | | | | | | | | | | | | | • | | | checkpoint kinase Chk1 |
| *CHK2* | • | | | | | | | | | | | | | | | | | | checkpoint kinase Chk2 |
| *CSPG2* | | | | | | | | | • | • | | | • | | | | | | chondroitin sulfate proteoglycan 2 (versican) |
| *EGF* | | | | | | | | | | | | | | | • | • | | | epidermal growth factor |
| *FGF5* | | | | | | | | | | • | | | • | | | | | | fibroblast growth factor 5 |

**Table 4.1 cont.**

| Gene symbol | Lamin A vs GFP Up 1 | 2 | 3 | Down 1 | 2 | 3 | Emerin vs GFP Up 1 | 2 | 3 | Down 1 | 2 | 3 | Lamin A vs Emerin Up 1 | 2 | 3 | Down 1 | 2 | 3 | Gene description |
|---|---|---|---|---|---|---|---|---|---|---|---|---|---|---|---|---|---|---|---|
| Cell cycle progression / cell proliferation and growth cont. | | | | | | | | | | | | | | | | | | | |
| *GPC3* | | | | | | | | | | • | | | | | | • | | | glypican 3 |
| *IGF2* | • | | | | | | | | | | | | | | • | | | | insulin-like growth factor 2 (somatomedin A) |
| *TGFA* | | | | | | | | | | | | | | | | • | | | transforming growth factor, alpha |
| *TGFBI / BIGH3* | | | | | | | | | | • | | | | | | | | | transforming growth factor, beta-induced, 68kDa |
| *VEGF* | | | | | | | | | | | | | • | | | | | | vascular endothelial growth factor |
| | | | | | | | | | | | | | | | | | | | |
| Cytoskeleton and nucleoskeleton | | | | | | | | | | | | | | | | | | | |
| *ACTG1* | | | | • | | | | | | | | | | | | | | | actin, gamma 1 |
| *KRT1* | | | | | | | • | | | | | | | | | | • | | keratin 1 |
| *KRT18* | | | | | | | | | | | | | | | • | | | | keratin 18 / Genbank® accession no. NM_000224 |
| *KRT8* | | | | | | | | | | | | | | | | • | | | keratin 8 / Genbank® accession no. X74929 |
| *LCP1* | • | | | | | | | | | | | | | | | • | | • | lymphocyte cytosolic protein 1 (L-plastin) |
| *LMNA (lamin C)* | | | | | | | | | | | | | • | | | | | | lamin C / Genbank® accession no. X03445 |
| *LMNB1* | | | | | | | | | | • | | | | | | | | | lamin B1 |
| *MACF1* | | | | | | | | | | | | | | | | | • | | microtubule-actin crosslinking factor 1 |
| *NEBL* | | | | | | | | | | | | | • | | | | | | nebulette |
| *NEFH* | | | | | | | | | | | | | | | | • | | | neurofilament, heavy polypeptide 200kDa |
| *paranemin* | | | | | • | • | | | | • | • | • | • | | | | | • | paranemin |
| *PLS3* | | | | | | | | | | • | | | • | | | | | • | plastin 3 (T isoform) |
| *PPL* | | | | | | | | | | | • | | | | | • | | | periplakin |
| *SYN* | | | | | • | • | | | | • | • | • | | | | • | | • | synemin |
| *TMPO (A)* | | | | | | | | | | | | | • | | | | | | thymopoietin alpha / lamina-associated polypeptide 2 alpha |
| *TMPO (B)* | | | | | | | | | | • | | | • | | | | • | | thymopoietin beta / lamina-associated polypeptide 2 beta |
| *TUBB2* | | | | | | | | | | | | | • | | | | | | tubulin, beta 2 |
| *TUBG* | | | | | | | | | | | | | | | | • | | | tubulin, gamma 1 |
| *VCL* | | | | | | | • | | | | | | | | | | | | vinculin |
| *VIL2* | | | | | | | | | | • | | | | | | | | | villin 2 (ezrin) |

**Table 4.1 cont.**

| Gene symbol | Lamin A vs GFP Up 1 | Lamin A vs GFP Up 2 | Lamin A vs GFP Up 3 | Lamin A vs GFP Down 1 | Lamin A vs GFP Down 2 | Lamin A vs GFP Down 3 | Emerin vs GFP Up 1 | Emerin vs GFP Up 2 | Emerin vs GFP Up 3 | Emerin vs GFP Down 1 | Emerin vs GFP Down 2 | Emerin vs GFP Down 3 | Lamin A vs Emerin Up 1 | Lamin A vs Emerin Up 2 | Lamin A vs Emerin Up 3 | Lamin A vs Emerin Down 1 | Lamin A vs Emerin Down 2 | Lamin A vs Emerin Down 3 | Gene description |
|---|---|---|---|---|---|---|---|---|---|---|---|---|---|---|---|---|---|---|---|
| Cytoskeleton and nucleoskeleton cont. | | | | | | | | | | | | | | | | | | | |
| *VIM* | | | | | | | | | | | | | | | | | • | | vimentin |
| | | | | | | | | | | | | | | | | | | | |
| DNA replication and repair | | | | | | | | | | | | | | | | | | | |
| *ATM* | | | | | | | | | | | | | • | | | | | | ataxia telangiectasia mutated |
| *MLH1* | • | | | | | | | | | | | | | | | • | | | mutL homolog 1, colon cancer, nonpolyposis type 2 |
| *MSH2* | | | | | | | | | | | | | • | | | | | | mutS homolog 2, colon cancer, nonpolyposis type 1 |
| *NBS1* | | | | | | | | | | | | | | | | • | | | Nijmegen breakage syndrome 1 (nibrin) |
| *PARP1* | | | | | | | | | | • | | | | | | | | | poly (ADP-ribose) polymerase family, member 1 |
| *PRKDC* | | | | | | | | | | | | | • | | | | | • | DNA-dependent protein kinase catalytic subunit |
| *RPA1* | | | | | | | | | | | | | • | | | | | | replication protein A1, 70kDa |
| *XRCC4* | | | | | | | | | | | | | • | | | | | | DNA-repair protein XRCC4 |
| *XRCC5* | | | | | | | | | | | | | • | | | | • | | Ku autoantigen, 80kDa |
| | | | | | | | | | | | | | | | | | | | |
| Extracellular matrix: components, processing, cellular attachment, proteases and protease inhibitors | | | | | | | | | | | | | | | | | | | |
| *BGN* | • | | | | | | | | | | | | | | | • | | | biglycan |
| *COL1A2* | | | | | | | | | | | | | | | | • | | | collagen, type I, alpha 2 Genbank® accession no. NM_000089 |
| *FN1 / FN* | | | | | | | | | | • | | | | | | | • | | fibronectin, alt splice / Genbank® accession no. X02761 |
| *HPSE* | | | | | | • | | | | • | | | | | | | • | | heparanase |
| *ITGA1* | | | | | | | | | | | | | • | | • | | | | integrin, alpha 1 |
| *ITGA2* | | | | | | | | | | • | | | | | | | | | integrin, alpha 2 |
| *ITGA3* | | | | | | | | | | | | | | | | • | | | integrin, alpha 3 |
| *ITGAV* | | | | | | • | | | | • | | | | | | | | | integrin, alpha V (vitronectin receptor) |
| *ITGB1* | | | | | | • | | | | • | | | | | | | | | integrin, beta 1 |
| *LAMA4* | | | | | | | | | | • | | | | | | | | | laminin, alpha 4 |
| *LAMB1* | | | | | | • | | | | • | | | | | | | | • | laminin, beta 1 |
| *MMP14* | | | | | | | | | | • | | | | | | • | | | matrix metalloproteinase 14 (membrane-inserted) |
| *MMP3* | | | | | | | | | | | | | | | | • | | | matrix metalloproteinase 3 (stromelysin 1, progelatinase) |

**Table 4.1 cont.**

| Gene symbol | Lamin A vs GFP Up 1 | Up 2 | Up 3 | Down 1 | Down 2 | Down 3 | Emerin vs GFP Up 1 | Up 2 | Up 3 | Down 1 | Down 2 | Down 3 | Lamin A vs Emerin Up 1 | Up 2 | Up 3 | Down 1 | Down 2 | Down 3 | Gene description |
|---|---|---|---|---|---|---|---|---|---|---|---|---|---|---|---|---|---|---|---|
| Extracellular matrix: components, processing, cellular attachment, proteases and protease inhibitors cont. | | | | | | | | | | | | | | | | | | | |
| *SDC4* | | | | | | | | | | • | | | | | | | | | syndecan 4 (amphiglycan, ryudocan) |
| *SPP1* | | | | | | | | | | • | | | | | | | | | secreted phosphoprotein 1 (osteopontin) |
| *TIMP1* | | | | • | | | | | | | | | | | | | | | tissue inhibitor of metalloproteinase 1 |
| | | | | | | | | | | | | | | | | | | | |
| Oncogenes | | | | | | | | | | | | | | | | | | | |
| *ABL1* | | | | | | | | | | • | | | | | | | | | v-abl Abelson murine leukemia viral oncogene homolog 1 |
| *HRAS* | | | | | | | | | | | | | • | | | | | | v-Ha-ras Harvey rat sarcoma viral oncogene homolog |
| *JUN* | | | | | | • | | | | | | | | | | • | | • | v-jun sarcoma virus 17 oncogene homolog |
| *KRAS* | | | | | • | | | | | | | | | | | | | | v-Ki-ras2 Kirsten rat sarcoma viral oncogene homolog |
| *MOS* | | | • | | | | | | | | | | | | | | | | v-mos Moloney murine sarcoma viral oncogene homolog |
| *MYC* | | | | • | • | | | | | • | • | | | | | • | • | | v-myc myelocytomatosis viral oncogene homolog |
| *MYCN* | | | | | | | | | | • | | | | | | | | | N-myc proto-oncogene protein |
| *RAF1* | • | | | | | | | | | • | • | | | | | • | • | • | v-raf-1 murine leukemia viral oncogene homolog 1 |
| *SRC* | | | | | | | | | | • | | | | | | | • | | v-src sarcoma (Schmidt-Ruppin A-2) viral oncogene homolog |
| | | | | | | | | | | | | | | | | | | | |
| Protein translation, processing, transport and degradation | | | | | | | | | | | | | | | | | | | |
| *AIM1* | | | | | | | | | | | | | | | | • | | • | absent in melanoma 1 |
| *EIF3S2* | | | | | | | | | | • | | | | | | | | | eukaryotic translation initiation factor 3, subunit 2 beta, 36kDa |
| *hsp20* | | | | | | | | | | | | | | | | | | • | Sequence 109 from Patent WO9954460 / hsp 20 |
| *HSP70-1* | | | | | | | | | | | | | | | | • | | | heat shock 70kD protein 1 |
| *HSPA8 / HSC70* | | | | | | | • | | | | • | | | | | | | | constitutive heat shock protein 70 |
| *HSPB2* | | | • | | | | | | | | | | | | | | | | heat shock 27kDa protein 2 |
| *NUP153* | | | | | | | | | | | | | • | | | | | | nucleoporin 153kDa |
| *RPL21* | | | | | | | | | | | | | • | | | | | | ribosomal protein L21 |
| *RPL31* | • | • | • | | | | • | • | • | | | | • | • | | | | | ribosomal protein L31 |

**Table 4.1 cont.**

| Gene symbol | Lamin A vs GFP Up 1 | Lamin A vs GFP Up 2 | Lamin A vs GFP Up 3 | Lamin A vs GFP Down 1 | Lamin A vs GFP Down 2 | Lamin A vs GFP Down 3 | Emerin vs GFP Up 1 | Emerin vs GFP Up 2 | Emerin vs GFP Up 3 | Emerin vs GFP Down 1 | Emerin vs GFP Down 2 | Emerin vs GFP Down 3 | Lamin A vs Emerin Up 1 | Lamin A vs Emerin Up 2 | Lamin A vs Emerin Up 3 | Lamin A vs Emerin Down 1 | Lamin A vs Emerin Down 2 | Lamin A vs Emerin Down 3 | Gene description |
|---|---|---|---|---|---|---|---|---|---|---|---|---|---|---|---|---|---|---|---|
| Regulation of gene expression (transcription) | | | | | | | | | | | | | | | | | | | |
| *GTF3A* | | | | | | | | | | | | | | | | | • | | general transcription factor IIIA |
| *RARA* | | | | • | | | | | | | | | | | | | | | retinoic acid receptor, alpha |
| *RXRA* | | | | | | | | | | | | | | | | | • | | retinoid X receptor, alpha |
| *TCF1* | | | | | | | | | | | | | | | | • | | | transcription factor 1, hepatic |
| *TCF4* | | | • | | | | | | | | | | • | | | | | | transcription factor 4 |
| *ZFP91* | | | | | • | | | | | • | • | | | | | | | | zinc finger protein 91 homolog (mouse) |
| | | | | | | | | | | | | | | | | | | | |
| Signal transduction | | | | | | | | | | | | | | | | | | | |
| *CCR7* | | | | | | | • | | • | | | | | | • | | | | chemokine (C-C motif) receptor 7 |
| *CD14* | • | | | | | | | | | | | | | | | | | | CD14 antigen |
| *FCGR2B* | | | | | | | | | | | | | | | | | • | | IGFR2 / Fc fragment of IgG, low affinity IIb, receptor |
| *GNAL* | | | | | | | | | | | | | | | | • | | | G-s-alpha / guanine nucleotide binding protein (G protein) |
| *MAPK1* | | | | | | | | | | • | | | | | | | | | mitogen-activated protein kinase 1 |
| *PIK3CG* | | | | | | | | | | • | | | | | | | | | phosphoinositide-3-kinase, catalytic, gamma polypeptide |
| *PTK2B / PKB* | | | | | | | | | | | | | | | • | | | | PTK2B protein tyrosine kinase 2 beta |
| *RAC1* | | | | | | | | | | | | | • | | | | | | rho family, small GTP binding protein Rac1 |
| *RGS2* | | | | | | | | | | • | | | | | | • | | | Regulator of G-protein signaling 2 (G0/G1 switch regulatory protein 8) |
| *TIAM1* | | | | | | | | | | | | | | | | • | | | T-cell lymphoma invasion and metastasis 1 |
| | | | | | | | | | | | | | | | | | | | |
| Stem cell differentiation | | | | | | | | | | | | | | | | | | | |
| *ANIL* | | | | | | | | | | • | | | | | | | | | astrocytic NOVA-like RNA-binding protein |
| *ASTN* | | | | | | | | | | • | | | | | | | | • | Astrotactin |
| *BMP4* | | | | | | | • | | | | | | | | | | | | bone morphogenetic protein 4 |
| *BMP6* | | | | | | | | | | | | | • | | | | | | bone morphogenetic protein 6 |
| *CRIPTO* | | | | | | | | | | • | | | | | | | | | cripto protein |
| *FN1* | | | | | | | | | | | | | • | | | | | • | cellular fibronectin / Genbank® accession no. M10905 |
| *FUT1* | | | | | | | • | | | | | | • | | | | | | fucosyltransferase 1 |

**Table 4.1 cont.**

| Gene symbol | Lamin A vs GFP Up 1 | Lamin A vs GFP Up 2 | Lamin A vs GFP Up 3 | Lamin A vs GFP Down 1 | Lamin A vs GFP Down 2 | Lamin A vs GFP Down 3 | Emerin vs GFP Up 1 | Emerin vs GFP Up 2 | Emerin vs GFP Up 3 | Emerin vs GFP Down 1 | Emerin vs GFP Down 2 | Emerin vs GFP Down 3 | Lamin A vs Emerin Up 1 | Lamin A vs Emerin Up 2 | Lamin A vs Emerin Up 3 | Lamin A vs Emerin Down 1 | Lamin A vs Emerin Down 2 | Lamin A vs Emerin Down 3 | Gene description |
|---|---|---|---|---|---|---|---|---|---|---|---|---|---|---|---|---|---|---|---|
| Stem cell differentiation cont. | | | | | | | | | | | | | | | | | | | |
| *FUT2* | | | | | | | | | | | | | | | | • | | | fucosyltransferase 2 (secretor status included) |
| *GAP43* | | | | | | | • | | | | | | | | | | | | growth associated protein 43 |
| *GJA1* | | | | | | | • | | | | | | | | | | | | gap junction protein, alpha 1, 43kDa (connexin 43) |
| *LAMB1* | | | | | | | | | • | • | | | | | | | | • | laminin, beta 1 |
| *MAPT / TAU* | | | | | | | | | | • | | | • | | | | | | microtubule-associated protein tau |
| *MASH1* | | | | | | | | | | | | | | | • | | | | Achaete-scute homolog 1 |
| *MASH2* | | | • | | | | | | | • | | | • | | | | | | achaete-scute complex-like 2 |
| *MYOD1* | | | | | | | | | | | • | | | | | | | | myogenic factor 3 |
| *NEFL* | | | | | | | • | | | | | | | | | | | | neurofilament, light polypeptide 68kDa |
| *NEFM* | | | | | • | | | | | • | | | | | | | | • | Neurofilament medium polypeptide |
| *NES* | | | | | • | | | | | • | | | | | | | | | nestin |
| *NEUROD2* | | | | | | | | | | • | | | | | | | | | neurogenic differentiation 2 |
| *NEUROD3* | | | | | • | | | | | • | | | | | | | | • | neurogenic differentiation 3 |
| *NEUROD4* | | | | | | | | | | • | | | | | | | | | neurogenic differentiation 4 |
| *NHLH2* | | | • | | • | | | | | | | | | | | | | | nescient helix loop helix 2 |
| *NOTCH2* | | | | | | | | | | | | | • | | | | | • | Notch homolog 2 (Drosophila) |
| *NSE* | | | | | • | | | | | • | | | | | | | | | Neuron-specific enolase |
| *PAX6* | | | • | | • | | | • | • | | | | | | | | | | paired box gene 6 (aniridia, keratitis) |
| *PLP* | | | | | | | • | | | | | | | | • | | | | proteolipid protein |
| *REST* | • | | • | | | | | • | • | | | | • | | • | | | | RE1-silencing transcription factor |
| *SOX1* | | | | | | | | | | | | | | | | | | • | SRY (sex determining region Y)-box 1 |
| *SOX17* | | | | | | | | | | | | | • | | | | | | SRY (sex determining region Y)-box 17 |
| *SOX2* | | | • | | | | | | | | | | | | | | | | SRY (sex determining region Y)-box 2 |
| *SYP* | | | | | | | | | | | | | • | | | | | | synaptophysin |
| *T* | | | | | • | | | | | • | | | | | | | | | T, brachyury homolog (mouse) |
| *TDGF1* | | | | | | | | | | • | | | | | | | | | teratocarcinoma-derived growth factor 1 |
| *TF* | | | | | | | | | | | | | | | | | | • | transferrin |

**Table 4.1 cont.**

| Gene symbol | Lamin A vs GFP Up 1 | 2 | 3 | Down 1 | 2 | 3 | Emerin vs GFP Up 1 | 2 | 3 | Down 1 | 2 | 3 | Lamin A vs Emerin Up 1 | 2 | 3 | Down 1 | 2 | 3 | Gene description |
|---|---|---|---|---|---|---|---|---|---|---|---|---|---|---|---|---|---|---|---|
| Stem cell differentiation cont. | | | | | | | | | | | | | | | | | | | |
| *VTN* | | | | | | | • | | | | | | | | • | | | | vitronectin |
| | | | | | | | | | | | | | | | | | | | |
| Stress response | | | | | | | | | | | | | | | | | | | |
| *SOD1* | | | | | | | | | | | | | • | | | | | | superoxide dismutase 1, soluble |
| *SOD2* | | | | | | | | | | | | | • | | | | • | | superoxide dismutase 2, mitochondrial |
| | | | | | | | | | | | | | | | | | | | |
| Transporters, carriers | | | | | | | | | | | | | | | | | | | |
| *ATP2A3* | | | | | | | | | | | | | • | | | | | | ATPase, Ca++ transporting, ubiquitous |
| *SLC16A1* | | | | | | | | | | | | | | | | • | | | solute carrier family 16 (monocarboxylic acid transporters), member 1 |
| *SLC2A1 / GLUT1* | | | | | | | • | | | | | | | | | | | | solute carrier family 2 (facilitated glucose transporter), member 1 |
| | | | | | | | | | | | | | | | | | | | |
| Tumour suppressor genes | | | | | | | | | | | | | | | | | | | |
| *APC* | | | | | | | | | | • | | | | | | | | | adenomatosis polyposis coli |
| *DCC* | | | | | | | | | | | | | | | | • | | | deleted in colorectal carcinoma |
| *RB1* | | | • | | | | | | | • | | | • | | | | | | retinoblastoma 1 |
| *TP53* | | | | | | | | | | • | | | • | | | | | | tumor protein p53 (Li-Fraumeni syndrome) |
| | | | | | | | | | | | | | | | | | | | |
| Wnt signalling | | | | | | | | | | | | | | | | | | | |
| *BIRC5* | | | | | | | | | | • | | | | | | | | | apoptosis inhibitor 4 - survivin |
| *CDKN1A* | | | | | | | | | | | | | • | | | | | | cyclin-dependent kinase inhibitor 1A (p21, Cip1) |
| *CEACAM1 / BGP1* | | | | | | | • | | | | | | | | | • | | | carcinoembryonic antigen-related cell adhesion molecule 1 (biliary glycoprotei |
| *CHAF1A* | | | | | | | | | | | | | | | | • | | | chromatin assembly factor 1, subunit A (p150) |
| *CLDN1* | | | | | | | | | | • | | | | | | | | | claudin 1 |
| *CLDN4* | | | • | | | | • | | • | | | | | | | | | | claudin 4 |
| *DLEU1* | | | | | | | | | | | | | • | | | | | • | deleted in lymphocytic leukemia, 1 |
| *ENC1* | | | | | | | | | • | | | | • | | • | | | | ectodermal-neural cortex (with BTB-like domain) |
| *EPHB1* | | | | | | | | | | | | | | | • | | | | EPH receptor B1 |

**Table 4.1 cont.**

| | Lamin A vs GFP | | | | | | Emerin vs GFP | | | | | | Lamin A vs Emerin | | | | | | |
|---|---|---|---|---|---|---|---|---|---|---|---|---|---|---|---|---|---|---|---|
| | Up | | | Down | | | Up | | | Down | | | Up | | | Down | | | |
| **Gene symbol** | **1** | **2** | **3** | **1** | **2** | **3** | **1** | **2** | **3** | **1** | **2** | **3** | **1** | **2** | **3** | **1** | **2** | **3** | **Gene description** |
| Wnt signalling cont. | | | | | | | | | | | | | | | | | | | |
| *EPHB2* | | | | | | | | | | | | | • | | | | | | EPH receptor B2 |
| *ETS2* | | | | | | | | | | | | | • | | | | | | v-ets erythroblastosis virus E26 oncogene homolog 2 |
| *FABP1* | | | | | | | | | | • | | | | | | | | | fatty acid binding protein 1, liver |
| *GPX2* | | | | | | | | | | | | | | | • | | | | glutathione peroxidase 2 (gastrointestinal) |
| *JPO1 / LOC442172* | | | | | | | | | • | | | | • | | | | | | c-Myc target JPO1 |
| *MCM3* | | | | | | | | | | | | | | | | • | | | MCM3 minichromosome maintenance deficient 3 |
| *MUC2* | | | | | | | | | | | | | • | | | | | | mucin 2, intestinal/tracheal |
| *MYB* | | | | | | | | | | | | | | | | • | | | Myb proto-oncogene protein (C-myb) |
| *PRKCD* | | | | | | | | | | | | | • | | | | | | protein kinase C, delta |
| *RBBP4* | | | | | | | | | | | | | | | | • | | | retinoblastoma binding protein 4 |
| *SCF / KITLG* | • | | | | | | | | | | | | | | | • | | | stem cell factor / kit ligand precursor / Mast cell growth factor (MGF) |
| *TCOF1* | | | • | | | | • | | | | | | | | | | | | Treacher Collins-Franceschetti syndrome 1 |
| *UNG* | • | | | | | | | | | | | | | | | | | | uracil-DNA glycosylase |
| | | | | | | | | | | | | | | | | | | | |
| Xenobiotic and drug metabolism / detoxification | | | | | | | | | | | | | | | | | | | |
| *ABCB1* | | | | | | • | | | | | | | | | | • | | | P glycoprotein 1/multiple drug resistance 1 |
| | | | | | | | | | | | | | | | | | | | |
| Miscellaneous enzymes | | | | | | | | | | | | | | | | | | | |
| *PTGS2 / COX2* | | | | | | | | | | | | | • | | | | | | prostaglandin-endoperoxide synthase 2 (cyclooxygenase) |
| *SI* | | | | | | | | | | | | | • | | | | | | sucrase-isomaltase (alpha-glucosidase) |
| | | | | | | | | | | | | | | | | | | | |
| Miscellaneous | | | | | | | | | | | | | | | | | | | |
| *CLCNKB* | | | | | | | • | | | | | | | | | | | | chloride channel Kb |
| *T18* | | | | | | | | | | | | | • | | | | | | T-18 |
| | | | | | | | | | | | | | | | | | | | |
| Function not well elucidated | | | | | | | | | | | | | | | | | | | |
| *KLRB1* | | | | | | | | | | | | | • | | | | | | NKR-P1A |

**Table 4.1 cont.**

| Gene symbol | Lamin A vs GFP Up 1 | 2 | 3 | Down 1 | 2 | 3 | Emerin vs GFP Up 1 | 2 | 3 | Down 1 | 2 | 3 | Lamin A vs Emerin Up 1 | 2 | 3 | Down 1 | 2 | 3 | Gene description |
|---|---|---|---|---|---|---|---|---|---|---|---|---|---|---|---|---|---|---|---|
| Function not well elucidated cont. | | | | | | | | | | | | | | | | | | | |
| *LGALS2* | | | | | | | | | | • | | | • | | | | | | galectin 2 |
| *PROX1* | | | | | • | | | | | • | | | | | | | | | prospero-related homeobox 1 |
| *REG1B* | | | | | | | | | | | | | • | | | | | | regenerating protein I beta |
| *RSAD2* | | | | | | | | | | | | | • | | • | | • | | radical S-adenosyl methionine domain containing 2 / cig5 / viperin |
| *ZBTB16* | | | | | | | • | | | | | | | | | | | | PLZF / zinc finger and BTB domain containing 16 |
| | | | | | | | | | | | | | | | | | | | |
| Negative controls | | | | | | | | | | | | | | | | | | | |
| *CHRM2* | | | | | | | | | | • | | | • | | | | | | cholinergic receptor, muscarinic 2 |
| *CHRM5* | | | | | | | | | | | | | • | | | | | | cholinergic receptor, muscarinic 5 |

**Figure 4.9**

**Expression of synemin, c-myc, c-raf and RPL31 in GFP-lamin A, GFP-emerin and GFP transfected SW480 colon carcinoma cells.** Microarray analysis identified reproducible changes in the levels of six RNA transcripts, four of which were further investigated by semi-quantitative RT-PCR. Primers were designed to amplify synemin (**A**), c-myc (**B**), c-raf (**C**) and RPL31 (**D**) in cell lines GFP 2 (lane 1), GFP-emerin 2 (lane 2) and GFP-lamin A 2bb3 (lane 3). RT-PCR products were distinguished according to their size: Synemin - 518 bp, c-myc - 557 bp, c-raf - 589 bp and RPL31 - 322 bp. Equal loading of starting material was verified by monitoring the transcriptional activity of β-actin (**E**), seen as an 834 bp product. M = DNA size markers, shown in base pairs (bp).

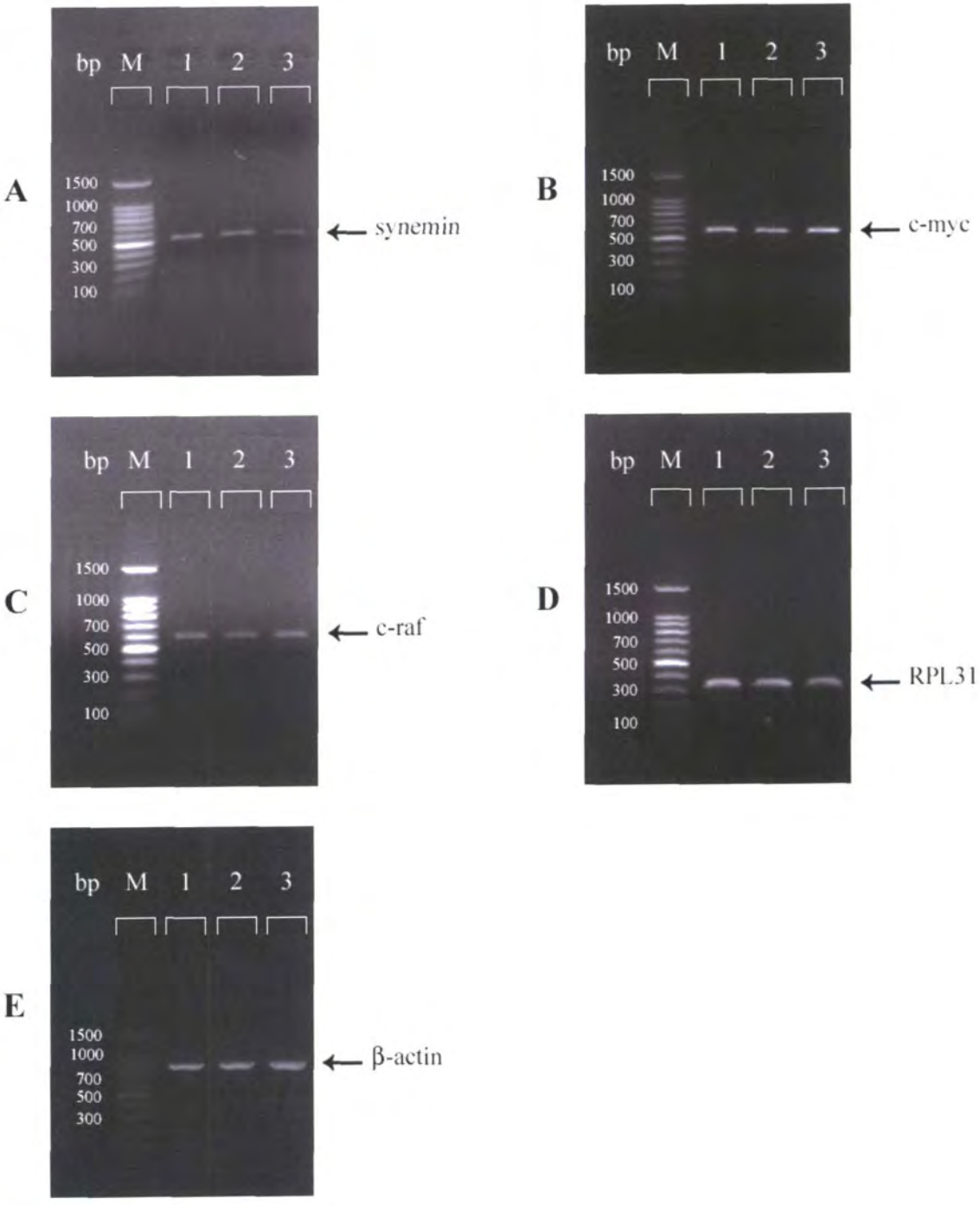
A
bp M 1 2 3
1500
1000
700
500
300
100
synemin
B
bp M 1 2 3
1500
1000
700
500
300
100
c-myc
C
bp M 1 2 3
1500
1000
700
500
300
100
c-raf
D
bp M 1 2 3
1500
1000
700
500
300
100
RPL31
E
bp M 1 2 3
1500
1000
700
500
300
β-actin

Figure 4.9

**Figure 4.10**

**Semi-quantitative RT-PCR confirmed a down-regulation of synemin in GFP-lamin A compared to GFP transfected SW480 colon carcinoma cells.** Messenger RNA expression levels for synemin (**A**), c-myc (**B**), c-raf (**C**) and RPL31 (**D**) in GFP 2 (**GFP**), GFP-emerin 2 (**GFP-emerin**) and GFP-lamin A 2bb3 (**GFP-lamin A**) cells were determined by semi-quantitative RT-PCR, followed by densitometry. Bands were digitally scanned (Fujifilm Intelligent Dark Box II) using Fujifilm Image Reader LAS-1000 Pro Ver. 2.11 software and quantified in Fujifilm Image Gauge, version 4.0. For each transcript three replicate RT-PCRs were completed. Messenger RNA expression was normalized against β-actin and relative expression of synemin, c-myc, c-raf and RPL31 was calculated. Values are mean ± standard deviation.

Differences in c-myc, c-raf and RPL31 expression between cell lines GFP 2, GFP-emerin 2 and GFP-lamin A 2bb3 were not statistically significant. However, the reduction in synemin mRNA levels in GFP-lamin A 2bb3 cells (mean = 45.5 ± 30.7%) compared to GFP 2 cells (mean = 100 ± 0.0%) is statistically significant ($t = 3.07$, $df = 4$, $P < 0.05$ in 'two-tailed' Student's $t$-test).

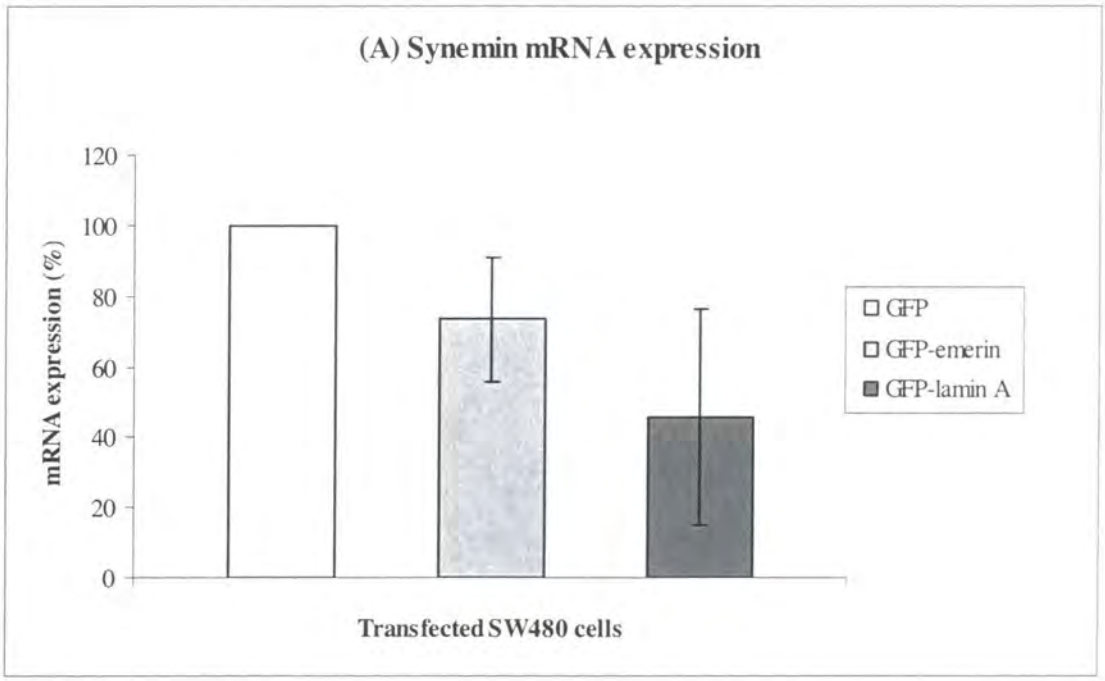


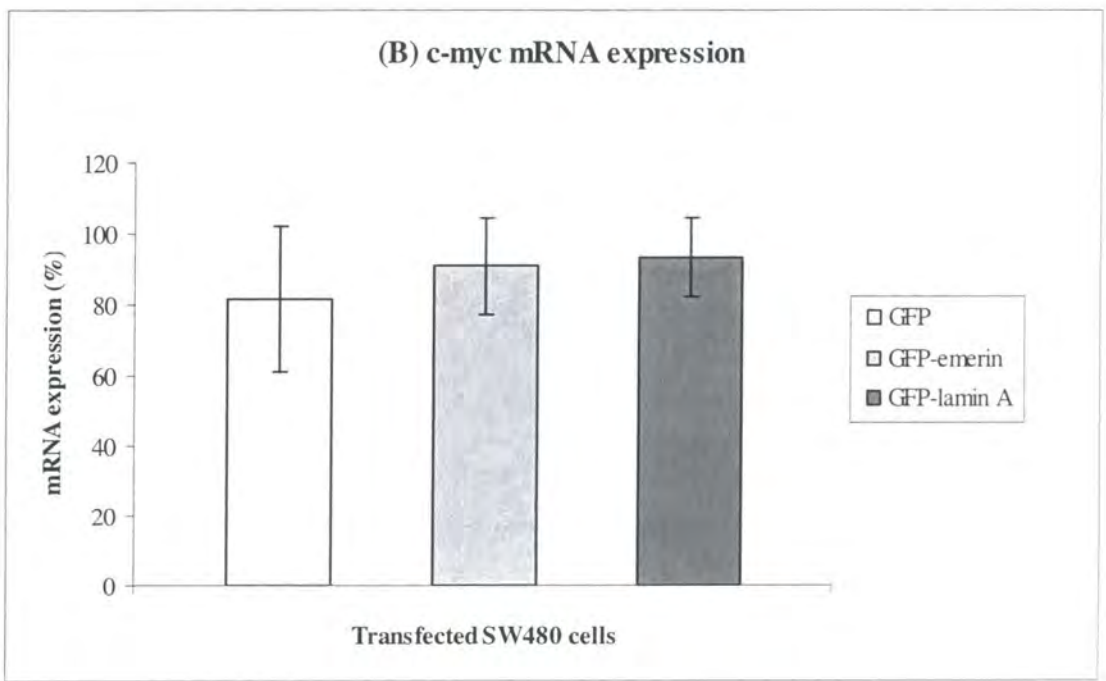


Figure 4.10 A & B

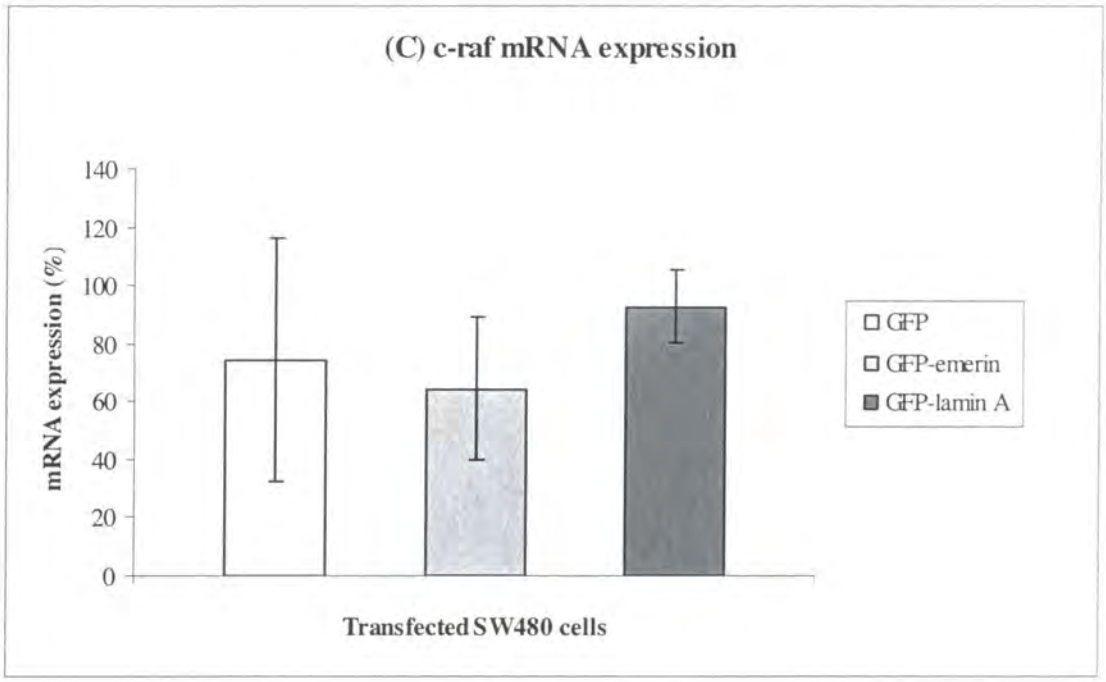


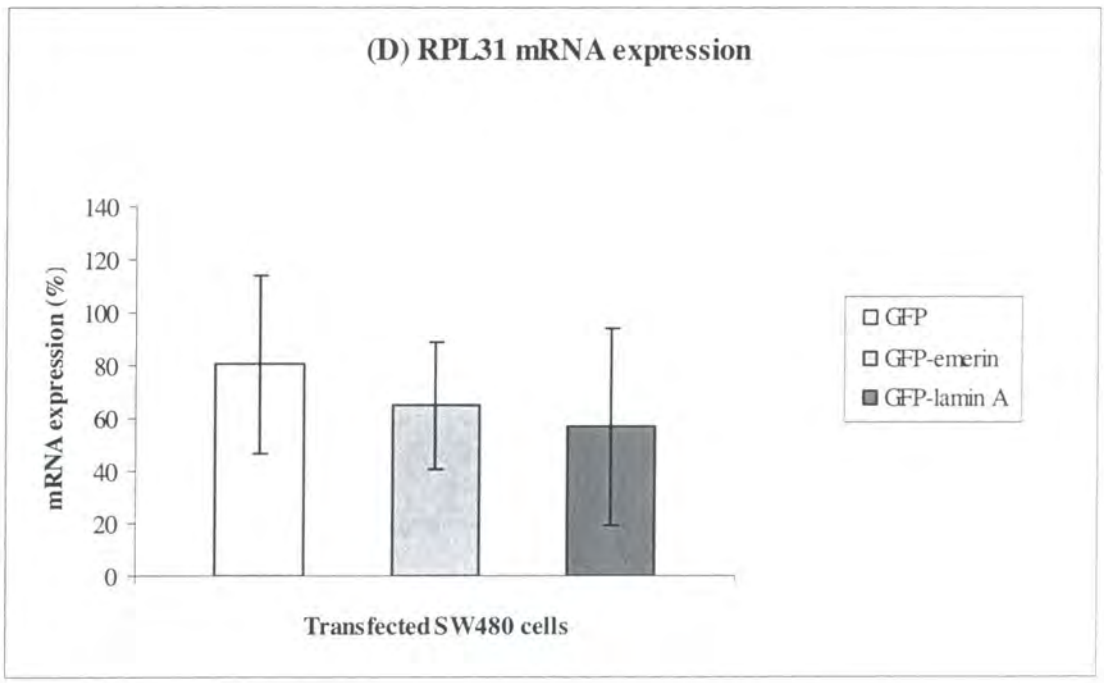


Figure 4.10 C & D

**Figure 4.11**

**Nucleotide – nucleotide BLAST results for synemin, c-myc, c-raf and RPL31 RT-PCR products**. Confirmation that the products amplified by RT-PCR from SW480 GFP 2, GFP-emerin 2 and GFP-lamin A 2bb3 cell lines using synemin-, c-myc-, c-raf- and RPL31-specific primers were genuine was sought. Each product was sequenced with the corresponding antisense primer using an ABI Prism® 377 XL automated DNA sequencer. The resulting sequences were compared with those on the BLASTN database and the three most significant hits and one example alignment are shown for synemin (**A**), c-myc (**B**), c-raf (**C**) and RPL31 (**D**).


## A. Synemin

| Sequences producing significant alignments: | Score (Bits) | E Value |
|---|---|---|
| gi\|18698323\|emb\|AJ310522.1\|HSA310522 Homo sapiens mRNA for synem | 198 | 5e-49 |
| gi\|18698321\|emb\|AJ310521.1\|HSA310521 Homo sapiens mRNA for synem | 198 | 5e-49 |
| gi\|22027637\|ref\|NM_145728.1\| Homo sapiens desmuslin (DMN), trans | 198 | 5e-49 |

> gi|18698323|emb|AJ310522.1|HSA310522 Homo sapiens mRNA for synemin (SYN gene), isoform H
Length=7337

Score = 198 bits (100), Expect = 5e-49
Identities = 100/100 (100%), Gaps = 0/100 (0%)
Strand=Plus/Plus

```
Query  1     ATCATCAACCTCGGCCTGAAAGGGAGGGAGGGGAGAGCAAAGGTCGTCAACGTGGAGATC  60
             ||||||||||||||||||||||||||||||||||||||||||||||||||||||||||||
Sbjct  2299  ATCATCAACCTCGGCCTGAAAGGGAGGGAGGGGAGAGCAAAGGTCGTCAACGTGGAGATC  2358

Query  61    GTGGAGGAGCCCGTGAGTTATGTCAGCGGGGAGAAGCCGG  100
             ||||||||||||||||||||||||||||||||||||||||
Sbjct  2359  GTGGAGGAGCCCGTGAGTTATGTCAGCGGGGAGAAGCCGG  2398
```

## B. c-myc

| Sequences producing significant alignments: | Score (Bits) | E Value |
|---|---|---|
| gi\|54696401\|gb\|BT019768.1\| Homo sapiens v-myc myelocytomatosi... | 198 | 5e-49 |
| gi\|31543215\|ref\|NM_002467.2\| Homo sapiens v-myc myelocytomato... | 198 | 5e-49 |
| gi\|34815\|emb\|V00568.1\|HSMYC1 Human mRNA encoding the c-myc oncog | 198 | 5e-49 |

> gi|34815|emb|V00568.1|HSMYC1 Human mRNA encoding the c-myc oncogene
Length=2121

Score = 198 bits (100), Expect = 5e-49
Identities = 100/100 (100%), Gaps = 0/100 (0%)
Strand=Plus/Plus

```
Query  1     CCAGCTTGTACCTGCAGGATCTGAGCGCCGCCGCCTCAGAGTGCATCGACCCCTCGGTGG  60
             ||||||||||||||||||||||||||||||||||||||||||||||||||||||||||||
Sbjct  1079  CCAGCTTGTACCTGCAGGATCTGAGCGCCGCCGCCTCAGAGTGCATCGACCCCTCGGTGG  1138

Query  61    TCTTCCCCTACCCTCTCAACGACAGCAGCTCGCCCAAGTC  100
             ||||||||||||||||||||||||||||||||||||||||
Sbjct  1139  TCTTCCCCTACCCTCTCAACGACAGCAGCTCGCCCAAGTC  1178
```

Figure 4.11 A & B


results of BLAST

## C. c-raf

| Sequences producing significant alignments: | Score (Bits) | E Value |
|---|---|---|
| gi\|52486392\|ref\|NM_002880.2\| Homo sapiens v-raf-1 murine leuk... | 198 | 5e-49 |
| gi\|34190937\|gb\|BC018119.2\| Homo sapiens v-raf-1 murine leukem... | 198 | 5e-49 |
| gi\|35841\|emb\|X03484.1\|HSRAFR Human mRNA for raf oncogene | 198 | 5e-49 |

> gi|35841|emb|X03484.1|HSRAFR Human mRNA for raf oncogene
Length=2977

Score = 198 bits (100), Expect = 5e-49
Identities = 100/100 (100%), Gaps = 0/100 (0%)
Strand=Plus/Plus

```
Query  1    TGCGTCTTTGATTGGAGAAGAACTTCAAGTAGATTTCCTGGATCATGTTCCCCTCACAAC  60
            ||||||||||||||||||||||||||||||||||||||||||||||||||||||||||||
Sbjct  483  TGCGTCTTTGATTGGAGAAGAACTTCAAGTAGATTTCCTGGATCATGTTCCCCTCACAAC  542

Query  61   ACACAACTTTGCTCGGAAGACGTTCCTGAAGCTTGCCTTC  100
            |||||||||||||||||||||||||||||||||||||||||
Sbjct  543  ACACAACTTTGCTCGGAAGACGTTCCTGAAGCTTGCCTTC  582
```

## D. RPL31

| Sequences producing significant alignments: | Score (Bits) | E Value |
|---|---|---|
| gi\|47682683\|gb\|BC070373.1\| Homo sapiens ribosomal protein L31... | 198 | 5e-49 |
| gi\|36129\|emb\|X15940.1\|HSRPL31 Human mRNA for ribosomal protein L | 198 | 5e-49 |
| gi\|15812219\|ref\|NM_000993.2\| Homo sapiens ribosomal protein L31 | 198 | 5e-49 |

> gi|15812219|ref|NM_000993.2| Homo sapiens ribosomal protein L31 (RPL31), mRNA
Length=442

Score = 198 bits (100), Expect = 5e-49
Identities = 100/100 (100%), Gaps = 0/100 (0%)
Strand=Plus/Plus

```
Query  1    GGTAACCCGAGAATACACCATCAACATTCACAAGCGCATCCATGGAGTGGGCTTCAAGAA  60
            ||||||||||||||||||||||||||||||||||||||||||||||||||||||||||||
Sbjct  87   GGTAACCCGAGAATACACCATCAACATTCACAAGCGCATCCATGGAGTGGGCTTCAAGAA  146

Query  61   GCGTGCACCTCGGGCACTCAAAGAGATTCGGAAATTTGCC  100
            |||||||||||||||||||||||||||||||||||||||||
Sbjct  147  GCGTGCACCTCGGGCACTCAAAGAGATTCGGAAATTTGCC  186
```

Figure 4.11 C & D

# CHAPTER 5 – IMMUNOHISTOCHEMICAL ANALYSIS OF A-TYPE LAMIN EXPRESSION IN COLORECTAL TUMOURS

## *5.1 Introduction*

### 5.1.1 Comparative value of using cell lines and tissue sections to study tumour progression

Human tumour-derived cell lines have proven themselves valuable models for studying the development and progression of cancer, as well as the efficacy and molecular pharmacology of potential anti-carcinogenic drugs [for example, Compagni and Christofori (2000), Ethier (1996), Paraskeva *et al.* (1990), Scherf *et al.* (2000) and Weinstein *et al.* (1997)]. Cancer cells, once established, are generally easy to grow in culture and provide an endless supply of living material with which to test scientific hypotheses. However their ability to faithfully maintain the same genotype / phenotype as that associated with the class or stage of tumour from which they were originally isolated has been called into question (Hewitt *et al.*, 2000; Virtanen *et al.*, 2002). Indeed it is prudent to consider that tumour cells grown *in vitro* on a plastic substrate, sometimes for over one hundred passages, may well lose some characteristics associated with the original tumour and possibly gain other attributes through further genetic mutations and/or chromosome translocations which have been reported in older cultures. However, evidence also suggests that many cancer cell lines do retain a genotype / phenotype which is representative of their progenitor tumour, despite long-term passage *in vitro*. Using cDNA microarray analysis Virtanen *et al.* (2002) have shown that lung cancer cell lines derived from small cell lung cancer and squamous cell

carcinoma generally display similar genetic signatures to their fresh tumour counterparts, such that they could be clustered accordingly. In another study, Hewitt et al. (2000) demonstrated that culture to a high passage number had no affect on the phenotypic features of two colorectal cancer cell lines. SW620 cells, which were originally explanted from a lymph node metastasis, were found to be poorly differentiated, more invasive and tumourigenic and to express a higher proliferation index compared to SW480 cells which were derived from a Dukes' B / Broders' grade IV carcinoma.

Comparatively few investigations have been undertaken to explore the nature of nuclear lamin expression in human neoplastic tissue and cell lines. The majority of studies that have been published concentrate on lung cancer (Broers *et al.*, 1993; Kaufmann *et al.*, 1991; Machiels *et al.*, 1995) and keratinocytic tumours of the skin (Oguchi *et al.*, 2002; Tilli *et al.*, 2003; Venables *et al.*, 2001). Encouragingly, in a study carried out by Broers *et al.* (1993) single label immunofluorescence and immunoblot analyses on lung cancer cell lines indicated a loss of A-type lamin expression in SCLCs compared to non-SCLCs which was later corroborated by immunoperoxidase staining of equivalent neoplastic tissues. This strongly suggests that neoplastic cell lines can prove accurate representative models for the examination of lamin expression in cancer.

Accordingly our investigations into the expression pattern of lamins in CRC began in cell lines representing Broders' grade II, III and IV and metastasis. This work is described in detail in Chapter 3 of this thesis. Preliminary findings in these cells lines suggested that lamins A and C were differentially expressed during the progression of colorectal cancer towards metastasis. While lamin C expression appeared unchanged, lamin A was down-regulated in cell lines representing grade III and grade IV tumours.

These cell lines, SW948 and SW480, are also known to be derived from Dukes' C and Dukes' B stage adenocarcinomas respectively (Leibovitz *et al.*, 1976). Loss of lamin A expression did not appear to be related to proliferation, but rather cellular dedifferentiation. No changes in expression of lamin B1 were observed. Although alterations in the levels of lamin B2 were clearly evident they did not follow a logical pattern, therefore it seemed that the contrasting patterns of lamin A and lamin C expression in the cell lines most warranted confirmation in colorectal tumour tissue.

### 5.1.2 Summary

In this chapter an immunohistochemical study of lamin A/C distribution in normal and malignant colorectal tissue is presented. Three anti-lamin antibodies, JoL2, RaLC and 133A2, were used. Both JoL2, which recognizes the lamin A/C common domain (Dyer *et al.*, 1997), and RaLC, which is lamin C specific (Venables *et al.*, 2001), were also used to chart A-type lamin expression in CRC cell lines in the first results chapter. Monoclonal antibody 133A2 was used exclusively for immunohistochemistry (IHC) in this chapter and detects only lamin A. Its epitope lies in the carboxy terminus of lamin A, between amino acids 598 and 611 (Hozak *et al.*, 1995).

## *5.2 Results*

### 5.2.1 Immunohistochemistry methodology

Immunoperoxidase staining of tissue sections first requires the sequestration of endogenous peroxidase activity, followed by a process of antigen retrieval (AR). The

two methods used most frequently to re-expose epitopes are proteolytic digestion and heating. AR by heating can be achieved using a microwave, pressure cooker, steamer, autoclave or water bath (Barker *et al.*, 1999; Igarashi *et al.*, 1994; Kawai *et al.*, 1994; Shi *et al.*, 1991; Taylor *et al.*, 1996). Although microwave heating is the most widely used method this is due more to its simplicity and time efficiency (Mighell *et al.*, 1995), rather than any perceivable difference in the quality of staining compared to that produced using other heating devices (Taylor *et al.*, 1996). Additionally comparative studies have shown that AR by microwave heating produces superior staining results to enzyme digestion (Hazelbag *et al.*, 1995), particularly after long periods of fixation (Cattoretti *et al.*, 1993; Kahveci *et al.*, 2003).

Despite the reported advantages of using microwave AR, I opted to use water bath heating to regenerate lamin epitopes. The reasons for this were two-fold. First, Barker *et al.* (1999) had already demonstrated successful antigen retrieval in colonic epithelium using the water bath method. Second, our own trials showed that water bath heating was significantly more gentle on tissues compared to microwave heating. Microwave heating consistently damaged the outer edge of the tissue sections tested, reducing the area available for effective staining and analysis by approximately 10 - 20%. Accordingly the method described by Barker *et al.* (1999) was adopted without making any alterations to their AR protocol.

### 5.2.2 Distribution of A-type lamin polypeptides in normal colonic tissue

The gastrointestinal tract is radially organized into four histological layers: the mucosa, submucosa, muscularis propria and serosa (Burkitt *et al.*, 1993). Immunoperoxidase staining of ultra-thin sections of healthy human colon with anti-lamin A/C antibody,

JoL2, showed that A-type lamins were expressed in a broad range of cell types and were always nuclear specific. Particular attention was paid to the two uppermost layers of colon histology (**Figure 5.1**). In the mucosa JoL2 decorated epithelial cells of the crypts and smooth muscle cells of the muscularis mucosae, as well as the majority of stromal cells. In the submucosa endothelial cells surrounding blood vessels were also positive for lamin A/C. In contrast, A-type lamin expression was not detected in infiltrating lymphocytes or lymphoid aggregates which thus constituted an internal negative control. This observation was not unexpected. B-type lamins are thought to be the sole components of the nuclear lamina in early human haematopoietic lineages, a phenomenon which has been frequently observed in immature, proliferating T- and B-lymphocytes (Cance *et al.*, 1992; Guilly *et al.*, 1987; Jansen *et al.*, 1997; Paulin-Levasseur *et al.*, 1988).

The pattern of expression of lamins A and C in healthy colonic epithelium was examined in detail. Using JoL2 a clear gradient of expression from the crypt base to the intercrypt table was observed (**Figures 5.1** & **5.2**). Lamin A/C was not completely absent from cells in the stem cell compartment, but was expressed very weakly. Low level expression was often maintained up to the mid-crypt point (that is, in the bottom 20 – 50% of cells). The transient amplifying region is characterized by rapid proliferation of precursor cells (Marshman *et al.*, 2002; Potten and Loeffler, 1990). This zone generally exhibited a steady, yet relatively incremental augmentation in lamin A/C expression, although an increase in staining intensity was often only perceivable from the mid-crypt point upwards. Intense up-regulation of A-type lamin expression was restricted specifically to the top 20% of the crypt. While specimen to specimen variation in the degree of lamin A/C staining in the lower 80% of the crypt was encountered, a dramatic increase in lamin A/C expression was consistently observed in the top 20% of

the crypt and, as such, appears to be connected to the differentiated state of cells in this region. The expression of lamin A and lamin C was also investigated independently (**Figure 5.2**). The results obtained exactly mirrored the pattern of expression identified by JoL2. Additionally, it is worth noting that in normal epithelium lamin staining was always most intense at the nuclear rim.

### 5.2.3 Immunohistochemical analysis of colorectal neoplasms reveals differential expression of lamins A and C in metastatic tumours

A-type lamin reactivity patterns were evaluated in relation to the clinical pathology of CRC. A small scale trial study incorporating two Dukes' stage A, 10 Dukes' stage B, 11 Dukes' stage C, two Dukes' stage D and 11 distant metastasis of colorectal carcinoma was set up. Serial sections of tumour were single-stained by immunoperoxidase with antibodies raised against lamin A/C, lamin A and lamin C. Subsequent microscopic analysis revealed variation in lamin A/C staining (as determined by JoL2) between different stages and amongst tumour samples classified into the same clinicopathological category (**Table 5.1** & **Figure 5.3**). Overall, expression of lamin A/C was very low in Duke's stage A tumours and at a medium level in Dukes' stage D tumours. However, due to the limited availability of these tumours, it is not possible to draw any definite conclusions. Instead it is more meaningful to focus on the Dukes' B, C and metastatic tumours for which a larger selection of samples were available. The majority of Dukes' stage B tumours expressed 'very low' levels of lamin A/C, whereas most Dukes' C tumours exhibited higher expression levels which were categorized as either 'low' or 'medium'. For the main part, metastatic tumours reacted most strongly with lamin A/C antibodies. Furthermore, staining was noticeably more heterogeneous in Dukes' C and metastatic tumours compared to those in the Dukes' B set. Independent of

stage, the staining of stomal cells was generally maximal with very little or no heterogeneity.

The expression of individual lamin polypeptides was assessed using antibodies to lamin A (133A2) and lamin C (RaLC) (**Table 5.1** & **Figure 5.3**). These investigations confirmed that both lamin A and lamin C follow a similar pattern of expression in Dukes' B and Dukes' C tumours, similar to that outlined by immunoperoxidase staining with JoL2. However, the reactivity patterns of individual A-type lamins appear to diverge in tumours removed from secondary sites. While the intensity of lamin C staining varied greatly between metastatic specimens, lamin A expression appeared to be preferentially down-regulated. Ninety percent of the samples examined displayed very low or no retrieval of lamin A antigens, whereas only 55% of samples expressed equally low levels of lamin C.

The colon carcinoma metastases used in this study were from different secondary sites. In **Table 5.1** all the metastases were clustered together to facilitate the assessment of the general nature of lamin expression during the progression of CRC. However, following the observation that lamin A is down-regulated relative to lamin C in most of the metastasis samples, I was intrigued to know whether the site of metastasis had any bearing on the expression level of lamin A. Therefore in **Table 5.2** the metastases are subdivided according to their location and accompanying levels of lamin A/C, lamin A and lamin C expression are tabulated.

All liver metastases had very low or absent expression of lamin A, generally medium levels of lamin A/C and an inconsistent pattern of lamin C expression, in that at least one specimen was assigned to each value on the intensity scale. Although the metastasis

to the pancreas / duodenum went against the trend of all the other samples and exhibited medium / high levels of lamin A, lamin C and lamin A/C, more data from the same site is required to determine if this is a predictable feature.

### 5.2.4 Down-regulation of A-type lamins in malignant polyps correlates with changes in nuclear morphology

Investigations into lamin A/C expression in the context of dysplasia were limited to the Dukes' A specimens. Both these specimens were malignant polyps which contained some area of relatively normal epithelium, therefore direct comparisons could be made between expression of lamins A and C in normal versus dysplastic tissue. Regions harbouring normal crypt-like structures could be found at the outer edge of these polyps juxtaposed dysplastic tissue. Normal epithelium is characterized by small, round nuclei with basal polarity. Clinically, nuclear morphology is a well-established marker of dysplasia. Enlargement and elongation of nuclei, concomitant with migration towards the apical pole are classic identifiers of dysplastic behaviour. On the whole expression of A-type lamins in these polyps was either very low or absent (**Table 5.1** & **Figure 5.3, panels A - C**). Closer inspection revealed that expression of A-type lamins was strongly related to nuclear morphology. Lamin A expression was lost and lamin A/C staining diminished in nuclei exhibiting a dysplastic phenotype, compared to those with a normal phenotype (**Figure 5.4**). Some cytoplasmic staining was apparent in dysplastic cells, but was completely absent from cells exhibiting normal nuclear morphology. A similar reduction in nuclear lamin C expression was observed, but the quality of staining was not good enough for reproduction in this thesis.

## *5.3 Discussion*

I endeavoured to set up a system of analysis suitable for charting the pattern of expression of nuclear lamins A and C in healthy colonic epithelium and neoplastic tissue. A preliminary immunohistochemical study was undertaken using archived material from Maastricht University Hospital, The Netherlands. A-type lamin epitopes were successfully re-exposed in formalin-fixed, paraffin-embedded colorectal tissue sections by heating in a citric acid AR solution. In normal colonic crypts increase in lamin A/C staining correlated with cellular differentiation. Two groups have previously reported augmented lamin A/C expression in the top third of the crypt and weak staining in the basal region, but they did not differentiate between lamin A and lamin C (Cance *et al.*, 1992; Moss *et al.*, 1999). This study demonstrates parallel topological expression patterns for lamins A and C along the crypt / villus axis and defines the area with highest lamin A/C expression to the upper 20% of the crypt.

These initial investigations revealed an ambiguous relationship between lamin expression and Dukes' stage. This is predominately due to insufficient availability of Dukes' stage A and D tumours which prevented the completion of a comprehensive analysis. Despite this drawback, some interesting observations were made from the analysis of Dukes' B, C and metastatic tumours that would be worthy of further research. In general, expression of lamin A/C appeared stronger in late stage tumours compared to early stage tumours. However in metastatic tumours lamins A and C became differentially expressed - a reproducible characteristic of liver metastases. The majority of metastatic samples analysed displayed reduced expression of lamin A compared to Dukes' C tumours, but a similar down-regulation was not seen in lamin C immunostained sections. Furthermore, A-type lamin expression was very heterogeneous

in the metastasis specimens which implies that down-regulation of lamin A in metastatic colon carcinoma cells is non-uniform.

Histological analysis of a small sample of malignant polyps suggested a link between morphological transformation of nuclei and down-regulation of lamin A/C expression. Aberrant nuclear shape and migration of nuclei to the apical pole of epithelial cells are strong indicators of dysplasia. Cells exhibiting such dysplastic characteristics were invariably negative for lamin A and negative or very weakly positive for lamin C and lamin A/C.

Taken *in toto* this immunohistochemical study confirms that alterations in nuclear lamin expression are a feature of colorectal cancer. It would appear that the most significant changes occur in the earliest and latest stages of the disease. Down-regulation of A-type lamins was associated with dysplastic behaviour in malignant polyps and lamin A appears preferentially reduced in metastatic tumours. Whether loss of both lamins A and C in the earliest stages of this disease promotes colorectal carcinogenesis remains to be further investigated. A possible role for lamin A in promoting metastasis is an interesting one. In normal colon tissue, A-type lamin expression is associated with differentiation [Cance *et al.* (1992), Moss *et al.* (1999) and this thesis]. Studies on lamin expression in other cancers have associated loss of lamin A/C with poor differentiation (Oguchi *et al.*, 2002). In particular, Machiels *et al.* (1997) observed that lamin A alone was absent from poorly differentiated nonseminomas of the testicular germ cell. Perhaps loss of lamin A in CRC promotes dedifferentiation and facilitates spread to a secondary site?

Further research is certainly warranted. This pilot study needs to be extended to incorporate at least 20 tumours of each stage to obtain a clear picture of A-type lamin expression in CRC. It would also be beneficial to compare lamin expression patterns with patient survival data. As changes in nuclear lamin expression do not appear to be directly related to clinical pathology, variation in lamin A and C expression within tumours of the same stage may therefore emerge as a good prognostic indicator.

### *5.4 Figures*

**Figure 5.1**

**Basic mucosal form of the colon illustrated by staining with lamin A/C antibodies.** Cells expressing lamin A/C antigens (brown) were labelled by immunoperoxidase staining of paraffin-embedded sections of healthy colon tissue. Nuclei were weakly counterstained with Ehrlich's haematoxylin. The two uppermost layers in colon histology, the mucosa and submucosa, are clearly distinguishable; the border between the two being demarcated by the muscularis mucosae. The majority of nuclei in both layers are positive for lamin A/C. This includes endothelial cells surrounding blood vessels (**b/v**), smooth muscle cells of the muscularis mucosae and epithelial cells of the colonic crypts (**C**). A distinct gradient of expression which increases from the base of the crypt to the lumenal surface is evident. There is no cytoplasmic staining. Lymphocytes were distributed as isolated cells throughout the lamina propria (**LP**) or in non-encapsulated aggregations (**L**) which were observed in the submucosa (as depicted here) or frequently breaching the muscularis mucosae and infiltrating the lamina propria. Lymphoid cells consistently demonstrated complete absence of lamin A/C expression and are therefore clearly identifiable in blue. The lamin A/C positive cells within the lymphoid follicles are likely to be analogous to the M cells of the small intestine. Scale bar = 250 μm.

**Figure 5.2**

**A-type lamins are expressed in a gradient from the crypt base to the lumenal pole.** The pattern of expression of lamin A/C, lamin A and lamin C (staining shown in brown) was assessed immunohistochemically in eleven examples of paraffin-embedded normal colonic mucosa. Nuclei not expressing lamins A or C were visualized by counterstaining with haematoxylin (shown in blue). The same region of one patient specimen is presented here. Independent of the anti-lamin antibody used, expression of lamin A and lamin C appears very low or absent in the bottom third of the crypt (sten cell / proliferative compartment) but increases towards the uppermost part of the cryp to a maximum level in the top 20% of the crypt (the differentiated compartment). Sca bar = 100 μm.

**Table 5.1**

**Immunoperoxidase staining pattern of A-type lamins in colorectal tumours.** Thirty-six formalin-fixed, paraffin-embedded colon tumour specimens representing Dukes' stage A (n = 2), Dukes' stage B (n = 10), Dukes' stage C (n = 11), Dukes' stage D (n = 2) and metastasis (n = 11) were stained individually with antibodies to lamin A/C (JoL2), lamin A (133A2) and lamin C (RaLC). The level and heterogeneity of expression of each antigen was examined in both crypt (epithelial) cells and adjacent stromal (mesenchymal) cells (where possible). Staining intensity was scored according to an arbitrary scale in which – indicates absent expression, ± indicates very low level expression, + indicates low level expression, ++ indicates medium level expression and +++ indicates high level expression. Heterogeneity was measured according to the following scale:

| Heterogeneity score | Lamin expression |
|---|---|
| - | no variation |
| ± | – to ±, ± to +, + to ++ or ++ to +++ |
| + | – to +, ± to ++ or + to +++ |
| ++ | – to ++ or ± to +++ |
| +++ | – to +++ |

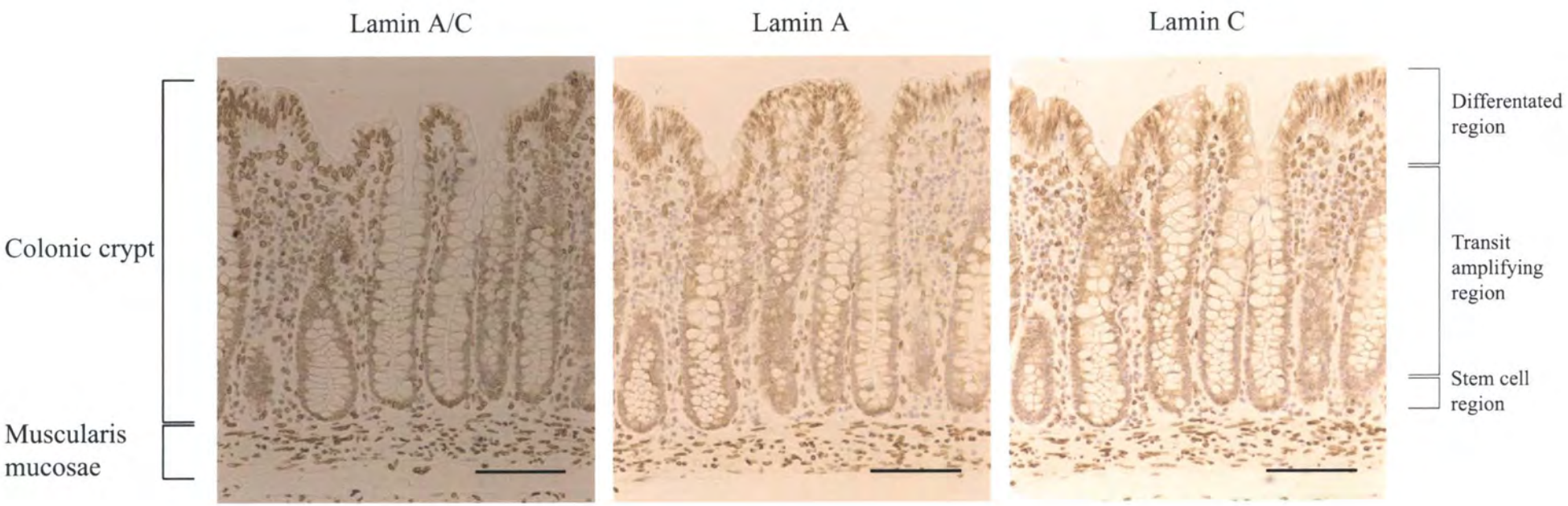
Lamin A/C
Lamin A
Lamin C
Colonic crypt
Muscularis mucosae
Differentated region
Transit amplifying region
Stem cell region

Figure 5.2

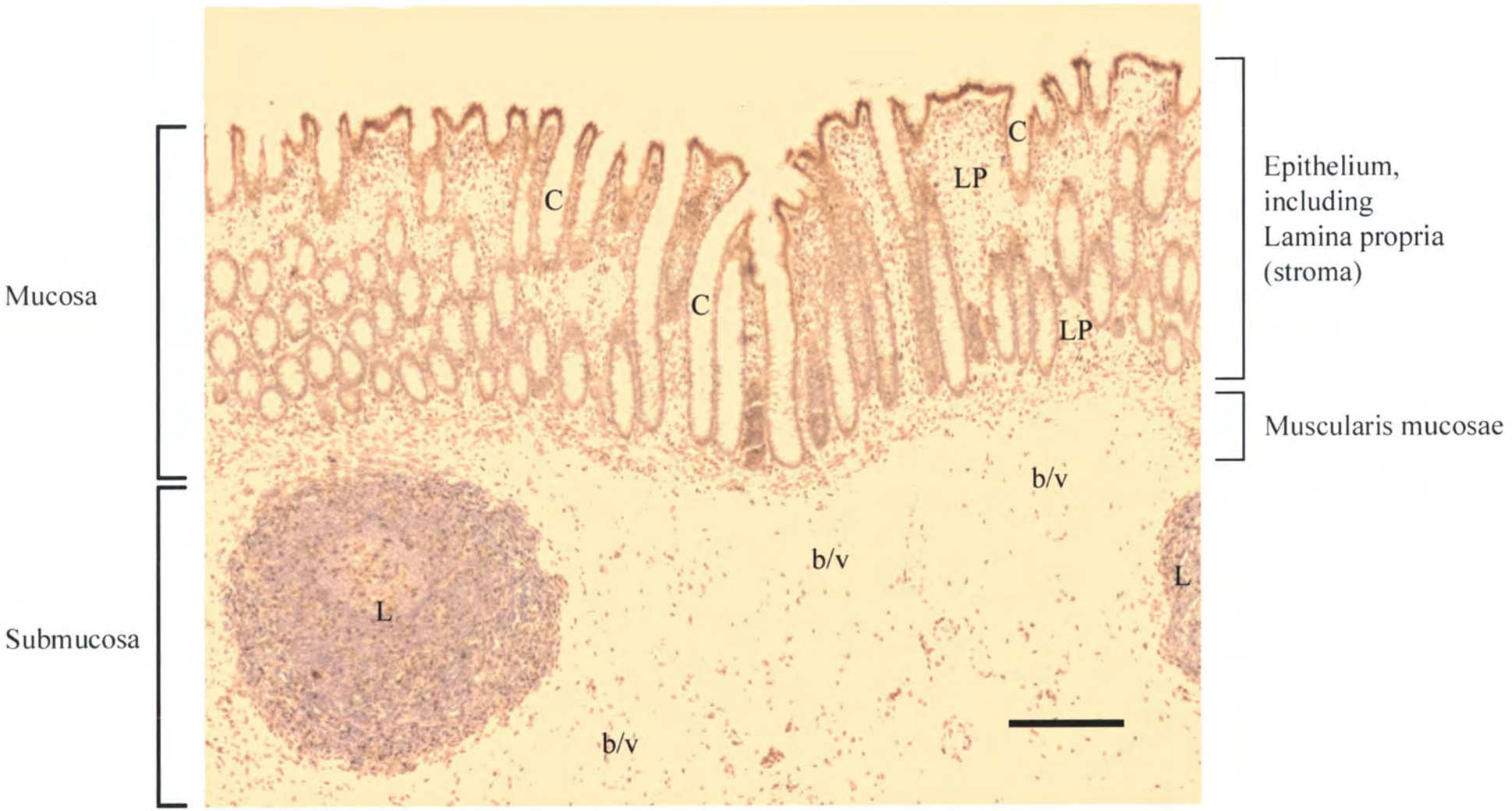
Mucosa
Submucosa
C
C
C
LP
LP
b/v
b/v
b/v
L
L
Epithelium,
including
Lamina propria
(stroma)
Muscularis mucosae

Figure 5.1

**Table 5.1 Immunoperoxidase staining pattern of A-type lamins in colorectal tumours.**

| | Lamin A/C (JoL2) | | | | | | Lamin A (133A2) | | | | | | Lamin C (RaLC) | | | | | |
|---|---|---|---|---|---|---|---|---|---|---|---|---|---|---|---|---|---|---|
| **Colorectal tumours** | **No.** | - | ± | + | ++ | +++ | **No.** | - | ± | + | ++ | +++ | **No.** | - | ± | + | ++ | +++ |
| Dukes' A | | | | | | | | | | | | | | | | | | |
| Aberrant crypt nuclei | | | | | | | | | | | | | | | | | | |
| Staining itensity | **2** | 0 | 2 | 0 | 0 | 0 | **2** | 2 | 0 | 0 | 0 | 0 | **2** | 0 | 2 | 0 | 0 | 0 |
| Heterogeneity | **2** | 0 | 0 | 2 | 0 | 0 | **2** | 1 | 1 | 0 | 0 | 0 | **2** | 0 | 0 | 2 | 0 | 0 |
| Stromal cell nuclei | | | | | | | | | | | | | | | | | | |
| Staining itensity | **1** | 0 | 0 | 0 | 1 | 0 | **1** | 0 | 0 | 0 | 0 | 1 | **1** | 0 | 0 | 0 | 0 | 1 |
| Heterogeneity | **1** | 1 | 0 | 0 | 0 | 0 | **1** | 0 | 1 | 0 | 0 | 0 | **1** | 1 | 0 | 0 | 0 | 0 |
| Dukes' B | | | | | | | | | | | | | | | | | | |
| Aberrant crypt nuclei | | | | | | | | | | | | | | | | | | |
| Staining itensity | **10** | 1 | 6 | 1 | 2 | 0 | **10** | 4 | 4 | 1 | 1 | 0 | **10** | 3 | 3 | 3 | 0 | 1 |
| Heterogeneity | **10** | 1 | 3 | 5 | 0 | 1 | **10** | 3 | 2 | 1 | 1 | 3 | **10** | 6 | 0 | 0 | 2 | 2 |
| Stromal cell nuclei | | | | | | | | | | | | | | | | | | |
| Staining itensity | **10** | 0 | 0 | 0 | 2 | 8 | **10** | 0 | 0 | 0 | 2 | 8 | **10** | 0 | 0 | 0 | 1 | 9 |
| Heterogeneity | **10** | 7 | 2 | 1 | 0 | 0 | **10** | 6 | 3 | 1 | 0 | 0 | **10** | 6 | 4 | 0 | 0 | 0 |
| Dukes' C | | | | | | | | | | | | | | | | | | |
| Aberrant crypt nuclei | | | | | | | | | | | | | | | | | | |
| Staining itensity | **11** | 0 | 1 | 7 | 3 | 0 | **10** | 2 | 3 | 4 | 1 | 0 | **11** | 2 | 3 | 4 | 2 | 0 |
| Heterogeneity | **11** | 0 | 0 | 3 | 7 | 1 | **10** | 1 | 3 | 2 | 4 | 0 | **11** | 1 | 2 | 3 | 4 | 1 |
| Stromal cell nuclei | | | | | | | | | | | | | | | | | | |
| Staining itensity | **10** | 0 | 0 | 0 | 1 | 9 | **9** | 0 | 0 | 0 | 4 | 5 | **10** | 0 | 0 | 0 | 3 | 7 |
| Heterogeneity | **10** | 5 | 5 | 0 | 0 | 0 | **9** | 4 | 3 | 2 | 0 | 0 | **10** | 6 | 2 | 2 | 0 | 0 |
| Dukes' D | | | | | | | | | | | | | | | | | | |
| Aberrant crypt nuclei | | | | | | | | | | | | | | | | | | |
| Staining itensity | **2** | 0 | 0 | 0 | 2 | 0 | **2** | 0 | 0 | 1 | 1 | 0 | **2** | 0 | 2 | 0 | 0 | 0 |
| Heterogeneity | **2** | 0 | 0 | 0 | 0 | 2 | **2** | 0 | 0 | 0 | 0 | 2 | **2** | 0 | 0 | 0 | 0 | 2 |
| Stromal cell nuclei | | | | | | | | | | | | | | | | | | |
| Staining itensity | **2** | 0 | 0 | 0 | 0 | 2 | **1** | 0 | 0 | 0 | 0 | 1 | **2** | 0 | 0 | 0 | 1 | 1 |
| Heterogeneity | **2** | 2 | 0 | 0 | 0 | 0 | **1** | 1 | 0 | 0 | 0 | 0 | **2** | 1 | 1 | 0 | 0 | 0 |
| Metastasis | | | | | | | | | | | | | | | | | | |
| Tumour cell nuclei | | | | | | | | | | | | | | | | | | |
| Staining itensity | **11** | 1 | 2 | 1 | 6 | 1 | **11** | 7 | 3 | 0 | 1 | 0 | **11** | 2 | 4 | 2 | 2 | 1 |
| Heterogeneity | **11** | 0 | 1 | 5 | 2 | 3 | **11** | 5 | 4 | 1 | 0 | 3 | **11** | 3 | 1 | 2 | 3 | 2 |
| Stromal cell nuclei | | | | | | | | | | | | | | | | | | |
| Staining itensity | **11** | 0 | 0 | 0 | 1 | 10 | **7** | 0 | 0 | 0 | 1 | 6 | **11** | 0 | 0 | 0 | 5 | 6 |
| Heterogeneity | **11** | 9 | 2 | 0 | 0 | 0 | **7** | 2 | 5 | 0 | 0 | 0 | **11** | 6 | 4 | 1 | 0 | 0 |

**Figure 5.3**

**Expression of lamin A/C, lamin A and lamin C in colorectal tumours.** Four micron thick sections of Dukes' stage A (panels A to C), Dukes' stage B (panels D to F), Dukes' stage C (panels G to I) and Dukes' stage D (panels J to L) colon tumours, along with metastases of colon carcinoma (panels M to O) were subjected to immunohistochemical detection of individual lamin antigens using three anti-lamin antibodies. Panels A, D, G, J & M – lamin A/C antibody (JoL2); panels B, E, H, K & N – lamin A antibody (133A2); and panels C, F, I, L & O – lamin C antibody (RaLC). Tissue sections were weakly counterstained with Ehrlich's haematoxylin, shown in blue where lamin staining is negative. Lamin staining appears brown. For each Dukes' stage and metastasis, examples of A-type lamin staining are presented from the same patient. Scale bar = 100 μm.

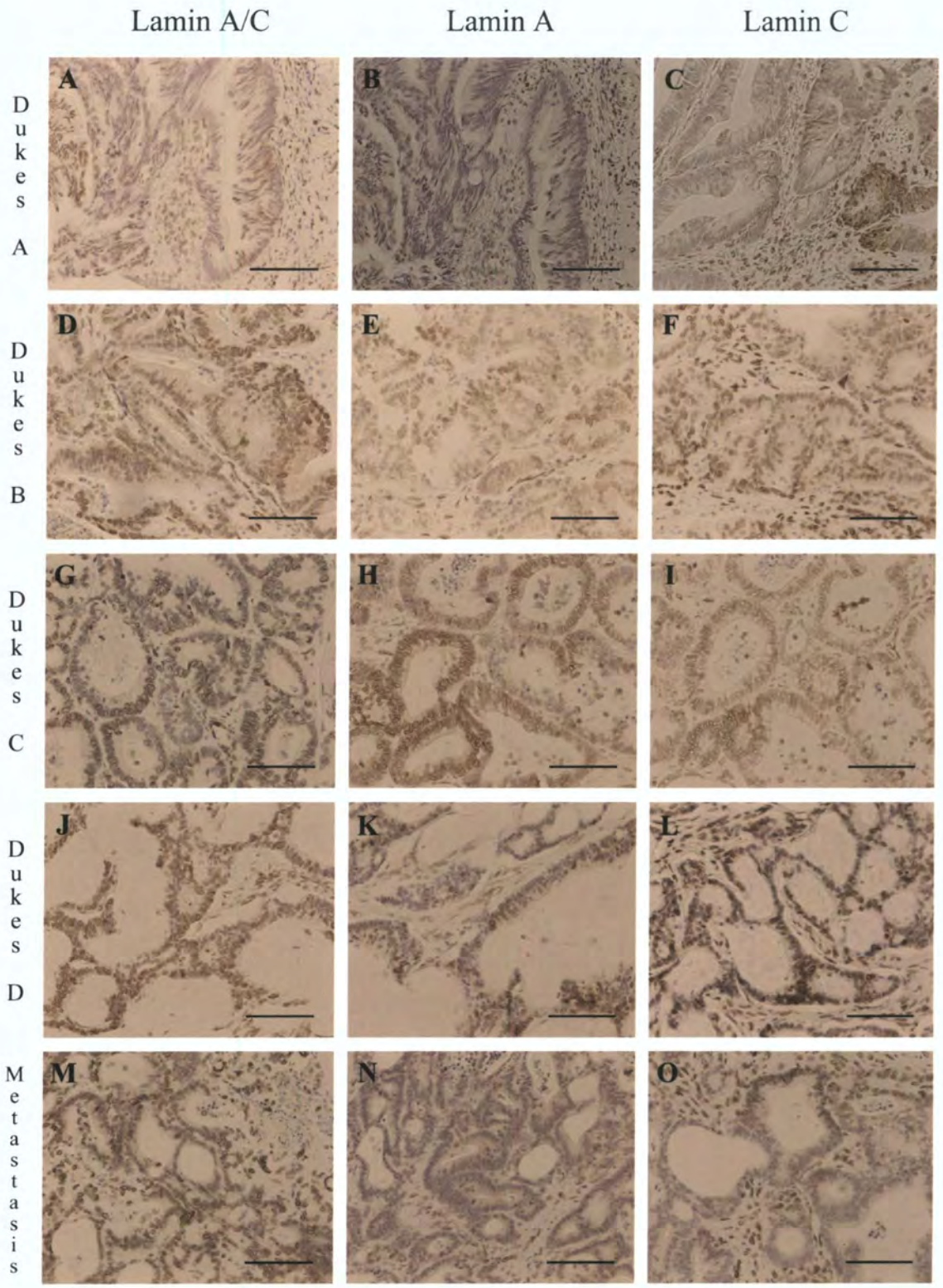
Lamin A/C
Lamin A
Lamin C
Dukes A
Dukes B
Dukes C
Dukes D
Metastasis
A
B
C
D
E
F
G
H
I
J
K
L
M
N
O

Figure 5.3

**Table 5.2**

**Expression of A-type lamins in secondary tumours of colorectal cancer.** Eleven examples of metastasis of colon carcinoma were labelled by immunoperoxidase with antibodies raised against lamin A/C (JoL2), lamin A (133A2) and lamin C (RaLC). Eight specimens represented metastasis to the liver and one example each of a lung, small intestine and pancreas / duodenum metastasis were included in the analysis. Staining intensity in both tumour cells and surrounding stromal cells (where possible) was scored based on an arbitrary scale where – = absent expression, ± = very low level expression, + = low level expression, ++ = medium level expression and +++ = high level expression. The different lamin polypeptides were generally expressed heterogeneously throughout the tissue sections and the degree of variation was measured following the scale below:

| Heterogeneity score | Lamin expression |
|---|---|
| - | no variation |
| ± | – to ±, ± to +, + to ++ or ++ to +++ |
| + | – to +, ± to ++ or + to +++ |
| ++ | – to ++ or ± to +++ |
| +++ | – to +++ |

**Table 5.2 Expression of A-type lamins in secondary tumours of colorectal cancer, determined by immunohistochemistry.**

| | Lamin A/C (JoL2) | | | | | | Lamin A (133A2) | | | | | | Lamin C (RaLC) | | | | | |
|---|---|---|---|---|---|---|---|---|---|---|---|---|---|---|---|---|---|---|
| **Colorectal metastases** | **No.** | - | ± | + | ++ | +++ | **No.** | - | ± | + | ++ | +++ | **No.** | - | ± | + | ++ | +++ |
| Metastasis | | | | | | | | | | | | | | | | | | |
| Liver | | | | | | | | | | | | | | | | | | |
| Tumour cell nuclei | | | | | | | | | | | | | | | | | | |
| Staining itensity | **8** | 1 | 1 | 1 | 5 | 0 | **8** | 6 | 2 | 0 | 0 | 0 | **8** | 2 | 3 | 1 | 1 | 1 |
| Heterogeneity | **8** | 0 | 1 | 3 | 2 | 2 | **8** | 3 | 4 | 1 | 0 | 0 | **8** | 3 | 1 | 1 | 3 | 0 |
| Stromal cell nuclei | | | | | | | | | | | | | | | | | | |
| Staining itensity | **8** | 0 | 0 | 0 | 1 | 7 | **5** | 0 | 0 | 0 | 1 | 4 | **8** | 0 | 0 | 0 | 4 | 4 |
| Heterogeneity | **8** | 7 | 1 | 0 | 0 | 0 | **5** | 0 | 5 | 0 | 0 | 0 | **8** | 6 | 2 | 1 | 0 | 0 |
| Lung | | | | | | | | | | | | | | | | | | |
| Tumour cell nuclei | | | | | | | | | | | | | | | | | | |
| Staining itensity | **1** | 0 | 0 | 0 | 1 | 0 | **1** | 0 | 1 | 0 | 0 | 0 | **1** | 0 | 0 | 1 | 0 | 0 |
| Heterogeneity | **1** | 0 | 0 | 0 | 0 | 1 | **1** | 1 | 0 | 0 | 0 | 0 | **1** | 0 | 0 | 0 | 0 | 1 |
| Stromal cell nuclei | | | | | | | | | | | | | | | | | | |
| Staining itensity | **1** | 0 | 0 | 0 | 0 | 1 | **0** | 0 | 0 | 0 | 0 | 0 | **1** | 0 | 0 | 0 | 0 | 1 |
| Heterogeneity | **1** | 1 | 0 | 0 | 0 | 0 | **0** | 0 | 0 | 0 | 0 | 0 | **1** | 0 | 1 | 0 | 0 | 0 |
| Small intestine | | | | | | | | | | | | | | | | | | |
| Tumour cell nuclei | | | | | | | | | | | | | | | | | | |
| Staining itensity | **1** | 0 | 1 | 0 | 0 | 0 | **1** | 1 | 0 | 0 | 0 | 0 | **1** | 0 | 1 | 0 | 0 | 0 |
| Heterogeneity | **1** | 0 | 0 | 1 | 0 | 0 | **1** | 1 | 0 | 0 | 0 | 0 | **1** | 0 | 0 | 1 | 0 | 0 |
| Stromal cell nuclei | | | | | | | | | | | | | | | | | | |
| Staining itensity | **1** | 0 | 0 | 0 | 0 | 1 | **1** | 0 | 0 | 0 | 0 | 1 | **1** | 0 | 0 | 0 | 1 | 0 |
| Heterogeneity | **1** | 1 | 0 | 0 | 0 | 0 | **1** | 1 | 0 | 0 | 0 | 0 | **1** | 0 | 1 | 0 | 0 | 0 |
| Pancreas / duodenum | | | | | | | | | | | | | | | | | | |
| Tumour cell nuclei | | | | | | | | | | | | | | | | | | |
| Staining itensity | **1** | 0 | 0 | 0 | 0 | 1 | **1** | 0 | 0 | 0 | 1 | 0 | **1** | 0 | 0 | 0 | 1 | 0 |
| Heterogeneity | **1** | 0 | 0 | 1 | 0 | 0 | **1** | 0 | 0 | 0 | 0 | 1 | **1** | 0 | 0 | 0 | 0 | 1 |
| Stromal cell nuclei | | | | | | | | | | | | | | | | | | |
| Staining itensity | **1** | 1 | 0 | 0 | 0 | 0 | **1** | 0 | 0 | 0 | 0 | 1 | **1** | 0 | 0 | 0 | 0 | 1 |
| Heterogeneity | **1** | 0 | 1 | 0 | 0 | 0 | **1** | 1 | 0 | 0 | 0 | 0 | **1** | 1 | 0 | 0 | 0 | 0 |

**Figure 5.4**

**Loss of lamin A/C expression in colorectal polyps appears to be associated with loss of nuclear morphology.** Serial sections of paraffin-embedded malignant polyps were subjected to immunoperoxidase staining with monoclonal antibodies raised against lamin A/C (panel A) and lamin A (panel B). Nuclei exhibiting normal polarity and size in crypt-like structures (fine arrows) were lamin A/C and lamin A positive. Nuclei displaying abnormal morphology and loss of polarity (broad arrows) were lamin A negative and showed significant down-regulation of lamin A/C. Lamin staining is shown in brown; haematoxylin counterstaining is shown in blue. Scale bar = 100 μm.

Lamin A/C

Lamin A

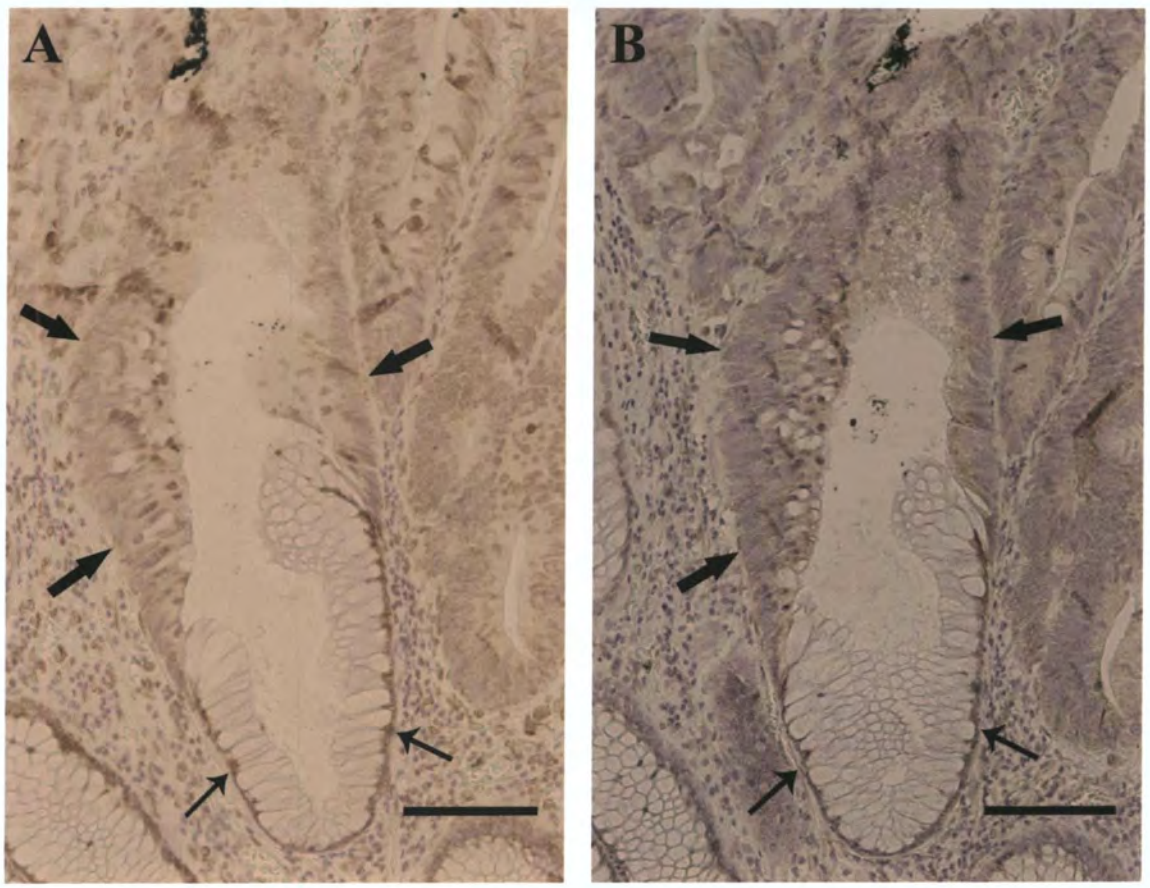


Figure 5.4

# CHAPTER 6 - GENERAL DISCUSSION

## *6.1 Background to project*

The implications of non-functional lamin A/C are borne out in tissue-specific familial disorders such as autosomal inherited EDMD, CMD-1A, Dunnigan type – FPLD, MAD and CMT2B1 (Bonne *et al.*, 1999; Cao and Hegele, 2000; De Sandre-Giovannoli *et al.*, 2002; Fatkin *et al.*, 1999; Novelli *et al.*, 2002; Raffaele Di Barletta *et al.*, 2000). Mutations in the lamin A binding region of emerin also give rise to an X-linked form of EDMD with identical clinical features to AD-EDMD (Bione *et al.*, 1994; Lee *et al.*, 2001). Therefore a role for A-type lamins and their binding partners in tissue-specific diseases is well-established. Considering that such disorders are not associated with the development of any malignancy, it is very interesting that altered expression and distribution of A-type lamins has also been reported in a growing number of neoplasms affecting epithelial, mesenchymal and lymphoid lineages.

The expression of nuclear lamins has been studied most extensively in lung cancer (Broers *et al.*, 1993; Kaufmann *et al.*, 1991) and keratinocytic tumours of the skin (Oguchi *et al.*, 2002; Tilli *et al.*, 2003; Venables *et al.*, 2001), but also in acute lymphoblastic leukaemia, non-Hodgkin's lymphoma (Stadelmann *et al.*, 1990) and colorectal cancer (Cance *et al.*, 1992; Moss *et al.*, 1999). In general these investigations have reported down-regulation of lamin A/C in association with increased proliferation and dedifferentiation of tumours. By comparison changes in expression of lamins B1 and B2 appear less common, although differential expression of B-type lamins has been noted in some healthy tissues (Broers *et al.*, 1997). These studies provided the first

indication that lamins may be important in the development and progression of cancer. However, immunological investigations into lamin expression in CRC have so far produced contradictory results (Cance *et al.*, 1992; Moss *et al.*, 1999).

Colorectal cancer is the third most commonly diagnosed malignancy and the second most important cause of cancer mortality (males and females combined) in the UK (Toms, 2004). While methods for early detection have been developed and, in the case of FOB testing, are being rolled out across the UK (Alexander and Weller, 2003), clinicians are still relying predominately on Dukes' and TNM classification (AJCC, 1997; Dukes, 1932; Gabriel *et al.*, 1935; Turnbull *et al.*, 1967) of colorectal tumours to determine patient treatment regimes and prognosis. Although one cannot deny the contribution made by pathologists such as C.E. Dukes in improving our understanding of this disease by determining a universal system through which it can be clinically described (Dukes, 1932), current morphological and pathological staging criteria are simply unable to provide detailed predictions of individual patient outcome [discussed by Johnston (2004)]. Biomarkers of tumour advancement and for prognosis have been proposed, including osteopontin (Agrawal *et al.*, 2002) and CEA (Galambos, 1973; Goldstein and Mitchell, 2005), but a definitive marker or genetic signature has yet to be demonstrated. Given the intriguing data currently being expounded on nuclear lamin expression in epithelial tumours of the lung and skin, it is perhaps surprising that detailed investigations into the expression and regulation of lamins in CRC have not been undertaken so far. This thesis aims to go some way in rectifying this.

### *6.2 Expression of nuclear lamins in CRC cell lines*

Expression and distribution of nuclear lamins A, C, B1 and B2 was examined using a model system incorporating colorectal cancer cell lines HT29, SW948 and SW480 which represented the progression of the disease from a relatively differentiated phenotype to a highly dedifferentiated phenotype. Also included in the study was cell line T84 which represented a lung metastasis of a colon carcinoma. Comparative analysis of protein profiles and single-label immunofluorescence identified diminished levels of lamin A in the most dedifferentiated cell lines SW948 and SW480, but unaltered expression of lamin C. These cultures displayed morphological abnormalities including loss of contact inhibition, stratified growth and an apparently weaker adherence to the tissue culture substrate. Concomitant with loss of protein expression, lamin A transcript levels were significantly reduced in SW948 cells compared to HT29 cells, indicating that loss of expression was regulated at the level of transcription. However in SW480 cells lamin A mRNA levels were not similarly down-regulated. This suggests that a different, post-transcriptional mechanism of lamin A regulation was functioning in this cell line.

Previously transcriptional and post-transcriptional regulation of A-type lamins has been reported. Broers *et al.* (1993) demonstrated that a decrease in lamin A and C mRNA levels accompanied down-regulation of protein expression in two SCLC cell lines. However, in the context of the observations made regarding SW948 colon cancer cells, work by Machiels *et al.* (1995) is particularly interesting. This group observed preferential repression of lamin A protein expression relative to lamin C in a human lung adenocarcinoma cell line and ascribed this imbalance to a reduction in the amount of lamin A transcript. Equally, up-regulation of lamin A/C protein expression can be

reflected in mRNA levels. Expression of the mutant v-Ha-*ras* oncogene in a SCLC cell line induced a 10 fold increase in lamin A/C protein levels which was paralleled by elevation in the corresponding mRNA species (Kaufmann *et al.*, 1991). Otherwise, a study on the premature ageing disease Hutchinson-Gilford progeria syndrome has illustrated a post-transcriptional mechanism by which lamin A expression may be abrogated but lamin C unaffected. *De novo* point mutations in the lamin A-specific tail domain are thought to prevent complete processing of prelamin A to lamin A, while lamin C is processed as normal (Eriksson *et al.*, 2003).

A reduction in lamin A/C expression has been reported previously in CRC by Moss *et al.* (1999), but they did not distinguish between individual A-type lamin polypeptides. The first evidence of a differential relationship between lamins A and C in tumours was presented by Venables *et al.* (2001). They reported a mutually exclusive pattern of lamin A and Ki67 staining in BCC of the skin and correlated loss of lamin A with fast growing tumours. Consequently it was considered that loss of lamin A in SW948 and SW480 cells may be related to their proliferative capacity. This was investigated using flow cytometry and double-label immunofluorscence. Flow cytometric analyses showed HT29 and SW948 cells to be slow growing and SW480 and T84 cells to be faster growing. Comparative immunofluorescence analyses identified no discernible relationship between the expression of Ki67 or PCNA and lamin A despite a clear reduction in lamin A expression in SW948 and SW480 cells. Thus no correlation between lamin A expression and growth rate or proliferation indices could be detected in the selected colorectal cancer cell lines. These findings are therefore not consistent with the observations made by Venables *et al.* (2001).

In general, a complex relationship between lamin A/C expression and cellular proliferation / differentiation is emerging in the literature. A decrease in A-type lamin levels has been correlated with proliferation in Swiss 3T3 murine fibroblasts (Pugh *et al.*, 1997). Similarly lamin A/C expression has been inversely correlated with proliferation in lung tumours (Coates *et al.*, 1996; Rowlands *et al.*, 1994). However, many groups have reported coincident appearance of lamin A/C during tissue and cellular differentiation, whereas at least one B-type lamin is always expressed (Lebel *et al.*, 1987; Paulin-Levasseur *et al.*, 1989; Rober *et al.*, 1989; Stewart and Burke, 1987). Further to the work by Venables *et al.* (2001) on BCC, Oguchi *et al.* (2002) examined a range of keratinocytic tumours of the skin and reported the greatest reduction in lamin A/C in poorly differentiated tumours. Tilli *et al.* (2003) also came to the conclusion that A-type lamin expression was most strongly associated with well-differentiated tumours, but that it does not follow that these cells possess no proliferative capacity. They observed simultaneous expression of lamin A/C and Ki67 in approximately 50% of the proliferating cells in BCC and SCC of the skin.

### *6.3 Effects of stable re-expression of lamin A in SW480 cells*

As changes in lamin A expression in the chosen CRC cell lines appeared to be unrelated to proliferation, I sought to investigate whether it was a dedifferentiation-driven event. To do this lamin A was stably re-expressed in SW480 cells and the downstream molecular targets were investigated using cDNA microarray analysis with a custom-designed oligonucleotide chip comprising 325 genes reported to be relevant to colorectal carcinogenesis and malignancy in general.

Untransfected SW480 cells were highly anchorage independent, frequently multinucleate and grew in multiple layers. They did not adhere strongly to the culture surface. Ectopic expression of full-length lamin A completely rescued two-dimensional growth. Transfection with GFP-emerin, which stabilized endogenous lamin A at a level equivalent to that in GFP-lamin A transfected cells, produced a partial rescue. Cells grew as a monolayer but a proportion remained multinucleate. Ectopic expression of GFP had no affect on the morphology of the parental cell line.

RNA profiles of each transfected cell line were compared and reproducible changes were confirmed by RT-PCR. Importantly, there were no significant changes in Wnt response elements. [Wnt controlled gene expression is essential for the maintenance of a proliferative phenotype in the base of normal colonic crypts. The β-catenin/TCF-4 complex which activates transcription of Wnt targets is switched on in CRC (van de Wetering *et al.*, 2002).] In particular c-*MYC*, which is up-regulated by β-catenin/TCF-4 and promotes cell proliferation (van de Wetering *et al.*, 2002), remained unchanged in the transfected cell lines. Consistent with this observation, cell proliferation indices also remained unaltered, supporting earlier findings that lamin A expression in CRC cells was not related to proliferation. However, RT-PCR did confirm significant down-regulation in the mRNA levels of synemin in GFP-lamin A transfected cells. Synemin is a type VI cytoplasmic IF protein (Mizuno *et al.*, 2001; Steinert *et al.*, 1999), therefore this finding suggests that the phenotypic manifestations of lamin A down-regulation observed in cultured cells may reflect alterations in the cytoskeleton.

It is worth noting that phenotypic changes have previously been associated with expression of lamin A/C in a SCLC cell line. Insertion of oncogenically activated v-Ha-*ras* into NCI-H249 cells induced a transition towards a non-SCLC phenotype,

coincident with a significant up-regulation of lamin A/C and vimentin, which is another cytoplasmic IF (Kaufmann *et al.*, 1991). Consequently functional connections between IF networks of the nucleus and cytoplasm were speculated to result in cytoskeletal alterations and account for the acquired change in cell shape and growth characteristics. Similar to GFP-lamin A transfected SW480 cells, NCI-H249*ras*$^{H}$ cells also began to grow as a monolayer (Mabry *et al.*, 1988). The question is, how could lamin A and synemin form a functional connection which regulates the morphology of CRC cells?

Synemin was originally identified as an IFAP, but was later demonstrated to be a *bona fide* member of the IF superfamily (Becker *et al.*, 1995; Bellin *et al.*, 1999). Now two splice variants of the human synemin gene have been identified, α and β (Titeux *et al.*, 2001). Synemin cannot self-assemble, but forms heteropolymers with one or both of the type III IF proteins desmin and vimentin, thereby linking them to other components of the cytoskeleton (Bellin *et al.*, 1999; Bilak *et al.*, 1998). As such synemin functions as an effective cytoskeletal cross-linker and could be very important in maintaining cytoskeletal architecture.

The majority of research so far has focused on understanding the nature of synemin's interactions in skeletal muscle where it associates with the myofibril Z-discs and is enriched at the neuromuscular and myotendinous junctions (Bellin *et al.*, 1999; Bilak *et al.*, 1998; Carlsson *et al.*, 2000; Granger and Lazarides, 1980; Mizuno *et al.*, 2004). Through multiprotein interactions, synemin is thought to perform a structural role during myofibre contraction and be involved in maintaining muscle integrity (Mizuno *et al.*, 2004). Synemin has been detected in smooth muscle cells of the colon, but not in epithelial cells (Hirako *et al.*, 2003). However synemin activity in the colon does not appear to have been studied extensively by any research group.

A role for synemin in promoting tumourigenicity has only recently been suggested (Jing *et al.*, 2005). Jing and co-workers discovered that both α- and β-synemin were up-regulated in reactive and malignant astrocytes compared to normal brain tissue. [Synemin is known to be absent from mature astrocytes of adult animals (Sultana *et al.*, 2000).] They reported that all astrocytoma tissues reacted with synemin antibodies, independent of grade. Additionally α- and β-synemin were differentially increased in some glioblastoma cell lines. Generally α-synemin appeared predominately up-regulated with comparable variation in expression seen at the mRNA level. Interestingly, in these cell lines synemin was found to associate specifically with α-actinin in ruffled membranes which are actin-rich semicircular leading edges important in cell motility. Both nesprin-1 giant and nesprin-2 giant isoforms have also been immunodetected in membrane ruffles / leading edges (Padmakumar *et al.*, 2004; Zhen *et al.*, 2002). Nesprin-1 was shown to largely colocalize with the actin-binding protein α-actinin, while nesprin-2 colocalized with the actin networks.

Nesprins are huge spectrin-repeat proteins belonging to the α-actinin superfamily. They possess an N-terminal α-actinin-related actin binding domain and are involved in actin bundling (Padmakumar *et al.*, 2004; Zhen *et al.*, 2002). Unlike other members of the spectrin family, nesprins harbour a transmembrane domain within a C-terminal Klarsicht-like domain and are consequently targeted to the nuclear membrane (Padmakumar *et al.*, 2004; Zhang *et al.*, 2001; Zhen *et al.*, 2002). In healthy colon tissue nesprin-1 mRNA is expressed at a medium level, whereas nesprin-2 mRNA is expressed at a low level. In SW480 colon carcinoma cells specifically, levels of nesprin-2 transcript are comparable to normal tissue, whereas nesprin-1 mRNA levels are down-regulated to an almost undetectable amount. Overall, cancer cell lines seem to express

little or no nesprin-1 mRNA and only traceable amounts of nesprin-2 transcript (Padmakumar *et al.*, 2004; Zhen *et al.*, 2002).

Nesprins are hypothesized to connect the nuclear lamina to elements of the microfilament system in the cytoplasm (Libotte *et al.*, 2005). Localization of nesprin-2 giant to both sides of the nuclear envelope has been demonstrated, as well as direct interaction of nesprin-2 giant with both lamin A/C and emerin (Libotte *et al.*, 2005; Zhen *et al.*, 2002). Likewise nesprin-1 giant and nesprin-1α immunostaining has been detected at the nuclear membrane of smooth and skeletal muscle and found to overlap with that of lamin A/C and emerin (Mislow *et al.*, 2002a; Zhang *et al.*, 2001). In addition, direct interaction between nesprin-1α, lamin A and emerin has been shown by Mislow et al. (2002b), as well as cytoplasmic staining of nesprin-1 giant in chick cardiac myocytes (COS7 cells) (Padmakumar *et al.*, 2004). Based on this evidence Libotte et al. (2005) have proposed a model in which giant nesprin isoforms congregate at the ONM, where they bind actin, and at the INM, where they interact with nuclear lamin A/C and emerin and lie in close proximity to heterochromatin. Via UNC-84/Sun and other hitherto unidentified peripheral and integral membrane proteins nesprins are predicted to form molecular bridges between lamins, emerin and the actin cytoskeleton. If this is the case alterations in nucleoskeletal elements might be expected to have an impact on the form and function of the cytoskeleton.

At this point only tentative proposals can be made regarding the possible connection between lamin A, synemin and the maintenance of cellular integrity. Currently, experiments undertaken in this thesis indicate the following: 1) Loss of lamin A affects nuclear and cellular morphology in SW480 cells. 2) Normal two-dimensional growth can be rescued by transfection of lamin A and to a lesser extent emerin. 3) Synemin is

significantly down-regulated in lamin A positive versus lamin A negative cells. It has been noted that synemin is expressed in reactive and neoplastic astrocytes but not in normal astrocytes, suggesting that expression of synemin may promote a tumourigenic phenotype (Jing *et al.*, 2005). It is therefore plausible that lamin A expression may promote a more normal epithelial-like phenotype in SW480 cells by influencing the expression of cytoskeletal linker proteins, such as synemin. Nesprins are recognized nucleus and cytoskeletal connecting elements which bind directly to A-type lamins on the nucleoplasmic side of the nuclear membrane and α-actinin and actin in the cytoplasm (Libotte *et al.*, 2005; Mislow *et al.*, 2002b; Padmakumar *et al.*, 2004; Zhen *et al.*, 2002). Therefore they are primary candidates to mediate lamin A – cytoplasmic IF interaction, thereby functionally connecting two IF networks on opposing sides of the nuclear envelope believed to regulate cellular integrity.

### *6.4 A-type lamin expression in CRC tissue*

To determine whether the aforementioned changes in A-type lamin expression seen in CRC cell lines were also a feature of neoplastic tissue, a small scale immunohistochemical study of colorectal tumours and normal colon tissue was undertaken. In normal colonic crypts lamin A/C activity correlated with cellular differentiation, resulting in a gradient of expression. Protein levels were barely detectable in the stem cell compartment but gradually increased to a maximal level at the intercrypt table. Two other groups have reported augmented lamin A/C expression in the top third of the crypt and weak staining in the basal region, but they did not differentiate between lamin A and lamin C (Cance *et al.*, 1992; Moss *et al.*, 1999). Using antibodies specific for individual A-type lamin polypeptides, this study demonstrates parallel topological expression patterns for lamins A and C along the crypt

/ villus axis and defines the area with highest lamin A/C expression to the upper 20% of the crypt.

Changes in nuclear morphology, including enlargement and elongation, as well as migration of nuclei from the basal to the apical pole of colonic epithelial cells are strong indicators of dysplasia. The earliest signs of dysplasia are associated with ACF, whereas the characteristic signs of severe dysplasia were apparent in the malignant colorectal polyps analysed in this study. Lamin A and lamin C antibodies noticeably decorated the marginal zones of these polyps which were essentially normal. However, dysplastic regions were invariably negative for lamin A and negative or very weakly positive for lamin C and lamin A/C. This suggests a link between morphological transformation of nuclei and down-regulation of lamin A/C. Clinically the degree of dysplasia within a tumour is determined predominately by nuclear morphology and migration. In the absence of a clinically relevant molecular marker of dysplasia in CRC, these data suggest lamin A may potentially be an ideal marker. To ascertain the suitability of lamin A as a marker of dysplasia, a larger immunohistochemical study will be required incorporating specimens with different degrees of dysplasia to establish whether a change in lamin expression is concomitant with the earliest signs of dysplasia or is associated only with the later stages.

### *6.5 Final conclusions*

In summary, I have examined the expression and distribution of nuclear lamins in CRC using a model system of colorectal cancer cell lines and specimens of normal and malignant colorectal mucosa. Initially it was discovered that lamin A expression is down-regulated over lamin C in the most dedifferentiated cell lines and that this process

can be regulated at both the level of transcription and by post-transcriptional mechanisms. Furthermore, the proportion of cells in each phase of the cell cycle was measured and the expression of proliferation indices also monitored. Consequently it was determined that loss of lamin A was not related to proliferation. Subsequently, loss of lamin A was correlated with severe dysplasia in malignant polyps and was therefore associated with aberrant nuclear morphology and migration. Re-expression of lamin A in SW480 cells rescued two-dimensional, epithelial-like growth and was correlated with a significant reduction in the transcription of synemin, a cytoplasmic IF. The corollary of this is that loss of lamin A in CRC appears to accompany cellular dedifferentiation, alterations in nuclear morphology and abnormal three-dimensional cell growth. RNA profiling suggests this may be the result of a breakdown in functional interactions between lamin A and components of the cytoskeleton, namely cytoplasmic IFs such as synemin.

Future work should focus on determining whether equivalent changes in synemin expression are seen at the protein level and whether changes in expression of synemin and lamin A correlate with cell motility and dysplastic behaviour. Identification of other genes involved in lamin A – cytoskeletal communication is of paramount importance. Comparing gene expression profiles between colon cancer cells with and without lamin A using Affymetrix GeneChip® microarray technology should facilitate the identification of different genes involved in lamin A regulated pathways or enable the prediction of signalling networks. Additionally it would be informative to sequence the tail domain of lamin A in each of the CRC cell lines used, particularly SW480, to look for similar destabilizing mutations as those seen in HGPS (Eriksson *et al.*, 2003) which give rise to aberrant lamin A, but normal lamin C.

# APPENDIX I

Additional information associated with Chapter 2, Material and Methods.

# APPENDIX I

## A. Mowiol mounting media

| | | |
|---|---|---|
| Mowiol® 4-88 | 2.4 g | 12% |
| Glycerol | 6 g | 30% |
| 0.2 M Tris-HCl, pH 8.5 | 12 ml | 120 mM |
| DABCO | 2.5% | 2.5% |
| DAPI | 1 µg/ml | 1 µg/ml |
| $dH_2O$ | 6 ml | |

## B. SDS-PAGE gel preparation

***Resolving gel***

| Component | 10% gel | 12% gel |
|---|---|---|
| Deionised water | 5.3 ml | 4.9 ml |
| ProSieve® 50 gel solution | 2.0 ml | 2.4 ml |
| 1.5 M Tris-HCl, pH 8.8 | 2.5 ml | 2.5 ml |
| 10% SDS | 0.1 ml | 0.1 ml |
| 10% APS (fresh) | 0.1 ml | 0.1 ml |
| TEMED | 0.004 ml | 0.004 ml |

***Stacking gel (5%)***

| Component | 5ml |
|---|---|
| Deionised water | 3.75 ml |
| ProSieve® 50 gel solution | 0.5 ml |
| 1 M Tris-HCl, pH 6.8 | 0.65 ml |
| 10% SDS | 0.05 ml |
| 10% APS (fresh) | 0.05 ml |
| TEMED | 0.005 ml |

# APPENDIX II

Information relating to the development of the Colorectal Cancer Oligonucleotide Chip which was designed and printed in-house (see Chapters 2 and 4) and data produced from the accompanying microarray experiments (see Chapter 4).

**Appendix II, A**

Table of functional groups into which the genes on the Colorectal Cancer Oligonucleotide Chip were organized.

## Appendix II, A. Table of functional groups into which the genes on the Colorectal Cancer Oligonucleotide Chip were organized.

| Gene symbol | Gene Description | Accession no. |
|---|---|---|
| Apoptosis and apoptotic inhibitors | | |
| *AMID / PRG3* | p53-responsive gene 3 | AF337957 |
| *BAD* | BCL2-antagonist of cell death | AF031523 |
| *BAK1* | BCL2-antagonist/killer 1 | U23765 |
| *BCL2* | B-cell CLL/lymphoma 2 | M14745 |
| *BCL2L1* | BCL2-like 1 / bcl-X | Z23115 |
| *BIRC2* | baculoviral IAP repeat-containing 2 / apoptosis inhibitor 1 | U45878 |
| *CASP3* | caspase 3, apoptosis-related cysteine protease | AY219866 |
| *CASP7* | caspase 7, apoptosis-related cysteine protease | NM_001227 |
| *CASP8* | caspase 8, apoptosis-related cysteine protease | NM_001228 |
| *CAST* | calpastatin | D16217 |
| *FAS* | Fas (TNF receptor superfamily, member 6) | X83493 |
| *FASLG* | Fas ligand (TNF superfamily, member 6) | D38122 |
| *LITAF* | lipopolysaccharide-induced TNF factor | NM_004862 |
| *NCKAP1 / NAP1* | NCK-associated protein 1 | AB014509 |
| *TERT* | telomerase reverse transcriptase | NM_003219 |
| *TNFRSF10A / TRAILR1* | tumor necrosis factor receptor superfamily, member 10a | U90875 |
| *TNFSF10 / TRAIL* | TNF-related apoptosis-inducing ligand | U37518 |
| Cell adhesion | | |
| *CDH1* | cadherin 1, type 1, E-cadherin (epithelial) | Z13009 |
| *CTNNA1* | catenin (cadherin-associated protein), alpha 1, 102kDa | NM_001903 |
| *CTNND1* | catenin (cadherin-associated protein), delta 1 / p120 catenin | AF062339 |
| Cell cycle progression / cell proliferation and growth | | |
| *CCNA1* | cyclin A1 | NM_003914 |
| *CCNB1* | cyclin B1 | NM_031966 |
| *CCNB2* | cyclin B2 | NM_004701 |
| *CCND1* | cyclin D1 | NM_053056 |
| *CCND2* | cyclin D2 | NM_001759 |
| *CCND3* | cyclin D3 | NM_001760 |
| *CCNE1* | cyclin E1 | NM_001238 |
| *CDC2* | cell division cycle 2, G1 to S and G2 to M / cdk1 | NM_001786 |
| *CDC25A* | cell division cycle 25A | NM_001789 |
| *CDC25B* | cell division cycle 25B | NM_021874 |
| *CDC42* | cell division cycle 42 (GTP binding protein, 25kDa) | NM_001791 |
| *CDK2* | cyclin-dependent kinase 2 | NM_001798 |
| *CDK4* | cyclin-dependent kinase 4 | NM_000075 |
| *CDK6* | cyclin-dependent kinase 6 | NM_001259 |
| *CDKN1B* | cyclin-dependent kinase inhibitor 1B (p27, Kip1) | NM_004064 |
| *CHK1* | checkpoint kinase Chk1 | AF016582 |
| *CHK2* | checkpoint kinase Chk2 | AF086904 |
| *CSPG2* | chondroitin sulfate proteoglycan 2 (versican) | X15998 |
| *CXCL2* | GRO-beta / chemokine (C-X-C motif) ligand 2 | M36820 |
| *EGF* | epidermal growth factor | NM_001963 |
| *EGFR* | epidermal growth factor receptor | X00588 |
| *FGF5* | fibroblast growth factor 5 | NM_004464 |
| *FGFR1* | fibroblast growth factor receptor 1 | X51803 |
| *FGFR4* | fibroblast growth factor receptor 4 | NM_002011 |
| *GPC3* | glypican 3 | NM_004484 |
| *IGF1R* | insulin-like growth factor 1 receptor | X04434 |

**Appendix II, A cont.**

| Gene symbol | Gene Description | Accession no. |
|---|---|---|
| Cell cycle progression / cell proliferation and growth cont. | | |
| *IGF2* | insulin-like growth factor 2 (somatomedin A) | NM_000612 |
| *IL3* | interleukin 3 (colony-stimulating factor, multiple) | NM_000588 |
| *MDM2* | Mdm2, transformed 3T3 cell double minute 2, p53 binding protein (mouse) | AF092844 |
| *MKI67* | antigen identified by monoclonal antibody Ki-67 | NM_002417 |
| *PDGFA* | platelet-derived growth factor alpha polypeptide | X06374 |
| *PDGFRA* | platelet-derived growth factor receptor, alpha polypeptide | J03278 |
| *SPARC* | secreted protein, acidic, cysteine-rich (osteonectin) | J03040 |
| *TGFA* | transforming growth factor, alpha | NM_003236 |
| *TGFB1* | transforming growth factor, beta 1 | NM_000660 |
| *TGFBI / BIGH3* | transforming growth factor, beta-induced, 68kDa | M77349 |
| *TGFBR2* | transforming growth factor, beta receptor II (70/80kDa) | NM_003242 |
| *VEGF* | vascular endothelial growth factor | NM_003376 |
| | | |
| Cytoskeleton and nucleoskeleton | | |
| *ACTA1* | actin, alpha 1, skeletal muscle | NM_001100 |
| *ACTA2* | actin, alpha 2, smooth muscle, aorta | K01747 |
| *ACTG1* | actin, gamma 1 | NM_001614 |
| *CFL1* | cofilin 1 (non-muscle) | D00682 |
| *DES* | desmin | NM_001927 |
| *DSP* | desmoplakin | NM_004415 |
| *FLNA* | filamin A, alpha (actin binding protein 280) | NM_001456 |
| *GFAP* | glial fibrillary acidic protein | NM_002055 |
| *JUP* | junction plakoglobin | NM_002230 |
| *KRT1* | keratin 1 | NM_006121 |
| *KRT10* | keratin 10 | NM_000421 |
| *KRT14* | keratin 14 | NM_000526 |
| *KRT18* | keratin 18 | NM_000224 |
| *KRT18* | keratin 18 | X12881 |
| *KRT19* | keratin 19 | NM_002276 |
| *KRT20* | keratin 20 | X73502 |
| *KRT5* | keratin 5 | NM_000424 |
| *KRT8* | keratin 8 | NM_002273 |
| *KRT8* | keratin 8 | X74929 |
| *LCP1* | lymphocyte cytosolic protein 1 (L-plastin) | NM_002298 |
| *LMNA* | lamin A | X03444 |
| *LMNA* | lamin C | X03445 |
| *LMNB1* | lamin B1 | NM_005573 |
| *LMNB2* | lamin B2 | M94362 |
| *MACF1* | microtubule-actin crosslinking factor 1 | NM_012090 |
| *NEBL* | nebulette | Y16241 |
| *NEFH* | neurofilament, heavy polypeptide 200kDa | NM_021076 |
| *NF2* | merlin / neurofibromin 2 (bilateral acoustic neuroma) | NM_000268 |
| *paranemin* | paranemin | XM_195022 |
| *PFN1* | profilin 1 | NM_005022 |
| *PLEC1* | plectin 1, intermediate filament binding protein 500kDa | NM_000445 |
| *PLS3* | plastin 3 (T isoform) | NM_005032 |
| *PPL* | periplakin | NM_002705 |
| *PRPH* | peripherin | NM_006262 |
| *PXN* | paxillin | U14588 |
| *SYN* | synemin | AJ310521 |
| *TMPO (A)* | thymopoietin alpha / lamina-associated polypeptide 2 alpha | U09086 |
| *TMPO (B)* | thymopoietin beta / lamina-associated polypeptide 2 beta | U09087 |
| *TUBA2* | tubulin, alpha 2 | K00558 |

**Appendix II, A cont.**

| Gene symbol | Gene Description | Accession no. |
|---|---|---|
| Cytoskeleton and nucleoskeleton cont. | | |
| *TUBB2* | tubulin, beta 2 | NM_001069 |
| *TUBG* | tubulin, gamma 1 | M61764 |
| *VCL* | vinculin | M33308 |
| *VIL2* | villin 2 (ezrin) | NM_003379 |
| *VIM* | vimentin | NM_003380 |
| DNA replication and repair | | |
| *ATM* | ataxia telangiectasia mutated | U33841 |
| *LIG4* | DNA ligase IV | X83441 |
| *MLH1* | mutL homolog 1, colon cancer, nonpolyposis type 2 (E. coli) | U07343 |
| *MSH2* | mutS homolog 2, colon cancer, nonpolyposis type 1 (E. coli) | NM_000251 |
| *NBS1* | Nijmegen breakage syndrome 1 (nibrin) | AF058696 |
| *PARP1* | poly (ADP-ribose) polymerase family, member 1 | NM_001618 |
| *PMS2* | PMS2 postmeiotic segregation increased 2 | NM_000535 |
| *PRKDC* | DNA-dependent protein kinase catalytic subunit | U47077 |
| *RPA1* | replication protein A1, 70kDa | NM_002945 |
| *XRCC4* | DNA-repair protein XRCC4 | NM_022550 |
| *XRCC5* | Ku autoantigen, 80kDa | NM_021141 |
| *XRCC6* | thyroid autoantigen 70kD (Ku antigen) | NM_001469 |
| Extracellular matrix: components, processing, cellular attachment, proteases and protease inhibitors | | |
| *BGN* | biglycan | J04599 |
| *COL1A2* | collagen, type I, alpha 2 | NM_000089 |
| *COL1A2* | collagen, type I, alpha 2 | V00503 |
| *FN1 / FN* | fibronectin, alt splice | X02761 |
| *HPSE* | heparanase | AF144325 |
| *ITGA1* | integrin, alpha 1 | X68742 |
| *ITGA2* | integrin, alpha 2 | X17033 |
| *ITGA3* | integrin, alpha 3 | M59911 |
| *ITGA5* | integrin, alpha 5 (fibronectin receptor) | NM_002205 |
| *ITGA6* | integrin, alpha 6 | NM_000210 |
| *ITGAV* | integrin, alpha V (vitronectin receptor) | NM_002210 |
| *ITGB1* | integrin, beta 1 | M34189 |
| *ITGB3* | integrin, beta 3 | NM_000212 |
| *ITGB4* | integrin, beta 4 | X53587 |
| *ITGB5* | integrin, beta 5 | X53002 |
| *LAMA4* | laminin, alpha 4 | NM_002290 |
| *LAMB1* | laminin, beta 1 | NM_002291 |
| *MMP1* | matrix metalloproteinase 1 (interstitial collagenase) | NM_002421 |
| *MMP14* | matrix metalloproteinase 14 (membrane-inserted) | NM_004995 |
| *MMP3* | matrix metalloproteinase 3 (stromelysin 1, progelatinase) | NM_002422 |
| *MMP9* | matrix metalloproteinase 9 | NM_004994 |
| *SDC1* | syndecan 1 | NM_002997 |
| *SDC4* | syndecan 4 (amphiglycan, ryudocan) | NM_002999 |
| *SERPINA1* | serine proteinase inhibitor, clade A (alpha-1 antiproteinase, antitrypsin), member 1 | X01683 |
| *SPP1* | secreted phosphoprotein 1 (osteopontin) | J04765 |
| *TIMP1* | tissue inhibitor of metalloproteinase 1 | NM_003254 |
| Metabolism | | |
| *FABP2* | fatty acid binding protein 2, intestinal | M18079 |
| Oncogenes | | |
| *ABL1* | v-abl Abelson murine leukemia viral oncogene homolog 1 | X16416 |

**Appendix II, A cont.**

| Gene symbol | Gene Description | Accession no. |
|---|---|---|
| Oncogenes cont. | | |
| *EP300* | E1A binding protein p300 | NM_001429 |
| *FOS* | v-fos FBJ murine osteosarcoma viral oncogene homolog | K00650 |
| *HER2* | v-erb-b2 erythroblastic leukemia viral oncogene homolog 2 | M11730 |
| *HRAS* | v-Ha-ras Harvey rat sarcoma viral oncogene homolog | NM_005343 |
| *JUN* | v-jun sarcoma virus 17 oncogene homolog | J04111 |
| *KRAS* | v-Ki-ras2 Kirsten rat sarcoma viral oncogene homolog | M54968 |
| *MOS* | v-mos Moloney murine sarcoma viral oncogene homolog | NM_005372 |
| *MYC* | v-myc myelocytomatosis viral oncogene homolog | V00568 |
| *MYCN* | N-myc proto-oncogene protein | Y00664 |
| *RAF1* | v-raf-1 murine leukemia viral oncogene homolog 1 | X03484 |
| *SRC* | v-src sarcoma (Schmidt-Ruppin A-2) viral oncogene homolog | NM_004383 |
| Protein translation, processing, transport and degradation | | |
| *AIM1* | absent in melanoma 1 | NM_016180 |
| *EIF3S2* | eukaryotic translation initiation factor 3, subunit 2 beta, 36kDa | NM_003757 |
| *IPO7 / RANBP7* | importin 7 | AF098799 |
| *NUP153* | nucleoporin 153kDa | NM_005124 |
| *RPL19* | ribosomal protein L19 | NM_000981 |
| *RPL21* | ribosomal protein L21 | NM_000982 |
| *RPL31* | ribosomal protein L31 | NM_000993 |
| *TPR* | nucleoprotein TPR / translocated promoter region | NM_003292 |
| Regulation of gene expression (transcription) | | |
| *BCL3* | B-cell CLL/lymphoma 3 | NM_005178 |
| *CDX2* | caudal type homeo box transcription factor 2 | AH007259 |
| *E2F4* | E2F transcription factor 4, p107/p130-binding | NM_001950 |
| *GTF3A* | general transcription factor IIIA | NM_002097 |
| *NFKB1* | nuclear factor of kappa light polypeptide gene enhancer in B-cells 1 (p105) | X61498 |
| *RARA* | retinoic acid receptor, alpha | NM_000964 |
| *RXRA* | retinoid X receptor, alpha | NM_002957 |
| *SP1* | Sp1 transcription factor | AF252284 |
| *TCF1* | transcription factor 1, hepatic | M57732 |
| *TCF3* | transcription factor 3 | AB031046 |
| *TCF4* | transcription factor 4 | AR067642 |
| *TGIF* | TGFB-induced factor (TALE family homeobox) | X89750 |
| *USF2* | upstream transcription factor 2, c-fos interacting | NM_003367 |
| *ZFP91* | zinc finger protein 91 homolog (mouse) | NM_053023 |
| Signal transduction | | |
| *CCR7* | chemokine (C-C motif) receptor 7 | AB000887 |
| *CD14* | CD14 antigen | M86511 |
| *FCGR2B* | IGFR2 / Fc fragment of IgG, low affinity IIb, receptor | J04162 |
| *GNAL* | G-s-alpha / guanine nucleotide binding protein (G protein) | AH002748 |
| *ILK* | integrin-linked kinase | NM_004517 |
| *MAPK1* | mitogen-activated protein kinase 1 | NM_002745 |
| *PAK1* | p21/Cdc42/Rac1-activated kinase 1 (STE20 homolog, yeast) | NM_002576 |
| *PIK3CG* | phosphoinositide-3-kinase, catalytic, gamma polypeptide | NM_002649 |
| *PTK2B / PKB* | PTK2B protein tyrosine kinase 2 beta | X61037 |
| *RAC1* | rho family, small GTP binding protein Rac1 | NM_006908 |
| *RGS2* | Regulator of G-protein signaling 2 (G0/G1 switch regulatory protein 8) | L13463 |
| *RHOA* | ras homolog gene family, member A | NM_001664 |
| *RHOC* | ras homolog gene family, member C | NM_005167 |
| *STAT1* | signal transducer and activator of transcription 1, 91kDa | NM_007315 |

**Appendix II, A cont.**

| Gene symbol | Gene Description | Accession no. |
|---|---|---|
| Signal transduction cont. | | |
| *TIAM1* | T-cell lymphoma invasion and metastasis 1 | NM_003253 |
| | | |
| Stem cell differentiation | | |
| *ANIL* | astrocytic NOVA-like RNA-binding protein | U70477 |
| *ASTN* | Astrotactin | AB006627 |
| *BMP1* | bone morphogenetic protein 1 | M22488 |
| *BMP4* | bone morphogenetic protein 4 | NM_001202 |
| *BMP6* | bone morphogenetic protein 6 | NM_001718 |
| *CRIPTO* | cripto protein | X14253 |
| *EPHA1* | EPH receptor A1 | M18391 |
| *FN1* | cellular fibronectin | M10905 |
| *FUT1* | fucosyltransferase 1 | M35531 |
| *FUT2* | fucosyltransferase 2 (secretor status included) | D87942 |
| *GAP43* | growth associated protein 43 | M25667 |
| *GATA4* | GATA binding protein 4 | L34357 |
| *GATA4* | GATA binding protein 4 | NM_002052 |
| *GJA1* | gap junction protein, alpha 1, 43kDa (connexin 43) | M65188 |
| *HATH1* | atonal protein homolog 1 | U61148 |
| *LAMB1* | laminin, beta 1 | M20206 |
| *MAP2* | microtubule-associated protein 2 | U01828 |
| *MAPT / TAU* | microtubule-associated protein tau | J03778 |
| *MASH1* | Achaete-scute homolog 1 | L08424 |
| *MASH2* | achaete-scute complex-like 2 | U77629 |
| *MYOD1* | myogenic factor 3 | X17650 |
| *NEFL* | neurofilament, light polypeptide 68kDa | NM_006158 |
| *NEFM* | Neurofilament medium polypeptide | Y00067 |
| *NES* | nestin | X65964 |
| *NEUROD1* | neurogenic differentiation 1 | AF045152 |
| *NEUROD2* | neurogenic differentiation 2 | U58681 |
| *NEUROD3* | neurogenic differentiation 3 | U63842 |
| *NEUROD4* | neurogenic differentiation 4 | U43843 |
| *NHLH2* | nescient helix loop helix 2 | M97508 |
| *NOTCH1* | Notch homolog 1 (Drosophila) | M73980 |
| *NOTCH2* | Notch homolog 2 (Drosophila) | X80115 |
| *NOTCH3* | Notch homolog 3 (Drosophila) | U97669 |
| *NOTCH4* | Notch homolog 4 (Drosophila) | U95299 |
| *NSE* | Neuron-specific enolase | X51956 |
| *PAX6* | paired box gene 6 (aniridia, keratitis) | M93650 |
| *PLP* | proteolipid protein | M27110 |
| *REST* | RE1-silencing transcription factor | U13879 |
| *SCG10* | Stathmin 2 (SCG10 protein) | S82024 |
| *SNAP25* | synaptosomal-associated protein, 25kDa | D21267 |
| *SOX1* | SRY (sex determining region Y)-box 1 | Y13436 |
| *SOX10* | SRY (sex determining region Y)-box 10 | AJ001183 |
| *SOX17* | SRY (sex determining region Y)-box 17 | NM_022454 |
| *SOX2* | SRY (sex determining region Y)-box 2 | L07335 |
| *SOX8* | SRY (sex determining region Y)-box 8 | AF226675 |
| *SOX9* | SRY (sex determining region Y)-box 9 | NM_000346 |
| *SYP* | synaptophysin | U93305 |
| *T* | T, brachyury homolog (mouse) | AJ001699 |
| *TDGF1* | teratocarcinoma-derived growth factor 1 | M96955 |
| *TF* | transferrin | S95936 |

**Appendix II, A cont.**

| Gene symbol | Gene Description | Accession no. |
|---|---|---|
| Stem cell differentiation cont. | | |
| *TLE2* | transducin-like enhancer of split 2 | M99436 |
| *VTN* | vitronectin | X03168 |
| *ZNF74* | zinc finger protein 74 (Cos52) | X92715 |
| Stress response | | |
| *CRYAA* | crystallin, alpha A | NM_000394 |
| *CRYAB* | crystallin, alpha B | NM_001885 |
| *HSP70-1* | heat shock 70kD protein 1 | M11717 |
| *HSPA8 / HSC70* | constitutive heat shock protein 70 | AF352832 |
| *HSPB2* | heat shock 27kDa protein 2 | NM_001541 |
| *HSPCA* | heat shock 90kDa protein 1, alpha | X15183 |
| *hsp 20* | Sequence 109 from Patent WO9954460 (hsp 20) | AX013767 |
| *ORM1* | Alpha-1-acid glycoprotein 1 precursor (AGP 1) (Orosomucoid 1) (OMD 1) | X02544 |
| *SOD1* | superoxide dismutase 1, soluble | NM_000454 |
| *SOD2* | superoxide dismutase 2, mitochondrial | NM_000636 |
| Transporters, carriers | | |
| *ATP2A3* | ATPase, Ca++ transporting, ubiquitous | AF068221 |
| *SLC16A1* | solute carrier family 16 (monocarboxylic acid transporters), member 1 | NM_003051 |
| *SLC2A1 / GLUT1* | solute carrier family 2 (facilitated glucose transporter), member 1 | AY034633 |
| Tumour supressor genes | | |
| *APC* | adenomatosis polyposis coli | NM_000038 |
| *DCC* | deleted in colorectal carcinoma | NM_005215 |
| *NF1* | neurofibromin 1 | NM_000267 |
| *RB1* | retinoblastoma 1 | NM_000321 |
| *TP53* | tumor protein p53 (Li-Fraumeni syndrome) | NM_000546 |
| *WT1* | Wilms tumor 1 | NM_000378 |
| Wnt signalling | | |
| *AQP3* | aquaporin 3 | NM_004925 |
| *ASL* | argininosuccinate lyase | NM_000048 |
| *BIRC5* | apoptosis inhibitor 4 - survivin | NM_001168 |
| *CA2* | carbonic anhydrase II | NM_000067 |
| *CD44* | CD44 antigen (Heparan sulfate proteoglycan) (Epican) | X66733 |
| *CDKN1A* | cyclin-dependent kinase inhibitor 1A (p21, Cip1) | NM_000389 |
| *CEACAM1 / BGP1* | carcinoembryonic antigen-related cell adhesion molecule 1 (biliary glycoprotei | NM_001712 |
| *CHAF1A* | chromatin assembly factor 1, subunit A (p150) | NM_005483 |
| *CLDN1* | claudin 1 | NM_021101 |
| *CLDN4* | claudin 4 | NM_001305 |
| *CTNNB1* | catenin (cadherin-associated protein), beta 1, 88kDa | NM_001904 |
| *DLEU1* | deleted in lymphocytic leukemia, 1 | NM_005887 |
| *DRG1* | developmentally regulated GTP binding protein 1 | AF271994 |
| *ENC1* | ectodermal-neural cortex (with BTB-like domain) | NM_003633 |
| *EPHB1* | EPH receptor B1 | NM_004429 |
| *EPHB2* | EPH receptor B2 | AF025304 |
| *ETS2* | v-ets erythroblastosis virus E26 oncogene homolog 2 | J04102 |
| *FABP1* | fatty acid binding protein 1, liver | BC032801 |
| *GPX2* | glutathione peroxidase 2 (gastrointestinal) | AF199441 |
| *JPO1 / LOC442172* | c-Myc target JPO1 | AY029179 |
| *KLF4* | Kruppel-like factor 4 (gut) | NM_004235 |
| *LGALS4* | galectin 4 | NM_006149 |
| *MCM3* | MCM3 minichromosome maintenance deficient 3 (S. cerevisiae) | NM_002388 |

**Appendix II, A cont.**

| Gene symbol | Gene Description | Accession no. |
|---|---|---|
| Wnt signalling cont. | | |
| *MCM5* | minichromosome maintenance deficient 5, cell division cycle 46 | NM_006739 |
| *MUC2* | mucin 2, intestinal/tracheal | NM_002457 |
| *MYB* | Myb proto-oncogene protein (C-myb) | M15024 |
| *NSAP1 / SYNCRIP* | NS1-associated protein 1 pseudogene | AF155568 |
| *PLCB2* | phospholipase C, beta 2 | NM_004573 |
| *PRKCD* | protein kinase C, delta | NM_006254 |
| *RBBP4* | retinoblastoma binding protein 4 | NM_005610 |
| *SCF / KITLG* | stem cell factor / kit ligand precursor / Mast cell growth factor (MGF) | M59964 |
| *SLC7A5* | solute carrier family 7 (cationic amino acid transporter, y+ system), member 5 | NM_003486 |
| *TCOF1* | Treacher Collins-Franceschetti syndrome 1 | NM_000356 |
| *TEAD4* | Transcriptional enhancer factor TEF-3 (TEA domain family member 4) | X94438 |
| *TFDP2* | transcription factor Dp-2 (E2F dimerization partner 2) | NM_006286 |
| *UNG* | uracil-DNA glycosylase | Y09008 |
| *XRCC3* | X-ray repair complementing defective repair in Chinese hamster cells 3 | AF035586 |
| Xenobiotic and drug metabolism / detoxification | | |
| *ABCB1* | P glycoprotein 1/multiple drug resistance 1 | M14758 |
| *ABCB4* | P glycoprotein 3/multiple drug resistance 3 | M23234 |
| *MT1A* | metallothionein 1A (functional) | K01383 |
| Miscellaneous enzymes | | |
| *ANPEP* | aminopeptidase N / CD13 | M22324 |
| *CA12* | carbonic anhydrase XII | AF037335 |
| *PTGS2 / COX2* | prostaglandin-endoperoxide synthase 2 (cyclooxygenase) | M90100 |
| *SI* | sucrase-isomaltase (alpha-glucosidase) | NM_001041 |
| Miscellaneous | | |
| *CEACAM3 / CEA* | carcinoembryonic antigen-related cell adhesion molecule 3 | M29540 |
| *CLCNKB* | chloride channel Kb | Z30644 |
| *FOXE3* | forkhead box E3 | AL607122 |
| *NPM1* | nucleophosmin (nucleolar phosphoprotein B23, numatrin) | M28699 |
| *SOX4* | SRY (sex determining region Y)-box 4 | X70683 |
| *T18* | T-18 | AF089811 |
| Function not well elucidated | | |
| *KLRB1* | NKR-P1A | U11276 |
| *LGALS2* | galectin 2 | BC029063 |
| *MXD3* | MAX dimerization protein 3 | NM_031300 |
| *PITX3* | paired-like homeodomain transcription factor 3 | AF041339 |
| *PROX1* | prospero-related homeobox 1 | BC024201 |
| *RALGPS1* | Ral GEF with PH domain and SH3 binding motif 1 | NM_014636 |
| *REG1B* | regenerating protein I beta | D17291 |
| *RSAD2* | radical S-adenosyl methionine domain containing 2 / cig5 / viperin | AF026941 |
| *SOX11* | SRY (sex determining region Y)-box 11 | AB028641 |
| *SOX3* | SRY (sex determining region Y)-box 3 | NM_005634 |
| *TPBG* | trophoblast glycoprotein | NM_006670 |
| *TSPAN1* | tetraspan NET-1 | AF065388 |
| *ZBTB16* | PLZF / zinc finger and BTB domain containing 16 | AF060568 |
| House keeping / positive controls | | |
| *ACTB* | actin, beta | NM_001101 |
| *GAPDH* | glyceraldehyde-3-phosphate dehydrogenase | AF261085 |

**Appendix II, A cont.**

| Gene symbol | Gene Description | Accession no. |
|---|---|---|
| Negative controls | | |
| *CHRM1* | cholinergic receptor, muscarinic 1 | AF385587 |
| *CHRM2* | cholinergic receptor, muscarinic 2 | AF385588 |
| *CHRM3* | cholinergic receptor, muscarinic 3 | NM_000740 |
| *CHRM4* | cholinergic receptor, muscarinic 4 | AF385590 |
| *CHRM5* | cholinergic receptor, muscarinic 5 | NM_012125 |
| *POU5F1* | POU domain, class 5, transcription factor 1 | NM_002701 |

**Appendix II, B**

Complete list of human genes on the CRC Oligonucleotide Chip, including gene symbol, description and GenBank® accession number. The corresponding well ID (position of gene on the chip), chip code (used to identify gene on plate template – see Appendix II, C) and protein name are also given.

## Appendix II, B. Details of all genes printed on the Colorectal Cancer Oligonucleotide Chip.

| Well ID[a] | Chip code[b] | Gene symbol | Gene description | Accession no. | Protein name[c] |
|---|---|---|---|---|---|
| A1.a1 | GAPDH | *GAPDH* | glyceraldehyde-3-phosphate dehydrogenase | AF261085 | GAPDH |
| A2.a1 | SOX11 | *SOX11* | SRY (sex determining region Y)-box 11 | AB028641 | SOX11 |
| A3.a1 | ND1 | *NEUROD1* | neurogenic differentiation 1 | AF045152 | NEUROD1 |
| A4.a1 | SOX8 | *SOX8* | SRY (sex determining region Y)-box 8 | AF226675 | SOX8 |
| A5.a1 | SOX10 | *SOX10* | SRY (sex determining region Y)-box 10 | AJ001183 | SOX10 |
| A6.a1 | BRACHY | *T* | T, brachyury homolog (mouse) | AJ001699 | brachyury |
| A7.a1 | SNAP25 | *SNAP25* | synaptosomal-associated protein, 25kDa | D21267 | SNAP25 |
| A8.a1 | FUT2 | *FUT2* | fucosyltransferase 2 (secretor status included) | D87942 | FUT2 |
| A9.a1 | NOTCH2 | *NOTCH2* | Notch homolog 2 (Drosophila) | X80115 | NOTCH2 |
| A10.a1 | MAPT | *MAPT / TAU* | microtubule-associated protein tau | J03778 | MAPT / TAU |
| A11.a1 | ASTN | *ASTN* | Astrotactin | AB006627 | Astrotactin |
| A12.a1 | ACTB | *ACTB* | actin, beta | NM_001101 | β-actin |
| A1.a5 | ACTA2 | *ACTA2* | actin, alpha 2, smooth muscle, aorta | K01747 | ACTSA |
| A2.a5 | SOX2 | *SOX2* | SRY (sex determining region Y)-box 2 | L07335 | SOX2 |
| A3.a5 | GATA4 | *GATA4* | GATA binding protein 4 | L34357 | GATA4 |
| A4.a5 | EPHA1 | *EPHA1* | EPH receptor A1 | M18391 | EPHA1 |
| A5.a5 | LAMB1 | *LAMB1* | laminin, beta 1 | M20206 | LAMBI |
| A6.a5 | BMP1 | *BMP1* | bone morphogenetic protein 1 | M22488 | BMP1 |
| A7.a5 | GAP43 | *GAP43* | growth associated protein 43 | M25667 | GAP43 |
| A8.a5 | PLP | *PLP* | proteolipid protein | M27110 | PLP |
| A9.a5 | FUT1 | *FUT1* | fucosyltransferase 1 | M35531 | FUT1 |
| A10.a5 | BMP6 | *BMP6* | bone morphogenetic protein 6 | NM_001718 | BMP6 |
| A11.a5 | GJA1 | *GJA1* | gap junction protein, alpha 1, 43kDa (connexin 43) | M65188 | GJA1 |
| A12.a5 | NOTCH1 | *NOTCH1* | Notch homolog 1 (Drosophila) | M73980 | NOTCH1 |
| A1.b1 | PAX6 | *PAX6* | paired box gene 6 (aniridia, keratitis) | M93650 | PAX6 |
| A2.b1 | TDGF1 | *TDGF1* | teratocarcinoma-derived growth factor 1 | M96955 | TDGF1 |
| A3.b1 | NHLH2 | *NHLH2* | nescient helix loop helix 2 | M97508 | NHLH2 |

[a] The position of each gene on the chip. [b] Code used to identify gene on the plate template (Appendix II, C).

[c] Name of the functional protein product of each gene on the chip.

**Appendix II, B cont.**

| Well ID[a] | Chip code[b] | Gene symbol | Gene description | Accession no. | Protein name[c] |
|---|---|---|---|---|---|
| A8.c1 | SOX1 | *SOX1* | SRY (sex determining region Y)-box 1 | Y13436 | SOX1 |
| A9.c1 | OCT4 | *POU5F1* | POU domain, class 5, transcription factor 1 | NM_002701 | Oct4 / POU5F1 |
| A10.c1 | CLCNKB | *CLCNKB* | chloride channel Kb | Z30644 | CLCNKB |
| A11.c1 | ZNF74 | *ZNF74* | zinc finger protein 74 (Cos52) | X92715 | ZNF74 |
| A12.c1 | MASH1 | *MASH1* | Achaete-scute homolog 1 | L08424 | MASH1 |
| A1.c5 | HATH1 | *HATH1* | atonal protein homolog 1 | U61148 | HATH1 |
| A2.c5 | MASH2 | *MASH2* | achaete-scute complex-like 2 | U77629 | ASH2 |
| A3.c5 | SOX17 | *SOX17* | SRY (sex determining region Y)-box 17 | NM_022454 | SOX17 |
| A4.c5 | FOXE3 | *FOXE3* | forkhead box E3 | AL607122 | FoxE3 |
| A5.c5 | PRPH | *PRPH* | peripherin | NM_006262 | peripherin |
| A6.c5 | AIM1 | *AIM1* | absent in melanoma 1 | NM_016180 | AIM1 |
| A7.c5 | SOD1 | *SOD1* | superoxide dismutase 1, soluble | NM_000454 | SOD1 |
| A8.c5 | MMP3 | *MMP3* | matrix metalloproteinase 3 (stromelysin 1, progelatinase) | NM_002422 | MMP3 |
| A9.c5 | VCL | *VCL* | vinculin | M33308 | vinculin |
| A10.c5 | PARNMN | *None*[d] | paranemin | XM_195022 | paranemin |
| A11.c5 | TUBG | *TUBG* | tubulin, gamma 1 | M61764 | gamma tubulin |
| A12.c5 | HSP70 | *HSP70-1* | heat shock 70kD protein 1 | M11717 | hsp 70 |
| A1.d1 | HSP90 | *HSPCA* | heat shock 90kDa protein 1, alpha | X15183 | hsp 90 |
| A2.d1 | CRYAB | *CRYAB* | crystallin, alpha B | NM_001885 | CRYAB |
| A3.d1 | PROX1 | *PROX1* | prospero-related homeobox 1 | BC024201 | prox1 |
| A4.d1 | CRYAA | *CRYAA* | crystallin, alpha A | NM_000394 | CRYAA |
| A5.d1 | SYN | *SYN* | synemin | AJ310521 | synemin |
| A6.d1 | ACTG1 | *ACTG1* | actin, gamma 1 | NM_001614 | ACTG1 |
| A7.d1 | HSP27 | *HSPB2* | heat shock 27kDa protein 2 | NM_001541 | hsp 27 |
| A8.d1 | PITX3 | *PITX3* | paired-like homeodomain transcription factor 3 | AF041339 | PITX3 |
| A9.d1 | HSP20 | *None*[d] | Sequence 109 from Patent WO9954460. | AX013767 | hsp 20 |
| A10.d1 | IGF1R | *IGF1R* | insulin-like growth factor 1 receptor | X04434 | IGF1 receptor |

[a] The position of each gene on the chip. [b] Code used to identify gene on the plate template (Appendix II, C).

[c] Name of the functional protein product of each gene on the chip.

[d] No gene name currently allocated.

**Appendix II, B cont.**

| Well ID[a] | Chip code[b] | Gene symbol | Gene description | Accession no. | Protein name[c] |
|---|---|---|---|---|---|
| A11.d1 | CDC42 | *CDC42* | cell division cycle 42 (GTP binding protein, 25kDa) | NM_001791 | CDC42 |
| A12.d1 | HSC70 | *HSPA8 / HSC70* | constitutive heat shock protein 70 | AF352832 | hsp 70 |
| A1.d5 | DSP | *DSP* | desmoplakin | NM_004415 | desmoplakin |
| A2.d5 | PAK1 | *PAK1* | p21/Cdc42/Rac1-activated kinase 1 (STE20 homolog, yeast) | NM_002576 | PAK1 |
| A3.d5 | MMP9 | *MMP9* | matrix metalloproteinase 9 | NM_004994 | MMP9 |
| A4.d5 | NF2 | *NF2* | merlin / neurofibromin 2 (bilateral acoustic neuroma) | NM_000268 | merlin |
| A5.d5 | TIAM1 | *TIAM1* | T-cell lymphoma invasion and metastasis 1 | NM_003253 | tiam1 |
| A6.d5 | MMP14 | *MMP14* | matrix metalloproteinase 14 (membrane-inserted) | NM_004995 | mmp14 |
| A7.d5 | ILK | *ILK* | integrin-linked kinase | NM_004517 | ilk |
| A8.d5 | RAC1 | *RAC1* | rhó family, small GTP binding protein Rac1 | NM_006908 | Rac1 |
| A9.d5 | VIL2 | *VIL2* | villin 2 (ezrin) | NM_003379 | ezrin |
| A10.d5 | GPC3 | *GPC3* | glypican 3 | NM_004484 | glypican 3 |
| A11.d5 | PPL | *PPL* | periplakin | NM_002705 | periplakin |
| A12.d5 | PLEC1 | *PLEC1* | plectin 1, intermediate filament binding protein 500kDa | NM_000445 | plectin 1 |
| B2.a1 | HRAS | *HRAS* | v-Ha-ras Harvey rat sarcoma viral oncogene homolog | NM_005343 | H-ras |
| B3.a1 | KRAS | *KRAS* | v-Ki-ras2 Kirsten rat sarcoma viral oncogene homolog | M54968 | K-ras |
| B4.a1 | CSRC | *SRC* | v-src sarcoma (Schmidt-Ruppin A-2) viral oncogene homolog | NM_004383 | c-src |
| B5.a1 | CABL | *ABL1* | v-abl Abelson murine leukemia viral oncogene homolog 1 | X16416 | c-abl |
| B6.a1 | CMOS | *MOS* | v-mos Moloney murine sarcoma viral oncogene homolog | NM_005372 | c-mos |
| B7.a1 | CRAF | *RAF1* | v-raf-1 murine leukemia viral oncogene homolog 1 | X03484 | c-raf |
| B8.a1 | CMYC | *MYC* | v-myc myelocytomatosis viral oncogene homolog | V00568 | c-myc |
| B9.a1 | CFOS | *FOS* | v-fos FBJ murine osteosarcoma viral oncogene homolog | K00650 | c-fos |
| B10.a1 | CJUN | *JUN* | v-jun sarcoma virus 17 oncogene homolog | J04111 | c-jun |
| B11.a1 | E1A | *EP300* | E1A binding protein p300 | NM_001429 | E1A |
| B2.a5 | APC | *APC* | adenomatosis polyposis coli | NM_000038 | APC |
| B3.a5 | DCC | *DCC* | deleted in colorectal carcinoma | NM_005215 | DCC |
| B4.a5 | TP53 | *TP53* | tumor protein p53 (Li-Fraumeni syndrome) | NM_000546 | p53 |
| B5.a5 | RB1 | *RB1* | retinoblastoma 1 | NM_000321 | Rb |

[a] The position of each gene on the chip. [b] Code used to identify gene on the plate template (Appendix II, C).

[c] Name of the functional protein product of each gene on the chip.

**Appendix II, B cont.**

| Well ID[a] | Chip code[b] | Gene symbol | Gene description | Accession no. | Protein name[c] |
|---|---|---|---|---|---|
| B6.a5 | WT1 | *WT1* | Wilms tumor 1 | NM_000378 | WT-1 |
| B7.a5 | NF1 | *NF1* | neurofibromin 1 | NM_000267 | NF-1 |
| B8.a5 | NFKB | *NFKB1* | nuclear factor of kappa light polypeptide gene enhancer in B-cells 1 (p105) | X61498 | NF-kappa-B |
| B9.a5 | ZFP91 | *ZFP91* | zinc finger protein 91 homolog (mouse) | NM_053023 | PZF |
| B10.a5 | RARA | *RARA* | retinoic acid receptor, alpha | NM_000964 | RAR-alpha |
| B11.a5 | RXRA | *RXRA* | retinoid X receptor, alpha | NM_002957 | RXR |
| B1.b1 | RHOC | *RHOC* | ras homolog gene family, member C | NM_005167 | RhoC |
| B2.b1 | 5T4 | *TPBG* | trophoblast glycoprotein | NM_006670 | 5T4 |
| B3.b1 | TCF1 | *TCF1* | transcription factor 1, hepatic | M57732 | TCF-1 |
| B4.b1 | TCF3 | *TCF3* | transcription factor 3 | AB031046 | TCF-3 |
| B5.b1 | TCF4 | *TCF4* | transcription factor 4 | AR067642 | TCF-4 |
| B6.b1 | OCT4 | *POU5F1* | POU domain, class 5, transcription factor 1 | NM_002701 | Oct4 / POU5F1 |
| B7.b1 | BCL2 | *BCL2* | B-cell CLL/lymphoma 2 | M14745 | BCL-2 |
| B8.b1 | BCLX | *BCL2L1* | BCL2-like 1 / bcl-X | Z23115 | BCL-x |
| B9.b1 | TERT | *TERT* | telomerase reverse transcriptase | NM_003219 | Tert |
| B10.b1 | MDR1 | *ABCB1* | P glycoprotein 1/multiple drug resistance 1 | M14758 | MDR-1 |
| B11.b1 | MDR3 | *ABCB4* | P glycoprotein 3/multiple drug resistance 3 | M23234 | MDR-3 |
| B2.b5 | PDGF | *PDGFA* | platelet-derived growth factor alpha polypeptide | X06374 | PDGF |
| B3.b5 | EGF | *EGF* | epidermal growth factor | NM_001963 | EGF |
| B4.b5 | FGF | *FGF5* | fibroblast growth factor 5 | NM_004464 | FGF |
| B5.b5 | TGFA | *TGFA* | transforming growth factor, alpha | NM_003236 | TGF alpha |
| B6.b5 | TGFB | *TGFB1* | transforming growth factor, beta 1 | NM_000660 | TGF beta |
| B7.b5 | PDGFR | *PDGFRA* | platelet-derived growth factor receptor, alpha polypeptide | J03278 | PDGF receptor |
| B8.b5 | EGFR | *EGFR* | epidermal growth factor receptor | X00588 | EGF receptor |
| B9.b5 | FGFR | *FGFR1* | fibroblast growth factor receptor 1 | X51803 | FGF receptor |
| B10.b5 | TGFR | *TGFBR2* | transforming growth factor, beta receptor II (70/80kDa) | NM_003242 | TGF receptor |
| B11.b5 | KRT1 | *KRT1* | keratin 1 | NM_006121 | keratin 1 |
| B1.c1 | MMP1 | *MMP1* | matrix metalloproteinase 1 (interstitial collagenase) | NM_002421 | MMP1 |

[a] The position of each gene on the chip. [b] Code used to identify gene on the plate template (Appendix II, C).

[c] Name of the functional protein product of each gene on the chip.

**Appendix II, B cont.**

| Well ID[a] | Chip code[b] | Gene symbol | Gene description | Accession no. | Protein name[c] |
|---|---|---|---|---|---|
| B2.c1 | KRT5 | *KRT5* | keratin 5 | NM_000424 | keratin 5 |
| B3.c1 | KRT8 | *KRT8* | keratin 8 | NM_002273 | keratin 8 |
| B4.c1 | KRT10 | *KRT10* | keratin 10 | NM_000421 | keratin 10 |
| B5.c1 | KRT14 | *KRT14* | keratin 14 | NM_000526 | keratin 14 |
| B6.c1 | KRT18 | *KRT18* | keratin 18 | NM_000224 | keratin 18 |
| B7.c1 | KRT19 | *KRT19* | keratin 19 | NM_002276 | keratin 19 |
| B8.c1 | KRT20 | *KRT20* | keratin 20 | X73502 | keratin 20 |
| B9.c1 | DES | *DES* | desmin | NM_001927 | desmin |
| B10.c1 | VIM | *VIM* | vimentin | NM_003380 | vimentin |
| B11.c1 | GFAP | *GFAP* | glial fibrillary acidic protein | NM_002055 | GFAP |
| B2.c5 | NEFH | *NEFH* | neurofilament, heavy polypeptide 200kDa | NM_021076 | NF-H |
| B3.c5 | TUBA | *TUBA2* | tubulin, alpha 2 | K00558 | α-tubulin |
| B4.c5 | TUBB | *TUBB2* | tubulin, beta 2 | NM_001069 | β-tubulin |
| B5.c5 | ACTA | *ACTA1* | actin, alpha 1, skeletal muscle | NM_001100 | α-actin |
| B6.c5 | ACTB | *ACTB* | actin, beta | NM_001101 | β-actin |
| B7.c5 | B1 INT | *ITGB1* | integrin, beta 1 | M34189 | beta-1 integrin |
| B8.c5 | B3 INT | *ITGB3* | integrin, beta 3 | NM_000212 | beta-3 integrin |
| B9.c5 | B4 INT | *ITGB4* | integrin, beta 4 | X53587 | beta-4 integrin |
| B10.c5 | B5 INT | *ITGB5* | integrin, beta 5 | X53002 | beta-5 integrin |
| B11.c5 | A1 INT | *ITGA1* | integrin, alpha 1 | X68742 | alpha-1 integrin |
| B1.d1 | FLNA | *FLNA* | filamin A, alpha (actin binding protein 280) | NM_001456 | filamin A |
| B2.d1 | A2 INT | *ITGA2* | integrin, alpha 2 | X17033 | alpha-2 integrin |
| B3.d1 | A3 INT | *ITGA3* | integrin, alpha 3 | M59911 | alpha-3 integrin |
| B4.d1 | A5 INT | *ITGA5* | integrin, alpha 5 (fibronectin receptor) | NM_002205 | alpha-5 integrin |
| B5.d1 | A6 INT | *ITGA6* | integrin, alpha 6 | NM_000210 | alpha-6 integrin |
| B6.d1 | AV INT | *ITGAV* | integrin, alpha V (vitronectin receptor) | NM_002210 | alpha-v integrin |
| B7.d1 | PXN | *PXN* | paxillin | U14588 | paxillin |
| B8.d1 | E CADHR | *CDH1* | cadherin 1, type 1, E-cadherin (epithelial) | Z13009 | E-cadherin |

[a] The position of each gene on the chip. [b] Code used to identify gene on the plate template (Appendix II, C).

[c] Name of the functional protein product of each gene on the chip.

**Appendix II, B cont.**

| Well ID[a] | Chip code[b] | Gene symbol | Gene description | Accession no. | Protein name[c] |
|---|---|---|---|---|---|
| B9.d1 | A CATEN | *CTNNA1* | catenin (cadherin-associated protein), alpha 1, 102kDa | NM_001903 | α-catenin |
| B10.d1 | B CATEN | *CTNNB1* | catenin (cadherin-associated protein), beta 1, 88kDa | NM_001904 | β-catenin |
| B11.d1 | PLAGBN | *JUP* | junction plakoglobin | NM_002230 | plakoglobin |
| B2.d5 | P120 | *CTNND1* | catenin (cadherin-associated protein), delta 1 / p120 catenin | AF062339 | p120 catenin |
| B3.d5 | SYN1 | *SDC1* | syndecan 1 | NM_002997 | syn-1 |
| B4.d5 | SYN4 | *SDC4* | syndecan 4 (amphiglycan, ryudocan) | NM_002999 | syn-4 |
| B5.d5 | LMNN A | *LAMA4* | laminin, alpha 4 | NM_002290 | laminin (alpha) |
| B6.d5 | LMNN B | *LAMB1* | laminin, beta 1 | NM_002291 | laminin (beta) |
| B7.d5 | COL | *COL1A2* | collagen, type I, alpha 2 | NM_000089 | collagen |
| B8.d5 | ALTFBR | *FN1 / FN* | fibronectin, alt splice | X02761 | fibronectin, alt splice |
| B9.d5 | NUP153 | *NUP153* | nucleoporin 153kDa | NM_005124 | Nup153 |
| B10.d5 | TPR | *TPR* | nucleoprotein TPR / translocated promoter region | NM_003292 | Tpr |
| B11.d5 | B23 | *NPM1* | nucleophosmin (nucleolar phosphoprotein B23, numatrin) | M28699 | B23 |
| C2.a1 | RPL31 | *RPL31* | ribosomal protein L31 | NM_000993 | RPL31 |
| C3.a1 | RPL21 | *RPL21* | ribosomal protein L21 | NM_000982 | RPL21 |
| C4.a1 | RPL19 | *RPL19* | ribosomal protein L19 | NM_000981 | RPL19 |
| C5.a1 | LAMA | *LMNA* | lamin A | X03444 | lamin A |
| C6.a1 | LAMC | *LMNA* | lamin C | X03445 | lamin C |
| C7.a1 | LAMB1 | *LMNB1* | lamin B1 | NM_005573 | lamin B1 |
| C8.a1 | LAMB2 | *LMNB2* | lamin B2 | M94362 | lamin B2 |
| C9.a1 | LAP2A | *TMPO (A)* | thymopoietin alpha / lamina-associated polypeptide 2 alpha | U09086 | LAP2α |
| C10.a1 | LAP2B | *TMPO (B)* | thymopoietin beta / lamina-associated polypeptide 2 beta | U09087 | LAP2β |
| C11.a1 | CDK1 | *CDC2* | cell division cycle 2, G1 to S and G2 to M / cdk1 | NM_001786 | Cdk1 / cdc2 |
| C2.a5 | CDK2 | *CDK2* | cyclin-dependent kinase 2 | NM_001798 | Cdk2 |
| C3.a5 | CDK4 | *CDK4* | cyclin-dependent kinase 4 | NM_000075 | Cdk4 |
| C4.a5 | CDK6 | *CDK6* | cyclin-dependent kinase 6 | NM_001259 | Cdk6 |
| C5.a5 | CYCA | *CCNA1* | cyclin A1 | NM_003914 | cyclin A |
| C6.a5 | CYCB1 | *CCNB1* | cyclin B1 | NM_031966 | cyclin B1 |

[a] The position of each gene on the chip. [b] Code used to identify gene on the plate template (Appendix II, C).

[c] Name of the functional protein product of each gene on the chip.

**Appendix II, B cont.**

| Well ID[a] | Chip code[b] | Gene symbol | Gene description | Accession no. | Protein name[c] |
|---|---|---|---|---|---|
| C7.a5 | CYCB2 | *CCNB2* | cyclin B2 | NM_004701 | cyclin B2 |
| C8.a5 | CYCD1 | *CCND1* | cyclin D1 | NM_053056 | cyclin D1 |
| C9.a5 | CYCD2 | *CCND2* | cyclin D2 | NM_001759 | cyclin D2 |
| C10.a5 | CYCD3 | *CCND3* | cyclin D3 | NM_001760 | cyclin D3 |
| C11.a5 | CYCE | *CCNE1* | cyclin E1 | NM_001238 | cyclin E |
| C2.b1 | CHK1 | *CHK1* | checkpoint kinase Chk1 | AF016582 | Chk1 |
| C3.b1 | CHK2 | *CHK2* | checkpoint kinase Chk2 | AF086904 | Chk2 |
| C4.b1 | CDC25A | *CDC25A* | cell division cycle 25A | NM_001789 | Cdc25(A) |
| C5.b1 | CDC25B | *CDC25B* | cell division cycle 25B | NM_021874 | Cdc25(B) |
| C6.b1 | KU70 | *XRCC6* | thyroid autoantigen 70kD (Ku antigen) | NM_001469 | Ku70 |
| C7.b1 | KU80 | *XRCC5* | Ku autoantigen, 80kDa | NM_021141 | Ku80 |
| C8.b1 | DNAPKC | *PRKDC* | DNA-dependent protein kinase catalytic subunit | U47077 | DNA-PKcs (p350) |
| C9.b1 | LIG IV | *LIG4* | DNA ligase IV | X83441 | DNA ligase IV |
| C10.b1 | XRCC4 | *XRCC4* | DNA-repair protein XRCC4 | NM_022550 | XRCC4 |
| C11.b1 | RPA1 | *RPA1* | replication protein A1, 70kDa | NM_002945 | replication protein A1 |
| C2.b5 | ATM | *ATM* | ataxia telangiectasia mutated | U33841 | ATM |
| C3.b5 | GATA4 | *GATA4* | GATA binding protein 4 | NM_002052 | GATA4 |
| C4.b5 | FGFR4 | *FGFR4* | fibroblast growth factor receptor 4 | NM_002011 | FGFR4 |
| C5.b5 | GAPDH | *GAPDH* | glyceraldehyde-3-phosphate dehydrogenase | AF261085 | GAPDH |
| C6.b5 | M1 | *CHRM1* | cholinergic receptor, muscarinic 1 | AF385587 | cholinergic receptor M1 |
| C7.b5 | M2 | *CHRM2* | cholinergic receptor, muscarinic 2 | AF385588 | cholinergic receptor M2 |
| C8.b5 | M3 | *CHRM3* | cholinergic receptor, muscarinic 3 | NM_000740 | cholinergic receptor M3 |
| C9.b5 | M4 | *CHRM4* | cholinergic receptor, muscarinic 4 | AF385590 | cholinergic receptor M4 |
| C10.b5 | M5 | *CHRM5* | cholinergic receptor, muscarinic 5 | NM_012125 | cholinergic receptor M5 |
| C2.c1 | ERB2 | *HER2* | v-erb-b2 erythroblastic leukemia viral oncogene homolog 2 | M11730 | erb-b2 |
| C3.c1 | CD14 | *CD14* | CD14 antigen | M86511 | CD14 |
| C4.c1 | CLDN1 | *CLDN1* | claudin 1 | NM_021101 | claudin 1 |
| C5.c1 | CA12 | *CA12* | carbonic anhydrase XII | AF037335 | carbonic anhydrase 12 |

[a] The position of each gene on the chip. [b] Code used to identify gene on the plate template (Appendix II, C).

[c] Name of the functional protein product of each gene on the chip.

**Appendix II, B cont.**

| Well ID[a] | Chip code[b] | Gene symbol | Gene description | Accession no. | Protein name[c] |
|---|---|---|---|---|---|
| C6.c1 | ASL | *ASL* | argininosuccinate lyase | NM_000048 | argininosuccinate lyase |
| C7.c1 | GLCTN2 | *LGALS2* | galectin 2 | BC029063 | galectin 2 |
| C8.c1 | IGF2 | *IGF2* | insulin-like growth factor 2 (somatomedin A) | NM_000612 | IGF2 |
| C9.c1 | AQP3 | *AQP3* | aquaporin 3 | NM_004925 | aquaporin 3 |
| C10.c1 | COX2 | *PTGS2 / COX2* | prostaglandin-endoperoxide synthase 2 (cyclooxygenase) | M90100 | cox-2 |
| C11.c1 | NKRP1A | *KLRB1* | NKR-P1A | U11276 | hNKR-P1a |
| C2.c5 | hPMS2 | *PMS2* | PMS2 postmeiotic segregation increased 2 | NM_000535 | mutL homolog hPMS2 |
| C3.c5 | SCL7A5 | *SLC7A5* | solute carrier family 7 (cationic amino acid transporter, y+ system), member 5 | NM_003486 | SCL7A5 |
| C4.c5 | PARP | *PARP1* | poly (ADP-ribose) polymerase family, member 1 | NM_001618 | PARP |
| C5.c5 | DRG1 | *DRG1* | developmentally regulated GTP binding protein 1 | AF271994 | DRG-1 |
| C6.c5 | TGIFP | *TGIF* | TGFB-induced factor (TALE family homeobox) | X89750 | TGIF protein |
| C7.c5 | SOD2 | *SOD2* | superoxide dismutase 2, mitochondrial | NM_000636 | SOD2 |
| C8.c5 | COL1A2 | *COL1A2* | collagen, type I, alpha 2 | V00503 | collagen |
| C9.c5 | NET1 | *TSPAN1* | tetraspan NET-1 | AF065388 | tetraspan NET-1 |
| C10.c5 | LITAF | *LITAF* | lipopolysaccharide-induced TNF factor | NM_004862 | TNF alpha / LITAF |
| C11.c5 | ATP2A3 | *ATP2A3* | ATPase, Ca++ transporting, ubiquitous | AF068221 | SERCA3 / ATP2A3 |
| C2.d1 | GLCTN4 | *LGALS4* | galectin 4 | NM_006149 | galectin 4 |
| C3.d1 | PIK3CG | *PIK3CG* | phosphoinositide-3-kinase, catalytic, gamma polypeptide | NM_002649 | PIK3CG |
| C4.d1 | GSA | *GNAL* | G-s-alpha / guanine nucleotide binding protein (G protein) | AH002748 | G-s-alpha |
| C5.d1 | STAT1 | *STAT1* | signal transducer and activator of transcription 1, 91kDa | NM_007315 | STAT 1 |
| C6.d1 | E2F4 | *E2F4* | E2F transcription factor 4, p107/p130-binding | NM_001950 | E2F-4 |
| C7.d1 | IgGR | *FCGR2B* | IGFR2 / Fc fragment of IgG, low affinity IIb, receptor | J04162 | leucocyte IgG receptor |
| C8.d1 | TRAILR | *TNFRSF10A / TRAIL* | tumor necrosis factor receptor superfamily, member 10a | U90875 | TRAIL receptor |
| C9.d1 | IFBP | *FABP2* | fatty acid binding protein 2, intestinal | M18079 | IFBP |
| C10.d1 | MSH2 | *MSH2* | mutS homolog 2, colon cancer, nonpolyposis type 1 (E. coli) | NM_000251 | MSH2 |
| C11.d1 | DLEU1 | *DLEU1* | deleted in lymphocytic leukemia, 1 | NM_005887 | DLEU1 |
| C2.d5 | GROB | *CXCL2* | GRO-beta / chemokine (C-X-C motif) ligand 2 | M36820 | GRO-beta |
| C3.d5 | CFL | *CFL1* | cofilin 1 (non-muscle) | D00682 | cofilin |

[a] The position of each gene on the chip. [b] Code used to identify gene on the plate template (Appendix II, C).

[c] Name of the functional protein product of each gene on the chip.

**Appendix II, B cont.**

| Well ID[a] | Chip code[b] | Gene symbol | Gene description | Accession no. | Protein name[c] |
|---|---|---|---|---|---|
| C4.d5 | RBBP4 | *RBBP4* | retinoblastoma binding protein 4 | NM_005610 | RBBP4 |
| C5.d5 | GPX2 | *GPX2* | glutathione peroxidase 2 (gastrointestinal) | AF199441 | GPX2 |
| C6.d5 | G0S8 | *RGS2* | Regulator of G-protein signaling 2 (G0/G1 switch regulatory protein 8) | L13463 | G0S8 |
| C7.d5 | PFN1 | *PFN1* | profilin 1 | NM_005022 | profilin 1 |
| C8.d5 | P27 | *CDKN1B* | cyclin-dependent kinase inhibitor 1B (p27, Kip1) | NM_004064 | p27, Kip1 |
| C9.d5 | CD13 | *ANPEP* | aminopeptidase N / CD13 | M22324 | CD13 |
| C10.d5 | FASL | *FASLG* | Fas ligand (TNF superfamily, member 6) | D38122 | FasL |
| C11.d5 | GTF3A | *GTF3A* | general transcription factor IIIA | NM_002097 | GTF3A |
| D1.a1 | M | Marker[e] | | | |
| D2.a1 | KLF4 | *KLF4* | Kruppel-like factor 4 (gut) | NM_004235 | Kruppel like factor 4 |
| D3.a1 | MLH1 | *MLH1* | mutL homolog 1, colon cancer, nonpolyposis type 2 (E. coli) | U07343 | MLH1 |
| D4.a1 | LCP1 | *LCP1* | lymphocyte cytosolic protein 1 (L-plastin) | NM_002298 | L-Plastin |
| D5.a1 | CMYB | *MYB* | Myb proto-oncogene protein (C-myb) | M15024 | cMYB |
| D6.a1 | DP2 | *TFDP2* | transcription factor Dp-2 (E2F dimerization partner 2) | NM_006286 | TFDP2 |
| D7.a1 | RALGPS | *RALGPS1* | Ral GEF with PH domain and SH3 binding motif 1 | NM_014636 | RALGPS1 |
| D8.a1 | NAP1 | *NCKAP1 / NAP1* | NCK-associated protein 1 | AB014509 | Nap1 |
| D9.a1 | BAK | *BAK1* | BCL2-antagonist/killer 1 | U23765 | Bak |
| D10.a1 | NSAP1 | *NSAP1 / SYNCRIP* | NS1-associated protein 1 pseudogene | AF155568 | NSAP1 |
| D11.a1 | CASP3 | *CASP3* | caspase 3, apoptosis-related cysteine protease | AY219866 | caspase 3 |
| D12.a1 | M | Marker[e] | | | |
| D2.a5 | PKB | *PTK2B / PKB* | PTK2B protein tyrosine kinase 2 beta | X61037 | protein kinase B |
| D3.a5 | HPG1 | *BGN* | biglycan | J04599 | hPG1, biglycan |
| D4.a5 | EPICAN | *CD44* | CD44 antigen (Heparan sulfate proteoglycan) (Epican) | X66733 | epican |
| D5.a5 | SCF | *SCF / KITLG* | stem cell factor / kit ligand precursor / Mast cell growth factor (MGF) | M59964 | SCF |
| D6.a5 | EIF3S2 | *EIF3S2* | eukaryotic translation initiation factor 3, subunit 2 beta, 36kDa | NM_003757 | P36, EIF3S2 |
| D7.a5 | CEA | *CEACAM3 / CEA* | carcinoembryonic antigen-related cell adhesion molecule 3 | M29540 | CEA |
| D8.a5 | ETS2 | *ETS2* | v-ets erythroblastosis virus E26 oncogene homolog 2 | J04102 | ets-2 |

[a] The position of each gene on the chip. [b] Code used to identify gene on the plate template (Appendix II, C).

[c] Name of the functional protein product of each gene on the chip.

[e] Marker = either GAPDH or β-actin, see well ID A1.a1 and A12.a1 for accession numbers.

**Appendix II, B cont.**

| Well ID[a] | Chip code[b] | Gene symbol | Gene description | Accession no. | Protein name[c] |
|---|---|---|---|---|---|
| D9.a5 | MCM5 | *MCM5* | minichromosome maintenance deficient 5, cell division cycle 46 | NM_006739 | MCM5 |
| D10.a5 | PKCD | *PRKCD* | protein kinase C, delta | NM_006254 | protein kinase C, delta |
| D11.a5 | TIMP1 | *TIMP1* | tissue inhibitor of metalloproteinase 1 | NM_003254 | TIMP1 |
| D2.b1 | OSTNCT | *SPARC* | secreted protein, acidic, cysteine-rich (osteonectin) | J03040 | osteonectin |
| D3.b1 | BIGH3 | *TGFBI / BIGH3* | transforming growth factor, beta-induced, 68kDa | M77349 | TGF beta induced |
| D4.b1 | RHOA | *RHOA* | ras homolog gene family, member A | NM_001664 | RhoA |
| D5.b1 | EPHB1 | *EPHB1* | EPH receptor B1 | NM_004429 | ephrin B1 |
| D6.b1 | MCM3 | *MCM3* | MCM3 minichromosome maintenance deficient 3 (S. cerevisiae) | NM_002388 | MCM3 |
| D7.b1 | TRAIL | *TNFSF10 / TRAIL* | TNF-related apoptosis-inducing ligand | U37518 | TRAIL |
| D8.b1 | PLS3 | *PLS3* | plastin 3 (T isoform) | NM_005032 | T-Plastin |
| D9.b1 | CASP8 | *CASP8* | caspase 8, apoptosis-related cysteine protease | NM_001228 | caspase 8 |
| D10.b1 | BCL3 | *BCL3* | B-cell CLL/lymphoma 3 | NM_005178 | bcl-3 |
| D11.b1 | AGP1 | *ORM1* | Alpha-1-acid glycoprotein 1 precursor (AGP 1) (Orosomucoid 1) (OMD 1) | X02544 | alpha-1-acid glycoprotein 1 |
| D2.b5 | UNG | *UNG* | uracil-DNA glycosylase | Y09008 | uracil DNA glycosylase |
| D3.b5 | CA2 | *CA2* | carbonic anhydrase II | NM_000067 | carbonic anhydrase 2 |
| D4.b5 | OSTPNT | *SPP1* | secreted phosphoprotein 1 (osteopontin) | J04765 | osteopontin |
| D5.b5 | MCT1 | *SLC16A1* | solute carrier family 16 (monocarboxylic acid transporters), member 1 | NM_003051 | MCT1 / SLC16a5 |
| D6.b5 | FABP1 | *FABP1* | fatty acid binding protein 1, liver | BC032801 | FABPL |
| D7.b5 | TEF3 | *TEAD4* | Transcriptional enhancer factor TEF-3 (TEA domain family member 4) | X94438 | TEF-3 |
| D8.b5 | IL3 | *IL3* | interleukin 3 (colony-stimulating factor, multiple) | NM_000588 | interleukin 3 |
| D9.b5 | P21 | *CDKN1A* | cyclin-dependent kinase inhibitor 1A (p21, Cip1) | NM_000389 | p21, Cip1 |
| D10.b5 | ENC1 | *ENC1* | ectodermal-neural cortex (with BTB-like domain) | NM_003633 | ENC1 |
| D11.b5 | VERSCN | *CSPG2* | chondroitin sulfate proteoglycan 2 (versican) | X15998 | versican |
| D2.c1 | FAS | *FAS* | Fas (TNF receptor superfamily, member 6) | X83493 | Fas |
| D3.c1 | VEGF | *VEGF* | vascular endothelial growth factor | NM_003376 | VEGF |
| D4.c1 | MAPK1 | *MAPK1* | mitogen-activated protein kinase 1 | NM_002745 | MAPK1 |
| D5.c1 | USF2 | *USF2* | upstream transcription factor 2, c-fos interacting | NM_003367 | USF2 |
| D6.c1 | KI67 | *MKI67* | antigen identified by monoclonal antibody Ki-67 | NM_002417 | Ki-67 antigen |

[a] The position of each gene on the chip. [b] Code used to identify gene on the plate template (Appendix II, C).

[c] Name of the functional protein product of each gene on the chip.

**Appendix II, B cont.**

| Well ID[a] | Chip code[b] | Gene symbol | Gene description | Accession no. | Protein name[c] |
|---|---|---|---|---|---|
| D7.c1 | IAP1 | *BIRC2* | baculoviral IAP repeat-containing 2 / apoptosis inhibitor 1 | U45878 | cIAP1 |
| D8.c1 | P150 | *CHAF1A* | chromatin assembly factor 1, subunit A (p150) | NM_005483 | p150 |
| D9.c1 | NBS1 | *NSB1* | Nijmegen breakage syndrome 1 (nibrin) | AF058696 | NBS1, p95 |
| D10.c1 | CLDN4 | *CLDN4* | claudin 4 | NM_001305 | claudin 4 |
| D11.c1 | CCR7 | *CCR7* | chemokine (C-C motif) receptor 7 | AB000887 | CCR7, EB1 ligand |
| D2.c5 | PLZF | *ZBTB16* | PLZF / zinc finger and BTB domain containing 16 | AF060568 | PLZF |
| D3.c5 | SURVVN | *BIRC5* | apoptosis inhibitor 4 - survivin | NM_001168 | survivin |
| D4.c5 | HP | *HPSE* | heparanase | AF144325 | heparanase |
| D5.c5 | RANBP7 | *IPO7 / RANBP7* | importin 7 | AF098799 | RANBP7 / importin 7 |
| D6.c5 | A1ATRY | *SERPINA1* | serine proteinase inhibitor, clade A (alpha-1 antiproteinase, antitrypsin), member 1 | X01683 | alpha-1-antitrypsin |
| D7.c5 | MACF1 | *MACF1* | microtubule-actin crosslinking factor 1 | NM_012090 | MACF1 |
| D8.c5 | CAST | *CAST* | calpastatin | D16217 | CAST |
| D9.c5 | PRG3 | *AMID / PRG3* | p53-responsive gene 3 | AF337957 | PRG3 |
| D10.c5 | JPO1 | *JPO1 / LOC442172* | c-Myc target JPO1 | AY029179 | c-myc target protein, JPO1 |
| D11.c5 | MXD3 | *MXD3* | MAX dimerization protein 3 | NM_031300 | MXD3 |
| D2.d1 | MDM2 | *MDM2* | Mdm2, transformed 3T3 cell double minute 2, p53 binding protein (mouse) | AF092844 | MDM2 |
| D3.d1 | REGPI | *REG1B* | regenerating protein I beta | D17291 | regenerating protein I beta |
| D4.d1 | SP1 | *SP1* | Sp1 transcription factor | AF252284 | Sp1 |
| D5.d1 | CIG5 | *RSAD2* | radical S-adenosyl methionine domain containing 2 / cig5 / viperin | AF026941 | cig5 |
| D6.d1 | PLCB2 | *PLCB2* | phospholipase C, beta 2 | NM_004573 | phosholipase C, beta 2 |
| D7.d1 | ALTFBR | *FN1 / FN* | fibronectin, alt splice | X02761 | fibronectin, alt splice |
| D8.d1 | CASP7 | *CASP7* | caspase 7, apoptosis-related cysteine protease | NM_001227 | caspase 7 |
| D9.d1 | NEBL | *NEBL* | nebulette | Y16241 | nebulette |
| D10.d1 | TCOF1 | *TCOF1* | Treacher Collins-Franceschetti syndrome 1 | NM_000356 | TCOF1 |
| D11.d1 | MT1A | *MT1A* | metallothionein 1A (functional) | K01383 | Metallothionein-1-A |
| D2.d5 | MUC2 | *MUC2* | mucin 2, intestinal/tracheal | NM_002457 | mucin 2 |
| D3.d5 | SI | *SI* | sucrase-isomaltase (alpha-glucosidase) | NM_001041 | sucrase isomaltase |
| D4.d5 | CDX2 | *CDX2* | caudal type homeo box transcription factor 2 | AH007259 | cdx2 |

[a] The position of each gene on the chip. [b] Code used to identify gene on the plate template (Appendix II, C).

[c] Name of the functional protein product of each gene on the chip.

**Appendix II, B cont.**

| Well ID[a] | Chip code[b] | Gene symbol | Gene description | Accession no. | Protein name[c] |
|---|---|---|---|---|---|
| D5.d5 | EPHB2 | *EPHB2* | EPH receptor B2 | AF025304 | EPHB2 |
| D6.d5 | BAD | *BAD* | BCL2-antagonist of cell death | AF031523 | BAD |
| D7.d5 | BGP1 | *CEACAM1 / BGP1* | carcinoembryonic antigen-related cell adhesion molecule 1 (biliary glycoprotein) | NM_001712 | BGP1 |
| D8.d5 | XRCC3 | *XRCC3* | X-ray repair complementing defective repair in Chinese hamster cells 3 | AF035586 | XRCC3 |
| D9.d5 | T18 | *T18* | T-18 | AF089811 | T-18 |
| D10.d5 | GLUT1 | *SLC2A1 / GLUT1* | solute carrier family 2 (facilitated glucose transporter), member 1 | AY034633 | GLUT1 |

[a] The position of each gene on the chip. [b] Code used to identify gene on the plate template (Appendix II, C).

[c] Name of the functional protein product of each gene on the chip.

**Appendix II, C**

The plate template shows the position of all genes on the Colorectal Cancer Oligonucleotide Chip.

**Appendix II, C. Plate template for Colorectal Cancer Oligonucleotide Chip. M = marker, either β-actin or GAPDH.**

| | 1 | | 2 | | 3 | | 4 | | 5 | | 6 | | 7 | | 8 | | 9 | | 10 | | 11 | | 12 | |
|---|---|---|---|---|---|---|---|---|---|---|---|---|---|---|---|---|---|---|---|---|---|---|---|---|
| A | GAPDH | ACTA2 | SOX11 | SOX2 | ND1 | GATA4 | SOX8 | EPHA1 | SOX10 | LAMB1 | BRACHY | BMP1 | SNAP25 | GAP43 | FUT2 | PLP | NOTCH2 | FUT1 | MAPT | BMP6 | ASTN | GJA1 | ACTB | NOTCH1 |
| | PAX6 | ND3 | TDGF1 | ANIL | NHLH2 | SYP | TLE2 | NOTCH4 | SOX9 | NOTCH3 | SCG10 | ACTB | TF | FN1 | MAP2 | VTN | REST | NEFL | BMP4 | KRT18 | ND4 | CRIPTO | ND2 | MYOD1 |
| | NSE | HATH1 | NES | MASH2 | SOX4 | SOX17 | SOX3 | FOXE3 | KRT8 | PRPH | NEFM | AIM1 | MYCN | SOD1 | SOX1 | MMP3 | OCT4 | VCL | CLCNKB | PARNMN | ZNF74 | TUBG | MASH1 | HSP70 |
| | HSP90 | DSP | CRYAB | PAK1 | PROX1 | MMP9 | CRYAA | NF2 | SYN | TIAM1 | ACTG1 | MMP14 | HSP27 | ILK | PITX3 | RAC1 | HSP20 | VIL2 | IGF1R | GPC3 | CDC42 | PPL | HSC70 | PLEC1 |
| B | | | HRAS | APC | KRAS | DCC | CSRC | P53 | CABL | RB1 | CMOS | WT1 | CRAF | NF1 | CMYC | NFKB1 | CFOS | ZFP91 | CJUN | RARA | E1A | RXRA | | |
| | RHOC | | 5T4 | PDGF | TCF1 | EGF | TCF3 | FGF | TCF4 | TGFA | OCT4 | TGFB | BCL2 | PDGFR | BCLX | EGFR | TERT | FGFR | MDR1 | TGFR | MDR3 | KRT1 | | |
| | MMP1 | | KRT5 | NEFH | KRT8 | TUBA | KRT10 | TUBB | KRT14 | ACTA | KRT18 | ACTB | KRT19 | B1INT | KRT20 | B3INT | DESMIN | B4INT | VIMNTN | B5INT | GFAP | A1INT | | |
| | FLNA | | A2INT | P120 | A3INT | SYN1 | A5INT | SYN4 | A6INT | LMNNA | AVINT | LMNNB | PAXLIN | COL | ECADHR | ALTFBR | ACATEN | NUP153 | BCATEN | TPR | PLAGBN | B23 | | |
| C | | | RPL31 | CDK2 | RPL21 | CDK4 | RPL19 | CDK6 | LAMA | CYCA | LAMC | CYCB1 | LAMB1 | CYCB2 | LAMB2 | CYCD1 | LAP2A | CYCD2 | LAP2B | CYCD3 | CDK1 | CYCE | | |
| | | | CHK1 | ATM | CHK2 | GATA4 | CDC25A | FGFR4 | CDC25B | GAPDH | KU70 | M1 | KU80 | M2 | DNAPKC | M3 | LIGIV | M4 | XRCC4 | M5 | RPA1 | | | |
| | | | ERB2 | HPMS2 | CD14 | SCL7A5 | CLDN1 | PARP | CA12 | DRG1 | ASL | TGIFP | GLCTN2 | SOD2 | IGF2 | COL1A2 | AQP3 | NET1 | COX2 | LITAF | NKRP1A | ATP2A3 | | |
| | | | GLCTN4 | GROB | PIKC3G | CFL | GSA | RBBP4 | STAT1 | GPX2 | E2F4 | G0S8 | IgGR | PFN1 | TRAILR | P27 | IFBP | CD13 | MSH2 | FASL | DLEU1 | GTF3A | | |
| D | M | | KLF4 | PKB | MLH1 | HPG1 | LCP1 | EPICAN | CMYB | SCF | DP2 | EIF3S2 | RALGPS | CEA | NAP1 | ETS2 | BAK | MCM5 | NSAP1 | PKCD | CASP3 | TIMP1 | M | |
| | | | OSTNCT | UNG | BIGH3 | CA2 | RHOA | OSTPNT | EPHB1 | MCT1 | MCM3 | FABP1 | TRAIL | TEF3 | PLS3 | IL3 | CASP8 | P21 | BCL3 | ENC1 | AGP1 | VERSCN | | |
| | | | FAS | PLZF | VEGF | SURVVN | MAPK1 | HPSE | USF2 | RANBP7 | KI67 | A1ATRY | IAP1 | MACF1 | P150 | CAST | NBS1 | PRG3 | CLDN4 | JPO1 | CCR7 | MXD3 | | |
| | | | MDM2 | MUC2 | REGPI | SI | SP1 | CDX2 | CIG5 | EPHB2 | PLCB2 | BAD | ALTFBR | BGP1 | CASP7 | XRCC3 | NEBL | T18 | TCOF1 | GLUT1 | MT1A | | | |

**Appendix II, D**

The mean fold change ± standard deviation (S.D.) for each gene in each replicate microarray experiment is tabulated here. A mean fold change between -1 and +1 indicates that the degree of hybridization varied between the spots and that the gene was not uniformly up- or down-regulated. Data highlighted in grey corresponds to the genes listed in Chapter 4, Table 4.1 which were at least 1.5 fold up- or down-regulated in test versus control samples. When only mean fold change is given without a S.D., this indicates that there were less that three good spots for a particular gene. X = all four spots bad, therefore gene was excluded from analysis in that particular experiment.

**Appendix II, D. Mean fold change ± S.D. for each gene in each replicate microarray experiment.**

| | LAMIN A vs GFP | | | | | | EMERIN vs GFP | | | | | | LAMIN A vs EMERIN | | | | | |
|---|---|---|---|---|---|---|---|---|---|---|---|---|---|---|---|---|---|---|
| | Replicate 1 | | Replicate 2 | | Replicate 3 | | Replicate 1 | | Replicate 2 | | Replicate 3 | | Replicate 1 | | Replicate 2 | | Replicate 3 | |
| Gene symbol | Mean | ±S.D. | Mean | ±S.D. | Mean | ±S.D. | Mean | ±S.D. | Mean | ±S.D. | Mean | ±S.D. | Mean | ±S.D. | Mean | ±S.D. | Mean | ±S.D. |
| *GAPDH* | 1.06 | 0.036 | 1.07 | 0.024 | 1.40 | 0.133 | 1.44 | 0.078 | 1.52 | 0.035 | 1.29 | 0.042 | 1.96 | | 1.18 | 0.128 | 0.07 | |
| *SOX11* | -0.61 | 1.160 | -1.56 | 0.361 | 1.63 | 0.342 | -1.19 | 0.076 | 1.27 | 0.040 | 0.49 | 1.090 | -1.61 | 0.491 | -1.25 | 0.087 | 1.31 | 0.103 |
| *NEUROD1* | 1.12 | 0.091 | -1.09 | | 0.42 | 1.240 | -1.32 | 0.231 | 1.08 | 0.057 | 1.09 | 0.056 | -0.70 | 1.770 | 1.14 | 0.022 | -0.74 | 1.240 |
| *SOX8* | -0.10 | 1.340 | -1.05 | 0.024 | 1.31 | 0.360 | -0.47 | 1.280 | -0.38 | 1.210 | 0.50 | 1.110 | -0.95 | 1.440 | -0.30 | 1.250 | -0.62 | 1.130 |
| *SOX10* | -1.06 | 0.006 | 0.00 | 1.170 | -1.01 | 0.013 | -1.06 | 0.017 | 0.01 | 1.180 | 0.02 | 1.210 | -1.29 | 0.153 | -1.05 | 0.021 | -1.09 | |
| *T* | 0.02 | 1.550 | -1.73 | 0.228 | 1.39 | 0.320 | -1.59 | 0.148 | 1.23 | 0.042 | 1.21 | 0.037 | 1.46 | 0.180 | -0.33 | 1.210 | -0.63 | 1.450 |
| *SNAP25* | 0.59 | 1.070 | -1.07 | 0.023 | 1.14 | 0.066 | 1.48 | 0.058 | -0.36 | 1.210 | 1.12 | 0.032 | -0.17 | 1.540 | 0.54 | 1.090 | -1.15 | 0.139 |
| *FUT2* | -1.13 | 0.111 | -0.52 | 1.070 | 1.27 | 0.046 | 1.10 | 0.075 | -1.05 | 0.036 | 1.16 | 0.039 | -2.44 | 0.165 | 0.03 | 1.210 | -1.28 | 0.075 |
| *NOTCH2* | X | X | -1.28 | 0.106 | 1.25 | 0.264 | -1.24 | 0.122 | 1.25 | 0.093 | 1.24 | 0.091 | 2.08 | 0.205 | -0.26 | 1.320 | -2.25 | 0.414 |
| *MAPT / TAU* | -1.46 | 0.280 | -1.47 | 0.170 | 1.23 | 0.024 | -1.60 | 0.525 | 7.57 | 5.370 | 0.09 | 1.310 | 2.57 | | -0.56 | 1.070 | -1.38 | 0.080 |
| *ASTN* | -0.87 | 2.200 | -2.99 | 0.529 | 0.41 | 1.260 | -7.18 | 2.840 | X | X | -3.13 | | 2.91 | 0.577 | 0.58 | 1.250 | -2.07 | 0.070 |
| *ACTB* | -1.09 | 0.081 | -0.05 | | -0.52 | 1.030 | 1.43 | 0.052 | 0.01 | 1.190 | 1.16 | 0.070 | -1.29 | 0.201 | -1.04 | 0.030 | 1.22 | 0.171 |
| *ACTA2* | -1.12 | 0.022 | -0.35 | 1.230 | 1.04 | 0.021 | -0.52 | 1.050 | 1.11 | 0.062 | 1.03 | 0.019 | 0.40 | 1.470 | 1.09 | 0.107 | -0.72 | 1.350 |
| *SOX2* | 1.12 | 0.057 | -0.41 | 1.230 | 1.74 | 0.109 | -1.10 | 0.068 | 1.35 | 0.033 | 1.31 | 0.097 | -1.22 | | 1.17 | 0.081 | 1.48 | 0.025 |
| *GATA4* | -1.10 | 0.031 | 1.15 | 0.061 | 1.40 | 0.057 | 1.21 | 0.014 | 1.13 | 0.035 | 1.15 | 0.021 | 0.94 | 1.470 | 1.26 | 0.019 | 1.40 | 0.083 |
| *EPHA1* | 1.27 | 0.290 | -94.10 | 165.000 | 2.93 | 1.710 | -13.80 | 9.570 | 4.86 | 2.320 | 0.61 | 1.470 | 1.52 | 0.329 | 1.35 | | -0.53 | 1.350 |
| *LAMB1* | 1.48 | 0.371 | 13.20 | 2.130 | 2.58 | 0.869 | -3.14 | 0.265 | 2.41 | 0.189 | 2.13 | 1.040 | 1.89 | 0.243 | -1.49 | 0.631 | -3.16 | 0.894 |
| *BMP1* | -1.43 | 0.340 | -0.82 | 1.300 | 1.11 | 0.073 | 1.32 | 0.086 | 1.06 | 0.025 | 0.58 | 1.070 | 1.43 | 0.067 | 1.10 | 0.025 | -1.10 | 0.119 |
| *GAP43* | -1.23 | 0.132 | 0.04 | 1.280 | 1.09 | 0.044 | 1.64 | 0.059 | 0.30 | 1.260 | 1.10 | 0.037 | 1.07 | | 0.02 | 1.210 | -1.26 | 0.172 |
| *PLP* | 0.03 | 1.310 | -0.33 | 1.200 | 1.49 | 0.045 | 1.59 | | 1.35 | 0.129 | 1.28 | | -1.19 | 0.101 | 1.15 | 0.066 | 1.79 | 0.133 |
| *FUT1* | -1.14 | 0.038 | -0.03 | | 1.55 | | 1.75 | 0.125 | 1.10 | | 1.21 | 0.070 | 1.73 | 0.553 | 1.20 | 0.041 | 1.17 | 0.131 |
| *BMP6* | -0.59 | 1.240 | -1.27 | 0.140 | 1.27 | 0.134 | 1.27 | 0.040 | 1.38 | 0.182 | -0.61 | 1.120 | 1.98 | 0.420 | 0.54 | 1.040 | 0.57 | 1.090 |
| *GJA1* | -1.13 | 0.015 | -0.53 | 1.020 | -1.02 | 0.010 | 1.65 | 0.019 | -0.37 | 1.220 | 1.22 | | -1.20 | 0.166 | -0.35 | 1.200 | 1.40 | 0.148 |
| *NOTCH1* | -1.05 | 0.014 | X | X | 0.33 | 1.160 | -1.08 | 0.008 | -1.05 | 0.021 | 1.02 | 0.026 | -1.16 | | -1.05 | 0.012 | -1.07 | |
| *PAX6* | 1.17 | | -1.75 | 0.236 | 2.33 | 0.196 | -3.58 | 0.585 | 6.64 | 3.560 | 1.87 | 0.593 | 18..38 | | 1.41 | 0.151 | 1.31 | 0.210 |
| *TDGF1* | -0.04 | | -11.84 | | 29.90 | | -29.10 | 16.600 | 3.33 | 0.550 | -0.72 | 1.300 | 1.83 | 0.566 | 2.06 | 0.671 | 0.82 | 1.240 |
| *NHLH2* | 0.36 | 1.270 | -1.89 | | 2.51 | 0.188 | -1.32 | 0.127 | 1.31 | 0.145 | 1.07 | 0.031 | -1.26 | | 1.26 | 0.038 | 1.08 | 0.061 |

**Appendix II, D cont.**

| | LAMIN A vs GFP | | | | | | EMERIN vs GFP | | | | | | LAMIN A vs EMERIN | | | | | |
|---|---|---|---|---|---|---|---|---|---|---|---|---|---|---|---|---|---|---|
| | Replicate 1 | | Replicate 2 | | Replicate 3 | | Replicate 1 | | Replicate 2 | | Replicate 3 | | Replicate 1 | | Replicate 2 | | Replicate 3 | |
| Gene symbol | Mean | ±S.D. | Mean | ±S.D. | Mean | ±S.D. | Mean | ±S.D. | Mean | ±S.D. | Mean | ±S.D. | Mean | ±S.D. | Mean | ±S.D. | Mean | ±S.D. |
| *TLE2* | 0.05 | 1.280 | 1.08 | 0.079 | 1.40 | 0.096 | 1.11 | 0.032 | 1.10 | 0.049 | 1.07 | 0.013 | -0.65 | 1.230 | 1.26 | 0.038 | 1.42 | 0.057 |
| *SOX9* | 0.00 | 1.240 | -1.15 | 0.054 | 1.32 | 0.167 | -1.16 | 0.049 | -0.35 | 1.210 | 1.04 | 0.029 | -1.44 | | 1.16 | 0.120 | 1.20 | 0.079 |
| *SCG10* | -1.35 | 0.080 | -0.06 | 1.280 | -1.16 | 0.050 | 1.23 | 0.042 | -0.36 | 1.200 | -0.57 | 1.050 | 1.39 | 0.115 | 1.15 | | -1.48 | |
| *TF* | -1.18 | 0.123 | 0.51 | 1.260 | -0.04 | 1.270 | 1.12 | 0.040 | 1.17 | 0.006 | 0.54 | 1.050 | 1.56 | 0.235 | 1.34 | 0.040 | -1.56 | 0.188 |
| *MAP2* | -1.11 | 0.042 | -1.06 | 0.030 | -1.03 | 0.026 | 1.15 | 0.006 | -1.08 | 0.029 | -1.05 | 0.028 | 1.19 | 0.106 | -0.02 | | 1.13 | 0.050 |
| *REST* | 1.61 | 0.095 | 1.12 | 0.039 | 2.69 | 0.160 | 1.15 | 0.054 | 1.84 | 0.079 | 1.66 | 0.293 | 2.27 | 0.178 | 1.27 | 0.204 | 1.95 | 0.236 |
| *BMP4* | -1.09 | 0.010 | -0.51 | 1.030 | -0.52 | 1.020 | 1.58 | 0.087 | 1.11 | 0.036 | 0.35 | 1.170 | 1.38 | 0.085 | 0.54 | 1.080 | 1.23 | 0.075 |
| *NEUROD4* | -1.75 | 0.172 | -1.16 | 0.172 | 1.20 | 0.095 | -3.56 | 0.759 | -0.35 | 1.200 | -0.40 | 1.230 | -0.32 | 1.410 | 1.33 | 0.084 | -1.47 | 0.146 |
| *NEUROD2* | 1.09 | | 0.02 | | 1.14 | 0.048 | -1.64 | 0.406 | -1.36 | 0.113 | 1.19 | 0.042 | 0.54 | 1.110 | 1.25 | 0.031 | 0.05 | |
| *NEUROD3* | 1.20 | 0.040 | -2.41 | | 1.30 | | -1.83 | 0.115 | 2.58 | 0.211 | -0.53 | 1.050 | 1.65 | 0.651 | 1.33 | 0.050 | -2.84 | |
| *ANIL* | -1.15 | 0.079 | -2.66 | 0.255 | 0.68 | 1.660 | -4.33 | 1.150 | X | X | -1.09 | 0.102 | 0.72 | 1.480 | 1.30 | 0.050 | -1.44 | 0.209 |
| *SYP* | -1.09 | 0.075 | 1.12 | 0.017 | 1.43 | 0.061 | 1.18 | 0.015 | 1.12 | 0.071 | 0.00 | 1.190 | 1.52 | 0.043 | 1.25 | 0.024 | 1.24 | 0.076 |
| *NOTCH4* | -0.54 | 1.070 | -1.24 | 0.138 | 1.25 | 0.096 | -1.32 | 0.101 | -0.05 | 1.220 | -0.52 | 1.010 | -0.06 | 1.510 | 1.11 | 0.035 | 0.01 | |
| *NOTCH3* | 0.01 | 1.290 | -0.59 | 1.090 | 1.34 | 0.148 | -1.18 | 0.032 | 1.08 | 0.044 | -0.54 | 1.050 | 1.46 | 0.200 | 1.13 | 0.067 | -1.46 | 0.323 |
| *ACTB* | -1.58 | | -1.28 | 0.110 | -1.15 | 0.080 | 0.58 | 1.060 | -1.01 | 0.012 | 0.02 | 1.230 | 1.43 | 0.167 | -1.05 | 0.045 | -1.95 | 0.197 |
| *FN1* | 1.22 | 0.067 | -3.32 | 0.501 | -0.56 | 1.480 | -3.63 | 0.947 | 1.86 | | 0.03 | 1.220 | 1.59 | 0.270 | -1.12 | 0.140 | -5.42 | 0.804 |
| *VTN* | 0.36 | 1.180 | 1.02 | 0.010 | 1.19 | 0.104 | 1.77 | 0.040 | 1.49 | 0.150 | 1.26 | 0.136 | 0.01 | 1.330 | 1.31 | 0.062 | 1.97 | 0.412 |
| *NEFL* | -1.06 | 0.042 | 0.57 | 1.050 | 0.03 | | 1.69 | 0.048 | -1.06 | | -1.13 | 0.073 | 0.04 | 1.250 | -0.32 | 1.380 | 0.56 | 1.080 |
| *KRT18* | 1.32 | 0.036 | 1.04 | 0.005 | 1.27 | 0.099 | 1.35 | 0.037 | 1.40 | 0.040 | 1.48 | | 1.49 | 0.297 | 1.22 | 0.154 | 1.94 | 0.033 |
| *CRIPTO* | -1.45 | 0.275 | -1.28 | 0.156 | 1.20 | 0.114 | -1.83 | 0.328 | 0.34 | 1.260 | 1.07 | | -0.52 | 1.420 | 1.25 | 0.096 | -1.25 | 0.100 |
| *MYOD1* | -1.15 | | X | X | -1.07 | | 1.19 | 0.176 | -1.58 | 0.286 | 1.05 | 0.026 | -1.64 | | 1.20 | 0.065 | -1.32 | 0.312 |
| *NSE* | 1.27 | 0.142 | -2.45 | | 1.30 | 0.240 | -1.52 | 0.015 | 1.68 | | -1.24 | 0.159 | 2.38 | | -0.10 | 2.580 | 0.56 | 1.100 |
| *NES* | -1.24 | 0.117 | -1.95 | 0.048 | 1.13 | 0.173 | -3.09 | 1.270 | 1.20 | 0.069 | -1.42 | 0.162 | 0.13 | 1.860 | 1.25 | 0.033 | -1.18 | 0.023 |
| *SOX4* | -1.14 | 0.018 | -0.55 | 1.050 | 1.06 | 0.058 | -0.03 | 1.200 | 0.37 | 1.240 | 0.02 | 1.220 | 1.26 | 0.172 | 1.31 | 0.056 | 1.07 | 0.057 |
| *SOX3* | -1.04 | 0.014 | -0.52 | 1.020 | 1.26 | 0.133 | -0.02 | 1.180 | 0.03 | 1.200 | 0.04 | 1.220 | 1.36 | 0.131 | -1.04 | 0.025 | -1.04 | 0.032 |
| *KRT8* | -1.09 | 0.008 | -1.02 | 0.010 | -1.05 | 0.005 | -1.11 | 0.022 | -1.08 | | -1.06 | 0.010 | 0.00 | 1.380 | -1.07 | | -1.06 | 0.016 |
| *NEFM* | -1.12 | 0.061 | -1.79 | 0.092 | 1.31 | 0.126 | -3.48 | 0.567 | 0.52 | 1.020 | -0.54 | 1.100 | 0.26 | | 1.05 | 0.035 | -2.11 | 0.210 |
| *MYCN* | -1.28 | 0.215 | -2.90 | 0.551 | -0.15 | 2.080 | -63.04 | | -0.12 | 1.350 | -1.45 | 0.101 | 2.97 | 1.430 | 0.55 | 1.040 | -4.38 | 1.810 |
| *SOX1* | -1.09 | | 0.26 | 1.490 | 1.04 | 0.021 | 0.52 | 1.060 | 0.52 | 1.040 | -0.41 | 1.260 | 0.36 | 1.220 | 0.59 | 1.090 | -1.55 | 0.106 |

**Appendix II, D cont.**

| | LAMIN A vs GFP | | | | | | EMERIN vs GFP | | | | | | LAMIN A vs EMERIN | | | | | |
|---|---|---|---|---|---|---|---|---|---|---|---|---|---|---|---|---|---|---|
| | Replicate 1 | | Replicate 2 | | Replicate 3 | | Replicate 1 | | Replicate 2 | | Replicate 3 | | Replicate 1 | | Replicate 2 | | Replicate 3 | |
| Gene symbol | Mean | ±S.D. | Mean | ±S.D. | Mean | ±S.D. | Mean | ±S.D. | Mean | ±S.D. | Mean | ±S.D. | Mean | ±S.D. | Mean | ±S.D. | Mean | ±S.D. |
| *POU5F1* | -1.16 | 0.113 | -1.20 | 0.079 | 1.27 | 0.052 | -1.18 | 0.065 | 1.24 | 0.148 | 0.03 | 1.210 | -0.56 | 1.160 | 1.24 | 0.055 | -1.39 | 0.121 |
| *CLCNKB* | 1.29 | 0.065 | 0.52 | 1.030 | -0.51 | 1.030 | 1.75 | 0.072 | 0.60 | 1.080 | 1.02 | 0.018 | 1.26 | 0.042 | 1.13 | | 0.86 | 1.290 |
| *ZNF74* | -1.07 | 0.015 | -1.03 | 0.029 | -1.08 | 0.033 | 1.23 | 0.124 | -1.07 | 0.029 | 0.53 | 1.050 | -0.76 | 1.340 | -1.04 | 0.021 | 1.22 | 0.085 |
| *MASH1* | 1.29 | 0.063 | -0.01 | | 0.63 | 1.090 | 1.24 | 0.119 | -1.22 | 0.104 | 1.18 | 0.091 | 1.53 | | 1.28 | 0.021 | 1.71 | 0.137 |
| *HATH1* | 1.40 | 0.252 | -18.30 | 26.800 | 1.61 | 2.280 | -3.61 | | 6.31 | | -0.60 | 1.090 | 1.56 | 1.780 | 2.34 | 0.948 | 0.37 | 1.200 |
| *MASH2* | 0.55 | 1.050 | -8.37 | 4.760 | 1.54 | 0.443 | -2.59 | 0.280 | 1.25 | 0.097 | -0.62 | 1.090 | 1.77 | 0.020 | 1.29 | 0.049 | 1.28 | 0.239 |
| *SOX17* | -1.15 | 0.079 | 0.52 | 1.050 | 1.09 | 0.061 | -1.20 | 0.078 | 1.16 | 0.070 | -1.10 | 0.043 | 1.51 | 0.087 | 1.20 | 0.050 | 1.08 | 0.049 |
| *FOXE3* | -1.08 | 0.014 | -1.04 | 0.045 | -1.04 | 0.021 | -1.14 | 0.008 | -1.04 | 0.005 | -1.03 | 0.010 | -1.42 | 0.097 | -1.02 | 0.019 | -1.09 | |
| *PRPH* | -1.13 | 0.035 | -0.51 | 1.010 | -0.53 | 1.020 | -1.14 | 0.021 | -1.06 | 0.024 | -1.11 | 0.022 | 0.52 | 1.030 | 0.34 | 1.170 | -0.55 | 1.080 |
| *AIM1* | -0.36 | 1.290 | -2.40 | 0.863 | -1.81 | 0.833 | -1.40 | 0.120 | 0.00 | 1.280 | -1.28 | 0.057 | -2.01 | 0.883 | 1.16 | 0.232 | -1.93 | 0.532 |
| *SOD1* | -0.49 | 1.340 | 1.04 | 0.040 | 0.02 | 1.310 | 1.33 | 0.070 | -1.04 | 0.031 | 0.01 | 1.200 | 1.56 | 0.131 | 1.25 | 0.087 | 1.09 | 0.117 |
| *MMP3* | -1.10 | | -0.54 | 1.060 | 1.15 | 0.095 | 1.51 | 0.083 | -0.52 | 1.030 | 0.35 | 1.190 | -1.55 | 0.478 | -0.54 | 1.030 | 1.08 | |
| *VCL* | 1.37 | 0.076 | 0.57 | 1.050 | 1.09 | 0.045 | 1.70 | 0.062 | 0.37 | 1.230 | 0.56 | 1.060 | -1.31 | 0.237 | 1.43 | 0.066 | -0.46 | 1.120 |
| *paranemin* | -1.47 | 0.165 | -1.56 | 0.176 | -1.96 | 0.852 | -3.84 | 0.913 | -1.58 | 0.332 | -1.56 | 0.219 | 1.67 | | 1.30 | 0.082 | -3.40 | 0.770 |
| *TUBG* | 0.54 | 1.080 | 0.55 | 1.060 | -1.09 | 0.017 | 1.50 | 0.060 | 1.21 | 0.176 | 0.01 | 1.190 | -3.13 | 0.871 | 0.03 | | 0.35 | 1.280 |
| *HSP70-1* | -1.08 | 0.024 | X | X | -1.04 | | -1.08 | 0.018 | -1.11 | 0.028 | -1.06 | 0.015 | -1.50 | 0.436 | -1.31 | 0.327 | -0.53 | 1.030 |
| *HSPCA* | -1.09 | 0.047 | 0.51 | 1.040 | 1.18 | 0.134 | 1.40 | | 1.45 | 0.061 | 1.08 | | 1.34 | 0.115 | 1.37 | 0.040 | -0.41 | 1.240 |
| *CRYAB* | -1.08 | 0.010 | -1.02 | 0.023 | -1.04 | 0.024 | 1.06 | 0.040 | -1.05 | 0.008 | -1.04 | 0.022 | -0.63 | 1.140 | -1.03 | | -0.53 | 1.040 |
| *PROX1* | -0.53 | 1.060 | -1.73 | 0.275 | -0.53 | 1.080 | -1.90 | 0.110 | -0.58 | 1.070 | -1.35 | 0.104 | 0.57 | 1.580 | 1.25 | 0.054 | -0.58 | 1.150 |
| *CRYAA* | -1.05 | 0.019 | -1.03 | 0.025 | -0.52 | 1.020 | -1.06 | 0.046 | -1.10 | 0.022 | -1.15 | 0.057 | -2.02 | 0.217 | -0.51 | 1.050 | -1.09 | 0.022 |
| *SYN* | -1.46 | 0.055 | -2.12 | 0.121 | -1.56 | 0.444 | -14.90 | 4.780 | -1.95 | 0.476 | -1.61 | 0.212 | -1.60 | 0.313 | -0.53 | 1.350 | -1.60 | 0.321 |
| *ACTG1* | -1.51 | 0.052 | -0.49 | 1.060 | -1.20 | 0.061 | 1.07 | 0.059 | -1.07 | 0.032 | -1.21 | 0.029 | -0.05 | | -1.04 | 0.035 | -1.20 | 0.076 |
| *HSPB2* | 1.33 | 0.247 | -1.17 | | 1.54 | 0.038 | 1.06 | 0.064 | 1.25 | 0.012 | 0.63 | 1.090 | 1.21 | 0.086 | 1.05 | 0.056 | -1.10 | 0.029 |
| *PITX3* | -1.08 | 0.025 | -1.06 | 0.015 | -0.01 | 1.200 | -0.35 | 1.180 | -1.06 | 0.033 | -1.06 | 0.025 | 1.36 | 0.076 | -1.10 | 0.017 | -1.15 | 0.010 |
| *hsp 20* | -0.04 | | -1.28 | 0.136 | -0.55 | 1.070 | -1.37 | 0.168 | -1.13 | 0.066 | -1.18 | 0.052 | 1.35 | 0.042 | 0.52 | 1.040 | -1.72 | 0.414 |
| *IGF1R* | -1.03 | 0.022 | -0.35 | 1.170 | 0.00 | 1.180 | 1.42 | 0.046 | 0.07 | 1.280 | 0.01 | 1.200 | 1.18 | 0.066 | -1.04 | 0.038 | 0.63 | 1.110 |
| *CDC42* | -0.52 | 1.040 | -1.05 | 0.028 | -1.04 | 0.024 | 1.18 | 0.036 | -1.06 | 0.030 | 0.41 | 1.250 | -1.43 | 0.386 | -1.06 | 0.021 | 1.11 | 0.070 |
| *HSPA8 / HSC70* | -1.19 | 0.105 | -1.06 | | -1.23 | 0.075 | 1.53 | 0.095 | -1.60 | 0.054 | -1.04 | 0.015 | -0.66 | 1.550 | 1.05 | 0.025 | 0.35 | 1.230 |
| *DSP* | 1.05 | 0.053 | -1.24 | 0.196 | -1.24 | 0.180 | -0.04 | 1.230 | 1.26 | 0.082 | -1.10 | 0.070 | -0.90 | 1.360 | 1.25 | 0.077 | -0.40 | 1.220 |

**Appendix II, D cont.**

| | LAMIN A vs GFP | | | | | | EMERIN vs GFP | | | | | | LAMIN A vs EMERIN | | | | | |
|---|---|---|---|---|---|---|---|---|---|---|---|---|---|---|---|---|---|---|
| | Replicate 1 | | Replicate 2 | | Replicate 3 | | Replicate 1 | | Replicate 2 | | Replicate 3 | | Replicate 1 | | Replicate 2 | | Replicate 3 | |
| Gene symbol | Mean | ±S.D. | Mean | ±S.D. | Mean | ±S.D. | Mean | ±S.D. | Mean | ±S.D. | Mean | ±S.D. | Mean | ±S.D. | Mean | ±S.D. | Mean | ±S.D. |
| *PAK1* | -1.05 | 0.024 | -1.03 | 0.021 | 1.23 | 0.050 | -0.01 | 1.260 | -0.52 | 1.010 | 0.01 | 1.180 | 1.41 | 0.363 | 0.00 | 1.170 | 1.14 | 0.055 |
| *MMP9* | -1.22 | 0.059 | -0.02 | 1.200 | -1.43 | 0.270 | -1.38 | 0.103 | -1.05 | 0.030 | -1.24 | 0.143 | 1.22 | | 1.06 | 0.047 | -1.32 | 0.006 |
| *NF2* | -1.05 | 0.055 | -0.57 | 1.060 | -1.22 | 0.149 | -1.25 | 0.033 | -1.08 | 0.021 | -1.17 | 0.022 | -1.38 | 1.920 | 1.23 | 0.018 | -1.21 | |
| *TIAM1* | -1.25 | 0.101 | 1.14 | 0.032 | -0.57 | 1.050 | 1.04 | 0.008 | -1.03 | 0.017 | -1.14 | 0.022 | -2.23 | 0.506 | X | X | -1.22 | 0.111 |
| *MMP14* | 0.52 | 1.020 | -1.17 | 0.066 | -1.15 | 0.008 | -1.50 | 0.086 | -1.10 | 0.024 | -1.31 | 0.084 | -1.72 | 0.362 | 0.06 | 1.240 | -1.49 | 0.081 |
| *ILK* | -1.22 | 0.104 | -1.22 | 0.110 | -1.17 | 0.038 | -1.21 | | -0.60 | 1.060 | -1.26 | 0.092 | -1.34 | | 1.10 | 0.100 | -1.38 | 0.125 |
| *RAC1* | -0.55 | 1.100 | -1.16 | 0.076 | 1.34 | 0.117 | 0.55 | 1.040 | 1.22 | 0.119 | -1.35 | 0.373 | 1.61 | 0.046 | 1.12 | | 1.05 | 0.067 |
| *VIL2* | 1.19 | | -1.05 | 0.022 | -0.35 | 1.180 | -2.78 | 0.555 | 0.52 | 1.050 | -0.02 | 1.210 | 1.48 | 0.137 | 1.27 | 0.056 | -0.01 | 1.230 |
| *GPC3* | -1.21 | 0.104 | 1.16 | | 1.05 | 0.022 | -1.75 | 0.089 | 0.55 | 1.110 | -1.26 | 0.130 | -2.25 | 0.902 | 1.40 | 0.096 | -0.58 | 1.080 |
| *PPL* | -1.43 | | -1.16 | 0.223 | -1.17 | 0.073 | -1.32 | 0.172 | -1.52 | 0.264 | -1.18 | 0.135 | -2.93 | 1.400 | 1.08 | 0.017 | -1.23 | 0.091 |
| *PLEC1* | -1.24 | 0.108 | X | X | -1.10 | | 1.42 | 0.072 | -1.27 | 0.019 | -1.15 | 0.021 | -1.26 | | -0.50 | 1.310 | 0.35 | 1.210 |
| *HRAS* | -0.54 | 1.030 | -0.54 | 1.060 | 1.19 | 0.045 | 1.23 | 0.079 | 1.26 | 0.069 | 0.52 | 1.010 | 1.66 | 0.285 | 1.27 | 0.029 | 1.16 | 0.111 |
| *KRAS* | X | X | -1.76 | 0.275 | 1.13 | 0.106 | -13.60 | 7.060 | -1.09 | 0.085 | -0.53 | 1.140 | -1.53 | 0.144 | -1.24 | 0.067 | -0.14 | 1.460 |
| *SRC* | 0.45 | 1.360 | -1.37 | 0.131 | -0.03 | 1.340 | 10.10 | 4.170 | -1.34 | | -1.05 | 0.010 | 0.34 | 1.970 | -1.76 | 0.441 | -1.46 | 0.282 |
| *ABL1* | 0.65 | 1.120 | -1.08 | 0.041 | -1.34 | 0.136 | -3.00 | 0.340 | -1.34 | 0.149 | -1.06 | 0.036 | 1.45 | 0.154 | -0.39 | 1.330 | -0.14 | |
| *MOS* | 1.33 | 0.105 | -0.56 | 1.040 | 1.55 | 0.057 | 0.53 | 1.120 | 1.12 | 0.066 | -0.40 | 1.230 | -1.40 | 0.135 | 1.08 | | -1.08 | 0.012 |
| *RAF1* | 1.53 | 0.400 | -1.43 | 0.154 | -0.97 | 1.530 | -12.20 | 5.190 | -1.69 | 0.395 | -1.34 | 0.133 | -1.86 | 0.620 | -2.02 | 0.558 | -2.00 | 0.222 |
| *MYC* | -1.78 | 0.248 | -1.95 | 0.121 | 0.54 | 1.180 | -2.16 | 0.428 | -1.69 | 0.100 | -1.23 | 0.123 | -1.63 | 0.191 | -3.65 | 1.420 | -1.23 | 0.028 |
| *FOS* | 1.04 | 0.014 | -1.01 | | 1.07 | 0.032 | -1.03 | 0.024 | 0.52 | 1.030 | -0.53 | 1.030 | -1.31 | 0.055 | 0.00 | 1.210 | 0.30 | 1.240 |
| *JUN* | -1.26 | 0.007 | -1.05 | 0.015 | -1.75 | 0.264 | -1.31 | 0.223 | -1.42 | 0.254 | -1.06 | 0.026 | -1.92 | 0.185 | 0.02 | 1.320 | -1.78 | 0.131 |
| *EP300* | -1.08 | 0.096 | 0.52 | 1.050 | -0.01 | 1.180 | -1.08 | 0.030 | 0.34 | 1.170 | -1.02 | 0.006 | -1.33 | | 0.34 | 1.160 | -0.02 | |
| *APC* | -1.24 | 0.173 | -1.33 | 0.079 | -0.03 | 1.580 | -2.24 | 0.621 | -0.61 | 1.210 | 0.52 | 1.070 | 1.75 | 0.476 | -1.33 | 0.216 | -1.28 | 0.166 |
| *DCC* | -1.13 | 0.023 | 0.52 | 1.080 | -1.19 | 0.057 | -1.33 | 0.069 | -1.17 | 0.044 | -1.17 | 0.018 | -3.72 | 0.675 | 1.04 | 0.017 | -1.33 | 0.060 |
| *TP53* | 1.36 | 0.100 | -0.11 | | 0.58 | 1.120 | -2.02 | 0.378 | -1.41 | 0.679 | -1.07 | 0.006 | 1.64 | 0.320 | 0.55 | 1.100 | 1.41 | |
| *RB1* | 1.31 | 0.076 | -1.41 | | 1.69 | 0.259 | -2.48 | 0.391 | 1.09 | 0.116 | 0.55 | 1.060 | 2.09 | | -1.18 | 0.099 | -0.04 | 1.240 |
| *WT1* | 1.14 | | 1.17 | 0.022 | 0.34 | 1.230 | -0.54 | 1.030 | -1.17 | 0.030 | -0.52 | 1.040 | 0.01 | 1.250 | 1.08 | 0.087 | 0.61 | 1.130 |
| *NF1* | 0.76 | 1.570 | -5.19 | 1.010 | -3.46 | 10.300 | X | X | X | X | -1.46 | 0.392 | 1.55 | 0.316 | X | X | -1.68 | 0.434 |
| *NFKB1* | -1.42 | 0.061 | 1.06 | 0.031 | -1.12 | 0.010 | 1.14 | 0.015 | -1.06 | 0.030 | -1.07 | 0.022 | -1.38 | 0.279 | -0.52 | 1.020 | 1.13 | 0.108 |
| *ZFP91* | 0.17 | 1.540 | -1.94 | 0.512 | 0.58 | 1.420 | -2.45 | 0.367 | -1.61 | 0.357 | -0.51 | 1.030 | -1.56 | | 0.01 | 1.210 | -1.69 | 0.659 |

**Appendix II, D cont.**

| | LAMIN A vs GFP | | | | | | EMERIN vs GFP | | | | | | LAMIN A vs EMERIN | | | | | |
|---|---|---|---|---|---|---|---|---|---|---|---|---|---|---|---|---|---|---|
| | Replicate 1 | | Replicate 2 | | Replicate 3 | | Replicate 1 | | Replicate 2 | | Replicate 3 | | Replicate 1 | | Replicate 2 | | Replicate 3 | |
| Gene symbol | Mean | ±S.D. | Mean | ±S.D. | Mean | ±S.D. | Mean | ±S.D. | Mean | ±S.D. | Mean | ±S.D. | Mean | ±S.D. | Mean | ±S.D. | Mean | ±S.D. |
| *RARA* | -2.02 | 0.086 | 0.04 | 1.210 | -1.06 | 0.034 | 1.06 | 0.017 | 0.50 | 1.050 | -0.37 | 1.190 | -0.20 | 1.420 | 0.55 | 1.070 | 1.10 | 0.056 |
| *RXRA* | -0.06 | | 0.52 | 1.020 | -1.07 | 0.035 | 1.26 | 0.029 | -1.08 | 0.047 | -1.04 | 0.006 | -0.65 | 1.440 | -1.98 | 0.276 | 1.21 | 0.079 |
| *RHOC* | 1.05 | 0.055 | -0.68 | 1.180 | -1.28 | 0.060 | X | X | 1.46 | 0.034 | 1.08 | | 2.75 | 0.280 | -1.66 | 0.584 | -23.42 | |
| *TPBG* | 0.00 | 1.180 | 0.35 | 1.270 | 0.53 | 1.030 | 1.15 | 0.025 | 1.14 | 0.061 | 1.06 | 0.036 | 0.94 | 1.370 | 0.64 | 1.100 | 0.36 | 1.280 |
| *TCF1* | -1.04 | 0.024 | 1.04 | 0.039 | -1.02 | 0.012 | -1.10 | 0.041 | -1.02 | 0.017 | -1.02 | 0.012 | -1.73 | 0.177 | -1.03 | 0.010 | -1.06 | 0.021 |
| *TCF3* | -1.19 | 0.017 | 0.53 | 1.030 | -1.27 | 0.075 | 1.09 | 0.079 | 0.03 | 1.240 | -1.03 | 0.012 | 1.49 | 0.425 | -0.34 | 1.170 | -1.04 | 0.054 |
| *TCF4* | 1.43 | 0.154 | 1.06 | 0.015 | 1.76 | 0.382 | -1.42 | 0.104 | 1.30 | 0.025 | -1.05 | 0.019 | 2.42 | | 1.17 | 0.050 | 1.25 | 0.040 |
| *POU5F1* | -0.04 | 1.220 | -1.16 | 0.055 | -1.09 | 0.015 | -1.40 | 0.260 | -1.16 | 0.048 | -1.16 | 0.033 | 1.24 | 0.068 | -0.05 | 1.240 | -0.60 | 1.090 |
| *BCL2* | -0.36 | 1.180 | -0.52 | 1.010 | 0.03 | 1.280 | -1.13 | | -1.05 | 0.029 | -1.06 | 0.021 | -1.06 | | -1.06 | 0.019 | -1.05 | 0.017 |
| *BCL2L1* | -1.06 | 0.030 | -1.01 | 0.010 | 1.07 | 0.010 | -1.13 | 0.021 | -1.06 | 0.030 | -1.03 | 0.022 | -1.47 | | -1.05 | 0.032 | -1.06 | 0.024 |
| *TERT* | 1.29 | 0.164 | 1.23 | | -1.08 | 0.067 | -0.01 | 1.180 | -1.08 | 0.047 | -1.04 | 0.021 | -0.45 | 1.330 | 1.11 | 0.034 | 1.18 | 0.096 |
| *ABCB1* | -1.21 | 0.098 | -1.16 | | -1.69 | 0.123 | 1.13 | 0.106 | -1.27 | 0.066 | -1.04 | 0.010 | -2.84 | | -1.07 | 0.043 | -1.30 | 0.151 |
| *ABCB4* | -1.07 | 0.076 | 1.05 | 0.006 | -0.01 | | -1.02 | 0.021 | -1.05 | | -0.52 | 1.010 | 0.35 | 1.210 | 0.33 | 1.170 | -0.01 | |
| *PDGFA* | -1.01 | 0.013 | -0.52 | 1.010 | 0.53 | 1.040 | -1.09 | 0.013 | -0.01 | 1.190 | 0.51 | 1.020 | -1.43 | 0.266 | -1.02 | | -1.02 | 0.010 |
| *EGF* | 1.20 | 0.012 | 1.17 | 0.041 | 1.37 | 0.099 | 1.14 | 0.046 | 1.08 | 0.021 | 1.13 | | -2.31 | 0.606 | 1.20 | 0.060 | 1.79 | 0.022 |
| *FGF5* | -0.59 | 1.310 | -1.27 | 0.167 | -1.34 | 0.159 | -2.02 | 0.050 | -1.10 | 0.028 | -1.16 | 0.022 | 1.54 | 0.055 | 0.01 | 1.170 | -1.16 | 0.031 |
| *TGFA* | -1.21 | 0.036 | -1.04 | 0.031 | -1.08 | 0.029 | -1.11 | 0.012 | -1.04 | 0.023 | -1.03 | 0.018 | -1.56 | 0.317 | -1.06 | 0.049 | -1.06 | 0.029 |
| *TGFB* | 0.00 | 1.170 | 0.53 | 1.020 | X | X | -1.07 | | 0.52 | 1.030 | -0.50 | 1.010 | -1.11 | 0.047 | -0.34 | 1.180 | 0.01 | 1.170 |
| *PDGFRA* | -1.05 | 0.012 | 0.00 | 1.160 | -1.03 | 0.005 | -1.13 | 0.026 | -1.02 | 0.017 | -1.03 | 0.010 | -1.14 | 0.021 | -1.02 | 0.033 | -1.10 | 0.021 |
| *EGFR* | -1.11 | 0.065 | -1.01 | 0.012 | 0.03 | 1.220 | -0.57 | 1.060 | -1.06 | 0.017 | -1.04 | 0.017 | -1.27 | 0.145 | -1.07 | 0.027 | -1.07 | 0.025 |
| *FGFR1* | 1.08 | | 1.05 | 0.005 | 0.53 | 1.030 | -1.07 | 0.025 | 1.02 | 0.017 | 1.04 | 0.015 | -1.12 | | 0.51 | 1.030 | 0.36 | 1.200 |
| *TGFBR2* | -0.33 | 1.460 | 1.40 | 0.045 | 0.01 | 1.200 | 1.26 | 0.058 | -1.09 | 0.022 | -0.35 | 1.180 | -1.57 | 0.292 | 1.23 | 0.057 | 1.13 | 0.059 |
| *KRT1* | -1.21 | | 1.17 | 0.008 | -1.32 | 0.139 | 1.66 | 0.069 | -1.15 | 0.052 | 0.35 | 1.190 | -1.41 | | -7.66 | 6.240 | 1.29 | 0.114 |
| *MMP1* | -1.36 | 0.092 | -1.17 | 0.089 | 0.61 | 1.150 | X | X | 2.34 | 0.292 | 1.16 | 0.058 | 3.74 | 0.311 | -1.34 | 0.203 | -18.03 | |
| *KRT5* | 0.54 | 1.030 | 0.57 | 1.040 | -1.06 | 0.029 | -1.04 | 0.024 | 0.51 | 1.040 | -0.32 | 1.200 | -1.01 | 1.430 | 1.27 | 0.017 | -1.11 | 0.021 |
| *KRT8* | -0.38 | 1.200 | 1.19 | 0.050 | -0.54 | 1.050 | -0.04 | 1.240 | -0.55 | 1.030 | -0.52 | 1.050 | -2.94 | 0.397 | 1.11 | 0.013 | 1.16 | 0.054 |
| *KRT10* | -0.35 | 1.180 | -1.02 | 0.021 | -1.12 | 0.010 | -1.09 | 0.023 | -0.38 | 1.200 | -0.36 | 1.200 | 0.02 | 1.650 | -0.03 | | -1.04 | |
| *KRT14* | 1.32 | 0.085 | 1.10 | 0.062 | -1.08 | 0.017 | 1.04 | 0.015 | -1.05 | 0.012 | -1.06 | 0.022 | -1.50 | 0.294 | 0.55 | 1.040 | -1.01 | 0.006 |
| *KRT18* | 1.17 | 0.010 | 0.01 | 1.170 | 0.32 | 1.190 | -0.55 | 1.040 | -1.03 | 0.031 | -1.03 | 0.015 | 0.40 | 1.240 | -1.02 | 0.017 | -1.03 | 0.014 |

**Appendix II, D cont.**

| | LAMIN A vs GFP | | | | | | EMERIN vs GFP | | | | | | LAMIN A vs EMERIN | | | | | |
|---|---|---|---|---|---|---|---|---|---|---|---|---|---|---|---|---|---|---|
| | Replicate 1 | | Replicate 2 | | Replicate 3 | | Replicate 1 | | Replicate 2 | | Replicate 3 | | Replicate 1 | | Replicate 2 | | Replicate 3 | |
| Gene symbol | Mean | ±S.D. | Mean | ±S.D. | Mean | ±S.D. | Mean | ±S.D. | Mean | ±S.D. | Mean | ±S.D. | Mean | ±S.D. | Mean | ±S.D. | Mean | ±S.D. |
| *KRT19* | 1.45 | 0.125 | 1.10 | 0.039 | -0.08 | 1.350 | 1.11 | 0.031 | -1.12 | | -1.06 | 0.029 | -1.17 | 0.202 | 1.07 | 0.006 | -0.56 | 1.050 |
| *KRT20* | 1.22 | 0.183 | -1.46 | 0.106 | 1.24 | | -25.70 | 17.300 | -1.37 | 0.180 | -1.08 | 0.041 | -0.91 | 1.860 | -2.85 | 1.170 | -1.53 | 0.217 |
| *DES* | -0.13 | 1.350 | 1.15 | | -1.32 | 0.194 | -1.44 | 0.044 | -1.13 | 0.057 | -1.05 | 0.021 | 0.82 | 1.290 | 1.12 | 0.054 | 1.12 | 0.032 |
| *VIM* | 0.01 | 1.200 | -1.19 | 0.087 | 1.25 | 0.031 | 1.50 | 0.071 | 1.35 | 0.180 | 1.23 | 0.050 | 1.42 | 0.246 | -1.82 | 0.119 | -0.60 | 1.930 |
| *GFAP* | 0.01 | 1.200 | 0.52 | 1.050 | 0.01 | 1.180 | -1.05 | 0.013 | -0.51 | 1.010 | -1.03 | 0.010 | 0.52 | 1.030 | -0.01 | | -1.03 | 0.014 |
| *NEFH* | -2.21 | 1.090 | -1.32 | 0.076 | -1.13 | 0.058 | 0.55 | 1.040 | 0.00 | 1.180 | 1.08 | 0.024 | -1.82 | 0.308 | 1.10 | 0.053 | 0.39 | 1.240 |
| *TUBA2* | -0.55 | 1.030 | -0.50 | 1.020 | -0.54 | 1.030 | -1.11 | 0.022 | -1.02 | 0.017 | -0.34 | 1.160 | 1.65 | 0.064 | -0.51 | 1.010 | -1.02 | 0.012 |
| *TUBB2* | 0.02 | 1.230 | 0.55 | 1.050 | -1.17 | 0.046 | -1.04 | 0.053 | -1.06 | 0.015 | -1.04 | 0.029 | 0.77 | 1.760 | -0.53 | 1.030 | -1.03 | 0.013 |
| *ACTA1* | -0.53 | 1.050 | 0.57 | 1.080 | -1.05 | 0.042 | 1.20 | 0.045 | -0.58 | 1.050 | -1.07 | 0.033 | -0.83 | 1.330 | 1.09 | 0.047 | -0.49 | 1.100 |
| *ACTB* | -0.35 | 1.180 | 0.53 | 1.030 | -0.34 | 1.190 | 0.36 | 1.180 | -0.01 | | -1.03 | 0.032 | -1.81 | 0.071 | -1.02 | 0.015 | -1.08 | 0.029 |
| *ITGB1* | -1.27 | | -2.21 | 0.423 | -3.35 | 1.850 | -2.63 | | X | X | -1.08 | | -1.40 | | -1.47 | 0.462 | -1.34 | 0.176 |
| *ITGB3* | 1.31 | 0.263 | -4.27 | 1.670 | -16.02 | | -219.75 | | X | X | 0.60 | 1.160 | 1.86 | 0.474 | 1.14 | | -1.50 | 0.253 |
| *ITGB4* | -0.30 | 1.270 | 1.13 | 0.025 | -1.03 | 0.013 | 1.32 | 0.049 | -0.50 | 1.050 | 1.05 | 0.021 | -0.13 | 1.570 | 1.10 | 0.033 | 1.26 | 0.098 |
| *ITGB5* | 1.10 | 0.036 | -1.02 | 0.024 | 1.23 | 0.123 | 0.51 | 1.010 | 1.07 | 0.032 | -1.03 | 0.006 | -1.28 | 0.181 | 0.01 | 1.200 | 0.03 | 1.190 |
| *ITGA1* | -1.24 | 0.155 | 1.16 | 0.072 | -1.25 | 0.280 | 0.54 | 1.040 | -1.10 | 0.068 | 0.55 | 1.350 | 1.88 | 0.059 | -15.30 | 6.160 | 1.53 | 0.102 |
| *FLNA* | 1.51 | 2.300 | -1.85 | 0.326 | 3.01 | | -18.10 | 14.600 | X | X | X | X | 376.00 | 733.000 | X | X | | |
| *ITGA2* | -1.16 | 0.044 | -1.28 | 0.157 | 0.57 | 1.410 | -1.66 | 0.312 | 1.24 | 0.069 | 1.10 | 0.098 | -0.43 | 1.700 | -1.27 | 0.205 | 1.23 | |
| *ITGA3* | -0.04 | 1.220 | 1.13 | 0.079 | -1.07 | 0.039 | 1.12 | 0.017 | 0.52 | 1.020 | 1.07 | 0.006 | -2.03 | 0.358 | -1.04 | 0.037 | 1.11 | 0.036 |
| *ITGA5* | 0.65 | 1.460 | -2.10 | 0.374 | -0.66 | 1.770 | -50.80 | 26.300 | -0.79 | 1.350 | -0.01 | | 1.79 | 0.546 | -1.60 | 0.175 | -1.22 | 0.234 |
| *ITGA6* | 2.58 | 0.049 | 1.16 | 0.038 | 1.25 | 0.055 | 1.39 | 0.017 | 1.06 | 0.025 | 1.08 | 0.030 | 1.35 | 0.375 | 1.17 | 0.031 | 1.27 | |
| *ITGAV* | -0.46 | 1.280 | -1.14 | 0.102 | -1.69 | 0.148 | -1.80 | 0.064 | -1.18 | 0.017 | -0.64 | 1.090 | 1.47 | 0.093 | 0.01 | 1.200 | -1.09 | 0.051 |
| *PXN* | 0.58 | 1.070 | 1.15 | 0.024 | 1.05 | 0.035 | 1.19 | 0.053 | 0.35 | 1.180 | 0.53 | 1.020 | -1.48 | 0.249 | 1.17 | 0.030 | 0.01 | 1.220 |
| *CDH1* | 1.25 | 0..09798 | 1.07 | 0.022 | 1.19 | 0.085 | 1.32 | 0.027 | 0.54 | 1.030 | -0.53 | 1.020 | -1.40 | 0.270 | -0.51 | 1.050 | 0.51 | 1.020 |
| *CTNNA1* | 2.22 | 0.278 | -0.02 | 1.210 | 1.09 | 0.086 | -0.09 | 1.320 | -1.09 | 0.028 | 1.05 | 0.042 | 1.54 | | -0.55 | 1.050 | 1.40 | 0.134 |
| *CTNNB1* | -1.23 | 0.025 | 1.04 | 0.013 | -1.03 | 0.012 | 1.32 | 0.095 | -1.06 | 0.015 | 1.15 | 0.051 | 1.31 | 0.089 | 1.09 | 0.046 | 0.63 | 1.100 |
| *JUP* | -0.55 | 1.040 | 0.51 | 1.050 | 0.36 | 1.190 | -1.06 | 0.008 | 0.00 | 1.170 | -1.01 | 0.015 | 1.06 | 0.038 | -0.51 | 1.020 | 0.51 | 1.020 |
| *CTNND1* | -1.29 | 0.152 | -5.09 | 2.160 | -0.12 | 1.470 | -60.70 | 35.200 | -1.14 | | 1.15 | 0.033 | X | X | -4.77 | 3.560 | 1.20 | |
| *SDC1* | 0.59 | 1.070 | 1.12 | 0.033 | -1.15 | 0.044 | 1.06 | 0.033 | 0.02 | | 0.05 | 1.220 | -1.45 | 0.468 | 0.52 | 1.020 | 1.12 | |
| *SDC4* | 0.08 | | -0.39 | 1.250 | -1.42 | 0.225 | -3.78 | 0.587 | -1.06 | 0.028 | -1.13 | 0.034 | 0.45 | 1.660 | 1.15 | 0.012 | 0.04 | |

**Appendix II, D cont.**

| | LAMIN A vs GFP | | | | | | EMERIN vs GFP | | | | | | LAMIN A vs EMERIN | | | | | |
|---|---|---|---|---|---|---|---|---|---|---|---|---|---|---|---|---|---|---|
| | Replicate 1 | | Replicate 2 | | Replicate 3 | | Replicate 1 | | Replicate 2 | | Replicate 3 | | Replicate 1 | | Replicate 2 | | Replicate 3 | |
| Gene symbol | Mean | ±S.D. | Mean | ±S.D. | Mean | ±S.D. | Mean | ±S.D. | Mean | ±S.D. | Mean | ±S.D. | Mean | ±S.D. | Mean | ±S.D. | Mean | ±S.D. |
| *LAMA4* | 1.06 | 0.051 | -1.06 | 0.036 | -1.44 | 0.044 | -2.17 | 0.298 | -1.12 | 0.025 | -1.17 | 0.006 | 0.65 | 1.280 | -0.55 | 1.050 | -1.18 | 0.038 |
| *LAMB1* | 1.13 | 0.096 | -1.31 | 0.097 | -2.70 | 0.929 | -14.23 | | -1.11 | 0.061 | 0.52 | 1.070 | -0.65 | 1.630 | 1.18 | 0.033 | -1.81 | 0.057 |
| *COL1A2* | -1.45 | 0.250 | 1.12 | 0.033 | -1.25 | 0.086 | 0.35 | 1.170 | -1.12 | 0.039 | -1.10 | 0.067 | -1.69 | 0.165 | 0.58 | 1.100 | -1.07 | 0.059 |
| *FN1 / FN* | 0.54 | 1.090 | -1.22 | 0.194 | -1.45 | 0.213 | -3.56 | 1.380 | -1.15 | 0.029 | -0.54 | 1.040 | 1.34 | 0.040 | -1.59 | 0.314 | -1.12 | |
| *NUP153* | -1.49 | 0.210 | -2.06 | 0.424 | -0.53 | 1.530 | -13.00 | 3.240 | -1.68 | 0.492 | 1.41 | | 1.60 | | -1.30 | 0.210 | -2.10 | 0.424 |
| *TPR* | 1.00 | 0.010 | 1.17 | 0.046 | 0.01 | 1.200 | 1.08 | 0.019 | 0.36 | 1.190 | -1.03 | 0.012 | 1.40 | | 1.23 | 0.031 | -0.34 | 1.200 |
| *NPM1* | 0.31 | 1.210 | 1.11 | 0.029 | -0.60 | 1.090 | 0.52 | 1.020 | 0.55 | 1.030 | 1.13 | 0.097 | 1.34 | | 0.03 | | 1.12 | 0.048 |
| *RPL31* | 2.03 | 0.310 | 1.60 | 0.112 | 2.30 | 0.132 | 1.59 | 0.084 | 2.48 | 0.113 | 3.17 | 0.348 | 3.71 | 0.648 | 1.58 | 0.076 | 1.13 | |
| *RPL21* | 1.21 | 0.045 | 1.26 | | 1.35 | 0.095 | 1.15 | 0.103 | 1.12 | 0.013 | 1.20 | 0.050 | 1.86 | 0.236 | 1.17 | 0.064 | 1.18 | 0.046 |
| *RPL19* | 1.18 | 0.055 | 1.03 | 0.024 | 1.05 | 0.043 | -1.05 | 0.010 | 1.05 | | 1.06 | | 1.14 | 0.049 | 1.05 | 0.035 | 1.09 | 0.022 |
| *LMNA (lamin A)* | 1.13 | 0.017 | 1.22 | 0.054 | 1.09 | 0.006 | -0.51 | 1.010 | 1.12 | 0.025 | 1.09 | 0.015 | 1.09 | 0.075 | 1.09 | | 1.16 | 0.081 |
| LMNA (lamin C) | 0.47 | 1.120 | 1.15 | 0.055 | 0.66 | 1.120 | -1.25 | 0.044 | 0.54 | 1.050 | 1.15 | | 1.72 | 0.046 | 0.02 | 1.220 | 1.35 | 0.103 |
| *LMNB1* | 0.01 | 1.280 | -1.27 | 0.176 | 1.22 | | -7.15 | | 1.04 | | -0.38 | 2.440 | 0.41 | 1.320 | -1.39 | 0.203 | -1.25 | 0.032 |
| *LMNB2* | 0.56 | 1.060 | 0.57 | 1.080 | -0.34 | 1.160 | 1.13 | 0.058 | 0.34 | 1.180 | -0.33 | 1.200 | 1.06 | 0.045 | -0.01 | 1.180 | 0.33 | 1.170 |
| *TMPO (A)* | 0.47 | 1.380 | 1.25 | 0.071 | -0.67 | 1.120 | -1.28 | 0.190 | -0.51 | 1.020 | 1.17 | 0.121 | 1.68 | 0.053 | 0.10 | 1.310 | 0.55 | 1.050 |
| *TMPO (B)* | 1.18 | 0.125 | -1.73 | 0.397 | 0.59 | 1.400 | -2.70 | 0.731 | -1.35 | | 1.31 | 0.133 | 1.74 | 0.365 | -2.55 | 1.550 | -1.11 | 0.131 |
| *CDC2* | -0.40 | 1.250 | -1.06 | 0.030 | -0.28 | 1.290 | 1.17 | 0.048 | -1.11 | 0.082 | 1.18 | 0.075 | 1.98 | 0.229 | 0.02 | | -1.22 | 0.150 |
| *CDK2* | 1.07 | 0.051 | 1.28 | 0.044 | -0.54 | 1.050 | 1.14 | 0.066 | 1.18 | 0.087 | 0.54 | 1.030 | 1.20 | 0.195 | 0.60 | 1.110 | 1.39 | 0.085 |
| *CDK4* | 1.28 | 0.044 | -1.10 | 0.081 | -1.08 | 0.055 | -1.22 | 0.091 | 1.14 | 0.034 | 1.10 | 0.044 | 1.21 | 0.166 | X | X | 1.23 | 0.044 |
| *CDK6* | 0.82 | 1.260 | 1.11 | 0.028 | 1.11 | 0.069 | 0.01 | 1.240 | 1.15 | 0.035 | 1.09 | 0.078 | 1.48 | 0.263 | 1.18 | 0.093 | 1.29 | 0.040 |
| *CCNA1* | 0.61 | 1.090 | 1.18 | 0.064 | 1.05 | 0.037 | -1.23 | 0.107 | 1.04 | 0.006 | 1.13 | 0.063 | 1.94 | 0.075 | 0.65 | 1.110 | 1.22 | 0.024 |
| *CCNB1* | -0.01 | 1.240 | 1.27 | 0.052 | 1.28 | 0.049 | 0.05 | 1.210 | 1.10 | 0.035 | 0.37 | 1.210 | 1.98 | 0.050 | 1.12 | 0.057 | 1.37 | 0.026 |
| *CCNB2* | 1.22 | 0.155 | -1.15 | 0.110 | 1.27 | 0.109 | -1.97 | 1.050 | 1.09 | 0.056 | -1.16 | 0.075 | 1.71 | 0.113 | -1.25 | | 1.25 | 0.058 |
| *CCND1* | 1.26 | 0.180 | 1.16 | 0.109 | 1.20 | | -1.31 | | 1.03 | | -1.08 | 0.051 | 0.80 | 1.200 | -1.19 | 0.155 | 1.66 | 0.071 |
| *CCND2* | 1.07 | 0.065 | 1.07 | 0.044 | 1.05 | 0.026 | 0.00 | 1.220 | 1.06 | 0.027 | 1.05 | 0.046 | 1.12 | 0.024 | 0.52 | 1.020 | 1.03 | 0.015 |
| *CCND3* | 1.56 | 0.042 | 0.39 | 1.220 | -0.01 | 1.190 | 1.49 | | 0.53 | 1.040 | 1.31 | 0.061 | 1.70 | | 1.18 | 0.012 | 1.29 | 0.088 |
| *CCNE1* | 1.04 | 0.032 | 1.07 | 0.026 | -0.31 | 1.190 | -1.03 | 0.019 | 1.04 | | 1.28 | 0.070 | 1.10 | 0.049 | -1.41 | 0.140 | 0.51 | 1.010 |
| *CHK1* | -0.55 | 1.050 | 1.28 | 0.071 | -1.21 | | -1.07 | 0.061 | 1.31 | 0.078 | -0.52 | 1.350 | -1.63 | 0.114 | 0.63 | 1.100 | 0.55 | 1.110 |
| *CHK2* | 1.52 | 0.047 | 1.11 | 0.042 | -1.05 | 0.045 | 0.56 | 1.070 | 1.08 | 0.033 | 1.13 | 0.043 | -0.70 | 1.340 | 1.22 | | 1.39 | 0.120 |

**Appendix II, D cont.**

| | LAMIN A vs GFP | | | | | | EMERIN vs GFP | | | | | | LAMIN A vs EMERIN | | | | | |
|---|---|---|---|---|---|---|---|---|---|---|---|---|---|---|---|---|---|---|
| | Replicate 1 | | Replicate 2 | | Replicate 3 | | Replicate 1 | | Replicate 2 | | Replicate 3 | | Replicate 1 | | Replicate 2 | | Replicate 3 | |
| Gene symbol | Mean | ±S.D. | Mean | ±S.D. | Mean | ±S.D. | Mean | ±S.D. | Mean | ±S.D. | Mean | ±S.D. | Mean | ±S.D. | Mean | ±S.D. | Mean | ±S.D. |
| *CDC25A* | 1.14 | 0.082 | 1.26 | 0.049 | -1.07 | 0..05508 | 0.51 | 1.020 | 0.56 | 1.070 | -1.10 | 0.063 | 0.70 | 1.170 | 1.32 | | 0.02 | 1.200 |
| *CDC25B* | 1.31 | 0.067 | -0.51 | 1.020 | 1.01 | 0.012 | 1.15 | 0.042 | 0.51 | 1.010 | -0.01 | 1.180 | 1.08 | | 0.52 | 1.020 | 1.06 | 0.036 |
| *XRCC6* | -1.08 | 0.026 | 1.12 | 0.056 | 0.53 | 1.020 | 1.16 | 0.042 | 1.03 | 0.026 | 0.35 | 1.190 | -1.10 | 0.107 | -0.35 | 1.190 | 0.00 | 1.180 |
| *XRCC5* | 1.30 | 0.260 | -1.33 | 0.137 | 1.06 | 0.062 | -4.82 | 0.577 | -1.07 | 0.025 | -2.04 | 1.130 | 1.86 | 0.145 | -2.28 | 0.572 | -1.10 | 0.079 |
| *PRKDC* | 0.76 | 1.710 | -2.12 | 0.531 | -0.12 | 3.400 | -132.00 | 193.000 | 0.02 | 1.310 | 1.00 | 4.850 | 1.82 | 0.186 | -4.03 | 1.960 | -1.65 | 0.211 |
| *LIG4* | 0.59 | 1.390 | -2.27 | 0.158 | 0.54 | 1.450 | -5.77 | 3.330 | -0.40 | 1.270 | 0.24 | 1.400 | 1.64 | 0.136 | -4.95 | 3.100 | -0.12 | |
| *XRCC4* | -0.37 | 1.200 | 1.15 | 0.144 | 1.27 | 0.062 | 1.33 | 0.047 | 0.35 | 1.170 | 0.56 | 1.080 | 1.78 | 0.130 | 1.16 | | -0.32 | 1.210 |
| *RPA1* | 0.02 | 1.350 | 0.05 | 1.250 | 0.02 | 1.190 | 0.38 | 1.230 | -1.26 | 0.181 | 0.55 | 1.050 | 2.17 | 0.079 | -1.20 | | -1.15 | 0.090 |
| *ATM* | 0.15 | 1.360 | 1.28 | 0.082 | 0.02 | 1.210 | -1.16 | 0.111 | 1.22 | 0.087 | -0.07 | 1.260 | 1.81 | 0.337 | 0.65 | 1.110 | 1.39 | 0.026 |
| *GATA4* | 1.04 | 0.028 | 1.06 | 0.019 | 1.03 | 0.008 | -1.09 | 0.024 | 1.03 | 0.015 | 1.05 | 0.006 | -0.40 | 1.220 | 0.35 | 1.170 | 1.04 | 0.019 |
| *FGFR4* | 1.08 | 0.037 | 0.00 | 1.180 | -0.35 | 1.190 | -1.03 | 0.029 | 0.34 | 1.170 | -0.50 | 1.020 | 0.53 | 1.050 | -1.01 | 0.005 | -1.02 | 0.015 |
| *GAPDH* | 1.03 | 0.031 | 1.06 | 0.029 | 1.05 | 0.012 | -1.09 | 0.017 | 1.04 | 0.036 | 0.51 | 1.010 | -1.07 | 0.052 | -0.33 | 1.160 | 1.05 | 0.015 |
| *CHRM1* | 0.01 | 1.170 | 1.04 | 0.041 | 0.52 | 1.020 | -1.05 | 0.017 | 1.02 | 0.015 | -1.03 | 0.017 | 0.50 | 1.040 | 0.35 | 1.180 | -0.34 | 1.170 |
| *CHRM2* | 1.42 | 0.435 | -1.47 | 0.178 | 1.50 | 0.077 | -1.96 | 0.222 | -0.49 | 1.110 | -1.53 | 0.387 | 1.73 | 0.040 | -2.24 | 0.785 | 0.02 | 1.220 |
| *CHRM3* | -1.18 | 0.021 | 1.10 | 0.029 | -0.34 | 1.160 | 1.08 | | -1.05 | | 0.00 | 1.220 | 1.28 | 0.046 | -0.01 | 1.160 | -1.04 | 0.021 |
| *CHRM4* | 1.09 | | 1.18 | 0.032 | 1.16 | 0.087 | 1.35 | 0.070 | -0.52 | 1.030 | 1.21 | 0.047 | 0.64 | 1.240 | 0.53 | 1.040 | 1.40 | 0.015 |
| *CHRM5* | 1.08 | 0.054 | 1.04 | | 0.38 | 1.230 | 1.38 | 0.063 | 0.01 | 1.190 | 1.16 | 0.066 | 1.78 | | 1.12 | 0.046 | 1.28 | 0.036 |
| *HER2* | 1.15 | 0.100 | 1.22 | 0.132 | -0.54 | 1.030 | 1.21 | 0.052 | 1.19 | 0.088 | 1.33 | 0.062 | 0.58 | 1.470 | 1.15 | 0.075 | 1.14 | 0.071 |
| *CD14* | 1.52 | 0.125 | 1.13 | 0.119 | -0.54 | 1.040 | 1.10 | 0.057 | 1.18 | 0.013 | 0.55 | 1.170 | 1.20 | | 1.19 | | 1.36 | 0.045 |
| *CLDN1* | 1.46 | 0.131 | 0.00 | 1.180 | -1.35 | 0.384 | -4.73 | 1.080 | 0.51 | 1.080 | -1.13 | 0.031 | 1.60 | | -1.17 | 0.070 | 0.54 | 1.040 |
| *CA12* | 1.12 | 0.052 | 0.53 | 1.040 | 0.52 | 1.010 | 0.51 | 1.010 | 0.51 | 1.030 | 1.03 | 0.030 | -1.42 | 0.021 | -0.53 | 1.050 | 0.51 | 1.020 |
| *ASL* | -1.25 | 0.048 | 1.27 | 0.070 | -1.03 | 0.019 | 0.01 | 1.190 | -0.52 | 1.020 | -0.03 | 1.200 | -1.49 | | 0.35 | 1.200 | 1.24 | 0.032 |
| *LGALS2* | 1.18 | 0.051 | -1.07 | 0.073 | 1.16 | 0.076 | -1.61 | 0.182 | -1.10 | | -1.26 | 0.257 | 1.81 | 0.039 | -1.47 | 0.113 | 1.31 | 0.157 |
| *IGF2* | 1.64 | 0.255 | 0.37 | 1.180 | 1.45 | 0.029 | 1.27 | 0.137 | 0.55 | 1.100 | 1.07 | 0.061 | 1.46 | | -1.13 | 0.120 | 1.58 | 0.074 |
| *AQP3* | 1.08 | 0.038 | 1.10 | 0.058 | 0.56 | 1.050 | -1.04 | 0.021 | 1.06 | 0.029 | 0..015 | 1.180 | 0.02 | 1.190 | 0.04 | | 1.03 | 0.010 |
| *PTGS2 / COX2* | 0.36 | 1.590 | -0.55 | 1.120 | 1.27 | 0.062 | 1.15 | 0.083 | -0.51 | 1.080 | 0.61 | 1.090 | 1.71 | 0.197 | -0.56 | 1.080 | 0.36 | 1.470 |
| *KLRB1* | -0.41 | 1.240 | -1.35 | 0.301 | 1.41 | 0.145 | -5.32 | 2.390 | X | X | 1.16 | 0.089 | 2.07 | 0.140 | -2.62 | | -36.60 | 62.600 |
| *PMS2* | 1.16 | 0.119 | 1.46 | 0.021 | -1.19 | 0.074 | 0.57 | 1.060 | 1.09 | 0.087 | -1.19 | 0.056 | -0.37 | 1.290 | 1.18 | 0.094 | 1.29 | 0.029 |
| *SCL7A5* | 1.37 | 0.255 | 1.18 | 0.040 | -0.01 | 1.180 | 1.22 | 0.052 | 1.22 | | 1.11 | 0.026 | 0.43 | 1.290 | 1.06 | 0.068 | 1.20 | 0.158 |

**Appendix II, D cont.**

| | LAMIN A vs GFP | | | | | | EMERIN vs GFP | | | | | | LAMIN A vs EMERIN | | | | | |
|---|---|---|---|---|---|---|---|---|---|---|---|---|---|---|---|---|---|---|
| | Replicate 1 | | Replicate 2 | | Replicate 3 | | Replicate 1 | | Replicate 2 | | Replicate 3 | | Replicate 1 | | Replicate 2 | | Replicate 3 | |
| Gene symbol | Mean | ±S.D. | Mean | ±S.D. | Mean | ±S.D. | Mean | ±S.D. | Mean | ±S.D. | Mean | ±S.D. | Mean | ±S.D. | Mean | ±S.D. | Mean | ±S.D. |
| *PARP1* | 1.32 | 0.189 | -2.06 | 0.945 | 1.41 | 0.303 | -2.97 | 0.940 | -0.30 | 1.240 | 0.02 | 1.620 | X | X | -2.15 | 0.880 | 1.47 | 0.053 |
| *DRG1* | -1.04 | 0.037 | 0.49 | 1.120 | 1.06 | 0.084 | -1.31 | 0.047 | -1.09 | | -1.08 | 0.014 | -0.94 | 1.360 | -1.07 | 0.055 | 1.24 | 0.069 |
| *TGIF* | -1.14 | 0.099 | 1.11 | 0.049 | -1.19 | 0.041 | 1.09 | 0.042 | -0.35 | 1.220 | -1.12 | 0.034 | -0.45 | 2.000 | -0.56 | 1.040 | 1.25 | 0.083 |
| *SOD2* | 1.36 | 0.122 | -0.50 | 1.030 | -1.13 | 0.036 | 1.04 | 0.006 | -1.05 | 0.037 | -1.29 | 0.377 | 1.65 | 0.094 | -1.62 | 0.129 | -0.73 | 1.220 |
| *COL1A2* | -0.51 | 1.190 | 1.16 | 0.081 | -0.53 | 1.020 | 1.22 | | -1.09 | 0.094 | -0.53 | 1.030 | 0.62 | 1.460 | -1.15 | 0.073 | 1.09 | 0.083 |
| *TSPAN1* | 0.34 | 1.200 | 0.37 | 1.190 | 0.36 | 1.190 | -1.07 | 0.054 | 0.01 | 1.190 | -0.33 | 1.230 | -1.31 | 0.074 | -0.51 | 1.020 | 0.00 | 1.160 |
| *LITAF* | -0.36 | 1.320 | 1.04 | | 1.40 | 0.047 | -1.48 | 0.210 | 0.53 | 1.030 | 0.34 | 1.390 | 2.06 | 0.200 | -1.11 | 0.071 | -1.21 | 0.124 |
| *ATP2A3* | 0.00 | 1.230 | 1.38 | 0.029 | 1.20 | 0.147 | 1.46 | 0.100 | 0.02 | | 0.58 | 1.080 | 1.77 | 0.198 | X | X | 1.05 | 0.022 |
| *LGALS4* | 0.65 | 1.220 | 0.01 | | 1.21 | 0.202 | 1.41 | 0.023 | 1.24 | 0.073 | 1.13 | 0.050 | X | X | 0.43 | 1.360 | 1.28 | 0.126 |
| *PIK3CG* | 1.32 | 0.147 | -1.27 | 0.190 | -1.33 | 0.361 | -1.73 | 0.348 | -1.10 | 0.090 | -1.10 | 0.107 | 1.57 | 0.162 | -1.37 | 0.098 | -0.53 | 1.020 |
| *GNAL* | 0.45 | 1.390 | 0.54 | 1.050 | -1.15 | 0.047 | 1.15 | 0.025 | 0.53 | 1.050 | 0.51 | 1.070 | -2.16 | 0.174 | -1.29 | 0.038 | 0.54 | 1.140 |
| *STAT1* | 0.45 | 1.390 | 1.18 | 0.062 | -1.10 | 0.082 | -1.03 | 0.036 | 1.08 | 0.041 | 0.54 | 1.040 | X | X | -1.12 | 0.018 | 1.40 | 0.021 |
| *E2F4* | 1.06 | 0.024 | 0.55 | 1.040 | 1.02 | 0.019 | -0.02 | 1.190 | -0.51 | 1.030 | 1.06 | 0.048 | -1.29 | 0.066 | -1.02 | 0.012 | -0.50 | 1.010 |
| *FCGR2B* | X | X | -1.13 | 0.073 | -1.24 | 0.150 | -1.38 | 0.079 | -0.61 | 1.100 | -1.43 | 0.373 | -1.49 | 0.121 | -1.59 | 0.149 | 0.37 | 1.220 |
| *TNFRSF10A / TRIALR* | -3.89 | 0.505 | 1.32 | 0.121 | 1.13 | 0.035 | 1.19 | 0.069 | 0.50 | 1.020 | 1.07 | 0.020 | 1.39 | 0.110 | 0.52 | 1.020 | 0.04 | 1.210 |
| *FABP2* | -0.32 | 1.250 | -1.26 | 0.116 | 1.34 | 0.038 | -0.38 | 1.200 | -1.08 | 0.087 | 1.32 | 0.144 | 1.11 | 0.100 | -1.32 | 0.142 | 1.40 | 0.081 |
| *MSH2* | 1.15 | 0.095 | -0.54 | 1.120 | 1.20 | | 1.12 | 0.058 | -1.09 | 0.067 | 0.05 | | 1.97 | 0.096 | 1.08 | 0.050 | -1.33 | 0.147 |
| *DLEU1* | -1.41 | 0.320 | -0.41 | 1.260 | 1.64 | 0.126 | -0.03 | 1.190 | 1.03 | 0.026 | 1.31 | 0.165 | 2.01 | | -1.17 | 0.309 | -1.81 | 0.280 |
| *CXCL2* | 1.03 | 0.010 | 1.07 | 0.049 | 1.04 | 0.032 | -1.08 | 0.014 | 0.34 | 1.170 | 1.08 | 0.029 | 0.15 | 1.530 | 0.00 | 1.170 | 1.02 | 0.017 |
| *CFL1* | 1.26 | 0.137 | 1.24 | 0.062 | -1.23 | 0.050 | 1.08 | 0.047 | 1.08 | 0.034 | 0.02 | 1.210 | 0.54 | 1.060 | -0.32 | 1.310 | 1.22 | 0.165 |
| *RBBP4* | 1.09 | 0.050 | 1.14 | 0.021 | -1.14 | 0.046 | 0.00 | 0.000 | 0.32 | 1.250 | -1.02 | 0.014 | -1.67 | 0.101 | -1.23 | 0.079 | 1.45 | 0.083 |
| *GPX2* | -0.54 | 1.080 | 0.68 | 1.130 | 0.36 | 1.210 | 1.11 | 0.026 | 1.08 | 0.026 | 0.53 | 1.040 | 1.13 | 1.480 | 0.52 | 1.030 | 1.51 | 0.025 |
| *RGS2* | -0.14 | 1.540 | 0.51 | 1.120 | -1.06 | 0.021 | -2.33 | 0.319 | -1.04 | 0.013 | -1.14 | 0.074 | -1.84 | 0.762 | -1.16 | 0.061 | -0.08 | 1.630 |
| *PFN1* | 1.42 | 0.435 | 1.03 | 0.029 | 1.37 | 0.056 | 1.28 | 0.120 | -0.33 | 1.200 | 1.04 | 0.042 | 0.90 | 1.450 | -1.04 | 0.031 | 0.76 | 1.170 |
| *CDKN1B* | -2.47 | 0.755 | -1.13 | 0.059 | 1.06 | 0.047 | 0.15 | | -1.37 | 0.062 | -0.02 | 1.240 | 1.06 | | -1.44 | 0.076 | -1.67 | 0.720 |
| *ANPEP* | -0.57 | 1.120 | 1.14 | 0.045 | 1.11 | 0.061 | 1.04 | 0.020 | 0.50 | 1.020 | 1.24 | 0.187 | 0.71 | 1.160 | 0.51 | 1.020 | -1.06 | 0.015 |
| *FASLG* | -1.18 | 0.053 | 1.48 | 0.075 | 1.36 | 0.062 | 1.41 | 0.103 | -0.39 | 1.260 | 0.64 | 1.110 | 1.81 | 0.087 | 1.15 | 0.060 | 1.27 | 0.120 |
| *GTF3A* | -0.04 | 1.440 | 1.27 | 0.061 | 1.32 | 0.064 | 1.37 | 0.057 | 1.08 | 0.024 | 1.18 | | -0.13 | 1.380 | -2.22 | 0.648 | 1.28 | 0.096 |
| Marker | 1.07 | 0.025 | 1.11 | 0.021 | X | X | -1.03 | | 1.12 | | 1.06 | 0.030 | 1.18 | 0.079 | 1.01 | | 1.06 | 0.021 |

**Appendix II, D cont.**

| | LAMIN A vs GFP | | | | | | EMERIN vs GFP | | | | | | LAMIN A vs EMERIN | | | | | |
|---|---|---|---|---|---|---|---|---|---|---|---|---|---|---|---|---|---|---|
| | Replicate 1 | | Replicate 2 | | Replicate 3 | | Replicate 1 | | Replicate 2 | | Replicate 3 | | Replicate 1 | | Replicate 2 | | Replicate 3 | |
| Gene symbol | Mean | ±S.D. | Mean | ±S.D. | Mean | ±S.D. | Mean | ±S.D. | Mean | ±S.D. | Mean | ±S.D. | Mean | ±S.D. | Mean | ±S.D. | Mean | ±S.D. |
| *KLF4* | 0.48 | 1.520 | 1.29 | 0.061 | 1.07 | 0.049 | 1.08 | | 1.23 | 0.112 | 1.36 | 0.051 | -0.19 | 1.910 | 0.02 | 1.220 | 1.21 | 0.046 |
| *MLH1* | 1.94 | 0.140 | -1.29 | 0.103 | -1.87 | 0.111 | -1.41 | 0.271 | 1.35 | 0.056 | 1.10 | 0.099 | -1.53 | 0.306 | 0.33 | 1.210 | 1.28 | |
| *LCP1* | 2.00 | 0.519 | -1.59 | 0.266 | -0.96 | 1.840 | -4.78 | 1.800 | -0.39 | 1.290 | 0.50 | 1.100 | -1.74 | 0.414 | -1.21 | 0.169 | -1.74 | 0.015 |
| *MYB* | 1.29 | 0.114 | 1.23 | 0.056 | -1.06 | 0.013 | 0.05 | 1.240 | 0.53 | 1.050 | 1.09 | 0.045 | -1.67 | | -1.13 | 0.131 | -0.43 | 1.290 |
| *TFDP2* | 1.11 | 0.025 | 1.12 | | 0.52 | 1.030 | 1.09 | 0.026 | 1.03 | 0.015 | 1.13 | 0.045 | -0.03 | 1.300 | 1.07 | 0.044 | -0.32 | 1.190 |
| *RALGPS1* | 1.25 | 0.265 | 1.11 | 0.061 | -1.23 | 0.102 | -1.41 | 0.303 | 0.52 | 1.030 | 1.13 | 0.065 | -1.61 | | -1.22 | 0.229 | -0.35 | 1.440 |
| *NCKAP1 / NAP1* | -1.13 | 0.134 | 1.22 | 0.042 | 1.40 | 0.044 | 2.11 | 0.058 | 1.20 | 0.089 | 1.39 | 0.093 | -1.33 | 0.124 | -1.25 | 0.061 | 1.33 | 0.019 |
| *BAK1* | 1.12 | 0.083 | X | X | 1.13 | 0.041 | 1.31 | 0.100 | -1.03 | 0.022 | 0.46 | 1.290 | 1.74 | 0.077 | 1.16 | 0.066 | 1.25 | 0.163 |
| *NSAP1 / SYNCRIP* | 1.06 | 0.022 | 1.07 | 0.029 | 1.05 | 0.032 | -0.53 | 1.030 | 1.05 | | 0.53 | 1.040 | 0.34 | 1.200 | 0.52 | 1.020 | 0.50 | 1.010 |
| *CASP3* | -1.98 | 1.100 | -1.10 | 0.055 | 1.30 | 0.346 | -2.17 | 0.429 | -0.56 | 1.450 | 1.33 | 0.193 | 2.56 | 0.195 | -2.91 | 1.240 | -1.76 | 0.549 |
| Marker | -1.95 | 0.204 | X | X | 1.18 | 0.030 | 1.20 | 0.017 | 1.07 | | X | X | 0.10 | | 1.13 | 0.050 | 1.23 | |
| *PTK2B / PKB* | 1.04 | 0.040 | 1.32 | 0.122 | -1.17 | 0.024 | 1.31 | 0.127 | 1.20 | 0.078 | 1.22 | 0.061 | -1.37 | 0.221 | 1.11 | 0.029 | 1.54 | 0.069 |
| *BGN* | 1.55 | 0.182 | 1.30 | 0.046 | -1.04 | 0.034 | -1.25 | 0.187 | 1.13 | 0.092 | 1.29 | | -1.79 | 0.084 | 1.14 | 0.047 | 1.42 | 0.062 |
| *CD44* | 1.05 | 0.051 | 1.05 | 0.021 | 0.51 | 1.020 | -1.07 | 0.021 | 1.02 | 0.005 | 1.03 | 0.017 | -1.25 | 0.055 | 1.09 | 0.039 | -0.52 | 1.010 |
| *SCF / KITLG* | 1.60 | 0.167 | -1.21 | 0.113 | 1.19 | 0.087 | -1.18 | 0.059 | 1.27 | 0.139 | 0.54 | 1.030 | -1.69 | | -1.31 | 0.206 | 1.49 | 0.079 |
| *EIF3S2* | 0.37 | 1.200 | -1.41 | 0.023 | 0.17 | | -2.34 | 0.350 | X | X | 1.28 | 0.151 | -1.92 | 0.488 | -3.08 | 0.670 | 0.64 | 1.130 |
| *CEACAM3 / CEA* | 1.42 | 0.071 | -1.36 | | 0.50 | 1.120 | -2.72 | 1.940 | 0.52 | 1.050 | -0.11 | 1.460 | -1.30 | | -1.59 | 0.493 | -0.53 | 1.180 |
| *ETS2* | 0.53 | 1.070 | 1.21 | | 1.10 | 0.035 | 1.39 | 0.067 | 0.53 | 1.020 | 1.12 | | 1.62 | 0.056 | 0.00 | 1.200 | -1.36 | |
| *MCM5* | 1.03 | 0.035 | 1.08 | | 1.04 | 0.020 | -0.34 | 1.170 | -0.01 | 1.200 | 1.08 | 0.039 | 1.34 | 0.132 | 0.32 | 1.210 | 1.04 | |
| *PRKCD* | -1.23 | 0.116 | 1.12 | 0.067 | 1.44 | 0.076 | 1.33 | 0.103 | 1.21 | 0.088 | 1.37 | 0.151 | 2.11 | 0.131 | -1.06 | 0.042 | 0.61 | 1.080 |
| *TIMP1* | -2.24 | 0.078 | 1.07 | | 1.04 | 0.014 | -0.36 | 1.180 | -0.67 | 1.140 | 1.35 | 0.127 | 1.13 | 0.021 | 0.01 | 1.170 | -0.33 | 1.200 |
| *SPARC* | 1.15 | 0.025 | 1.04 | | 1.13 | | -1.06 | 0.013 | -0.33 | 1.180 | 1.09 | 0.012 | 0.07 | 1.460 | 1.03 | 0.028 | -0.34 | 1.170 |
| *TGFB1 / BIGH3* | -0.28 | 1.430 | -0.09 | 1.290 | -1.88 | 0.673 | -1.65 | 0.666 | 1.52 | 0.042 | 1.22 | 0.040 | 0.24 | 1.580 | -1.26 | 0.116 | 1.18 | 0.128 |
| *RHOA* | -0.38 | 1.190 | 1.40 | 0.025 | -1.10 | 0.076 | -0.53 | 1.030 | 1.16 | | 0.58 | 1.060 | -1.35 | 0.116 | 1.11 | 0.022 | 1.22 | 0.087 |
| *EPHB1* | 1.23 | 0.220 | 1.27 | 0.040 | 1.07 | 0.035 | 0.62 | 1.090 | 1.24 | | 1.23 | 0.024 | -1.37 | 0.107 | -0.50 | 1.020 | 1.56 | 0.087 |
| *MCM3* | 1.30 | 0.263 | 1.24 | 0.064 | -1.17 | 0.078 | 1.31 | 0.017 | 0.37 | 1.210 | 0.63 | 1.120 | -2.53 | 0.095 | 0.01 | 1.170 | 1.27 | 0.099 |
| *TNFSF10 / TRAIL* | -0.13 | | 1.29 | | -1.38 | 0.010 | 0.35 | 1.390 | -0.36 | 1.240 | 1.08 | 0.033 | -0.64 | 1.680 | -1.22 | 0.104 | -1.54 | 0.841 |
| *PLS3* | 0.58 | 1.070 | 1.17 | 0.090 | -1.37 | 0.065 | -1.91 | 0.737 | 0.09 | 1.280 | 0.34 | 1.190 | 1.73 | 0.265 | -1.25 | 0.098 | -1.70 | 0.348 |
| *CASP8* | 0.37 | 1.230 | -1.26 | 0.113 | 1.27 | 0.265 | -3.56 | 1.170 | 1.37 | 0.095 | 1.35 | 0.229 | 1.78 | 0.197 | 2.83 | 1.370 | -1.28 | 0.135 |

**Appendix II, D cont.**

| | LAMIN A vs GFP | | | | | | EMERIN vs GFP | | | | | | LAMIN A vs EMERIN | | | | | |
|---|---|---|---|---|---|---|---|---|---|---|---|---|---|---|---|---|---|---|
| | Replicate 1 | | Replicate 2 | | Replicate 3 | | Replicate 1 | | Replicate 2 | | Replicate 3 | | Replicate 1 | | Replicate 2 | | Replicate 3 | |
| Gene symbol | Mean | ±S.D. | Mean | ±S.D. | Mean | ±S.D. | Mean | ±S.D. | Mean | ±S.D. | Mean | ±S.D. | Mean | ±S.D. | Mean | ±S.D. | Mean | ±S.D. |
| *BCL3* | 1.07 | 0.013 | 1.03 | 0.013 | 1.34 | 0.080 | 1.14 | 0.087 | -0.33 | 1.190 | 1.20 | 0.051 | 2.19 | | 0.57 | 1.070 | 1.18 | |
| *ORM1* | -1.03 | 0.021 | 1.04 | | 1.32 | 0.170 | 1.08 | 0.033 | -0.03 | 1.250 | 1.08 | 0.105 | 1.24 | 0.070 | 1.14 | 0.030 | -0.04 | |
| *UNG* | 1.64 | 0.036 | 0.03 | 1.220 | -1.11 | 0.026 | 1.48 | 0.045 | 1.29 | 0.124 | 1.35 | 0.039 | -1.08 | 0.038 | 1.20 | 0.018 | 1.41 | 0.175 |
| *CA2* | -1.15 | | 1.17 | 0.036 | -1.13 | 0.032 | 0.36 | 1.190 | 1.20 | 0.010 | 1.16 | 0.079 | -1.39 | 0.205 | 1.09 | 0.019 | 1.16 | 0.052 |
| *SPP1* | 0.48 | 1.310 | 1.15 | 0.110 | -1.13 | 0.032 | -1.73 | | 1.18 | 0.015 | 1.06 | 0.044 | -1.08 | 1.500 | -1.14 | 0.095 | 1.23 | 0.075 |
| *SLC16A1* | -1.12 | 0.034 | 1.37 | 0.010 | -1.25 | 0.039 | 1.14 | 0.060 | 1.06 | 0.043 | 1.13 | 0.055 | -1.82 | 0.134 | 0.55 | 1.180 | 0.66 | 1.130 |
| *FABP1* | 0.55 | 1.110 | -1.47 | 0.264 | -4.23 | 3.280 | -3.90 | 0.884 | X | X | 0.66 | 1.120 | 1.63 | | -17.90 | 19.600 | -0.20 | 1.480 |
| *TEAD4* | 1.17 | 0.071 | 1.06 | 0.036 | -1.12 | 0.034 | 1.40 | 0.117 | -0.01 | 1.190 | 0.56 | 1.110 | 0.03 | | -0.56 | 1.060 | 1.25 | 0.045 |
| *IL3* | 1.19 | 0.074 | 1.31 | 0.032 | 0.52 | 1.030 | 1.41 | | 1.19 | 0.056 | 1.21 | 0.071 | -3.87 | | -0.51 | 1.030 | 1.19 | 0.056 |
| *CDKN1A* | 0.54 | 1.020 | 1.13 | | 1.13 | 0.075 | 1.40 | 0.026 | 0.02 | 1.180 | 1.37 | 0.076 | 1.79 | 0.163 | -0.57 | 1.080 | 1.17 | |
| *ENC1* | 1.10 | 0.062 | 1.33 | 0.055 | 1.14 | 0.033 | 1.34 | 0.046 | 1.36 | 0.055 | 1.56 | 0.047 | 1.87 | 0.430 | 0.55 | 1.080 | 1.55 | 0.029 |
| *CSPG2* | -3.10 | 0.722 | 0.04 | | 1.15 | 0.047 | -4.97 | 0.797 | X | X | 1.62 | 0.240 | 1.97 | 0.010 | -1.56 | 0.904 | -16.04 | |
| *FAS* | 0.36 | 1.340 | -1.33 | 0.150 | -1.99 | 0.434 | 0.37 | 1.200 | 0.33 | 1.410 | 1.34 | 0.278 | 1.75 | | -3.18 | 0.876 | -1.11 | 0.045 |
| *VEGF* | 0.08 | | -0.55 | 1.060 | -1.38 | 0.015 | 0.38 | 1.300 | 0.64 | 1.110 | 1.15 | 0.026 | 1.94 | 0.064 | -1.07 | 0.037 | 1.24 | 0.102 |
| *MAPK1* | -0.35 | 1.190 | -0.01 | | -1.56 | | -1.78 | 0.038 | 1.11 | 0.042 | -0.50 | 1.030 | -0.56 | 1.170 | -1.41 | 0.115 | 0.42 | 1.260 |
| *USF2* | 0.57 | 1.140 | 1.12 | 0.029 | 0.51 | 1.010 | 1.19 | 0.120 | 1.11 | 0.021 | 1.21 | 0.022 | -1.12 | 0.090 | 0.01 | | 1.22 | 0.133 |
| *MKI67* | -0.03 | | 1.33 | 0.041 | 1.06 | 0.024 | 1.28 | 0.041 | 1.18 | 0.064 | 1.15 | 0.100 | -1.49 | 0.333 | 0.52 | 1.020 | 1.21 | 0.046 |
| *BIRC2* | -0.42 | 1.520 | -1.36 | 0.116 | -1.69 | 0.146 | -92.60 | 138.000 | 1.18 | | -1.06 | 1.890 | -0.04 | | -1.59 | 1.730 | -1.11 | |
| *CHAF1A* | 1.20 | 0.068 | 1.42 | 0.035 | -0.52 | 1.050 | 1.36 | 0.076 | 1.21 | 0.038 | 0.59 | 1.070 | -1.58 | 0.142 | -1.16 | 0.081 | 1.37 | 0.219 |
| *NBS1* | 0.32 | 1.250 | 1.19 | 0.062 | -1.28 | 0.203 | -1.12 | | 1.26 | 0.079 | 1.39 | 0.215 | -1.63 | 0.068 | -2.14 | | 0.01 | |
| *CLDN4* | 1.10 | 0.056 | 1.09 | 0.059 | 1.63 | 0.030 | 1.78 | 0.068 | 1.16 | 0.055 | 1.50 | 0.048 | 1.69 | 0.822 | 1.15 | 0.039 | X | X |
| *CCR7* | -1.09 | 0.045 | 1.06 | 0.017 | 1.42 | 0.130 | 1.59 | 0.044 | 0.49 | 1.180 | 1.58 | 0.054 | 0.65 | 1.150 | 1.15 | 0.076 | 1.59 | |
| *ZBTB16* | 1.14 | | 0.39 | 1.270 | 1.06 | 0.024 | 1.53 | 0.040 | 1.30 | 0.126 | 1.40 | 0.063 | 1.47 | | -0.52 | 1.030 | 1.40 | 0.114 |
| *BIRC5* | -0.42 | 1.360 | -1.67 | 0.332 | 1.19 | | -4.31 | 0.807 | 1.25 | 0.189 | 1.25 | 0.161 | 1.28 | 0.229 | -4.05 | 1.890 | -1.16 | 0.093 |
| *HPSE* | 1.31 | 0.303 | -1.25 | 0.057 | -2.01 | 0.274 | -2.33 | 0.111 | -1.21 | 0.128 | -1.06 | 0.026 | -1.55 | 0.255 | -2.13 | 0.395 | -0.54 | 1.070 |
| *IPO7 / RANBP7* | -1.21 | 0.058 | 0.02 | | -1.25 | 0.069 | 0.38 | 1.230 | -1.07 | 0.050 | 1.03 | 0.017 | -1.33 | 0.338 | -1.41 | 0.071 | 0.62 | 1.130 |
| *SERPINA1* | -0.61 | 1.080 | 1.16 | | -1.14 | 0.065 | 1.09 | 0.010 | 1.24 | 0.026 | -1.09 | 0.093 | -3.25 | | -1.58 | 0.286 | 1.36 | 0.065 |
| *MACF1* | -1.27 | 0.121 | -1.05 | 0.026 | -1.31 | 0.146 | -1.33 | 0.158 | 0.03 | | -1.35 | 0.084 | -1.24 | 0.228 | -1.58 | 0.101 | -1.16 | 0.057 |
| *CAST* | 0.53 | 1.090 | 1.33 | 0.055 | -0.63 | 1.180 | 1.32 | | 1.15 | 0.076 | 0.61 | 1.100 | -2.49 | | -1.26 | | 1.17 | 0.072 |

**Appendix II, D cont.**

| | LAMIN A vs GFP | | | | | | EMERIN vs GFP | | | | | | LAMIN A vs EMERIN | | | | | |
|---|---|---|---|---|---|---|---|---|---|---|---|---|---|---|---|---|---|---|
| | Replicate 1 | | Replicate 2 | | Replicate 3 | | Replicate 1 | | Replicate 2 | | Replicate 3 | | Replicate 1 | | Replicate 2 | | Replicate 3 | |
| Gene symbol | Mean | ±S.D. | Mean | ±S.D. | Mean | ±S.D. | Mean | ±S.D. | Mean | ±S.D. | Mean | ±S.D. | Mean | ±S.D. | Mean | ±S.D. | Mean | ±S.D. |
| *AMID / PRG3* | 1.15 | 0.029 | 1.44 | | 1.42 | 0.050 | 1.93 | | 1.23 | 0.024 | 1.47 | 0.180 | 0.04 | 1.310 | 0.42 | 1.250 | 1.57 | 0.032 |
| *JPO1 / LOC442172* | 0.51 | 1.030 | 1.26 | 0.108 | 1.29 | 0.156 | -0.32 | 1.230 | 1.35 | 0.062 | 1.67 | 0.073 | 1.91 | 0.038 | -1.24 | 0.126 | 1.18 | 0.087 |
| *MXD3* | 0.01 | 1.170 | X | X | 1.12 | 0.075 | -0.54 | 1.040 | X | X | 1.08 | 0.017 | -1.10 | 0.055 | 0.37 | 1.200 | -1.07 | |
| *MDM2* | 1.09 | 0.076 | -0.51 | 1.030 | -1.32 | 0.085 | 1.43 | 0.095 | 1.15 | 0.094 | 1.23 | 0.071 | 1.61 | | -0.57 | 1.070 | 0.06 | |
| *REG1B* | 0.53 | 1.050 | 1.19 | 0.048 | -1.32 | 0.076 | -0.34 | 1.280 | 1.07 | 0.033 | 1.02 | 0.021 | 1.97 | 0.917 | -0.58 | 1.120 | 1.20 | |
| *SP1* | 1.01 | 0.005 | 1.04 | | 0.51 | 1.020 | -1.11 | 0.010 | 1.05 | 0.017 | -0.01 | 1.170 | -1.04 | 0.005 | 0.01 | 1.170 | 1.03 | 0.010 |
| *RSAD2* | -0.01 | 1.230 | 0.56 | 1.050 | 1.17 | 0.066 | -1.20 | 0.114 | 1.16 | 0.075 | 1.12 | 0.029 | 2.51 | 0.071 | -1.59 | 0.378 | 1.55 | 0.286 |
| *PLCB2* | 0.51 | 1.030 | 1.04 | 0.035 | -1.04 | 0.013 | -1.09 | 0.013 | -1.01 | 0.015 | -1.03 | 0.010 | 1.07 | 0.044 | -1.07 | | -1.03 | 0.019 |
| *FN1 / FN* | 1.23 | 0.096 | 1.05 | 0.062 | 1.03 | 0.010 | 1.48 | 0.051 | 0.56 | 1.060 | 1.13 | 0.024 | 0.22 | 1.550 | -0.55 | 1.050 | 1.01 | |
| *CASP7* | 1.24 | 0.115 | 1.30 | 0.065 | -1.11 | 0.032 | 1.36 | 0.074 | 1.24 | 0.035 | 0.58 | 1.060 | -1.14 | 0.072 | -1.47 | 0.070 | 1.30 | 0.101 |
| *NEBL* | 1.18 | 0.012 | 1.27 | 0.020 | 0.54 | 1.130 | 1.33 | 0.070 | 1.34 | 0.068 | 1.38 | 0.190 | 0.95 | 1.750 | -1.32 | | 1.24 | 0.052 |
| *TCOF1* | -1.01 | 0.008 | 0.00 | 1.160 | 1.50 | 0.055 | 1.80 | 0.147 | -0.01 | 1.170 | 0.59 | 1.070 | 1.14 | 0.081 | -1.05 | 0.040 | -1.06 | |
| *MTIA* | 0.51 | 1.030 | 1.06 | 0.022 | 1.06 | 0.038 | -1.07 | 0.010 | 1.06 | 0.021 | 0.52 | 1.020 | -1.06 | 0.015 | 1.03 | 0.012 | -0.34 | 1.190 |
| *MUC2* | 1.19 | 0.059 | -1.02 | 0.021 | 1.11 | 0.054 | -1.08 | 0.006 | -1.03 | 0.021 | 1.27 | 0.078 | 1.78 | 0.144 | -0.49 | 1.090 | -1.04 | 0.013 |
| *SI* | 1.28 | 0.110 | 1.10 | 0.050 | -0.65 | 1.620 | -1.24 | 0.073 | 1.18 | 0.069 | 1.16 | 0.041 | 2.58 | 0.402 | 1.05 | | 1.45 | 0.074 |
| *CDX2* | 0.06 | 1.280 | 1.33 | | 0.57 | 1.070 | -1.10 | 0.097 | 1.12 | 0.021 | 1.03 | 0.013 | 3.15 | | -0.61 | 1.080 | 1.31 | 0.036 |
| *EPHB2* | -0.55 | 1.040 | 1.09 | | -1.21 | 0.101 | 1.17 | 0.081 | 1.10 | 0.054 | 1.16 | 0.046 | 2.01 | 0.244 | -1.58 | | 1.09 | |
| *BAD* | 1.18 | 0.154 | -0.35 | 1.180 | -1.05 | 0.000 | -0.01 | 1.170 | -1.05 | 0.017 | -1.03 | 0.017 | 1.45 | 0.198 | -1.06 | 0.038 | -1.07 | 0.021 |
| *CEACAM1 / BGP1* | 1.46 | 0.062 | 1.24 | 0.024 | 1.05 | 0.037 | 1.62 | 0.064 | 1.15 | 0.026 | 0.00 | 1.170 | -1.56 | 0.065 | -1.02 | | -0.36 | 1.190 |
| *XRCC3* | 1.02 | 0.012 | 1.07 | 0.025 | -0.50 | 1.010 | -1.04 | 0.024 | 0.01 | 1.180 | 1.13 | 0.048 | -1.56 | 0.065 | -0.54 | 1.040 | 1.38 | |
| *T18* | 1.47 | 0.124 | 1.13 | 0.085 | 1.15 | 0.129 | -1.80 | | 1.54 | 0.127 | 0.93 | 1.300 | 2.21 | 0.157 | -92.00 | 155.000 | -0.54 | 1.430 |
| *SLC2A1 / GLUT1* | -0.35 | 1.180 | -1.01 | 0.008 | 1.32 | 0.042 | 1.63 | 0.120 | 1.05 | 0.027 | 1.17 | 0.024 | 1.42 | 0.280 | -0.01 | 1.200 | X | X |

# REFERENCES


Aarnio, M., Mecklin, J.P., Aaltonen, L.A., Nystrom-Lahti, M. and Jarvinen, H.J. (1995). Life-time risk of different cancers in hereditary non-polyposis colorectal cancer (HNPCC) syndrome. *Int J Cancer* **64**(6): 430-433.

Aaronson, R.P. and Blobel, G. (1975). Isolation of nuclear pore complexes in association with a lamina. *Proc Natl Acad Sci U S A* **72**(3): 1007-1011.

Aebi, U., Cohn, J., Buhle, L. and Gerace, L. (1986). The nuclear lamina is a meshwork of intermediate-type filaments. *Nature* **323**(6088): 560-564.

Agrawal, D., Chen, T., Irby, R., Quackenbush, J., Chambers, A.F., Szabo, M., Cantor, A., Coppola, D. and Yeatman, T.J. (2002). Osteopontin identified as lead marker of colon cancer progression, using pooled sample expression profiling. *J Natl Cancer Inst* **94**(7): 513-521.

Agrelo, R., Setien, F., Espada, J., Artiga, M.J., Rodriguez, M., Perez-Rosado, A., Sanchez-Aguilera, A., Fraga, M.F., Piris, M.A. and Esteller, M. (2005). Inactivation of the Lamin A/C Gene by CpG Island Promoter Hypermethylation in Hematologic Malignancies, and Its Association With Poor Survival in Nodal Diffuse Large B-Cell Lymphoma. *J Clin Oncol* **23**(17): 3940-3947.

AJCC (1997). Colon and rectum. In: *American Joint Committee on Cancer: AJCC Cancer Staging Manual.* Philadelphia: Lippincott-Raven, 5th ed., pp. 83.

Akerblad, P., Mansson, R., Lagergren, A., Westerlund, S., Basta, B., Lind, U., Thelin, A., Gisler, R., Liberg, D., Nelander, S., Bamberg, K. and Sigvardsson, M. (2005). Gene expression analysis suggests that EBF-1 and PPARgamma2 induce adipogenesis of NIH-3T3 cells with similar efficiency and kinetics. *Physiol Genomics* **23**(2): 206-216.

Alden, T.D., Gianino, J.W. and Saclarides, T.J. (1996). Brain metastases from colorectal cancer. *Dis Colon Rectum* **39**(5): 541-545.

Alexander, F. and Weller, D. (2003). Evaluation of UK Colorectal Cancer Screening Pilot, Final Report. NHS executive, UK.

Allen, T.D., Cronshaw, J.M., Bagley, S., Kiseleva, E. and Goldberg, M.W. (2000). The nuclear pore complex: mediator of translocation between nucleus and cytoplasm. *J Cell Sci* **113**(Pt 10): 1651-1659.

Altschul, S.F., Madden, T.L., Schaffer, A.A., Zhang, J., Zhang, Z., Miller, W. and Lipman, D.J. (1997). Gapped BLAST and PSI-BLAST: a new generation of protein database search programs. *Nucleic Acids Res* **25**(17): 3389-3402.

Alvarez-Reyes, M. (2003). Interactions between nuclear lamins and their binding partners in EDMD fibroblasts. In *School of Biological and Biomedical Sciences* Durham: University of Durham.

Apel, E.D., Lewis, R.M., Grady, R.M. and Sanes, J.R. (2000). Syne-1, a dystrophin- and Klarsicht-related protein associated with synaptic nuclei at the neuromuscular junction. *J Biol Chem* **275**(41): 31986-31995.

Astler, V.B. and Coller, F.A. (1954). The prognostic significance of direct extension of carcinoma of the colon and rectum. *Ann Surg* **139**(6): 846-852.

Atkin, W.S. (2002). Single flexible sigmoidoscopy screening to prevent colorectal cancer: baseline findings of a UK multicentre randomised trial. *Lancet* **359**(9314): 1291-1300.

Bagley, S., Goldberg, M.W., Cronshaw, J.M., Rutherford, S. and Allen, T.D. (2000). The nuclear pore complex. *J Cell Sci* **113**(Pt 22): 3885-3886.

Baker, S.J., Fearon, E.R., Nigro, J.M., Hamilton, S.R., Preisinger, A.C., Jessup, J.M., vanTuinen, P., Ledbetter, D.H., Barker, D.F., Nakamura, Y., White, R. and

Vogelstein, B. (1989). Chromosome 17 deletions and p53 gene mutations in colorectal carcinomas. *Science* **244**(4901): 217-221.

Barker, N., Huls, G., Korinek, V. and Clevers, H. (1999). Restricted high level expression of Tcf-4 protein in intestinal and mammary gland epithelium. *Am J Pathol* **154**(1): 29-35.

Basik, M., Mousses, S. and Trent, J. (2003). Integration of genomic technologies for accelerated cancer drug development. *Biotechniques* **35**(3): 580-582, 584, 586 passim.

Batlle, E., Henderson, J.T., Beghtel, H., van den Born, M.M., Sancho, E., Huls, G., Meeldijk, J., Robertson, J., van de Wetering, M., Pawson, T. and Clevers, H. (2002). Beta-catenin and TCF mediate cell positioning in the intestinal epithelium by controlling the expression of EphB/ephrinB. *Cell* **111**(2): 251-263.

Beaudouin, J., Gerlich, D., Daigle, N., Eils, R. and Ellenberg, J. (2002). Nuclear envelope breakdown proceeds by microtubule-induced tearing of the lamina. *Cell* **108**(1): 83-96.

Becker, B., Bellin, R.M., Sernett, S.W., Huiatt, T.W. and Robson, R.M. (1995). Synemin contains the rod domain of intermediate filaments. *Biochem Biophys Res Commun* **213**(3): 796-802.

Belgareh, N., Rabut, G., Bai, S.W., van Overbeek, M., Beaudouin, J., Daigle, N., Zatsepina, O.V., Pasteau, F., Labas, V., Fromont-Racine, M., Ellenberg, J. and Doye, V. (2001). An evolutionarily conserved NPC subcomplex, which redistributes in part to kinetochores in mammalian cells. *J Cell Biol* **154**(6): 1147-1160.

Benavente, R., Krohne, G. and Franke, W.W. (1985). Cell type-specific expression of nuclear lamina proteins during development of Xenopus laevis. *Cell* **41**(1): 177-190.

Benavente, R. and Krohne, G. (1986). Involvement of nuclear lamins in postmitotic reorganization of chromatin as demonstrated by microinjection of lamin antibodies. *J Cell Biol* **103**(5): 1847-1854.

Bellin, R.M., Sernett, S.W., Becker, B., Ip, W., Huiatt, T.W. and Robson, R.M. (1999). Molecular characteristics and interactions of the intermediate filament protein synemin. Interactions with alpha-actinin may anchor synemin-containing heterofilaments. *J Biol Chem* **274**(41): 29493-29499.

Berger, R., Theodor, L., Shoham, J., Gokkel, E., Brok-Simoni, F., Avraham, K.B., Copeland, N.G., Jenkins, N.A., Rechavi, G. and Simon, A.J. (1996). The characterization and localization of the mouse thymopoietin/lamina-associated polypeptide 2 gene and its alternatively spliced products. *Genome Res* **6**(5): 361-370.

Bhutani, M.S. and Pacheco, J. (1992). Metastatic colon carcinoma to oral soft tissues. *Spec Care Dentist* **12**(4): 172-173.

Biamonti, G., Giacca, M., Perini, G., Contreas, G., Zentilin, L., Weighardt, F., Guerra, M., Della Valle, G., Saccone, S., Riva, S. and et al. (1992). The gene for a novel human lamin maps at a highly transcribed locus of chromosome 19 which replicates at the onset of S-phase. *Mol Cell Biol* **12**(8): 3499-3506.

Bienz, M. and Clevers, H. (2000). Linking colorectal cancer to Wnt signaling. *Cell* **103**(2): 311-320.

Bilak, S.R., Sernett, S.W., Bilak, M.M., Bellin, R.M., Stromer, M.H., Huiatt, T.W. and Robson, R.M. (1998). Properties of the novel intermediate filament protein synemin and its identification in mammalian muscle. *Arch Biochem Biophys* **355**(1): 63-76.

Bione, S., Tamanini, F., Maestrini, E., Tribioli, C., Poustka, A., Torri, G., Rivella, S. and Toniolo, D. (1993). Transcriptional organization of a 450-kb region of the human X chromosome in Xq28. *Proc Natl Acad Sci U S A* **90**(23): 10977-10981.

Bione, S., Maestrini, E., Rivella, S., Mancini, M., Regis, S., Romeo, G. and Toniolo, D. (1994). Identification of a novel X-linked gene responsible for Emery-Dreifuss muscular dystrophy. *Nat Genet* **8**(4): 323-327.

Bird, R.P. (1987). Observation and quantification of aberrant crypts in the murine colon treated with a colon carcinogen: preliminary findings. *Cancer Lett* **37**(2): 147-151.

Bird, R.P. and Good, C.K. (2000). The significance of aberrant crypt foci in understanding the pathogenesis of colon cancer. *Toxicol Lett* **112-113**: 395-402.

Blixt, A., Mahlapuu, M., Aitola, M., Pelto-Huikko, M., Enerback, S. and Carlsson, P. (2000). A forkhead gene, FoxE3, is essential for lens epithelial proliferation and closure of the lens vesicle. *Genes Dev* **14**(2): 245-254.

Bodoor, K., Shaikh, S., Salina, D., Raharjo, W.H., Bastos, R., Lohka, M. and Burke, B. (1999). Sequential recruitment of NPC proteins to the nuclear periphery at the end of mitosis. *J Cell Sci* **112**(Pt 13): 2253-2264.

Bonne, G., Di Barletta, M.R., Varnous, S., Becane, H.M., Hammouda, E.H., Merlini, L., Muntoni, F., Greenberg, C.R., Gary, F., Urtizberea, J.A., Duboc, D., Fardeau, M., Toniolo, D. and Schwartz, K. (1999). Mutations in the gene encoding lamin A/C cause autosomal dominant Emery-Dreifuss muscular dystrophy. *Nat Genet* **21**(3): 285-288.

Bonne, G., Mercuri, E., Muchir, A., Urtizberea, A., Becane, H.M., Recan, D., Merlini, L., Wehnert, M., Boor, R., Reuner, U., Vorgerd, M., Wicklein, E.M., Eymard, B., Duboc, D., Penisson-Besnier, I., Cuisset, J.M., Ferrer, X., Desguerre, I., Lacombe, D., Bushby, K., Pollitt, C., Toniolo, D., Fardeau, M., Schwartz, K. and Muntoni, F. (2000). Clinical and molecular genetic spectrum of autosomal dominant Emery-Dreifuss muscular dystrophy due to mutations of the lamin A/C gene. *Ann Neurol* **48**(2): 170-180.

Booth, C. and Potten, C.S. (2000). Gut instincts: thoughts on intestinal epithelial stem cells. *J Clin Invest* **105**(11): 1493-1499.

Bridger, J.M., Kill, I.R., O'Farrell, M. and Hutchison, C.J. (1993). Internal lamin structures within G1 nuclei of human dermal fibroblasts. *J Cell Sci* **104**(Pt 2): 297-306.

Broders, A.C. (1925). The grading of carcinoma. *Minnesota Med* **8**: 726-730.

Bossie, C.A. and Sanders, M.M. (1993). A cDNA from Drosophila melanogaster encodes a lamin C-like intermediate filament protein. *J Cell Sci* **104**(Pt 4): 1263-1272.

Bouhouche, A., Benomar, A., Birouk, N., Mularoni, A., Meggouh, F., Tassin, J., Grid, D., Vandenberghe, A., Yahyaoui, M., Chkili, T., Brice, A. and LeGuern, E. (1999). A locus for an axonal form of autosomal recessive Charcot-Marie-Tooth disease maps to chromosome 1q21.2-q21.3. *Am J Hum Genet* **65**(3): 722-727.

Brodsky, G.L., Muntoni, F., Miocic, S., Sinagra, G., Sewry, C. and Mestroni, L. (2000). Lamin A/C gene mutation associated with dilated cardiomyopathy with variable skeletal muscle involvement. *Circulation* **101**(5): 473-476.

Broers, J.L., Raymond, Y., Rot, M.K., Kuijpers, H., Wagenaar, S.S. and Ramaekers, F.C. (1993). Nuclear A-type lamins are differentially expressed in human lung cancer subtypes. *Am J Pathol* **143**(1): 211-220.

Broers, J.L., Machiels, B.M., Kuijpers, H.J., Smedts, F., van den Kieboom, R., Raymond, Y. and Ramaekers, F.C. (1997). A- and B-type lamins are differentially expressed in normal human tissues. *Histochem Cell Biol* **107**(6): 505-517.

Broers, J.L., Machiels, B.M., van Eys, G.J., Kuijpers, H.J., Manders, E.M., van Driel, R. and Ramaekers, F.C. (1999). Dynamics of the nuclear lamina as monitored by GFP-tagged A-type lamins. *J Cell Sci* **112**(Pt 20): 3463-3475.

Broers, J.L., Peeters, E.A., Kuijpers, H.J., Endert, J., Bouten, C.V., Oomens, C.W., Baaijens, F.P. and Ramaekers, F.C. (2004). Decreased mechanical stiffness in LMNA-/- cells is caused by defective nucleo-cytoskeletal integrity: implications for the development of laminopathies. *Hum Mol Genet* **13**(21): 2567-2580.

Buendia, B., Courvalin, J.C. and Collas, P. (2001). Dynamics of the nuclear envelope at mitosis and during apoptosis. *Cell Mol Life Sci* **58**(12-13): 1781-1789.

Burke, B. and Gerace, L. (1986). A cell free system to study reassembly of the nuclear envelope at the end of mitosis. *Cell* **44**(4): 639-652.

Burkitt, H.G., Young, B. and Heath, J.W. (1993). Gastrointestinal tract. In: *Wheater's Functional Histology: A Text and Colour Atlas*. Edinburgh: Churchill Livingstone, pp. 247-270.

Cance, W.G., Chaudhary, N., Worman, H.J., Blobel, G. and Cordon-Cardo, C. (1992). Expression of the nuclear lamins in normal and neoplastic human tissues. *J. Exp. Clin. Cancer Res.* **11**(4): 233-246.

Cancer Research UK (October 2005). http://info.cancerresearchuk.org/cancerstats/incidence/commoncancers/.

Cancer Research UK (October 2005). http://info.cancerresearchuk.org/cancerstats/mortality/cancerdeaths/.

Cao, H. and Hegele, R.A. (2000). Nuclear lamin A/C R482Q mutation in canadian kindreds with Dunnigan-type familial partial lipodystrophy. *Hum Mol Genet* **9**(1): 109-112.

Capanni, C., Mattioli, E., Columbaro, M., Lucarelli, E., Parnaik, V.K., Novelli, G., Wehnert, M., Cenni, V., Maraldi, N.M., Squarzoni, S. and Lattanzi, G. (2005). Altered pre-lamin A processing is a common mechanism leading to lipodystrophy. *Hum Mol Genet* **14**(11): 1489-1502.

Carlsson, L., Li, Z.L., Paulin, D., Price, M.G., Breckler, J., Robson, R.M., Wiche, G. and Thornell, L.E. (2000). Differences in the distribution of synemin, paranemin, and plectin in skeletal muscles of wild-type and desmin knock-out mice. *Histochem Cell Biol* **114**(1): 39-47.

Cartegni, L., di Barletta, M.R., Barresi, R., Squarzoni, S., Sabatelli, P., Maraldi, N., Mora, M., Di Blasi, C., Cornelio, F., Merlini, L., Villa, A., Cobianchi, F. and Toniolo, D. (1997). Heart-specific localization of emerin: new insights into Emery-Dreifuss muscular dystrophy. *Hum Mol Genet* **6**(13): 2257-2264.

Cattoretti, G., Pileri, S., Parravicini, C., Becker, M.H., Poggi, S., Bifulco, C., Key, G., D'Amato, L., Sabattini, E., Feudale, E. and et al. (1993). Antigen unmasking on formalin-fixed, paraffin-embedded tissue sections. *J Pathol* **171**(2): 83-98.

Cavallo, R.A., Cox, R.T., Moline, M.M., Roose, J., Polevoy, G.A., Clevers, H., Peifer, M. and Bejsovec, A. (1998). Drosophila Tcf and Groucho interact to repress Wingless signalling activity. *Nature* **395**(6702): 604-608.

Chaudhary, N. and Courvalin, J.C. (1993). Stepwise reassembly of the nuclear envelope at the end of mitosis. *J Cell Biol* **122**(2): 295-306.

Chellappan, S.P., Hiebert, S., Mudryj, M., Horowitz, J.M. and Nevins, J.R. (1991). The E2F transcription factor is a cellular target for the RB protein. *Cell* **65**(6): 1053-1061.

Chen, L., Lee, L., Kudlow, B.A., Dos Santos, H.G., Sletvold, O., Shafeghati, Y., Botha, E.G., Garg, A., Hanson, N.B., Martin, G.M., Mian, I.S., Kennedy, B.K. and Oshima, J. (2003). LMNA mutations in atypical Werner's syndrome. *Lancet* **362**(9382): 440-445.

Clarke, P.A., te Poele, R., Wooster, R. and Workman, P. (2001). Gene expression microarray analysis in cancer biology, pharmacology, and drug development: progress and potential. *Biochem Pharmacol* **62**(10): 1311-1336.

Coates, P.J., Hobbs, R.C., Crocker, J., Rowlands, D.C., Murray, P., Quinlan, R. and Hall, P.A. (1996). Identification of the antigen recognized by the monoclonal antibody BU31 as lamins A and C. *J Pathol* **178**(1): 21-29.

Cohen, M., Lee, K.K., Wilson, K.L. and Gruenbaum, Y. (2001). Transcriptional repression, apoptosis, human disease and the functional evolution of the nuclear lamina. *Trends Biochem Sci* **26**(1): 41-47.

Collas, P., Thompson, L., Fields, A.P., Poccia, D.L. and Courvalin, J.C. (1997). Protein kinase C-mediated interphase lamin B phosphorylation and solubilization. *J Biol Chem* **272**(34): 21274-21280.

Compagni, A. and Christofori, G. (2000). Recent advances in research on multistage tumorigenesis. *Br J Cancer* **83**(1): 1-5.

Csoka, A.B., English, S.B., Simkevich, C.P., Ginzinger, D.G., Butte, A.J., Schatten, G.P., Rothman, F.G. and Sedivy, J.M. (2004). Genome-scale expression profiling of Hutchinson-Gilford progeria syndrome reveals widespread transcriptional misregulation leading to mesodermal/mesenchymal defects and accelerated atherosclerosis. *Aging Cell* **3**(4): 235-243.

Cutler, D.L., Kaufmann, S. and Freidenberg, G.R. (1991). Insulin-resistant diabetes mellitus and hypermetabolism in mandibuloacral dysplasia: a newly recognized form of partial lipodystrophy. *J Clin Endocrinol Metab* **73**(5): 1056-1061.

Dabauvalle, M.C., Loos, K., Merkert, H. and Scheer, U. (1991). Spontaneous assembly of pore complex-containing membranes ("annulate lamellae") in Xenopus egg extract in the absence of chromatin. *J Cell Biol* **112**(6): 1073-1082.

Daigle, N., Beaudouin, J., Hartnell, L., Imreh, G., Hallberg, E., Lippincott-Schwartz, J. and Ellenberg, J. (2001). Nuclear pore complexes form immobile networks and have a very low turnover in live mammalian cells. *J Cell Biol* **154**(1): 71-84.

Dechat, T., Gotzmann, J., Stockinger, A., Harris, C.A., Talle, M.A., Siekierka, J.J. and Foisner, R. (1998). Detergent-salt resistance of LAP2alpha in interphase nuclei and phosphorylation-dependent association with chromosomes early in nuclear assembly implies functions in nuclear structure dynamics. *Embo J* **17**(16): 4887-4902.

Dechat, T., Korbei, B., Vaughan, O.A., Vlcek, S., Hutchison, C.J. and Foisner, R. (2000). Lamina-associated polypeptide 2alpha binds intranuclear A-type lamins. *J Cell Sci* **113**(Pt 19): 3473-3484.

de la Chapelle, A. (2004). Genetic predisposition to colorectal cancer. *Nat Rev Cancer* **4**(10): 769-780.

De Sandre-Giovannoli, A., Chaouch, M., Kozlov, S., Vallat, J.M., Tazir, M., Kassouri, N., Szepetowski, P., Hammadouche, T., Vandenberghe, A., Stewart, C.L., Grid, D. and Levy, N. (2002). Homozygous defects in LMNA, encoding lamin A/C nuclear-envelope proteins, cause autosomal recessive axonal neuropathy in human (Charcot-Marie-Tooth disorder type 2) and mouse. *Am J Hum Genet* **70**(3): 726-736.

de Santa Barbara, P., van den Brink, G.R. and Roberts, D.J. (2003). Development and differentiation of the intestinal epithelium. *Cell Mol Life Sci* **60**(7): 1322-1332.

Dessev, G., Iovcheva-Dessev, C., Bischoff, J.R., Beach, D. and Goldman, R. (1991). A complex containing p34cdc2 and cyclin B phosphorylates the nuclear lamin and disassembles nuclei of clam oocytes in vitro. *J Cell Biol* **112**(4): 523-533.

Dhanasekaran, S.M., Barrette, T.R., Ghosh, D., Shah, R., Varambally, S., Kurachi, K., Pienta, K.J., Rubin, M.A. and Chinnaiyan, A.M. (2001). Delineation of prognostic biomarkers in prostate cancer. *Nature* **412**(6849): 822-826.

Dharmsathaphorn, K., McRoberts, J.A., Mandel, K.G., Tisdale, L.D. and Masui, H. (1984). A human colonic tumor cell line that maintains vectorial electrolyte transport. *Am J Physiol* **246**(2 Pt 1): G204-208.

Dreifuss, F.E. and Hogan, G.R. (1961). Survival in x-chromosomal muscular dystrophy. *Neurology* **11**: 734-737.

Drummond, S., Ferrigno, P., Lyon, C., Murphy, J., Goldberg, M., Allen, T., Smythe, C. and Hutchison, C.J. (1999). Temporal differences in the appearance of NEP-B78 and an LBR-like protein during Xenopus nuclear envelope reassembly reflect the ordered recruitment of functionally discrete vesicle types. *J Cell Biol* **144**(2): 225-240.

Duband-Goulet, I., Courvalin, J.C. and Buendia, B. (1998). LBR, a chromatin and lamin binding protein from the inner nuclear membrane, is proteolyzed at late stages of apoptosis. *J Cell Sci* **111**(Pt 10): 1441-1451.

Dukes, C.E. (1932). The classification of cancer of the rectum. *Journal of Pathology and Bacteriology* **35**: 323-332.

Dunnigan, M.G., Cochrane, M.A., Kelly, A. and Scott, J.W. (1974). Familial lipoatrophic diabetes with dominant transmission. A new syndrome. *Q J Med* **43**(169): 33-48.

Dunstone, G.H. and Knaggs, T.W. (1972). Familial cancer of the colon and rectum. *J Med Genet* **9**(4): 451-456.

Dwyer, N. and Blobel, G. (1976). A modified procedure for the isolation of a pore complex-lamina fraction from rat liver nuclei. *J Cell Biol* **70**(3): 581-591.

Dyer, J.A., Kill, I.R., Pugh, G., Quinlan, R.A., Lane, E.B. and Hutchison, C.J. (1997). Cell cycle changes in A-type lamin associations detected in human dermal fibroblasts using monoclonal antibodies. *Chromosome Res* **5**(6): 383-394.

Dyer, J.A., Lane, B.E. and Hutchison, C.J. (1999). Investigations of the pathway of incorporation and function of lamin A in the nuclear lamina. *Microsc Res Tech* **45**(1): 1-12.

Ellenberg, J., Siggia, E.D., Moreira, J.E., Smith, C.L., Presley, J.F., Worman, H.J. and Lippincott-Schwartz, J. (1997). Nuclear membrane dynamics and reassembly in living cells: targeting of an inner nuclear membrane protein in interphase and mitosis. *J Cell Biol* **138**(6): 1193-1206.

Ellis, J.A., Yates, J.R., Kendrick-Jones, J. and Brown, C.A. (1999). Changes at P183 of emerin weaken its protein-protein interactions resulting in X-linked Emery-Dreifuss muscular dystrophy. *Hum Genet* **104**(3): 262-268.

Emery, A.E. and Dreifuss, F.E. (1966). Unusual type of benign x-linked muscular dystrophy. *J Neurol Neurosurg Psychiatry* **29**(4): 338-342.

Erber, A., Riemer, D., Bovenschulte, M. and Weber, K. (1998). Molecular phylogeny of metazoan intermediate filament proteins. *J Mol Evol* **47**(6): 751-762.

Eriksson, M., Brown, W.T., Gordon, L.B., Glynn, M.W., Singer, J., Scott, L., Erdos, M.R., Robbins, C.M., Moses, T.Y., Berglund, P., Dutra, A., Pak, E., Durkin, S., Csoka, A.B., Boehnke, M., Glover, T.W. and Collins, F.S. (2003). Recurrent de novo point mutations in lamin A cause Hutchinson-Gilford progeria syndrome. *Nature* **423**(6937): 293-298.

Ethier, S.P. (1996). Human breast cancer cell lines as models of growth regulation and disease progression. *J Mammary Gland Biol Neoplasia* **1**(1): 111-121.

Farnsworth, C.C., Wolda, S.L., Gelb, M.H. and Glomset, J.A. (1989). Human lamin B contains a farnesylated cysteine residue. *J Biol Chem* **264**(34): 20422-20429.

Fatkin, D., MacRae, C., Sasaki, T., Wolff, M.R., Porcu, M., Frenneaux, M., Atherton, J., Vidaillet, H.J., Jr., Spudich, S., De Girolami, U., Seidman, J.G., Seidman, C., Muntoni, F., Muehle, G., Johnson, W. and McDonough, B. (1999). Missense mutations in the rod domain of the lamin A/C gene as causes of dilated

cardiomyopathy and conduction-system disease. *N Engl J Med* **341**(23): 1715-1724.

Fawcett, D.W. (1966). On the occurrence of a fibrous lamina on the inner aspect of the nuclear envelope in certain cells of vertebrates. *Am J Anat* **119**(1): 129-145.

Fearon, E.R., Cho, K.R., Nigro, J.M., Kern, S.E., Simons, J.W., Ruppert, J.M., Hamilton, S.R., Preisinger, A.C., Thomas, G., Kinzler, K.W. and et al. (1990). Identification of a chromosome 18q gene that is altered in colorectal cancers. *Science* **247**(4938): 49-56.

Fearon, E.R. and Vogelstein, B. (1990). A genetic model for colorectal tumorigenesis. *Cell* **61**(5): 759-767.

Firmbach-Kraft, I. and Stick, R. (1993). The role of CaaX-dependent modifications in membrane association of Xenopus nuclear lamin B3 during meiosis and the fate of B3 in transfected mitotic cells. *J Cell Biol* **123**(6 Pt 2): 1661-1670.

Fisher, D.Z., Chaudhary, N. and Blobel, G. (1986). cDNA sequencing of nuclear lamins A and C reveals primary and secondary structural homology to intermediate filament proteins. *Proc Natl Acad Sci U S A* **83**(17): 6450-6454.

Fodde, R., Smits, R. and Clevers, H. (2001). APC, signal transduction and genetic instability in colorectal cancer. *Nat Rev Cancer* **1**(1): 55-67.

Fogh, J. and Trempe, G. (1975). New Human Tumor Cell Lines. In: *Human Tumor Cells In Vitro*. Fogh, J. (ed). New York: Plenum Press, pp. 115-159.

Foisner, R. and Gerace, L. (1993). Integral membrane proteins of the nuclear envelope interact with lamins and chromosomes, and binding is modulated by mitotic phosphorylation. *Cell* **73**(7): 1267-1279.

Foisner, R. (2001). Inner nuclear membrane proteins and the nuclear lamina. *J Cell Sci* **114**(Pt 21): 3791-3792.

Franke, W.W., Scheer, U., Krohne, G. and Jarasch, E.D. (1981). The nuclear envelope and the architecture of the nuclear periphery. *J Cell Biol* **91**(3 Pt 2): 39s-50s.

Fuchs, E. and Weber, K. (1994). Intermediate filaments: structure, dynamics, function, and disease. *Annu Rev Biochem* **63**: 345-382.

Fuller, G.N., Hess, K.R., Rhee, C.H., Yung, W.K., Sawaya, R.A., Bruner, J.M. and Zhang, W. (2002). Molecular classification of human diffuse gliomas by multidimensional scaling analysis of gene expression profiles parallels morphology-based classification, correlates with survival, and reveals clinically-relevant novel glioma subsets. *Brain Pathol* **12**(1): 108-116.

Furukawa, K. and Hotta, Y. (1993). cDNA cloning of a germ cell specific lamin B3 from mouse spermatocytes and analysis of its function by ectopic expression in somatic cells. *Embo J* **12**(1): 97-106.

Furukawa, K., Inagaki, H. and Hotta, Y. (1994). Identification and cloning of an mRNA coding for a germ cell-specific A-type lamin in mice. *Exp Cell Res* **212**(2): 426-430.

Furukawa, K. (1999). LAP2 binding protein 1 (L2BP1/BAF) is a candidate mediator of LAP2-chromatin interaction. *J Cell Sci* **112**(Pt 15): 2485-2492.

Gabriel, V.B., Dukes, C. and Bussey, H.J.R. (1935). Lymphatic spread in cancer of the rectum. *Br J Surg* **23**: 395.

Galambos, J.T. (1973). Carcinoembryonic antigen and neoplastic disease. *South Med J* **66**(11): 1216-1217.

Genschel, J., Bochow, B., Kuepferling, S., Ewert, R., Hetzer, R., Lochs, H. and Schmidt, H. (2001). A R644C mutation within lamin A extends the mutations causing dilated cardiomyopathy. *Hum Mutat* **17**(2): 154.

Georgatos, S.D., Pyrpasopoulou, A. and Theodoropoulos, P.A. (1997). Nuclear envelope breakdown in mammalian cells involves stepwise lamina disassembly

and microtubule-drive deformation of the nuclear membrane. *J Cell Sci* **110**(Pt 17): 2129-2140.

Gerace, L., Blum, A. and Blobel, G. (1978). Immunocytochemical localization of the major polypeptides of the nuclear pore complex-lamina fraction. Interphase and mitotic distribution. *J Cell Biol* **79**(2 Pt 1): 546-566.

Gerace, L. and Blobel, G. (1980). The nuclear envelope lamina is reversibly depolymerized during mitosis. *Cell* **19**(1): 277-287.

Gerace, L., Comeau, C. and Benson, M. (1984). Organization and modulation of nuclear lamina structure. *J Cell Sci Suppl* **1**: 137-160.

Gerace, L. (1986). Nuclear lamina and organisation of nuclear architecture. *Trends Biochem Sci* **11**: 443-445.

Gerace, L. and Burke, B. (1988). Functional organization of the nuclear envelope. *Annu Rev Cell Biol* **4**: 335-374.

Giles, R.H., van Es, J.H. and Clevers, H. (2003). Caught up in a Wnt storm: Wnt signaling in cancer. *Biochim Biophys Acta* **1653**(1): 1-24.

Goldberg, M., Harel, A. and Gruenbaum, Y. (1999). The nuclear lamina: molecular organization and interaction with chromatin. *Crit Rev Eukaryot Gene Expr* **9**(3-4): 285-293.

Goldberg, M.W. and Allen, T.D. (1995). Structural and functional organization of the nuclear envelope. *Curr Opin Cell Biol* **7**(3): 301-309.

Goldman, R.D., Gruenbaum, Y., Moir, R.D., Shumaker, D.K. and Spann, T.P. (2002). Nuclear lamins: building blocks of nuclear architecture. *Genes Dev* **16**(5): 533-547.

Goldman, R.D., Shumaker, D.K., Erdos, M.R., Eriksson, M., Goldman, A.E., Gordon, L.B., Gruenbaum, Y., Khuon, S., Mendez, M., Varga, R. and Collins, F.S. (2004). Accumulation of mutant lamin A causes progressive changes in nuclear architecture in Hutchinson-Gilford progeria syndrome. *Proc Natl Acad Sci U S A* **101**(24): 8963-8968.

Goldstein, M.J. and Mitchell, E.P. (2005). Carcinoembryonic antigen in the staging and follow-up of patients with colorectal cancer. *Cancer Invest* **23**(4): 338-351.

Golub, T.R., Slonim, D.K., Tamayo, P., Huard, C., Gaasenbeek, M., Mesirov, J.P., Coller, H., Loh, M.L., Downing, J.R., Caligiuri, M.A., Bloomfield, C.D. and Lander, E.S. (1999). Molecular classification of cancer: class discovery and class prediction by gene expression monitoring. *Science* **286**(5439): 531-537.

Gordon, J.I. and Hermiston, M.L. (1994). Differentiation and self-renewal in the mouse gastrointestinal epithelium. *Curr Opin Cell Biol* **6**(6): 795-803.

Granger, B.L. and Lazarides, E. (1980). Synemin: a new high molecular weight protein associated with desmin and vimentin filaments in muscle. *Cell* **22**(3): 727-738.

Gruenbaum, Y., Landesman, Y., Drees, B., Bare, J.W., Saumweber, H., Paddy, M.R., Sedat, J.W., Smith, D.E., Benton, B.M. and Fisher, P.A. (1988). Drosophila nuclear lamin precursor Dm0 is translated from either of two developmentally regulated mRNA species apparently encoded by a single gene. *J Cell Biol* **106**(3): 585-596.

Gruenbaum, Y., Lee, K.K., Liu, J., Cohen, M. and Wilson, K.L. (2002). The expression, lamin-dependent localization and RNAi depletion phenotype for emerin in C. elegans. *J Cell Sci* **115**(Pt 5): 923-929.

Gruenbaum, Y., Goldman, R.D., Meyuhas, R., Mills, E., Margalit, A., Fridkin, A., Dayani, Y., Prokocimer, M. and Enosh, A. (2003). The nuclear lamina and its functions in the nucleus. *Int Rev Cytol* **226**: 1-62.

Gruenbaum, Y., Margalit, A., Goldman, R.D., Shumaker, D.K. and Wilson, K.L. (2005). The nuclear lamina comes of age. *Nat Rev Mol Cell Biol* **6**(1): 21-31.

Guilly, M.N., Bensussan, A., Bourge, J.F., Bornens, M. and Courvalin, J.C. (1987). A human T lymphoblastic cell line lacks lamins A and C. *Embo J* **6**(12): 3795-3799.

Hammoud, M.A., McCutcheon, I.E., Elsouki, R., Schoppa, D. and Patt, Y.Z. (1996). Colorectal carcinoma and brain metastasis: distribution, treatment, and survival. *Ann Surg Oncol* **3**(5): 453-463.

Hardcastle, J.D., Chamberlain, J.O., Robinson, M.H., Moss, S.M., Amar, S.S., Balfour, T.W., James, P.D. and Mangham, C.M. (1996). Randomised controlled trial of faecal-occult-blood screening for colorectal cancer. *Lancet* **348**(9040): 1472-1477.

Hatch, K.F., Blanchard, D.K., Hatch, G.F., 3rd, Wertheimer-Hatch, L., Davis, G.B., Foster, R.S., Jr. and Skandalakis, J.E. (2000). Tumors of the appendix and colon. *World J Surg* **24**(4): 430-436.

Hazelbag, H.M., van den Broek, L.J., van Dorst, E.B., Offerhaus, G.J., Fleuren, G.J. and Hogendoorn, P.C. (1995). Immunostaining of chain-specific keratins on formalin-fixed, paraffin-embedded tissues: a comparison of various antigen retrieval systems using microwave heating and proteolytic pre-treatments. *J Histochem Cytochem* **43**(4): 429-437.

He, T.C., Sparks, A.B., Rago, C., Hermeking, H., Zawel, L., da Costa, L.T., Morin, P.J., Vogelstein, B. and Kinzler, K.W. (1998). Identification of c-MYC as a target of the APC pathway. *Science* **281**(5382): 1509-1512.

Hegele, R.A., Anderson, C.M., Wang, J., Jones, D.C. and Cao, H. (2000). Association between nuclear lamin A/C R482Q mutation and partial lipodystrophy with hyperinsulinemia, dyslipidemia, hypertension, and diabetes. *Genome Res* **10**(5): 652-658.

Heitlinger, E., Peter, M., Haner, M., Lustig, A., Aebi, U. and Nigg, E.A. (1991). Expression of chicken lamin B2 in Escherichia coli: characterization of its structure, assembly, and molecular interactions. *J Cell Biol* **113**(3): 485-495.

Heitlinger, E., Peter, M., Lustig, A., Villiger, W., Nigg, E.A. and Aebi, U. (1992). The role of the head and tail domain in lamin structure and assembly: analysis of bacterially expressed chicken lamin A and truncated B2 lamins. *J Struct Biol* **108**(1): 74-89.

Hemminki, A., Markie, D., Tomlinson, I., Avizienyte, E., Roth, S., Loukola, A., Bignell, G., Warren, W., Aminoff, M., Hoglund, P., Jarvinen, H., Kristo, P., Pelin, K., Ridanpaa, M., Salovaara, R., Toro, T., Bodmer, W., Olschwang, S., Olsen, A.S., Stratton, M.R., de la Chapelle, A. and Aaltonen, L.A. (1998). A serine/threonine kinase gene defective in Peutz-Jeghers syndrome. *Nature* **391**(6663): 184-187.

Herman, J.G. and Baylin, S.B. (2003). Gene silencing in cancer in association with promoter hypermethylation. *N Engl J Med* **349**(21): 2042-2054.

Herrmann, H. and Aebi, U. (2000). Intermediate filaments and their associates: multi-talented structural elements specifying cytoarchitecture and cytodynamics. *Curr Opin Cell Biol* **12**(1): 79-90.

Hewitt, R.E., McMarlin, A., Kleiner, D., Wersto, R., Martin, P., Tsokos, M., Stamp, G.W. and Stetler-Stevenson, W.G. (2000). Validation of a model of colon cancer progression. *J Pathol* **192**(4): 446-454.

Hirako, Y., Yamakawa, H., Tsujimura, Y., Nishizawa, Y., Okumura, M., Usukura, J., Matsumoto, H., Jackson, K.W., Owaribe, K. and Ohara, O. (2003). Characterization of mammalian synemin, an intermediate filament protein present in all four classes of muscle cells and some neuroglial cells: co-localization and interaction with type III intermediate filament proteins and [illegible]s. *Cell Tissue Res* **313**(2): 195-207.

Hobdy, E.M., Ciesielski, T.E. and Kummar, S. (2003). Unusual sites of colorectal cancer metastasis. *Clin Colorectal Cancer* **3**(1): 54-57.

Hofemeister, H., Kuhn, C., Franke, W.W., Weber, K. and Stick, R. (2002). Conservation of the gene structure and membrane-targeting signals of germ cell-specific lamin LIII in amphibians and fish. *Eur J Cell Biol* **81**(2): 51-60.

Hoger, T.H., Grund, C., Franke, W.W. and Krohne, G. (1991). Immunolocalization of lamins in the thick nuclear lamina of human synovial cells. *Eur J Cell Biol* **54**(1): 150-156.

Hozak, P., Sasseville, A.M., Raymond, Y. and Cook, P.R. (1995). Lamin proteins form an internal nucleoskeleton as well as a peripheral lamina in human cells. *J Cell Sci* **108**(Pt 2): 635-644.

Hutchison, C.J., Alvarez-Reyes, M. and Vaughan, O.A. (2001). Lamins in disease: why do ubiquitously expressed nuclear envelope proteins give rise to tissue-specific disease phenotypes? *J Cell Sci* **114**(Pt 1): 9-19.

Hutchison, C.J. (2002). Lamins: building blocks or regulators of gene expression? *Nat Rev Mol Cell Biol* **3**(11): 848-858.

Igarashi, H., Sugimura, H., Maruyama, K., Kitayama, Y., Ohta, I., Suzuki, M., Tanaka, M., Dobashi, Y. and Kino, I. (1994). Alteration of immunoreactivity by hydrated autoclaving, microwave treatment, and simple heating of paraffin-embedded tissue sections. *Apmis* **102**(4): 295-307.

Iwashita, T., Kruger, G.M., Pardal, R., Kiel, M.J. and Morrison, S.J. (2003). Hirschsprung disease is linked to defects in neural crest stem cell function. *Science* **301**(5635): 972-976.

Jansen, M.P., Machiels, B.M., Hopman, A.H., Broers, J.L., Bot, F.J., Arends, J.W., Ramaekers, F.C. and Schouten, H.C. (1997). Comparison of A and B-type lamin expression in reactive lymph nodes and nodular sclerosing Hodgkin's disease. *Histopathology* **31**(4): 304-312.

Jen, J., Powell, S.M., Papadopoulos, N., Smith, K.J., Hamilton, S.R., Vogelstein, B. and Kinzler, K.W. (1994). Molecular determinants of dysplasia in colorectal lesions. *Cancer Res* **54**(21): 5523-5526.

Jenne, D.E., Reimann, H., Nezu, J., Friedel, W., Loff, S., Jeschke, R., Muller, O., Back, W. and Zimmer, M. (1998). Peutz-Jeghers syndrome is caused by mutations in a novel serine threonine kinase. *Nat Genet* **18**(1): 38-43.

Jing, R., Pizzolato, G., Robson, R.M., Gabbiani, G. and Skalli, O. (2005). Intermediate filament protein synemin is present in human reactive and malignant astrocytes and associates with ruffled membranes in astrocytoma cells. *Glia* **50**(2): 107-120.

Johnston, P.G. (2004). Of what value genomics in colorectal cancer? Opportunities and challenges. *J Clin Oncol* **22**(9): 1538-1539.

Jones, P.A. and Laird, P.W. (1999). Cancer epigenetics comes of age. *Nat Genet* **21**(2): 163-167.

Kahveci, Z., Minbay, F.Z., Noyan, S. and Cavusoglu, I. (2003). A comparison of microwave heating and proteolytic pretreatment antigen retrieval techniques in formalin fixed, paraffin embedded tissues. *Biotech Histochem* **78**(2): 119-128.

Karnovsky, M.J. (1965). A formaldehyde-glutaraldehyde fixative of high osmolarity for use in electron microscopy. *J Cell Biol* **27**: 137A-138A.

Kaufmann, S.H., Mabry, M., Jasti, R. and Shaper, J.H. (1991). Differential expression of nuclear envelope lamins A and C in human lung cancer cell lines. *Cancer Res* **51**(2): 581-586.

Kawai, K., Serizawa, A., Hamana, T. and Tsutsumi, Y. (1994). Heat-induced antigen retrieval of proliferating cell nuclear antigen and p53 protein in formalin-fixed, paraffin-embedded sections. *Pathol Int* **44**(10-11): 759-764.

Kedinger, M., Lefebvre, O., Duluc, I., Freund, J.N. and Simon-Assmann, P. (1998). Cellular and molecular partners involved in gut morphogenesis and differentiation. *Philos Trans R Soc Lond B Biol Sci* **353**(1370): 847-856.

Kill, I.R. and Hutchison, C.J. (1995). S-phase phosphorylation of lamin B2. *FEBS Lett* **377**(1): 26-30.

Kinzler, K.W. and Vogelstein, B. (1996). Lessons from hereditary colorectal cancer. *Cell* **87**(2): 159-170.

Korenjak, M. and Brehm, A. (2005). E2F-Rb complexes regulating transcription of genes important for differentiation and development. *Curr Opin Genet Dev* **15**(5): 520-527.

Korinek, V., Barker, N., Morin, P.J., van Wichen, D., de Weger, R., Kinzler, K.W., Vogelstein, B. and Clevers, H. (1997). Constitutive transcriptional activation by a beta-catenin-Tcf complex in APC-/- colon carcinoma. *Science* **275**(5307): 1784-1787.

Korkola, J.E., DeVries, S., Fridlyand, J., Hwang, E.S., Estep, A.L., Chen, Y.Y., Chew, K.L., Dairkee, S.H., Jensen, R.M. and Waldman, F.M. (2003). Differentiation of lobular versus ductal breast carcinomas by expression microarray analysis. *Cancer Res* **63**(21): 7167-7175.

Korkola, J.E., Houldsworth, J., Dobrzynski, D., Olshen, A.B., Reuter, V.E., Bosl, G.J. and Chaganti, R.S. (2005). Gene expression-based classification of nonseminomatous male germ cell tumors. *Oncogene* **24**(32): 5101-5107.

Krimm, I., Ostlund, C., Gilquin, B., Couprie, J., Hossenlopp, P., Mornon, J.P., Bonne, G., Courvalin, J.C., Worman, H.J. and Zinn-Justin, S. (2002). The Ig-like structure of the C-terminal domain of lamin A/C, mutated in muscular dystrophies, cardiomyopathy, and partial lipodystrophy. *Structure (Camb)* **10**(6): 811-823.

Lazarides, E. (1980). Intermediate filaments as mechanical integrators of cellular space. *Nature* **283**(5744): 249-256.

Leal, A., Morera, B., Del Valle, G., Heuss, D., Kayser, C., Berghoff, M., Villegas, R., Hernandez, E., Mendez, M., Hennies, H.C., Neundorfer, B., Barrantes, R., Reis, A. and Rautenstrauss, B. (2001). A second locus for an axonal form of autosomal recessive Charcot-Marie-Tooth disease maps to chromosome 19q13.3. *Am J Hum Genet* **68**(1): 269-274.

Lebel, S., Lampron, C., Royal, A. and Raymond, Y. (1987). Lamins A and C appear during retinoic acid-induced differentiation of mouse embryonal carcinoma cells. *J Cell Biol* **105**(3): 1099-1104.

Lee, K.K., Haraguchi, T., Lee, R.S., Koujin, T., Hiraoka, Y. and Wilson, K.L. (2001). Distinct functional domains in emerin bind lamin A and DNA-bridging protein BAF. *J Cell Sci* **114**(Pt 24): 4567-4573.

Lee, K.K., Starr, D., Cohen, M., Liu, J., Han, M., Wilson, K.L. and Gruenbaum, Y. (2002). Lamin-dependent localization of UNC-84, a protein required for nuclear migration in Caenorhabditis elegans. *Mol Biol Cell* **13**(3): 892-901.

Lehner, C.F., Stick, R., Eppenberger, H.M. and Nigg, E.A. (1987). Differential expression of nuclear lamin proteins during chicken development. *J Cell Biol* **105**(1): 577-587.

Leibovitz, A. (1963). The Growth and Maintenance of Tissue-Cell Cultures in Free Gas Exchange with the Atmosphere. *Am J Hyg* **78**: 173-180.

Leibovitz, A., Stinson, J.C., McCombs, W.B., 3rd, McCoy, C.E., Mazur, K.C. and Mabry, N.D. (1976). Classification of human colorectal adenocarcinoma cell lines. *Cancer Res* **36**(12): 4562-4569.

Lenz-Bohme, B., Wismar, J., Fuchs, S., Reifegerste, R., Buchner, E., Betz, H. and Schmitt, B. (1997). Insertional mutation of the Drosophila nuclear lamin Dm0

gene results in defective nuclear envelopes, clustering of nuclear pore complexes, and accumulation of annulate lamellae. *J Cell Biol* **137**(5): 1001-1016.

Li, J., Yen, C., Liaw, D., Podsypanina, K., Bose, S., Wang, S.I., Puc, J., Miliaresis, C., Rodgers, L., McCombie, R., Bigner, S.H., Giovanella, B.C., Ittmann, M., Tycko, B., Hibshoosh, H., Wigler, M.H. and Parsons, R. (1997). PTEN, a putative protein tyrosine phosphatase gene mutated in human brain, breast, and prostate cancer. *Science* **275**(5308): 1943-1947.

Libotte, T., Zaim, H., Abraham, S., Padmakumar, V.C., Schneider, M., Lu, W., Munck, M., Hutchison, C., Wehnert, M., Fahrenkrog, B., Sauder, U., Aebi, U., Noegel, A.A. and Karakesisoglou, I. (2005). Lamin A/C-dependent localization of Nesprin-2, a giant scaffolder at the nuclear envelope. *Mol Biol Cell* **16**(7): 3411-3424.

Lin, F. and Worman, H.J. (1993). Structural organization of the human gene encoding nuclear lamin A and nuclear lamin C. *J Biol Chem* **268**(22): 16321-16326.

Lin, F. and Worman, H.J. (1995). Structural organization of the human gene (LMNB1) encoding nuclear lamin B1. *Genomics* **27**(2): 230-236.

Lin, F. and Worman, H.J. (1997). Expression of nuclear lamins in human tissues and cancer cell lines and transcription from the promoters of the lamin A/C and B1 genes. *Exp Cell Res* **236**(2): 378-384.

Liu, J., Rolef Ben-Shahar, T., Riemer, D., Treinin, M., Spann, P., Weber, K., Fire, A. and Gruenbaum, Y. (2000). Essential roles for Caenorhabditis elegans lamin gene in nuclear organization, cell cycle progression, and spatial organization of nuclear pore complexes. *Mol Biol Cell* **11**(11): 3937-3947.

Loewinger, L. and McKeon, F. (1988). Mutations in the nuclear lamin proteins resulting in their aberrant assembly in the cytoplasm. *Embo J* **7**(8): 2301-2309.

Logan, C.Y. and Nusse, R. (2004). The Wnt signaling pathway in development and disease. *Annu Rev Cell Dev Biol* **20**: 781-810.

Lynch, H.T. and de la Chapelle, A. (1999). Genetic susceptibility to non-polyposis colorectal cancer. *J Med Genet* **36**(11): 801-818.

Lui, j. and et al. (2000). Essential roles of *Caenorhabditis elegans* lamin gene in nuclear organisation, cell cycle progression, and spatial organisation of nuclear pore complexes. *Mol. Biol. Cell* **11**: 3937-3947.

Mabry, M., Nakagawa, T., Nelkin, B.D., McDowell, E., Gesell, M., Eggleston, J.C., Casero, R.A., Jr. and Baylin, S.B. (1988). v-Ha-ras oncogene insertion: a model for tumor progression of human small cell lung cancer. *Proc Natl Acad Sci U S A* **85**(17): 6523-6527.

Machiels, B.M., Broers, J.L., Raymond, Y., de Ley, L., Kuijpers, H.J., Caberg, N.E. and Ramaekers, F.C. (1995). Abnormal A-type lamin organization in a human lung carcinoma cell line. *Eur J Cell Biol* **67**(4): 328-335.

Machiels, B.M., Zorenc, A.H., Endert, J.M., Kuijpers, H.J., van Eys, G.J., Ramaekers, F.C. and Broers, J.L. (1996). An alternative splicing product of the lamin A/C gene lacks exon 10. *J Biol Chem* **271**(16): 9249-9253.

Machiels, B.M., Ramaekers, F.C., Kuijpers, H.J., Groenewoud, J.S., Oosterhuis, J.W. and Looijenga, L.H. (1997). Nuclear lamin expression in normal testis and testicular germ cell tumours of adolescents and adults. *J Pathol* **182**(2): 197-204.

Mandel, J.S., Bond, J.H., Church, T.R., Snover, D.C., Bradley, G.M., Schuman, L.M. and Ederer, F. (1993). Reducing mortality from colorectal cancer by screening for fecal occult blood. Minnesota Colon Cancer Control Study. *N Engl J Med* **328**(19): 1365-1371.

Mandel, J.S., Church, T.R., Ederer, F. and Bond, J.H. (1999). Colorectal cancer mortality: effectiveness of biennial screening for fecal occult blood. *J Natl Cancer Inst* **91**(5): 434-437.

Manilal, S., Nguyen, T.M., Sewry, C.A. and Morris, G.E. (1996). The Emery-Dreifuss muscular dystrophy protein, emerin, is a nuclear membrane protein. *Hum Mol Genet* **5**(6): 801-808.

Manilal, S., Sewry, C.A., Pereboev, A., Man, N., Gobbi, P., Hawkes, S., Love, D.R. and Morris, G.E. (1999). Distribution of emerin and lamins in the heart and implications for Emery-Dreifuss muscular dystrophy. *Hum Mol Genet* **8**(2): 353-359.

Markiewicz, E., Dechat, T., Foisner, R., Quinlan, R.A. and Hutchison, C.J. (2002). Lamin A/C binding protein LAP2alpha is required for nuclear anchorage of retinoblastoma protein. *Mol Biol Cell* **13**(12): 4401-4413.

Marsh, D.J., Coulon, V., Lunetta, K.L., Rocca-Serra, P., Dahia, P.L., Zheng, Z., Liaw, D., Caron, S., Duboue, B., Lin, A.Y., Richardson, A.L., Bonnetblanc, J.M., Bressieux, J.M., Cabarrot-Moreau, A., Chompret, A., Demange, L., Eeles, R.A., Yahanda, A.M., Fearon, E.R., Fricker, J.P., Gorlin, R.J., Hodgson, S.V., Huson, S., Lacombe, D., Eng, C. and et al. (1998). Mutation spectrum and genotype-phenotype analyses in Cowden disease and Bannayan-Zonana syndrome, two hamartoma syndromes with germline PTEN mutation. *Hum Mol Genet* **7**(3): 507-515.

Marshman, E., Booth, C. and Potten, C.S. (2002). The intestinal epithelial stem cell. *Bioessays* **24**(1): 91-98.

Marton, M.J., DeRisi, J.L., Bennett, H.A., Iyer, V.R., Meyer, M.R., Roberts, C.J., Stoughton, R., Burchard, J., Slade, D., Dai, H., Bassett, D.E., Jr., Hartwell, L.H., Brown, P.O. and Friend, S.H. (1998). Drug target validation and identification of secondary drug target effects using DNA microarrays. *Nat Med* **4**(11): 1293-1301.

McKeon, F.D., Kirschner, M.W. and Caput, D. (1986). Homologies in both primary and secondary structure between nuclear envelope and intermediate filament proteins. *Nature* **319**(6053): 463-468.

McKusick, V.A. (1963). Medical Genetics 1962. *J Chronic Dis* **16**: 457-634.

Meier, J., Campbell, K.H., Ford, C.C., Stick, R. and Hutchison, C.J. (1991). The role of lamin LIII in nuclear assembly and DNA replication, in cell-free extracts of Xenopus eggs. *J Cell Sci* **98**(Pt 3): 271-279.

Mighell, A.J., Robinson, P.A. and Hume, W.J. (1995). Patterns of immunoreactivity to an anti-fibronectin polyclonal antibody in formalin-fixed, paraffin-embedded oral tissues are dependent on methods of antigen retrieval. *J Histochem Cytochem* **43**(11): 1107-1114.

Miller, R.G., Layzer, R.B., Mellenthin, M.A., Golabi, M., Francoz, R.A. and Mall, J.C. (1985). Emery-Dreifuss muscular dystrophy with autosomal dominant transmission. *Neurology* **35**(8): 1230-1233.

Misiewicz, J.J., Bartram, C.I., Cotton, P.B., Mee, A.S., Price, A.B. and Thompson, R.P.H. (1988). Diseases of the colon and rectum: A guide to diagnosis. In: *Gastroenterology*. Vol. 3. London: Gower Medical Publishing.

Mislow, J.M., Kim, M.S., Davis, D.B. and McNally, E.M. (2002a). Myne-1, a spectrin repeat transmembrane protein of the myocyte inner nuclear membrane, interacts with lamin A/C. *J Cell Sci* **115**(Pt 1): 61-70.

Mislow, J.M., Holaska, J.M., Kim, M.S., Lee, K.K., Segura-Totten, M., Wilson, K.L. and McNally, E.M. (2002b). Nesprin-1alpha self-associates and binds directly to emerin and lamin A in vitro. *FEBS Lett* **525**(1-3): 135-140.

Mittnacht, S. and Weinberg, R.A. (1991). G1/S phosphorylation of the retinoblastoma protein is associated with an altered affinity for the nuclear compartment. *Cell* **65**(3): 381-393.

Mizuno, Y., Thompson, T.G., Guyon, J.R., Lidov, H.G., Brosius, M., Imamura, M., Ozawa, E., Watkins, S.C. and Kunkel, L.M. (2001). Desmuslin, an intermediate filament protein that interacts with alpha -dystrobrevin and desmin. *Proc Natl Acad Sci U S A* **98**(11): 6156-6161.

Mizuno, Y., Guyon, J.R., Watkins, S.C., Mizushima, K., Sasaoka, T., Imamura, M., Kunkel, L.M. and Okamoto, K. (2004). Beta-synemin localizes to regions of high stress in human skeletal myofibers. *Muscle Nerve* **30**(3): 337-346.

Moir, R.D., Donaldson, A.D. and Stewart, M. (1991). Expression in Escherichia coli of human lamins A and C: influence of head and tail domains on assembly properties and paracrystal formation. *J Cell Sci* **99**(Pt 2): 363-372.

Moir, R.D., Spann, T.P., Lopez-Soler, R.I., Yoon, M., Goldman, A.E., Khuon, S. and Goldman, R.D. (2000a). Review: the dynamics of the nuclear lamins during the cell cycle-- relationship between structure and function. *J Struct Biol* **129**(2-3): 324-334.

Moir, R.D., Yoon, M., Khuon, S. and Goldman, R.D. (2000b). Nuclear lamins A and B1: different pathways of assembly during nuclear envelope formation in living cells. *J Cell Biol* **151**(6): 1155-1168.

Morin, P.J., Sparks, A.B., Korinek, V., Barker, N., Clevers, H., Vogelstein, B. and Kinzler, K.W. (1997). Activation of beta-catenin-Tcf signaling in colon cancer by mutations in beta-catenin or APC. *Science* **275**(5307): 1787-1790.

Moss, S.F., Krivosheyev, V., de Souza, A., Chin, K., Gaetz, H.P., Chaudhary, N., Worman, H.J. and Holt, P.R. (1999). Decreased and aberrant nuclear lamin expression in gastrointestinal tract neoplasms. *Gut* **45**(5): 723-729.

Mounkes, L.C., Kozlov, S., Hernandez, L., Sullivan, T. and Stewart, C.L. (2003). A progeroid syndrome in mice is caused by defects in A-type lamins. *Nature* **423**(6937): 298-301.

Muchir, A., Bonne, G., van der Kooi, A.J., van Meegen, M., Baas, F., Bolhuis, P.A., de Visser, M. and Schwartz, K. (2000). Identification of mutations in the gene encoding lamins A/C in autosomal dominant limb girdle muscular dystrophy with atrioventricular conduction disturbances (LGMD1B). *Hum Mol Genet* **9**(9): 1453-1459.

Muller, H.H., Heinimann, K. and Dobbie, Z. (2000). Genetics of hereditary colon cancer - a basis for prevention? *Eur J Cancer* **36**(10): 1215-1223.

Murakami, H. and Masui, H. (1980). Hormonal control of human colon carcinoma cell growth in serum-free medium. *Proc Natl Acad Sci U S A* **77**(6): 3464-3468.

Murakami, S., Terakado, M., Hashimoto, T., Tsuji, Y., Okubo, K. and Hirayama, R. (2003). Adrenal metastasis from rectal cancer: report of a case. *Surg Today* **33**(2): 126-130.

Nagano, A., Koga, R., Ogawa, M., Kurano, Y., Kawada, J., Okada, R., Hayashi, Y.K., Tsukahara, T. and Arahata, K. (1996). Emerin deficiency at the nuclear membrane in patients with Emery-Dreifuss muscular dystrophy. *Nat Genet* **12**(3): 254-259.

Nagase, H. and Nakamura, Y. (1993). Mutations of the APC (adenomatous polyposis coli) gene. *Hum Mutat* **2**(6): 425-434.

Narayan, S. and Roy, D. (2003). Role of APC and DNA mismatch repair genes in the development of colorectal cancers. *Mol Cancer* **2**: 41.

Newport, J.W., Wilson, K.L. and Dunphy, W.G. (1990). A lamin-independent pathway for nuclear envelope assembly. *J Cell Biol* **111**(6 Pt 1): 2247-2259.

Nigg, E.A. (1992). Assembly and cell cycle dynamics of the nuclear lamina. *Semin Cell Biol* **3**(4): 245-253.

Nigro, J.M., Baker, S.J., Preisinger, A.C., Jessup, J.M., Hostetter, R., Cleary, K., Bigner, S.H., Davidson, N., Baylin, S., Devilee, P. and et al. (1989). Mutations in the p53 gene occur in diverse human tumour types. *Nature* **342**(6250): 705-708.

Nili, E., Cojocaru, G.S., Kalma, Y., Ginsberg, D., Copeland, N.G., Gilbert, D.J., Jenkins, N.A., Berger, R., Shaklai, S., Amariglio, N., Brok-Simoni, F., Simon, A.J. and Rechavi, G. (2001). Nuclear membrane protein LAP2beta mediates transcriptional repression alone and together with its binding partner GCL (germ-cell-less). *J Cell Sci* **114**(Pt 18): 3297-3307.

NORCCAG (2004). Northern Region Colorectal Cancer Audit Group - 6th Annual Report.

Novelli, G., Muchir, A., Sangiuolo, F., Helbling-Leclerc, A., D'Apice, M.R., Massart, C., Capon, F., Sbraccia, P., Federici, M., Lauro, R., Tudisco, C., Pallotta, R., Scarano, G., Dallapiccola, B., Merlini, L. and Bonne, G. (2002). Mandibuloacral dysplasia is caused by a mutation in LMNA-encoding lamin A/C. *Am J Hum Genet* **71**(2): 426-431.

Oguchi, M., Sagara, J., Matsumoto, K., Saida, T. and Taniguchi, S. (2002). Expression of lamins depends on epidermal differentiation and transformation. *Br J Dermatol* **147**(5): 853-858.

Olson, T.M. and Keating, M.T. (1996). Mapping a cardiomyopathy locus to chromosome 3p22-p25. *J Clin Invest* **97**(2): 528-532.

Oster, S.K., Ho, C.S., Soucie, E.L. and Penn, L.Z. (2002). The myc oncogene: MarvelouslY Complex. *Adv Cancer Res* **84**: 81-154.

Ottaviano, Y. and Gerace, L. (1985). Phosphorylation of the nuclear lamins during interphase and mitosis. *J Biol Chem* **260**(1): 624-632.

Ozaki, T., Saijo, M., Murakami, K., Enomoto, H., Taya, Y. and Sakiyama, S. (1994). Complex formation between lamin A and the retinoblastoma gene product: identification of the domain on lamin A required for its interaction. *Oncogene* **9**(9): 2649-2653.

Padmakumar, V.C., Abraham, S., Braune, S., Noegel, A.A., Tunggal, B., Karakesisoglou, I. and Korenbaum, E. (2004). Enaptin, a giant actin-binding protein, is an element of the nuclear membrane and the actin cytoskeleton. *Exp Cell Res* **295**(2): 330-339.

Paraskeva, C., Corfield, A.P., Harper, S., Hague, A., Audcent, K. and Williams, A.C. (1990). Colorectal carcinogenesis: sequential steps in the in vitro immortalization and transformation of human colonic epithelial cells. *Anticancer Res* **10**(5A): 1189-1200.

Parsons, R., Li, G.M., Longley, M.J., Fang, W.H., Papadopoulos, N., Jen, J., de la Chapelle, A., Kinzler, K.W., Vogelstein, B. and Modrich, P. (1993). Hypermutability and mismatch repair deficiency in RER+ tumor cells. *Cell* **75**(6): 1227-1236.

Paulin-Levasseur, M., Scherbarth, A., Traub, U. and Traub, P. (1988). Lack of lamins A and C in mammalian hemopoietic cell lines devoid of intermediate filament proteins. *Eur J Cell Biol* **47**(1): 121-131.

Paulin-Levasseur, M., Giese, G., Scherbarth, A. and Traub, P. (1989). Expression of vimentin and nuclear lamins during the in vitro differentiation of human promyelocytic leukemia cells HL-60. *Eur J Cell Biol* **50**(2): 453-461.

Perou, C.M., Sorlie, T., Eisen, M.B., van de Rijn, M., Jeffrey, S.S., Rees, C.A., Pollack, J.R., Ross, D.T., Johnsen, H., Akslen, L.A., Fluge, O., Pergamenschikov, A., Williams, C., Zhu, S.X., Lonning, P.E., Borresen-Dale, A.L., Brown, P.O. and

Botstein, D. (2000). Molecular portraits of human breast tumours. *Nature* **406**(6797): 747-752.

Peter, M., Nakagawa, J., Doree, M., Labbe, J.C. and Nigg, E.A. (1990). In vitro disassembly of the nuclear lamina and M phase-specific phosphorylation of lamins by cdc2 kinase. *Cell* **61**(4): 591-602.

Pinto, D., Gregorieff, A., Begthel, H. and Clevers, H. (2003). Canonical Wnt signals are essential for homeostasis of the intestinal epithelium. *Genes Dev* **17**(14): 1709-1713.

Pinto, D. and Clevers, H. (2005). Wnt control of stem cells and differentiation in the intestinal epithelium. *Exp Cell Res* **306**(2): 357-363.

Potten, C.S. and Loeffler, M. (1990). Stem cells: attributes, cycles, spirals, pitfalls and uncertainties. Lessons for and from the crypt. *Development* **110**(4): 1001-1020.

Potten, C.S., Booth, C. and Pritchard, D.M. (1997). The intestinal epithelial stem cell: the mucosal governor. *Int J Exp Pathol* **78**(4): 219-243.

Potter, J.D. (1999). Colorectal cancer: molecules and populations. *J Natl Cancer Inst* **91**(11): 916-932.

Promega (2002). Wizard SV Gel and PCR Clean-Up System Technical Bulletin #TB308.

Pugh, G.E., Coates, P.J., Lane, E.B., Raymond, Y. and Quinlan, R.A. (1997). Distinct nuclear assembly pathways for lamins A and C lead to their increase during quiescence in Swiss 3T3 cells. *J Cell Sci* **110 ( Pt 19)**: 2483-2493.

Radtke, F. and Clevers, H. (2005). Self-renewal and cancer of the gut: two sides of a coin. *Science* **307**(5717): 1904-1909.

Raffaele Di Barletta, M., Ricci, E., Galluzzi, G., Tonali, P., Mora, M., Morandi, L., Romorini, A., Voit, T., Orstavik, K.H., Merlini, L., Trevisan, C., Biancalana, V., Housmanowa-Petrusewicz, I., Bione, S., Ricotti, R., Schwartz, K., Bonne, G. and Toniolo, D. (2000). Different mutations in the LMNA gene cause autosomal dominant and autosomal recessive Emery-Dreifuss muscular dystrophy. *Am J Hum Genet* **66**(4): 1407-1412.

Rankin, F.W. and Broders, A.C. (1928). Factors influencing prognosis in carcinoma of the rectum. *Surg Gynecol Obstet* **46**: 660-667.

Raven, P.H. and Johnson, G.B. (1996). Cellular Mechanisms of Development. In: *Biology*. Dubuque: Wm. C. Brown Publishers, pp. 371-400.

Rao, L., Perez, D. and White, E. (1996). Lamin proteolysis facilitates nuclear events during apoptosis. *J Cell Biol* **135**(6 Pt 1): 1441-1455.

Reid, L., Holland, J., Jones, C., Wolfe, B., Niwayama, G., Williams, R., Kaplan, N. and Sato, G. (1978). Some of the variables affecting the success of transplantation of human tumours into the athymic nude mouse. In: *Proceedings of the Symposium on the Use of Athymic (Nude) Mice in Cancer Research*. Overje, A. (ed). New York: Fischer, pp. 107-121.

Reintgen, D.S., Thompson, W., Garbutt, J. and Seigler, H.F. (1984). Radiologic, endoscopic, and surgical considerations of melanoma metastatic to the gastrointestinal tract. *Surgery* **95**(6): 635-639.

Reynolds, E.S. (1963). The use of lead citrate at high pH as an electron-opaque stain in electron microscopy. *J Cell Biol* **17**: 208-212.

Riemer, D., Stuurman, N., Berrios, M., Hunter, C., Fisher, P.A. and Weber, K. (1995). Expression of Drosophila lamin C is developmentally regulated: analogies with vertebrate A-type lamins. *J Cell Sci* **108**(Pt 10): 3189-3198.

Rober, R.A., Weber, K. and Osborn, M. (1989). Differential timing of nuclear lamin A/C expression in the various organs of the mouse embryo and the young animal: a developmental study. *Development* **105**(2): 365-378.

Roncucci, L., Pedroni, M., Vaccina, F., Benatti, P., Marzona, L. and De Pol, A. (2000). Aberrant crypt foci in colorectal carcinogenesis. Cell and crypt dynamics. *Cell Prolif* **33**(1): 1-18.

Rowlands, D.C., Bunce, C.M., Crocker, J., Ayres, J.G., Johnson, G.D., Ling, N. and Brown, G. (1994). Expression of a nuclear envelope protein recognized by the monoclonal antibody BU31 in lung tumours: relationship to Ki-67 antigen expression. *J Pathol* **173**(2): 89-96.

Sadler, T.W. and Langman, J. (2000). *Langman's Medical Embryology, 8th ed.* New York: Lippincott Williams & Wilkins.

Salina, D., Bodoor, K., Eckley, D.M., Schroer, T.A., Rattner, J.B. and Burke, B. (2002). Cytoplasmic dynein as a facilitator of nuclear envelope breakdown. *Cell* **108**(1): 97-107.

Sancho, E., Batlle, E. and Clevers, H. (2004). Signaling pathways in intestinal development and cancer. *Annu Rev Cell Dev Biol* **20**: 695-723.

Sasseville, A.M. and Raymond, Y. (1995). Lamin A precursor is localized to intranuclear foci. *J Cell Sci* **108**(Pt 1): 273-285.

Scheer, U., Kartenbeck, J., Trendelenburg, M.F., Stadler, J. and Franke, W.W. (1976). Experimental disintegration of the nuclear envelope. Evidence for pore-connecting fibrils. *J Cell Biol* **69**(1): 1-18.

Scherf, U., Ross, D.T., Waltham, M., Smith, L.H., Lee, J.K., Tanabe, L., Kohn, K.W., Reinhold, W.C., Myers, T.G., Andrews, D.T., Scudiero, D.A., Eisen, M.B., Sausville, E.A., Pommier, Y., Botstein, D., Brown, P.O. and Weinstein, J.N. (2000). A gene expression database for the molecular pharmacology of cancer. *Nat Genet* **24**(3): 236-244.

Schirmer, E.C., Guan, T. and Gerace, L. (2001). Involvement of the lamin rod domain in heterotypic lamin interactions important for nuclear organization. *J Cell Biol* **153**(3): 479-489.

Sgonc, R. and Gruber, J. (1998). Apoptosis detection: an overview. *Exp Gerontol* **33**(6): 525-533.

Shi, S.R., Key, M.E. and Kalra, K.L. (1991). Antigen retrieval in formalin-fixed, paraffin-embedded tissues: an enhancement method for immunohistochemical staining based on microwave oven heating of tissue sections. *J Histochem Cytochem* **39**(6): 741-748.

Sigma (1999). Tri Reagent Technical Bulletin MB-205.

Simha, V. and Garg, A. (2002). Body fat distribution and metabolic derangements in patients with familial partial lipodystrophy associated with mandibuloacral dysplasia. *J Clin Endocrinol Metab* **87**(2): 776-785.

Simha, V., Agarwal, A.K., Oral, E.A., Fryns, J.P. and Garg, A. (2003). Genetic and phenotypic heterogeneity in patients with mandibuloacral dysplasia-associated lipodystrophy. *J Clin Endocrinol Metab* **88**(6): 2821-2824.

Sinensky, M., Fantle, K., Trujillo, M., McLain, T., Kupfer, A. and Dalton, M. (1994). The processing pathway of prelamin A. *J Cell Sci* **107**(Pt 1): 61-67.

Siu, I.M., Pretlow, T.G., Amini, S.B. and Pretlow, T.P. (1997). Identification of dysplasia in human colonic aberrant crypt foci. *Am J Pathol* **150**(5): 1805-1813.

Smythe, C., Jenkins, H.E. and Hutchison, C.J. (2000). Incorporation of the nuclear pore basket protein nup153 into nuclear pore structures is dependent upon lamina assembly: evidence from cell-free extracts of Xenopus eggs. *Embo J* **19**(15): 3918-3931.

Sobotka-Briner, C. and Chelsky, D. (1992). COOH-terminal methylation of lamin B and inhibition of methylation by farnesylated peptides corresponding to lamin B and other CAAX motif proteins. *J Biol Chem* **267**(17): 12116-12122.

Spann, T.P., Moir, R.D., Goldman, A.E., Stick, R. and Goldman, R.D. (1997). Disruption of nuclear lamin organization alters the distribution of replication factors and inhibits DNA synthesis. *J Cell Biol* **136**(6): 1201-1212.

Spann, T.P., Goldman, A.E., Wang, C., Huang, S. and Goldman, R.D. (2002). Alteration of nuclear lamin organization inhibits RNA polymerase II-dependent transcription. *J Cell Biol* **156**(4): 603-608.

Speckman, R.A., Garg, A., Du, F., Bennett, L., Veile, R., Arioglu, E., Taylor, S.I., Lovett, M. and Bowcock, A.M. (2000). Mutational and haplotype analyses of families with familial partial lipodystrophy (Dunnigan variety) reveal recurrent missense mutations in the globular C-terminal domain of lamin A/C. *Am J Hum Genet* **66**(4): 1192-1198.

Stadelmann, B., Khandjian, E., Hirt, A., Luthy, A., Weil, R. and Wagner, H.P. (1990). Repression of nuclear lamin A and C gene expression in human acute lymphoblastic leukemia and non-Hodgkin's lymphoma cells. *Leuk Res* **14**(9): 815-821.

Stainier, D.Y. (2005). No organ left behind: tales of gut development and evolution. *Science* **307**(5717): 1902-1904.

Starr, D.A., Hermann, G.J., Malone, C.J., Fixsen, W., Priess, J.R., Horvitz, H.R. and Han, M. (2001). unc-83 encodes a novel component of the nuclear envelope and is essential for proper nuclear migration. *Development* **128**(24): 5039-5050.

Steen, R.L. and Collas, P. (2001). Mistargeting of B-type lamins at the end of mitosis: implications on cell survival and regulation of lamins A/C expression. *J Cell Biol* **153**(3): 621-626.

Steinert, P.M., Chou, Y.H., Prahlad, V., Parry, D.A., Marekov, L.N., Wu, K.C., Jang, S.I. and Goldman, R.D. (1999). A high molecular weight intermediate filament-associated protein in BHK-21 cells is nestin, a type VI intermediate filament protein. Limited co-assembly in vitro to form heteropolymers with type III vimentin and type IV alpha-internexin. *J Biol Chem* **274**(14): 9881-9890.

Stewart, C. and Burke, B. (1987). Teratocarcinoma stem cells and early mouse embryos contain only a single major lamin polypeptide closely resembling lamin B. *Cell* **51**(3): 383-392.

Stick, R. and Hausen, P. (1985). Changes in the nuclear lamina composition during early development of Xenopus laevis. *Cell* **41**(1): 191-200.

Stick, R. (1988). cDNA cloning of the developmentally regulated lamin LIII of Xenopus laevis. *Embo J* **7**(10): 3189-3197.

Stick, R., Angres, B., Lehner, C.F. and Nigg, E.A. (1988). The fates of chicken nuclear lamin proteins during mitosis: evidence for a reversible redistribution of lamin B2 between inner nuclear membrane and elements of the endoplasmic reticulum. *J Cell Biol* **107**(2): 397-406.

Stoffler, D., Fahrenkrog, B. and Aebi, U. (1999). The nuclear pore complex: from molecular architecture to functional dynamics. *Curr Opin Cell Biol* **11**(3): 391-401.

Stremmel, C., Wein, A., Hohenberger, W. and Reingruber, B. (2002). DNA microarrays: a new diagnostic tool and its implications in colorectal cancer. *Int J Colorectal Dis* **17**(3): 131-136.

Stadelmann, B., Khandjian, E., Hirt, A., Luthy, A., Weil, R. and Wagner, H.P. (1990). Repression of nuclear lamin A and C gene expression in human acute lymphoblastic leukemia and non-Hodgkin's lymphoma cells. *Leuk Res* **14**(9): 815-821.

Stewart, C. and Burke, B. (1987). Teratocarcinoma stem cells and early mouse embryos contain only a single major lamin polypeptide closely resembling lamin B. *Cell* **51**(3): 383-392.

Stuurman, N., Heins, S. and Aebi, U. (1998). Nuclear lamins: their structure, assembly, and interactions. *J Struct Biol* **122**(1-2): 42-66.

Sullivan, K.M., Busa, W.B. and Wilson, K.L. (1993). Calcium mobilization is required for nuclear vesicle fusion in vitro: implications for membrane traffic and IP3 receptor function. *Cell* **73**(7): 1411-1422.

Sullivan, T., Escalante-Alcalde, D., Bhatt, H., Anver, M., Bhat, N., Nagashima, K., Stewart, C.L. and Burke, B. (1999). Loss of A-type lamin expression compromises nuclear envelope integrity leading to muscular dystrophy. *J Cell Biol* **147**(5): 913-920.

Sultana, S., Sernett, S.W., Bellin, R.M., Robson, R.M. and Skalli, O. (2000). Intermediate filament protein synemin is transiently expressed in a subset of astrocytes during development. *Glia* **30**(2): 143-153.

Sundermeyer, M.L., Meropol, N.J., Rogatko, A., Wang, H. and Cohen, S.J. (2005). Changing patterns of bone and brain metastases in patients with colorectal cancer. *Clin Colorectal Cancer* **5**(2): 108-113.

Takahashi, A., Musy, P.Y., Martins, L.M., Poirier, G.G., Moyer, R.W. and Earnshaw, W.C. (1996). CrmA/SPI-2 inhibition of an endogenous ICE-related protease responsible for lamin A cleavage and apoptotic nuclear fragmentation. *J Biol Chem* **271**(51): 32487-32490.

Taylor, C.R., Shi, S.R., Chen, C., Young, L., Yang, C. and Cote, R.J. (1996). Comparative study of antigen retrieval heating methods: microwave, microwave and pressure cooker, autoclave, and steamer. *Biotech Histochem* **71**(5): 263-270.

Terry, P., Giovannucci, E., Michels, K.B., Bergkvist, L., Hansen, H., Holmberg, L. and Wolk, A. (2001). Fruit, vegetables, dietary fiber, and risk of colorectal cancer. *J Natl Cancer Inst* **93**(7): 525-533.

Thibodeau, S.N., Bren, G. and Schaid, D. (1993). Microsatellite instability in cancer of the proximal colon. *Science* **260**(5109): 816-819.

Tilli, C.M., Ramaekers, F.C., Broers, J.L., Hutchison, C.J. and Neumann, H.A. (2003). Lamin expression in normal human skin, actinic keratosis, squamous cell carcinoma and basal cell carcinoma. *Br J Dermatol* **148**(1): 102-109.

Titeux, M., Brocheriou, V., Xue, Z., Gao, J., Pellissier, J.F., Guicheney, P., Paulin, D. and Li, Z. (2001). Human synemin gene generates splice variants encoding two distinct intermediate filament proteins. *Eur J Biochem* **268**(24): 6435-6449.

Toms, J.R., (ed) (2004). *CancerStats Monograph 2004.* London: Cancer Research UK.

Torosian, M.H., Botet, J.F. and Paglia, M. (1987). Colon carcinoma metastatic to the thigh--an unusual site of metastasis. Report of a case. *Dis Colon Rectum* **30**(10): 805-808.

Touchette, N. (1994). Finding clues about how embryo structures form. *Science* **266**(5185): 564-565.

Turnbull, R.B., Jr., Kyle, K., Watson, F.R. and Spratt, J. (1967). Cancer of the colon: the influence of the no-touch isolation technic on survival rates. *Ann Surg* **166**(3): 420-427.

Tzur, Y.B., Hersh, B.M., Horvitz, H.R. and Gruenbaum, Y. (2002). Fate of the nuclear lamina during Caenorhabditis elegans apoptosis. *J Struct Biol* **137**(1-2): 146-153.

van de Wetering, M., Cavallo, R., Dooijes, D., van Beest, M., van Es, J., Loureiro, J., Ypma, A., Hursh, D., Jones, T., Bejsovec, A., Peifer, M., Mortin, M. and Clevers, H. (1997). Armadillo coactivates transcription driven by the product of the Drosophila segment polarity gene dTCF. *Cell* **88**(6): 789-799.

van de Wetering, M., Sancho, E., Verweij, C., de Lau, W., Oving, I., Hurlstone, A., van der Horn, K., Batlle, E., Coudreuse, D., Haramis, A.P., Tjon-Pon-Fong, M., Moerer, P., van den Born, M., Soete, G., Pals, S., Eilers, M., Medema, R. and

Clevers, H. (2002). The beta-catenin/TCF-4 complex imposes a crypt progenitor phenotype on colorectal cancer cells. *Cell* **111**(2): 241-250.

van der Kooi, A.J., Ledderhof, T.M., de Voogt, W.G., Res, C.J., Bouwsma, G., Troost, D., Busch, H.F., Becker, A.E. and de Visser, M. (1996). A newly recognized autosomal dominant limb girdle muscular dystrophy with cardiac involvement. *Ann Neurol* **39**(5): 636-642.

van der Kooi, A.J., van Meegen, M., Ledderhof, T.M., McNally, E.M., de Visser, M. and Bolhuis, P.A. (1997). Genetic localization of a newly recognized autosomal dominant limb-girdle muscular dystrophy with cardiac involvement (LGMD1B) to chromosome 1q11-21. *Am J Hum Genet* **60**(4): 891-895.

Vaughan, A., Alvarez-Reyes, M., Bridger, J.M., Broers, J.L., Ramaekers, F.C., Wehnert, M., Morris, G.E., Whitfield, W.G.F. and Hutchison, C.J. (2001). Both emerin and lamin C depend on lamin A for localization at the nuclear envelope. *J Cell Sci* **114**(Pt 14): 2577-2590.

Venables, R.S., McLean, S., Luny, D., Moteleb, E., Morley, S., Quinlan, R.A., Lane, E.B. and Hutchison, C.J. (2001). Expression of individual lamins in basal cell carcinomas of the skin. *Br J Cancer* **84**(4): 512-519.

Vigers, G.P. and Lohka, M.J. (1991). A distinct vesicle population targets membranes and pore complexes to the nuclear envelope in Xenopus eggs. *J Cell Biol* **112**(4): 545-556.

Vigouroux, C., Auclair, M., Dubosclard, E., Pouchelet, M., Capeau, J., Courvalin, J.C. and Buendia, B. (2001). Nuclear envelope disorganization in fibroblasts from lipodystrophic patients with heterozygous R482Q/W mutations in the lamin A/C gene. *J Cell Sci* **114**(Pt 24): 4459-4468.

Virtanen, C., Ishikawa, Y., Honjoh, D., Kimura, M., Shimane, M., Miyoshi, T., Nomura, H. and Jones, M.H. (2002). Integrated classification of lung tumors and cell lines by expression profiling. *Proc Natl Acad Sci U S A* **99**(19): 12357-12362.

Vogelstein, B., Fearon, E.R., Hamilton, S.R., Kern, S.E., Preisinger, A.C., Leppert, M., Nakamura, Y., White, R., Smits, A.M. and Bos, J.L. (1988). Genetic alterations during colorectal-tumor development. *N Engl J Med* **319**(9): 525-532.

Ward, G.E. and Kirschner, M.W. (1990). Identification of cell cycle-regulated phosphorylation sites on nuclear lamin C. *Cell* **61**(4): 561-577.

Weber, K., Plessmann, U. and Traub, P. (1989). Maturation of nuclear lamin A involves a specific carboxy-terminal trimming, which removes the polyisoprenylation site from the precursor; implications for the structure of the nuclear lamina. *FEBS Lett* **257**(2): 411-414.

Weiss, L. and Ward, P.M. (1988). Effects of metastatic cascades on metastatic patterns: studies on colon-26 carcinomas in mice. *Int J Cancer* **41**(3): 450-455.

Weinstein, J.N., Myers, T.G., O'Connor, P.M., Friend, S.H., Fornace, A.J., Jr., Kohn, K.W., Fojo, T., Bates, S.E., Rubinstein, L.V., Anderson, N.L., Buolamwini, J.K., van Osdol, W.W., Monks, A.P., Scudiero, D.A., Sausville, E.A., Zaharevitz, D.W., Bunow, B., Viswanadhan, V.N., Johnson, G.S., Wittes, R.E. and Paull, K.D. (1997). An information-intensive approach to the molecular pharmacology of cancer. *Science* **275**(5298): 343-349.

Wilson, R.G. (2001). Personal communication.

Wolpert, L. (1994). Do we understand development? *Science* **266**(5185): 571-572.

Wulff, K., Ebener, U., Wehnert, C.S., Ward, P.A., Reuner, U., Hiebsch, W., Herrmann, F.H. and Wehnert, M. (1997). Direct molecular genetic diagnosis and heterozygote identification in X-linked Emery-Dreifuss muscular dystrophy by heteroduplex analysis. *Dis Markers* **13**(2): 77-86.

Wydner, K.L., McNeil, J.A., Lin, F., Worman, H.J. and Lawrence, J.B. (1996). Chromosomal assignment of human nuclear envelope protein genes LMNA, LMNB1, and LBR by fluorescence in situ hybridization. *Genomics* **32**(3): 474-478.

Xue, Z.G., Cheraud, Y., Brocheriou, V., Izmiryan, A., Titeux, M., Paulin, D. and Li, Z. (2004). The mouse synemin gene encodes three intermediate filament proteins generated by alternative exon usage and different open reading frames. *Exp Cell Res* **298**(2): 431-444.

Yang, L., Guan, T. and Gerace, L. (1997). Integral membrane proteins of the nuclear envelope are dispersed throughout the endoplasmic reticulum during mitosis. *J Cell Biol* **137**(6): 1199-1210.

Ye, Q., Callebaut, I., Pezhman, A., Courvalin, J.C. and Worman, H.J. (1997). Domain-specific interactions of human HP1-type chromodomain proteins and inner nuclear membrane protein LBR. *J Biol Chem* **272**(23): 14983-14989.

Young, L.W., Radebaugh, J.F., Rubin, P., Sensenbrenner, J.A., Fiorelli, G. and McKusick, V.A. (1971). New syndrome manifested by mandibular hypoplasia, acroosteolysis, stiff joints and cutaneous atrophy (mandibuloacral dysplasia) in two unrelated boys. *Birth Defects Orig Artic Ser* **7**(7): 291-297.

Zhang, Q., Skepper, J.N., Yang, F., Davies, J.D., Hegyi, L., Roberts, R.G., Weissberg, P.L., Ellis, J.A. and Shanahan, C.M. (2001). Nesprins: a novel family of spectrin-repeat-containing proteins that localize to the nuclear membrane in multiple tissues. *J Cell Sci* **114**(Pt 24): 4485-4498.

Zhen, Y.Y., Libotte, T., Munck, M., Noegel, A.A. and Korenbaum, E. (2002). NUANCE, a giant protein connecting the nucleus and actin cytoskeleton. *J Cell Sci* **115**(Pt 15): 3207-3222.

http://frodo.wi.mit.edu/primer3/primer3_code.html

http://www.premierbiosoft.com/netprimer/index.html